DsRNA-mediated antiviral immunity in fish cells: visualization, sensors, and innate immune responses

by

Sarah Jacqueline Poynter

A thesis

presented to the University of Waterloo

in fulfilment of the

thesis requirement for the degree of

Doctor of Philosophy

in

Biology

Waterloo, Ontario, Canada, 2018

Examining committee membership

The following served on the Examining Committee for this thesis. The decision of the Examining Committee is by majority vote.

External Examiner	SARAH WOOTTON Associate Professor, Pathobiology, University of Guelph
Supervisors	STEPHANIE DEWITTE-ORR Associate Professor, Department of Health Sciences and Biology, Wilfrid Laurier University
	BRIAN DIXON Professor, Canada Research Chair in Fish and Environmental Immunology, Department of Biology, University of Waterloo
Internal Members	CHRISTINE DUPONT Continuing Lecturer, Biology Teaching Fellow, Undergraduate Advisor, Department of Biology, University of Waterloo
	PAUL CRAIG Assistant Professor, Department of Biology, University of Waterloo
Internal-External Member	MARC AUCOIN Academic Director WatPD- Engineering and Associate Professor, Department of Chemical Engineering, University of Waterloo

Author's declaration

This thesis consists of material all of which I authored or co-authored: see Statement of Contributions included in the thesis. This is a true copy of the thesis, including any required final revisions, as accepted by my examiners.

I understand that my thesis may be made electronically available to the public

Statement of contributions

In the case of published chapters, the numbering system of any published chapters has been updated to fit this thesis.

Chapter 1 – Sections of this chapter, namely the descriptions of specific ISGs, came from a review that I am first author on and can be found in Appendix B in its entirety. This review was published in Developmental & Comparative Immunology, volume 65, pp. 218-225.

Chapter 2 – No additional contributors. This chapter was published in Frontiers in Immunology, volume 9, article 829.

Chapter 3 – A. Monjo and G. Micheli performed experiments to identify the MARCO-1 sequence, and to clone this sequence into an expression vector. A. Monjo completed a preliminary notation of conserved domains for MARCO-1. A. Monjo contributed 1/3 of the introduction to this manuscript. This chapter was published in 2017 in Developmental & Comparative Immunology, volume *77*, pp. 95-105. All other experiments, analysis, and manuscript preparation were completed by S. Poynter.

Chapter 4 – A. Monjo cloned the full-length SCARA5 sequence and identified conserved domains in the SCARA5 sequence. This chapter was published in 2018 in Fish & shellfish immunology, volume 76, pp. 121-125. All other experiments, analysis, and manuscript preparation were completed by S. Poynter.

Chapter 5 – S. Herrington-Krause performed PCR reactions for identification of partial sequences from DDX3 and DHX9 under the mentorship of S. Poynter. All other experiments, analysis, and manuscript preparation were completed by S. Poynter.

Chapter 6 – The novel cell line used in this study was established by E. Leis from the U.S. Fish and Wildlife Service in La Crosse Wisconsin, USA and E. Leis performed DNA barcoding on the cell line. All other experiments, analysis, and manuscript preparation (with the exception of the materials and methods sections relevant to E. Leis experiments) were completed by S. Poynter.

Permission to use copyrighted material has been obtained from the publishers (Elsevier, Frontiers in Immunology, and Springer Nature) and all joint authors.

Abstract

The global aquaculture industry is a multibillion dollar business that is threatened by pathogens, including a wide array of aquatic viruses. Currently there are no antiviral treatments available to combat viral outbreaks, and as such viral infection can cause vast economic loss. Two important species for aquaculture include rainbow trout (*Oncorhynchus mykiss*), destined for human consumption, and fathead minnow (*Pimephales promelas*), a common species grown for bait purposes. Double-stranded (ds)RNA is a potent immunomodulating molecule produced during viral replication; dsRNA treatment induces a robust antiviral state that makes host cells refractive to viral replication. This thesis explored dsRNA-induced innate antiviral pathways from two angles. Firstly, the differences in dsRNA-induced responses between virally-produced dsRNA, synthesized dsRNA with natural sequence variation, and synthesized dsRNA with a homogenous sequence were analyzed in rainbow trout cells. The dsRNA, regardless of source, was sensed at the cell surface by a common receptor in rainbow trout cells and induced an innate immune response and antiviral state against two aquatic viruses, viral hemorrhagic septicemia virus and infectious pancreatic necrosis virus; the virally-produced and lab-synthesized dsRNA molecules with natural sequence variation produced the most similar responses. The second angle of approach was to better understand the host's response to exogenous dsRNA treatment. To this end, novel dsRNA sensors were identified and characterized in rainbow trout. This included class A scavenger receptors, the purported surface receptors for dsRNA, including MARCO, SCARA3, SCARA4, and SCARA5, as well as two novel cytoplasmic dsRNA sensors from the DExH/D-box family, DDX3 and DHX9. The receptors found in rainbow trout contained the same conserved domains that are found in their mammalian counterparts, a first indication of conserved functionality. Two MARCO variants were identified and found to bind

to two gram-negative and one gram–positive bacteria, but surprisingly not to dsRNA. Rainbow trout DDX3 and DHX9 are both functional in their ability to bind to dsRNA. The culmination of these findings was the development of a dsRNA molecule with sequence variation that can act as a potent antiviral therapy *in vitro* in fathead minnow cells. The findings from this thesis demonstrate the importance of 'natural' dsRNA as an innate immune signalling molecule and its potential to function as a prophylactic antiviral therapeutic for fish.

Acknowledgments

I would like to first acknowledge my parents and family. No one else in the world can provide unconditional support quite like mom and dad, and brothers aren't so bad either. Thank you for making science a part of my life from such a young age and fostering my love of science throughout my life. I would like to thank my fiancé Cody Partridge for absolutely everything that he does, thank you for your encouragement and for supporting me when I put my research first, I hope you know how special that makes you and I look forward to every moment we spend together, FOREVER. To my friends I truly appreciate you, I appreciate you for listening to me muse and ruminate for hours over problems and puzzles in my life. I am so lucky to have such wonderful people in my life.

I want to express my gratitude to all the current and past members of the DeWitte-Orr lab. Every single person who has passed through our lab has been a part of this journey and has had so much to teach me. Andrea Monjo, thank you for being my rock for two years, you truly are my kindred science spirit. Jondavid de Jong thank you for enduring a year of my non-stop talking and an almost constant stream of questions, you have some pretty good ideas about science too. I would also like to thank my extended scientific family, including "Grandpa" Niels Bols and "Uncle" Nguyen Vo; the growing community that exists from this lineage is so incredibly supportive and wonderful, I am grateful to get to be a part of the clan. I would also like to thank the support staff at the University of Waterloo and Wilfrid Laurier University, as well as Jim from the Curling Club for my daily greeting.

I thank my co-supervisor Brian Dixon for his support and providing me with new perspectives into the fish immunology area of science. Thank you for all the scientific and volunteer opportunities you have provided me to push me as a scientist and a person. Thank you

to my Ph.D. committee members, Drs. Christine Dupont, Paul Craig, and Matt Smith for your valuable advice and input to my research projects over the years.

And saving my biggest thank you for last, I want to thank Stephanie DeWitte-Orr, or as she will always be to me, Dr. D. As your first Ph.D. student, I have at least four years to be your uncontested favourite, most successful, most intelligent, and most amazing PhD student. I will savor the next four years. As my supervisor for the past six years you will *always* be my favourite, most successful, most intelligent, and most amazing M.Sc. and Ph.D. supervisor. I will always cherish our memories together, like Alanis car karaoke, the waterslide in Tucson, and our lab catch phrase. Thank you for inventing and perfecting the selfie. Thank you for taking a chance on a student from McMaster with little lab experience and bad grades. Your genuine love of research is inspirational and contagious, as a mentor and a friend you have taught me so many valuable lessons I will carry with me always. I could not have asked for a better mentor. I will always consider myself a student in the DeWitte-Orr lab.

Dedication

I dedicate this thesis to Danika Kelland and Holden McCollom-Foote. I know that you will both achieve such big wonderful things in your life, and I hope to continue passing on my love of science to you baby geniuses.

Table of Contents

List of figures

Chapter 1

Chapter 2

Chapter 3

Chapter 4

Chapter 5

Chapter 6

Appendix A

Appendix B

List of tables

List of abbreviations

AO – acridine orange
AP-1 – activator protein 1
APS – ammonium persulfate
ATP – adenosine triphosphate
BSA – bovine serum albumin
CARD – caspase activation and recruitment domain
CHSE-214 – Chinook salmon embryonic cell line
CDS – coding sequence
CRFB – cytokine receptor family B
CSV – chum salmon reovirus
DDX – DEAD box polypeptide
DHX – DExH box polypeptide
DAPI – 4',6-diamidino-2-phenylindole
dsRNA – double-stranded (ds) ribonucleic acid (RNA)
EDTA – ethylenediaminetetraacetic acid
eIF – eukaryotic translation initiation factor
ELISA – enzyme-linked immunosorbent assay
EPC – Epithelioma papulosum cyprini
EtBr – ethidium bromide
FAO – Food and Agriculture Organization of the United Nations
FHMskin – fathead minnow skin cell line
FBS – fetal bovine serum
GFP – green fluorescent protein
GIG – grass carp hemorrhagic virus-induced gene
GTP – guanosine triphosphate
HA – Human influenza hemagglutinin
HIV-1 – human immunodeficiency virus -1
HMW – high-molecular weight poly I:C
HRP – horseradish peroxidase
ICC – immunocytochemistry
IF – immunofluorescence
IFIT – interferon-induced protein with tetratricopeptide repeats
IFN – type I interferon
IFNAR – interferon-α/β receptor
IKKε – Inhibitor of nuclear factor kappa-B kinase subunit epsilon
IPNV – infectious pancreatic necrosis virus
IPS-1 – interferon-β promoter stimulator 1
ISG – interferon-stimulated gene
ISGF3 – interferon-stimulated gene factor 3
ISRE – interferon-sensitive response element
JAK – Janus kinase
LDL – low-density lipoprotein
LMW - low-molecular weight poly I:C
LPS – lipopolysaccharide

LTA – lipoteichoic acid
MARCO – macrophage receptor with collagenous structure
MEFs – mouse embryonic fibroblasts
MDA5 – Melanoma differentiation-associated protein 5
miRNA – micro RNA
MOI – multiplicity of infection
Mx1 – myxoma resistant gene-1
NF-kB – nuclear factor kappa-B
NNV – nervous necrosis virus
NRT – no-reverse transcriptase
NTP – nucleotide triphosphate
NV – nonvirion
OAS – oligoadenylate synthetase
PAGE – polyacrylamide gel electrophoreses
PAMP – pathogen-associated molecular pattern
PBS – phosphate buffered saline
PI – post-infection
PKR – protein kinase R
Poly C – polycytidylic acid
Poly I – polyinosinic acid
Poly I:C – polyinosinic: polycytidylic acid
PRR – pattern recognition receptor
P/S – penicillin/streptomycin
PVDF – polyvinylidene fluoride
qRT-PCR – quantitative reverse-transcription polymerase chain reaction
RdRp – RNA-dependent RNA polymerase
RIG-I – retinoic acid-inducible gene-I
RIPA buffer – Radioimmunoprecipitation assay buffer
RLRs – retinoic acid-inducible gene (RIG)-I like receptors
RNase – ribonuclease
RTG2 – rainbow trout gonadal cell line
RTgill-W1 – rainbow trout gill cell line
RTgutGC – rainbow trout gut cell line
SCARA3 – Class A scavenger receptor member 3
SCARA4 – Class A scavenger receptor member 4
SCARA5 – Class A scavenger receptor member 5
siRNA – short interfering RNA
SR-A – class A scavenger receptor
SRCR – scavenger receptor cysteine rich domain
ssRNA – single-stranded (ss) ribonucleic acid (RNA)
STAT – signal transducer and activator of transcription
TAE – tris-acetate ethylenediaminetetraacetic acid
TBK1 – TANK-binding kinase-1
TCID50/mL – 50% tissue culture infective dose per milliliter
TEMED – tetramethylethylenediamine
TBE – tris-borate ethylenediaminetetraacetic acid

TBS – tris-buffered saline
TICAM-1 – TIR domain-containing adaptor molecule 1
TIR – toll-interleukin-1 receptor
TLR – toll-like receptor
TYK – tyrosine-protein kinase
VHSV – viral hemorrhagic septicemia virus
Vig – viral hemorrhagic septicemia virus-induced gene
ivt-dsRNA – *in vitro* transcribed dsRNA
v- or (v)dsRNA – viral dsRNA

Chapter 1: General introduction

Double-stranded (ds)RNA is a potent inducer of antiviral immune responses. Long (>30bp) dsRNA is not found in healthy cells, but is produced by viruses during their replication cycle; dsRNA has been identified from viruses of every genome type (Jacobs and Langland, 1996; Lee et al., 1994; viral dsRNA reviewed by DeWitte-Orr and Mossman, 2010). While dsRNA is able to modulate the adaptive immune response, the focus of this thesis is on its effects within innate immunity (Desmet and Ishii, 2012). DsRNA is sensed by host sensors on the cell surface, in the cytoplasm, and in the endosome, leading to the production of type I interferons (IFNs), Fig. 1.1 (IFNs; DeWitte-Orr and Mossman, 2010). IFNs are secreted cytokines that signal through their cognate receptor in an autocrine and paracrine fashion, activating a signalling cascade that culminates in the expression of a large subset of genes known as IFN-stimulated genes (ISGs; Poynter and DeWitte-Orr, 2016; Crosse et al., 2018). The protein products from these genes can be involved in the dsRNA-signalling pathway, or can directly limit viral infection by interacting with viral components or host machinery necessary for replication (Poynter and DeWitte-Orr, 2016; Crosse et al., 2018). This pathway is very effective and efficient; low concentrations of dsRNA are able to produce robust and broad spectrum antiviral states (Jacobs and Langland, 1996; Poynter and DeWitte-Orr, 2015). Our long-term goal is to utilize this pathway to produce more efficacious viral vaccine adjuvants and antiviral treatments for aquaculture purposes. The following sections provide details regarding the steps in this pathway, the current state of knowledge in fish, and the importance of the aquaculture industry and the threat of pathogen outbreaks.

A

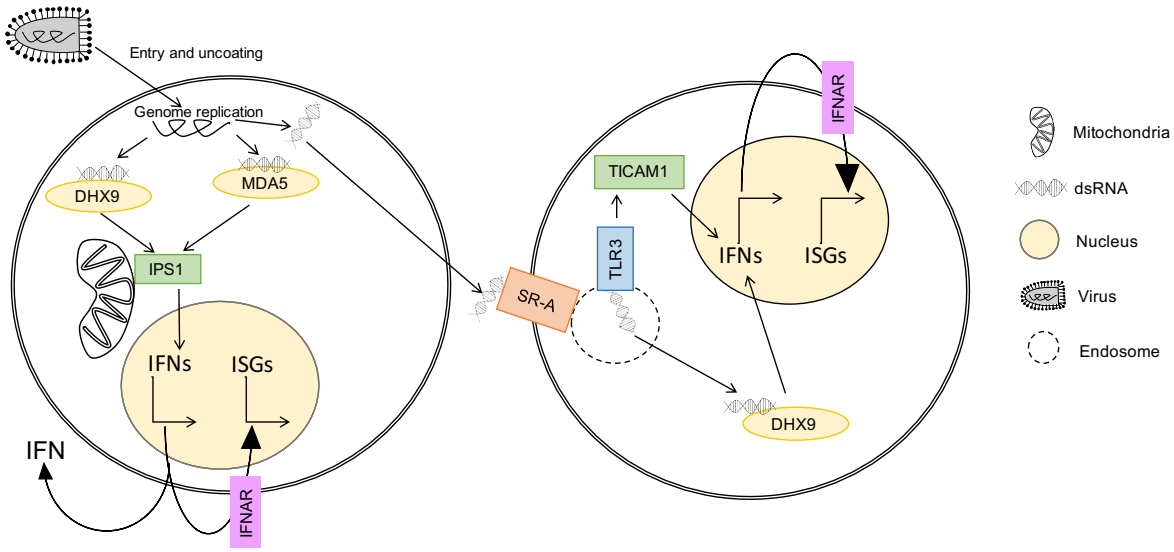
Entry and uncoating
Genome replication
DHX9
MDA5
IPS1
IFNs
ISGs
IFN
IFNAR
SR-A
TICAM1
TLR3
IFNAR
IFNs
ISGs
DHX9
Mitochondria
dsRNA
Nucleus
Virus
Endosome

B

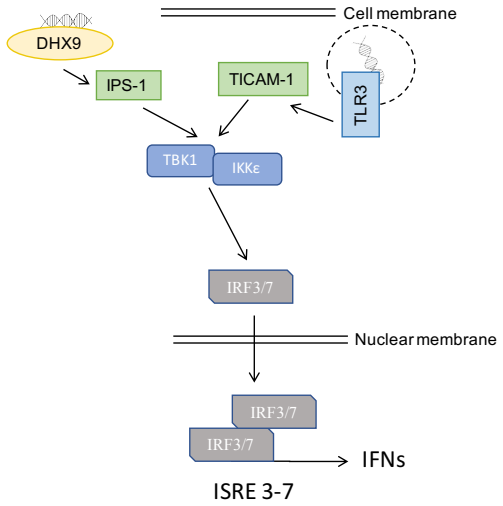
Cell membrane
DHX9
IPS-1
TICAM-1
TLR3
TBK1
IKKε
IRF3/7
Nuclear membrane
IRF3/7
IRF3/7
IFNs
ISRE 3-7

C

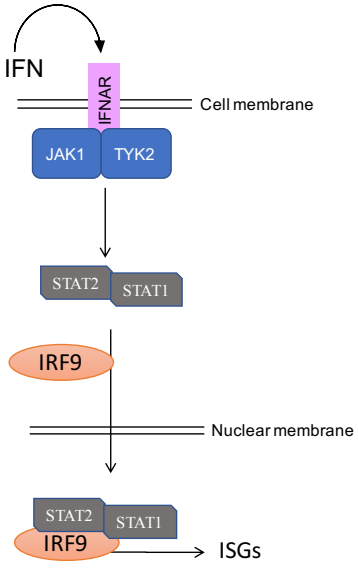
IFN
IFNAR
Cell membrane
JAK1
TYK2
STAT2
STAT1
IRF9
Nuclear membrane
STAT2
STAT1
IRF9
ISGs

Figure 1.1. dsRNA-mediated signaling pathways, involving type I IFNs, ISGs and the antiviral state. (A) When a virus infects a host cell dsRNA is produced during replication; this dsRNA will initially be found in the cellular compartment where viral replication is occurring. This dsRNA can be recognized by cytoplasmic sensors, such as the DExD/H-box helicase DHX9, which signals through an adaptor protein such as interferon-β promoter stimulator 1 (IPS-1) to produce type I interferon (IFN). IFNs are secreted cytokines that can bind to their cognate receptor, the interferon-α/β receptor (IFNAR), in an autocrine or paracrine fashion, triggering a signaling cascade that results in the production of IFN-stimulated genes (ISGs). Intracellular dsRNA can be released into the extracellular milieu the cytoplasm by cell lysis where it is bound by class A scavenger receptors (SR-A) on the surface of neighbouring cells and internalized through endocytosis. From the endosome dsRNA can be sensed by endosomal sensors or escape the endosome into the cytoplasm. Endosomal sensors such as toll-like receptor 3 (TLR3) and cytoplasmic sensors, such as DHX9, bind dsRNA and induce IFNs and ISGs, establishing an antiviral state within the cells. **(B)** Intracellular dsRNA is sensed in the cytoplasm (ex. DHX9) or the endosome (ex. TLR3), which recruits adapter proteins IPS-1 and TIR domain-containing adapter molecule 1 (TICAM-1) respectively. These adaptor proteins stimulate activation of kinases TANK-binding kinase 1 (TBK1)/inhibitor of nuclear factor kappa-B kinase subunit epsilon (IKKε), which phosphorylate interferon regulatory factor (IRF)3 and IRF7. IRF3 and IRF7 homo- or hetero-dimerize and translocate to the nucleus, where they bind to the IFN promoter region, along with activator protein 1 (AP-1) and nuclear factor kappa-B (NF-kB), inducing IFN transcription**. (C)** IFN is produced via the secretory protein synthesis pathway of the cell, and released in the extracellular space, where it binds to its cognate receptor, IFNAR. Binding to IFNAR triggers a signaling cascade that results in the phosphorylation and dimerization of signal transducer and activator of transcription (STAT1) and STAT2, IRF9 is recruited to for a complex which translocates to the nucleus and binds to the interferon-sensitive response element (ISRE) of ISGs, stimulating their expression within the cell. The accumulation of ISGs within the cell establishes an antiviral state.

1.1 Pathogen-associated molecular patterns

Innate immunity is centered around the ability for the host to distinguish self from non-self. Pathogen-associated molecular patterns (PAMPs) are proteins, nucleic acids, and other molecules that are produced by pathogens and associated with an infection. PAMPs are either exclusively produced by microbes or have a distinguishing feature that separates them from host molecules, such as cellular location or nucleotide modifications (Brubaker et al., 2015). Examples of bacterial PAMPs are lipopolysaccharides (LPS), unmethylated CpG DNA, or peptidoglycan (Akira and Hemmi, 2003). Fungi produce PAMPs such as zymosan, β-glucan, or chitin (Taghavi et al., 2017; van de Veerdonk et al., 2008). Viral PAMPs tend to be nucleic acids but also include some proteins; examples include endosomal DNA, long dsRNA, endosomal

single-stranded (ss)RNA, or certain viral membrane proteins (Desmet and Ishii, 2012; Compton et al., 2003).

The viral PAMP dsRNA is the focus of the present thesis. DsRNA consists of two antiparallel RNA strands with Watson-Crick base pairing that form a right-handed double helix; this helix is A-form and underwound compared to a B-helix (Nicholson, 1996; Tang and Draper, 1994). The minor groove of dsRNA has free 2'-hydroxyl groups that facilitate interactions with binding partners (Nicholson, 1996; Bevilacqua et al., 1996). DsRNA can be identified using differential digestion; under high salt conditions dsRNA is not degraded by ribonuclease (RNase) A, B, or TI, and dsRNA, not ssRNA, is susceptible to degradation by RNase III (DeWitte-Orr and Mossman, 2010). There are three commercially available monoclonal antibodies available from Scicons that bind specifically to long (>40bp) dsRNA; these antibodies can be used for enzyme-linked immunosorbent assays (ELISAs), immunoblots, and immunofluorescence to identify dsRNA (Schönborn et al., 1991; Doherty et al., 2016). Appendix A of this thesis provides a detailed protocol for four methods of identifying viral dsRNA, both antibody-dependent and -independent.

The mechanism by which dsRNA is produced depends on the genome of the virus and replication strategy. DsRNA viruses produce dsRNA as their genome, and while this nucleic acid is contained within the capsid to prevent detection, there is evidence small amounts of genome are improperly encapsidated and can be found outside the capsid (Lloyd and Shatkin, 1992). Viruses with ssRNA genomes make dsRNA as replicative intermediates during the replication of their genomic RNA (Kumar and Carmichael, 1998). DsRNA associated with DNA virus replication has been observed with several viruses (Jacquemont and Roizman, 1975). Converging bidirectional transcription can produce overlapping regions within RNA transcripts

that anneal to produce dsRNA; alternatively RNA polymerase III has been shown to transcribe cytoplasmic DNA into dsRNA that can trigger the type I IFN response (Kumar and Carmichael, 1998; Chiu et al., 2009).

DsRNA receptors are able to recognize dsRNA based on the unique helical structure of dsRNA, the length of dsRNA, the presence of 5' triphosphate groups, and differences in nucleoside modifications (Kariko and Weissman, 2007, Myong et al., 2009; Okahira et al., 2005; Kato et al., 2008). The main feature explored in this thesis is length. Host dsRNA molecules, such as short interfering (si)RNAs or micro (mi)RNAs, are short molecules (<30bp), viruses produce much longer molecules during replication (endogenous dsRNA reviewed by DeWitte-Orr and Mossman, 2010). The majority of dsRNA sensors are able to bind shorter dsRNA molecules, however dimerization is needed for activation and this requires a greater length; longer and more abundant dsRNA molecules induce a more robust response from receptor clustering (Heinicke et al., 2009; Kato et al., 2008; Peisley and Hur, 2013). The most common form of dsRNA used in research to date is polyinosinic: polycytidylic acid (poly I:C); while an IFN-inducing molecule, poly I:C does not have natural sequence variation and has a different structure than molecules with sequence variation (Okahira et al., 2005; Löseke et al., 2006). Poly I:C has limited biological relevancy as it is not a naturally produced molecule. The focus of this thesis is to transition to the use of more biologically relevant dsRNA molecules that have natural sequence variation and nucleotides. In the 1960s poly I:C was a prospective candidate as a broad antiviral drug, however due to the high-potency of poly I:C in mammalian cells, there were adverse physiological effects; attempts to decrease the potency of poly I:C have had some success, however these therapies are still in development (DeWitte-Orr and Mossman, 2010).

1.2 dsRNA signalling pathways: adaptor molecules, kinases and transcription factors

The recognition of dsRNA by a cognate pattern-recognition receptor (PRR) initiates a signalling pathway within the cell that culminates in the production of type I IFN, Fig. 1.1A (Sparrer and Gack, 2015). Many steps of the dsRNA sensing pathway have been elucidated in fish, however as different fish species show variability in immune pathways, further research is needed to understand species-specific differences. The downstream pathway to IFN induction can be separated into adaptor proteins, kinases, and transcription factor activation.

1.2.1 Adaptor proteins

Adaptor proteins function as linkage partners, matching the dsRNA-sensors to a specific signaling pathway. For example, toll-like receptor (TLR)3 recruits the adaptor molecule toll-interleukin-1 receptor (TIR)-containing adapter molecule 1 (TICAM-1; also known as TRIF) and the RIG-I-like receptors (RLRs) and non-RLR DExD/H-box helicases recruit interferon-β promoter stimulator 1 (IPS-1; also known as MAVS, CARDIF, or VISA; Yoneyama et al., 2015; Kawai and Akira, 2008; Zhang et al., 2011; Oshiumi et al., 2010A). Interestingly, the dsRNA surface receptors class A scavenger receptors (SR-As) do not seem to have substantial signalling capabilities themselves, and likely function as dsRNA carriers, bringing dsRNA into the cell to endosomal sensors such as TLR3 (Nellimarla et al., 2015; Dansako et al., 2013). These two adaptors have been identified in multiple fish species; and these proteins, like their mammalian homologs, interact with dsRNA receptors (Matsuo et al., 2008; Zou et al., 2015). In mammals IPS-1 interacts with RLRs through caspase recruitment domains (CARDs) found on both the receptors and IPS-1; IPS-1 is found on the mitochondria and associates with receptors at the mitochondria upon receptor-ligand binding (Belgnaoui et al., 2011). IPS-1 in fish also has CARDs and forms aggregates on the mitochondria after viral infection; there is evidence that IPS-1 in fish is involved in RLR signalling (Xiao et al., 2017; Zhang et al., 2014B; Huang et al.,

2018). In zebrafish (*Danio rerio*), co-immunoprecipitation assays have demonstrated interactions between IPS-1 and the RLRs (Zou et al., 2014B; Zou et al., 2015).

1.2.2 Kinases and transcription factors

IPS-1 and TICAM-1 activate the kinases TANK-binding kinase 1 (TBK1)/inhibitor of nuclear factor kappa-B kinase subunit epsilon (IKKε); these kinases phosphorylate transcription factors, including interferon regulatory factor (IRF)3 and IRF7; IRF3 and IRF7 homo- or hetero-dimerize and translocate to the nucleus to bind to the IFN-promoter, Fig. 1.1B (Reikine et al., 2014; Levy et al., 2011). Nuclear factor kappa-B (NFκB) and activator protein (AP)-1 are two additional transcription factors activated by dsRNA receptor-binding that together with IRF3/7 bind to the IFN promoter region and cause the production of IFN (Levy et al., 2011). In fish, both kinases have been cloned and have kinase domains; their role in the IFN pathway is less well understand but there is evidence they have a similar function to mammalian counterparts (Li et al., 2015; Hu et al., 2018A, Hu et al., 2018B). For example, zebrafish TBK1 overexpression increased levels of phosphorylated IRF3, whereas inactivate isoforms did not (Hu et al., 2018B). The exact role of these kinases in the teleost dsRNA-mediated immune pathway still requires further elucidation. The transcription factors IRF3 and IRF7 have been cloned and functionally characterized in fish. IRF3 and IRF7 are sufficient to activate fish IFN gene promoters; as is seen in mammals, these proteins are localized to the cytoplasm and upon stimulation with poly I:C or infection with virus they translocate to the nucleus and activate the IFN promoter (Cui et al., 2011; Holland et al., 2009; Sun et al., 2010; Chen et al., 2017).

1.3 Type I interferon, its receptor and signaling

1.3.1 Type I interferon

In mammals, viral infection or dsRNA stimulation leads to the production of IFN-α and IFN-β, both type I IFNs (Pestka et al., 2004). IFN-α and IFN-β are differentially expressed after

viral infection and these differences depend on the species, cell-type, and nature of the viral infection (Pestka et al., 2004). IFN is secreted from the cells and binds to the interferon-α/β receptor (IFNAR)1/2. This binding activates tyrosine kinase 2 (TYK2) and Janus kinase 1 (JAK1), these kinases phosphorylate signal transducer and activator of transcription (STAT)1 and STAT2. STAT1 and STAT2 homo- or hetero-dimerize and bind to phosphorylated IRF9 to form the interferon-stimulated gene factor 3 (ISGF3) complex, which translocates to the nucleus and upregulates ISGs through binding to the interferon-sensitive response element (ISRE) sequences in the promoter region of these genes, Fig. 1.1C (Au-Yeung et al., 2013). Accumulation of ISGs within the cell establishes an 'antiviral state', a state in which a cell is refractory to virus replication (Poynter and DeWitte-Orr, 2016).

Many type I IFNs have been identified in a variety of fish species; indeed, IFNs in fish have a greater diversity than IFNs than mammals. Twenty-two full-length type I IFN genes have been identified in rainbow trout (*Oncorhynchus mykiss*) (Zou et al., 2014A). Fish type I IFN are sub-grouped into groups a-f and are classified as group I or group II, if they possess two or four cysteine residues respectively (Zou et al., 2014A). The subgroups a and b are not reflective of mammalian IFN-α and IFN-β, however there is some evidence based on expression profiles that group I IFNs may be similar to IFN-β and group II may be more similar to IFN-α (Zou et al., 2014A). Fish type I IFNs are highly upregulated in response to viral infection and stimulation with dsRNA of different sources (Zou et al., 2007; Poynter and DeWitte-Orr, 2015; Svingerud et al., 2012; Jensen and Robertsen, 2002; Milne et al., 2018).

The JAK/STAT pathway in fish also shows similar features to mammals and many of the components of this pathway have been identified in fish (Oates et al., 1999; Skjesol et al., 2010). STAT1 from zebrafish was able to rescue the phenotype of a STAT1 deficient human cells;

suggesting the fish protein has similar function to the mammalian homolog (Oates et al., 1999). Atlantic salmon (*Salmo salar*) STAT1 is phosphorylated and moves into the nucleus upon IFN1a stimulation (Skjesol et al., 2010). IRF9 and STAT2 from crucian carp (*Carassius carassius*) were shown to activate an ISRE-containing promoter (Shi et al., 2012).

1.3.2 Type I interferon receptor(s)

There is only one known type I IFN receptor in mammals, composed of subunits IFNAR1 and IFNAR2, this is not the case in fish. Studies in zebrafish and the mandarin fish (*Siniperca chuatsi*) have identified three subunits of the IFN receptor, the cytokine receptor family B (CRFB)5, CRFB1, and CRFB2 (Laghari et al., 2018; Aggad et al., 2009; Levraud et al., 2007). CRFB5 is homologous to IFNAR1 and CRFB1/CRFB2 are homologous to IFNAR2 (Laghari et al., 2018). These three subunits form different complexes that preferentially bind different IFNs, for example in the mandarin fish IFNc preferentially binds CRFB2/CRFB5 and IFNd binds to CRFB1/CRFB5 (Laghari et al., 2018).

1.3.3 Interferon-stimulated genes

IFN stimulation in fish and mammals results in the production of a wide array of different genes, collectively termed IFN-stimulated genes (ISGs). These ISGs work together to block virus propagation at every step of the replication cycle. A detailed review of fish ISGs was published by Poynter and DeWitte-Orr in 2016, and is included in Appendix B of this thesis. In general fish possess a similar variety of ISGs to that of mammals, including sensors (ex. protein kinase R; PKR), signaling molecules (ex. IRF3 and IRF7) and antiviral effectors (ex. myxoma resistant gene-1 (Mx1) and ISG15; Holland et al., 2008; Poynter and DeWitte-Orr, 2016; Liu et al., 2011). In this thesis, the regulation of four ISGs has been explored: viperin/viral hemorrhagic septicemia virus (VHSV)-induced gene (vig)-1, ISG15/vig-3, ISG56/vig-4, and Mx1.

Viperin (also known as vig-1) is a well-characterized ISG with multiple antiviral mechanisms in mammals; these include interfering with viral budding through inhibition of specific enzymes, and inhibiting viral genome replication through binding to viral proteins required for replication and assembly (Chin and Cresswell, 2001; Helbig et al., 2011; Wang et al., 2007). Fish express an ISG with a high sequence similarity to human and murine viperin; however, its mechanism of action in fish is not well understood (Boudinot et al., 1999). The antiviral effects of viperin in both fish cells and whole animals have been shown; for example overexpression of viperin resulted in an antiviral state in crucian carp cells against grass carp hemorrhagic virus and in rock bream (*Oplegnathus fasciatus*) fish against megalocytivirus (Wang et al., 2014; Zhang et al., 2014A).

ISG15 (also known as vig-3) is a small protein with many roles in mammalian immunity; it is a ubiquitin-like protein that covalently binds to its target protein in a process known as ISGylation (O'Farrell et al., 2002; Schneider et al., 2014). Current evidence suggests that ISG15's antiviral activity may be non-specific, as it conjugates to both host and viral proteins, thus its mechanism for preferentially targeting viral proteins might be its ability to conjugate newly synthesized proteins of which there would be many in a virus infected cell (Durfee et al., 2010). Interestingly, ISGylation has been found to have both stabilizing and destabilizing effects on its target proteins, but it is not clear how this is accomplished (Durfee et al., 2010; Lu et al., 2006; Schneider et al., 2014). Fish ISG15 conjugates to viral proteins within infected cells, however the effect of this ISGylation is not understood (Langevin et al., 2013; Røkenes et al., 2007). Zebrafish ISG15 was found to conjugate to the P and NV proteins of infectious hematopoietic necrosis virus (Langevin et al., 2013). ISG15 in fish shows broad antiviral activity against many fish viruses, as seen with overexpression of orange-spotted grouper (*Epinephelus coioides*)

ISG15 in grouper spleen cells inhibiting grouper nervous necrosis virus and after knockdown of ISG15 by RNAi led to an increase in megalocytivirus viral load in tongue sole (*Cynoglossus semilaevis*) head kidney lymphocytes (Huang et al., 2013; Wang et al., 2012).

Mammalian ISG56 (also known as the IFN-induced protein with tetratricopeptide repeats (IFIT)-1) is a member of the IFIT family of proteins (Zhou et al., 2013). ISG56 in mammals has demonstrated antiviral properties; however, its mechanism is not thoroughly elucidated and appears complex. One antiviral mechanism of ISG56 is interference with viral transcription through binding to eukaryotic initiation factor (eIF)3 or binding/sequestering viral 5`PPP-RNA or non-2`-O methylated viral RNA (Zhou et al., 2013; Diamond, 2014). Fish also express members of the IFIT family, including ISG56 (O'Farrell et al., 2002). As in mammals, fish ISG56 proteins contain tetratricopeptide repeat domains and transcription is upregulated in response to viral infection (Long and Sun, 2014; O'Farrell et al., 2002; Zhou et al., 2013). While fish ISG56 has been shown to have antiviral effects, its mechanism of action is poorly understood. Overexpression of ISG56 in tongue sole limited megalocytivirus replication and knockdown of ISG56 enhanced replication (Long and Sun, 2014).

Mx proteins are dynamin-like guanosine triphosphate (GTP)ases with antiviral activity. In mammals, Mx1 induces a broad antiviral state by forming oligomers around viral nucleocapsids, ultimately targeting them for degradation (Schneider et al., 2014). Fish Mx is also interferon inducible and exhibits broad antiviral activity (Alvarez-Torres et al., 2013; Holland et al., 2008). As with mammals, fish Mx proteins have different mechanisms of action. In grouper Mx was shown to limit grouper nervous necrosis virus replication through direct interactions, specifically it was seen that the coat protein of the virus binds to the effector domain of Mx (Chen et al., 2008). In barramundi (*Lates calcarifer*) it was found that increased Mx expression led to

a decrease in nervous necrosis virus RNA-dependent RNA polymerase (RdRp) activity; Mx co-localized and co-precipitated with viral RdRp indicating a direct interaction (Wu et al., 2010).

1.4 Pattern-recognition receptors

PAMPs are recognized by their cognate receptors known as pattern-recognition receptors (PRRs). dsRNA-specific PRRs belong to a wide variety of different receptor families, including toll-like receptors (TLRs), retinoic acid-inducible gene (RIG)-I-like receptors (RLRs), non-RLR DExH/D-box (DHX or DDX) helicases, class A scavenger receptors (SR-As), and ISG receptors (PKR and oligoadenylate synthetase (OAS)) (Olive, 2012; Brubaker et al., 2015). TLR3 is the only known endosomal sensor of dsRNA in mammals; TLR3 is also found in fish and recently a novel role for TLR19 as an endosomal dsRNA receptor in fish has been identified (Matsuo et al., 2008; Ji et al., 2018; Kawai and Akira, 2008). The RIG-I-like (RLR) family of sensors (RIG-I and melanoma differentiation-associated protein 5 (MDA5)) are cytoplasmic, and both have been identified in fish species, with MDA5 expression found in a wider range of fish species compared to RIG-I, as RIG-I is not present in Acanthopterygii or rainbow trout (Yoneyama et al., 2015; Chen et al., 2017). OAS and PKR are cytoplasmic proteins that act as sensors for dsRNA and also as direct effector proteins, limiting virus replication at the transcription and translation level of protein production respectively; PKR is found in teleost fish, however OAS has not yet been identified (Hovanessian and Justesen, 2007; Garcia et al., 2007; Robertsen, 2006). There are a number of review papers discussing these sensors in mammals (Kawai and Akira, 2010; Thompson et al., 2011; Ranjan et al., 2009) and fish (Poynter et al., 2015A; Chen et al., 2017; Rebl et al., 2010; Zou et al., 2010). However, the focus of the present thesis is the role of SR-As and non-RLR DExH/D-box helicases as dsRNA sensors in rainbow trout, and as such, they will be the focus below.

1.4.1 Class A scavenger receptors (SR-As)

The SR-A family are surface expressed sensors that consists of five members, SR-AI/II, macrophage receptor with collagenous structure (MARCO), class A scavenger receptor (SCARA) member 3 (SCARA3), member 4 (SCARA4), and member 5 (SCARA5). SR-As all contain conserved features including a cytoplasmic domain, a transmembrane region, an α-helical domain, a collagenous domain, and a variable terminal domain that may end at the collagenous domain, as is seen in SCARA3, or a scavenger-receptor cysteine rich (SRCR) domain as is the case for MARCO, SR-AI/II, and SCARA5, or for SCARA4 a C-type lectin domain (Zani et al., 2015). SR-As were first discovered in macrophages, where they play important roles in recognizing chemically modified low-density lipoproteins (LDLs), converting macrophages to lipid-laden foam cells in atherosclerotic lesions (Gough and Gordon, 2000). SR-As can also bind to proteoglycans of the extracellular matrix and apoptotic cells, facilitating a macrophage's role as a phagocyte, removing debris from the body (Plüddemann et al., 2007; Santiago-Garcia et al., 2003).

More recently, SR-A expression has been identified in cells other than macrophages and their role in innate immunity has begun to be understood (DeWitte-Orr et al., 2010). SR-As are able to bind gram-negative and -positive bacteria as well as bacterial components including LPS and lipoteichoic acid (Dunne et al., 1994; Peiser et al., 2000). SR-As can act as co-receptors for other receptors to mediate the pro-inflammatory response to bacterial ligands (Bowdish et al., 2009). Of particular interest to this project, SR-As play a role in virus-host interactions. Viruses such as vaccinia virus and herpes simplex virus type 1 use SR-As as surface receptors for cell entry (MacLeod et al., 2015; MacLeod et al., 2013). SR-As also play a role in innate immunity by sensing extracellular viral dsRNA (Limmon et al., 2008).

In mammals, dsRNA is recognized and internalized by SR-As, as was demonstrated by use of SR-A specific ligands, anti-SR-A antibodies, and SR-A knockout mice, all of which decreased the host response to dsRNA treatment (Limmon et al., 2008; DeWitte-Orr et al., 2010). The exact SR-As that are dsRNA-receptors has not yet been elucidate, compensatory effects of some SR-As have been identified, as the most dramatic inhibition of the dsRNA response was seen when multiple candidate SR-As were knocked down together (DeWitte-Orr et al., 2010). SR-As do not appear to be signalling receptors, instead they deliver ligands, such as dsRNA, to other receptors with signalling capabilities, such as TLR3 (Dansako et al., 2013; Nellimarla et al., 2015). SR-AI in mammals has been the best studied member for a role in dsRNA-mediated responses. SR-AI binds to dsRNA through the conserved collagenous domain and knockdown of SRAI hinders cells ability to take up poly I:C; teleost fish do not have a homolog to SR-AI (Dansako et al., 2013). The study of individual SR-As is complicated by several factors; functional full-length receptors are membrane bound and trimeric; in overexpression studies the proteins often appear to accumulate within the endoplasmic reticulum, failing to reach the membrane, thus are non-functional (unpublished data). Producing soluble recombinant protein is made complicated by the trimeric and membrane-bound nature of SR-As; however removal of the transmembrane domain does allow for production of soluble protein and this method has been a promising route to study SR-A ligand binding (Sankala et al., 2002).

SR-A sequences have been cloned in several fish species, and these receptors bind to gram-negative and –positive bacteria and modified LDLs (He et al., 2014; Feng et al., 2016; Zhang et al., 2018; Poynter et al., 2017). A study in rainbow trout gut cells found that poly I:C binding was blocked by pre-treatment with SR-A specific ligands and poly I:C blocked the

binding of acetylated LDL, a classic SR-A ligand (Poynter et al., 2015B). While a role for SR-As has been elucidated, it remains unknown which receptors bind dsRNA in fish species.

1.4.2 Non-RLR DExH/D-box helicases

The DExH/D-box helicases are a family of proteins that contain several conserved motifs, one of which being a DExH/D motif, DEIH (DHX) or DEAD (DDX) (Shih and Lee, 2014). While they are called RNA helicases, many also have DNA unwinding functions (Shih and Lee, 2014). Indeed, DExH/D-box helicases play a number of important roles in both cellular homeostasis and antiviral immunity as both sensors of nucleic acids, and as signalling molecules or even transcription factors (Shih and Lee, 2014). Very little is known about these receptors and their role in viral infection in fish.

DHX9 (also known as nuclear DNA helicase II or RNA helicase A) is a nucleotide triphosphate (NTP)-dependent RNA and DNA helicase. DHX9 is primarily a nuclear protein, however it can shuttle to the cytoplasm (Zhang et al., 1999). DHX9 plays an essential role in embryonic development, DNA replication, genomic stability, and in both transcriptional and translational control through miRNA processing and mRNA processing and transport (reviewed in Lee and Pelletier, 2016; Lee et al., 2014; Lee et al., 1998). DHX9 is a dsRNA sensor that interacts with IPS-1 for IFN signalling; knockdown of DHX9 hinders the ability of mammalian cells to produce an IFN response to poly I:C, influenza A or reovirus (Zhang et al., 2011). Minimal research has explored teleost DHX9, with the exception of identification in channel catfish (*Ictalurus punctatus;* Tian et al., 2017) and goldfish (*Carassius auratus;* Silva de Assis et al., 2013).

DDX3 is primarily a RNA helicase, with DNA helicase abilities, and is a gene regulator through transcription, splicing, export, and translational initiation (Ariumi et al., 2014; Lai et al., 2008; Garbelli et al., 2011; Soto-Rifo and Ohlmann, 2013). DDX3 has been found to be a

component of cytoplasmic stress granules, this is hypothesized to be due to its ability to interact with other RNA-binding proteins, as opposed to interacting with stress granule factors; stress granules can provide antiviral protection against some viruses such as influenza A (Soto-Rifo and Ohlamnn, 2013; Raman et al., 2016). DDX3 also plays a role in IFN-β production; there are several potential mechanisms by which this occurs. A direct interaction of DDX3 and TBK1/IKKε has been identified (Soulat et al., 2008; Schröder et al., 2008). After bacterial infection DDX3 was recruited to the IFN-promoter, suggesting it may be directly affecting transcription (Soulat et al., 2008). DDX3 also binds viral RNA and interacts with the adaptor protein IPS-1 to upregulate IFN production (Oshiumi et al., 2010A). New studies are beginning to elucidate a role for these helicases in fish immunity. DDX3 from fathead minnow (*Pimephales promelas*) binds the non-virion proteins of two fish novirhabdoviruses (Biacchesi et al., 2017). DDX3 expression in grouper (*Epinephelus coioides*) cells upregulated IFN and ISGs, and overexpression protected against viral infection (Liu et al., 2017).

Both DHX9 and DDX3 are proteins that are hijacked by several viruses to promote replication; albeit by many different mechanisms. DDX3 is an interacting partner with the hepatitis C virus core protein, this interaction is not required for replication of viral RNA but instead hinders a DDX3-mediated immune response by preventing the interaction between DDX3 and IPS-1 (Angus et al., 2010; Oshiumi et al., 2010B). A similar strategy is also utilized by vaccinia virus and hepatitis B virus; these viruses interfere with the interaction between DDX3 and TBK1/IKKε (Wang and Ryu, 2010; Schröder et al., 2008). DDX3 is required for Japanese encephalitis virus infection; DDX3 directly interacts with viral proteins and viral RNA, positively affecting viral RNA translation (Li et al., 2014). DDX3 interacts with human immunodeficiency virus (HIV)-1 replication in several ways, including facilitating reverse

transcription, mRNA transcription, transport, and packaging of viral RNA (Ariumi et al., 2014). DHX9 promotes infectivity of a broad range of viruses, including HIV-1, influenza A, and myxoma virus (reviewed in Lee and Pelletier, 2016). DHX9 interacts with HIV-1 genomic RNA in a structure-dependent manner to support infectivity (Boeras et al., 2016). DHX9 interacts with viral proteins form influenza A and myxoma virus to promote viral replication (Lin et al., 2011; Rhaman et al., 2013). It is currently unknown whether any aquatic viruses utilize DDX3 or DHX9 to promote their replication or infectivity.

1.5 Aquaculture

Aquaculture is an important industry for its contributions to the economy and to human food consumption. According to the Food and Agriculture Organization of the United Nations (FAO), total aquaculture of finfish in 2014 was 49.8 million tons worth $99.2 billion USD; in 2014, 146.3 million tonnes out of 167.2 million tonnes of aquaculture production was used for human consumption (FAO, 2016). In Canadian aquaculture, trout production accounted for 9607 tonnes of fish worth 14 million CAD in 2016 (Fisheries and Oceans Canada, 2016). A major source of loss for the aquaculture industry is infectious disease, approximately fifty percent of production loss, almost six billion dollars, is attributed to diseases (Assefa and Abunna, 2018). At Canadian latitudes the estimated loss of fish stocks due to disease is 34% (Leong and Bates, 2013). Viral outbreaks in fish aquaculture can cause high levels or mortality, for example viral hemohorrhagic septicemia outbreaks can cause mortality rates up to 90% (Benmansour et al., 1997).

1.6 Thesis objectives

The aim of this thesis was to better understand viral dsRNA and its role in inducing innate antiviral immune responses in fish, with the goal of demonstrating its viability as an antiviral

therapy. The hypothesis for this thesis was that dsRNA will be sensed and activate innate antiviral pathways in fish cells similar to those in mammals; in particular dsRNA with natural sequence variation will be an effective antiviral therapy in fish. The main objectives of this thesis were to:

i) Determine whether *in vitro* transcribed dsRNA is a reasonable surrogate for viral dsRNA with respect to antiviral induction capabilities.

ii) Identify and clone putative surface and cytoplasmic dsRNA receptors in rainbow trout cells. These included class A scavenger receptors and DExH/D-box helicases, DDX3 and DHX9.

iii) Demonstrate *in vitro* transcribed dsRNA's ability to protect fish cells *in vitro* from economically and ecologically relevant fish viruses.

Chapter 2: Understanding viral dsRNA-mediated innate immune responses at the cellular level using a rainbow trout model

Sarah J. Poynter[1] and Stephanie J. DeWitte-Orr[2]

1. University of Waterloo, Department of Biology, Waterloo, Canada
2. Wilfrid Laurier University, Department of Health Sciences, Waterloo, Canada

Frontiers in Immunology, 9, article 829. 2018.

2.1 Overview

Viruses across genome types produce long dsRNA molecules during replication (viral (v-) dsRNA). DsRNA is a potent signaling molecule and inducer of type I interferon (IFN), leading to the production of interferon-stimulated genes (ISGs), and a protective antiviral state within the cell. Research on dsRNA-induced immune responses has relied heavily on a commercially available, and biologically irrelevant dsRNA, polyinosinic:polycytidylic acid (poly I:C). Alternatively, dsRNA can be produced by *in vitro* transcription, (ivt-) dsRNA, with a defined sequence and length. We hypothesized that ivt-dsRNA, containing legitimate viral sequence and length, would be a more appropriate proxy for v-dsRNA, compared to poly I:C. This is the first study to investigate the effects of v-dsRNA on the innate antiviral response and to compare v-dsRNA to ivt-dsRNA induced responses in fish cells, specifically rainbow trout. Previously, class A scavenger receptors (SR-As) were found to be surface receptors for poly I:C in rainbow trout cells. In the current study, ivt-dsRNA binding was blocked by poly I:C and v-dsRNA, as well as SR-A competitive ligands, suggesting all three dsRNA molecules are recognised by SR-As. Downstream innate antiviral effects were determined by measuring IFN and ISG transcript levels using qRT-PCR and antiviral assays. Similar to what has been shown previously with ivt-dsRNA, v-dsRNA was able to induce IFN and ISG transcript production between 3h and 24h, and its effects were length dependent (ie. longer v-dsRNA produced a stronger response). Interestingly, when v-dsRNA and ivt-dsRNA were length and sequence matched both molecules induced statistically similar IFN and ISG transcript levels, which resulted in similar antiviral states against two aquatic viruses. To pursue sequence effects further, three ivt-dsRNA molecules of the same length but different sequences (including host and viral sequences) were tested for their ability to induce IFN/ISG transcripts and an antiviral state. All three induced responses similarly. This study is the first of its kind to look at the effects v-dsRNA in fish cells

as well as to compare ivt-dsRNA to v-dsRNA, and suggests that ivt-dsRNA may be a good surrogate for v-dsRNA in the study of dsRNA-induced responses and potential future antiviral therapies.

2.2 Introduction

Long dsRNA molecules (>30bp) are immunomodulatory nucleic acids that can induce interferon and an antiviral state across vertebrate species (DeWitte-Orr et al., 2010; Secombes and Zou, 2017). DsRNA is an important pathogen-associated molecule pattern (PAMP) produced by viruses; as demonstrated by the sheer number and diversity of receptors in the cytoplasm, endosome, and surface used by host cells to detect dsRNA (Desmet and Ishii, 2012). In vertebrates, dsRNA is a potent inducer of the type I interferon (IFN) response, which produces a broad-spectrum antiviral state. Viral dsRNA is sensed in the cytoplasm by a wide range of receptors, such as Retinoic acid-inducible gene-I (RIG-I), RNA helicase A/DHX9, and Melanoma Differentiation-Associated protein 5 (MDA5), Toll-like receptor 3 (TLR3) in the endosome, and class A scavenger receptors (SR-As) on the cell's surface (Desmet and Ishii, 2012; DeWitte-Orr et al., 2010; Zhang et al., 2011).

When dsRNA is sensed in a cell it triggers a signaling cascade through various adaptor proteins, such as interferon-β promoter stimulator 1 (IPS-1) or TIR-domain-containing adaptor-inducing interferon-β (TRIF, also known as TICAM-1), activating transcription factors, such as interferon-regulator factor (IRF)3/7, and causing the production of IFN. IFNs are secreted from the cell and signal in an autocrine and paracrine fashion via their cognate receptor, interferon-α/β receptor (IFNAR), to initiate the Janus kinase (JAK) and Signal Transducer and Activator of Transcription (STAT) signaling pathway resulting in the expression of a group of genes containing an interferon-sensitive response element (ISRE) known cumulatively as IFN-stimulated genes (ISGs; Ivashkiv and Donlin, 2014; Poynter and DeWitte-Orr, 2016). In rainbow trout (*Oncorhynchus mykiss)*, there is an incredibly large repertoire of type I IFNs, as many as 22 members have been identified. Type I IFNs in fish have an intricate naming system, teleost type I IFNs are subdivided into group 1 or group 2 based on the number of cysteine residues and

further into subgroups (a-f) based on phylogenetic analysis (Zou et al., 2014). These naming systems have no relation to the alpha or beta system used in mammals (Zou et al., 2014). IFN1 is a type I IFN, belonging to group I and subgroup a (Zou et al., 2014) and is used in the present study as a representative transcript indicative of type I IFN expression.

IFNs in fish stimulate expression of a panel of ISGs including molecules from the IFN signaling pathway such as IRF3/7 and antiviral effectors that limit viral infection, including myxovirus resistance gene -1 (Mx1), viral hemorrhagic septicemia virus (VHSV)-induced gene (vig)-1, vig-3, and vig-4 (Holland et al., 2008; Poynter and DeWitte-Orr, 2016, O'Farrell et al., 2002). Vig-4 is a VHSV – induced gene; the deduced protein contains tetratricopeptide repeat motifs and shows similarities to the ISG56/IFIT1 family of ISGs (O'Farrell et al., 2002; Robertsen et al., 2008). The present study chose vig-4 as a representative transcript indicative of ISG expression because it has been used as a representative ISG in previous studies (Saito et al., 2007; Scagnolari et al., 2012; Virtue et al., 2011; Goubau et al., 2014) and is up-regulated more strongly than other ISGs, such as Mx1 (Poynter and DeWitte-Orr, 2015). The dsRNA-induced accumulation of ISG proteins produces a protective antiviral state in rainbow trout cells against a variety of viruses (Poynter and DeWitte-Orr, 2015; Saint-Jean and Pérez-Prieto, 2006).

DsRNA sensed by a host cell in a natural system would be produced by viral infection, described here as v-dsRNA. As viruses replicate, dsRNA is produced as a by-product of replication, a genomic fragment, or transcribed from DNA by host proteins (Ablasser et al., 2009, Weber et al., 2006; Majde et al., 1991; Loo et al., 2008). The potent immune stimulatory nature of dsRNA makes it a candidate molecule for antiviral therapies and vaccine adjuvants, as well as for use in type I IFN studies. Unfortunately, v-dsRNA is difficult to collect from viruses in quantities useful for experimental scenarios and likely impossible for industrial applications. In

the late sixties a synthetic form of dsRNA, polyinosinic:polycytidylic acid (poly I:C), was identified as a potent IFN-inducer and was considered a "viral mimic" (DeWitte-Orr and Mossman, 2010; Richmond and Hamilton, 1969; Schafer and Lockart, 1970). Poly I:C is clearly different from dsRNA produced by a virus; poly I:C lacks sequence variation and natural structures, contains a range of lengths and one strand contains exclusively a modified inosine nucleotide (Löseke et al., 2006). Owing to these differences, poly I:C is not sensed the same nor does it induce responses exactly the same as *in vitro* transcribed (ivt-) dsRNA (Kato et al., 2006; Löseke et al., 2006, Jiang et al., 2011; DeWitte-Orr et al., 2009). In plasmacytoid dendritic cells only ivt-dsRNA was able to stimulate IFN-α production, poly I:C did not (Löseke et al., 2006). In rainbow trout cells, ivt-dsRNA induced a faster, stronger IFN1 and IFN2 response compared to poly I:C even when poly I:C was of much longer lengths (Poynter and DeWitte-Orr, 2015). Additionally, in mice, poly I:C is recognized by MDA5 whereas ivt-dsRNA and v-dsRNA activated RIG-I (Kato et al., 2006; Kato et al., 2008). For TLR3, human TLR3 but not teleost TLR3 has a much higher affinity for poly I:C than ivt-dsRNA (Kato et al., 2006; Matsuo et al., 2008).

The current state of research regarding responses to dsRNA largely relies on the use of poly I:C; however, studies of individual receptors are shifting towards ivt-dsRNA, likely for the ease of controlling length (Kato et al., 2006; DeWitte-Orr et al., 2009; Peisley et al., 2012). Length has been shown to influence the magnitude of immune response in cells and dsRNA receptor types show length requirements and specificities (DeWitte-Orr et al., 2009; Kato et al., 2006; Matsuo et al., 2008; Poynter and DeWitte-Orr, 2015). For example, longer dsRNA molecules have been shown to inducer a strong IFN response (DeWitte-Orr et al., 2009) and RIG-I has been shown to sense dsRNA molecules under 1000 bp in length, while MDA5 senses

lengths greater than 1000 bp (Peisley et al., 2012; Kato et al., 2008). The effect of dsRNA sequence on IFN-induction is also poorly studied; there were no detectable sequence motifs for MDA5 activation identified from vaccinia virus-derived dsRNA (Pichlmair et al., 2009). One example of sequence-dependence is the cytoplasmic dsRNA receptor oligoadenylate synthetase (OAS) that requires a four-base pair specific motif for binding (Kodym et al., 2009). Few studies have looked at the antiviral response induced by v-dsRNA, and any studies that do exist have all used mammalian models. Specifically, v-dsRNA derived from encephalomyocarditis virus, vaccinia virus and reovirus induced potent IFN responses in vero, HeLa and murine embryonic fibroblasts respectively (Pichlmair et al., 2009; Kato et al., 2008). ivt-dsRNA is an alternative source of synthetic dsRNA that retains some features of v-dsRNA and can be produced on a larger scale. To our knowledge there have been no studies directly comparing a v-dsRNA and an ivt-dsRNA molecule of matched length and sequence, therefore it is unknown if ivt-dsRNA induces a comparable immune response to v-dsRNA.

Rainbow trout were used in this study as a model fish species for their importance in aquaculture and the existing knowledge base of the rainbow trout type I IFN and antiviral response (Poynter and DeWitte-Orr, 2015; Chang et al., 2009). In rainbow trout cell lines ivt-dsRNA or poly I:C induces type I IFN and an antiviral state and similarly whole rainbow trout pretreated with poly I:C also showed decrease susceptibility to a fish virus (Poynter and DeWitte-Orr, 2015; Kim et al., 2009). Three aquatic viruses were used in this study: chum salmon reovirus (CSV), which has a segmented dsRNA genome that consists of 11 segments between 3947bp and 783bp (Lannan et al., 1981), infectious pancreatic necrosis virus (IPNV), which is a non-enveloped *Aquabirnavirus* with a bisegmented dsRNA genome (Ørpetveit et al., 2012) and viral hemhorrhagic septicemia virus (VHSV), which is an enveloped *Rhabodovirus* with a negative-

sense ssRNA genome (Purcell et al., 2012). All three viruses readily infect rainbow trout cells, including RTG-2, a rainbow trout gonadal cell line (Kelly et al., 1978; Lorenzen et al., 1999). Mammalian reoviruses have previously been used as a source of dsRNA of different lengths and total genomic dsRNA has been used as an immune stimulus (Kato et al., 2008; Alexopoulou et al., 2001; Goubau et al., 2014). VHSV and IPNV both represent important disease in the fish aquaculture industry and ecology as they have wide host ranges and can cause large die-offs of fish (Ørpetveit et al., 2012; Mortensen et al., 1999; Purcell et al., 2012).

This study compares IFN-mediated responses induced by three forms of dsRNA: v-dsRNA, ivt-dsRNA, and poly I:C. The dsRNA is this study was delivered extracellularly. In a viral infection, the dsRNA would be intracellular during its production and released to the extracellular space in the case of cell lysis where it could be recognized by neighbouring cells. In the case of a dsRNA-based therapy the dsRNA would be delivered to the cell surface and not to the cytoplasm. Because the dsRNA was delivered extracellularly, the surface receptor for these dsRNA molecules was investigated. The ability of v-dsRNA from aquatic viruses to induce IFNs, ISGs and an antiviral response was quantified. Length and sequence matched v-dsRNA and ivt-dsRNA were compared with poly I:C for their ability to induce IFNs, ISGs, and mount an antiviral state against IPNV and VHSV. The results from this study provides valuable insight with regards to how fish cells respond to viral dsRNA as opposed to poly I:C, with applications for novel dsRNA-based therapies.

2.3 Materials and methods

2.3.1 Cell culture

Two rainbow trout cell lines were used in the present study to measure dsRNA-mediated responses: RTG-2, derived from rainbow trout gonad (Wolf and Quimby, 1962) and RTgutGC, derived from rainbow trout intestine (Kawano et al., 2011). *Epithelioma Papulosum*

Cyprini (EPC) and Chinook salmon embryonic cell line (CHSE-214) were used for viral propagation. All cell lines used in this study were obtained from N. Bols (University of Waterloo, Waterloo, ON). All cell lines were grown in 75 cm^2 plastic tissue culture flasks (BD Falcon, Bedford, MA, USA) at room temperature in Leibovitz's L-15 media (HyClone, Logan, UT, USA) supplemented with 10% v/v fetal bovine serum (FBS; Fisher Scientific, Fair Lawn, NJ, USA) and 1% v/v penicillin/streptomycin (P/S) (10 mg/mL streptomycin and 10000U/mL penicillin; Fisher Scientific). All dsRNA treatments were delivered extracellularly by addition of dsRNA to cell culture media.

2.3.2 Virus propagation

Viral hemorrhagic septicemia virus (VHSV)-IVb (strain U13653) was propagated on monolayers of EPC (Fijan et al., 1983) cells, Chum salmon reovirus and infectious pancreatic necrosis virus (IPNV) were propagated on CHSE-214; all viruses were propagated at at 17°C (Nims et al., 1970). Virus containing media (L-15 with 2% v/v FBS (Fisher Scientific)) was collected 4–7 days post-infection, filtered through a 0.45μm filter (Nalgene, Rochester NY, USA) and kept frozen at −80 °C. The 50% tissue culture infective dose ($TCID_{50}$)/mL values were estimated according to the Reed and Muench method (Reed and Muench, 1988). The origin of the viruses used in this study has been described previously (Pham et al., 2014).

2.3.3 Poly I:C

High-molecular weight (HMW) poly I:C (InvivoGen, San Diego, CA, USA) stocks were prepared at 1mg/mL and low-molecular weight (LMW) poly I:C (InvivoGen) stocks were prepared at 10mg/mL, both were diluted in phosphate buffered saline (PBS) (HyClone) and aliquots were stored at −20°C. Before use aliquots were heated to 55°C for 15 min and then allowed to cool to room temperature for 20 min.

2.3.4 Synthesis of in vitro molecules

In vitro transcribed dsRNA molecules were produced as previously described using the MegaScript RNAi kit (Fisher Scientific; Poynter and DeWitte-Orr, 2015). All primers used for synthesizing dsRNA, Table 1, had the T7 promoter sequence added to the 5' end, TAATACGACTCACTATAGGGAG. The following molecules were prepared: the full-length Chum salmon reovirus segment 6 (2052 bp); a 300bp internal segment of Chum salmon reovirus segment 1 (CSVseg1); a 200bp segment of rainbow trout GAPDH, rainbow trout Mx3, and an internal segment of the VHSV G gene (v200; 3851bp-4048bp) that has been previously described (Poynter and DeWitte-Orr, 2015). Where needed, nucleotide distribution was calculated using Genomatix: DNA sequence toolbox (http://www.genomatix.de/cgi-bin/tools).

2.3.5 Extraction of v-dsRNA and isolation of segments

To extract the CSV viral genome, CSV was propagated as described above; after complete destruction of the monolayer the viral-containing media was collected and cell debris was pelleted by centrifugation at 3000 x g for 5 min. The supernatant was mixed with poly ethylene glycol BioUltra 8000 to a final concentration of 10% w/v (Sigma-Aldrich, St. Louis, MO, USA; catalogue number: 89510) and sodium chloride to a final concentration of 0.6% w/v and mixed on a Corning LSE Digital Microplate Shaker at 1400 RPM 4^{o}C overnight (Corning Tewksbury, MA, USA; Dopazo et al., 1996). The solution was then centrifuged at 17000 x g in a Sorvall Legend Micro 17 microcentrifuge for 20 min (Fisher Scientific). The resulting pellet was resuspended in 100µL PBS overnight at 4^{o}C and the RNA was extracted using TRIzol reagent (Invitrogen, Carlsbad, CA, USA) as per manufacturers' instructions. To isolate segments of the genome, total genomic CSV dsRNA was run on a 1% agarose TAE gel containing GelGreen (1:10000 dilution; Biotium Inc, Fremont, CA, USA).

Table 2.1. Primers used for *in vitro* transcription of dsRNA and qRT-PCR. Forward (F) and reverse (R) primer sequences (5'-3'), length of product (bp), annealing temperature (Ta), and accession number of source sequence are provided. For dsRNA the length of the final dsRNA product is provided.

Target	5'-3'	Length (bp)	Ta	Accession number
dsRNA				
GAPDH (seq1)	F - TGGCATCTCCTTCAACGACAA R - GCTGGGGGTACTATGGGTGT	200	55	NM_001124246.1
Mx3 (seq2)	F - AGGACTCGGCAGAAAGGATA R - TTCTCCCTCGATCCTCTGGT	200	55	U47946.1
V200 (seq3)	F - TCAGATGAGGGGAGCCACA R - CGCATGATCTGGCCATCAA	200	52	Poynter and DeWitte-Orr, 2015
CSV seg1	F - TATGGTCCCCACGTCCTGAT R - GCCTCCTACGTCACTCATCG	300	50	AF418294.1
CSV seg6	F - TATCTCCTTGCGCCCTTCTC R - AATAGTCATCCCCCTCCGGC	2052	60	AF418299.1
qRT-PCR				
IFN1	F - AAAACTGTTTGATGGGAATATGAAA R - CGTTTCAGTCTCCTCTCAGGTT	141	55	Chaves-Pozo et al., 2010
vig-4	F - GGGCTATGCCATTGTCCTGT R - AAGCTTCAGGGCTAGGAGGA	151	55	Poynter and DeWitte-Orr, 2015
β-Actin	F - GTCACCAACTGGGACGACAT R - GTACATGGCAGGGGTGTTGA	174	55	Poynter et al., 2015

The band of interest was cut out and purified using the QIAquick gel extraction kit (Qiagen, Hilden, Germany) and quantified using a NanoDrop Lite Spectrophotometer (Thermo Fisher Scientific). The v-dsRNA preparation was validated as pure dsRNA by two methods: acridine orange stained gel to confirm only red stained nucleic acids were visible, and differential nuclease degradation using RNase A and RNaseIII to ensure degradation by RNaseIII alone. These methods for visualizing dsRNA have been described previously (Poynter and DeWitte-Orr, 2017). Resulting products (20 ng) were re-quantified by gel densitometry to confirm the

NanoDrop readings. The matched ivt-dsRNA molecule was also gel purified and quantified as above for consistency.

2.3.6 Labelling of dsRNA

The CSV seg1 ivt-dsRNA was labelled using the Ulysis Alexa Fluor 546 Nucleic Acid Labeling Kit (Fisher Scientific) as previously described (Poynter and DeWitte-Orr, 2015). Unbound fluorophores were removed using a Bio-Rad p30 spin column (Bio-Rad, Hercules, CA, USA).

2.3.7 Competitive binding assay

RTgutGC cells were seeded at a density of $1x10^5$ cells/well on glass coverslips in a 12-well tissue culture plate. After attaching overnight cells were pretreated with 200µL of L-15 containing LMW, HMW, poly I, or poly C at 100 µg/mL, total native dsRNA at 40 µg/mL, or control L-15 alone for 30 min. After this incubation 1.25µg (5µg/mL) of labelled CSVseg1 dsRNA was added to the well with 50µg/mL of DEAE-dextran. DEAE-dextran is used in this context as a method of ensuring dsRNA reaches the cells in quantities sufficient for detection by fluorescence microscopy (DeWitte-Orr et al., 2010). Six hours post treatment cells were washed 3x with PBS, fixed for 10 min with 10% neutral buffered formalin (Fisher Scientific), nuclei were counterstained with 10 µg/mL 4',6-diamidino-2-phenylindole (DAPI; Fisher Scientific) and mounted on coverslips with SlowFade Gold mounting medium (Fisher Scientific) for visualization. Images were captured using an inverted fluorescence microscope (Nikon Eclipse TiE with Qi1 camera) and analyzed using Nikon NIS-elements. A blinded third-party researcher performed the fluorescence quantification measurements. Three images were captured of each treatment for each independent replicate. Alexa Fluor 546 fluorescence intensity was measured by automatic selection of the area surrounding DAPI stained nuclei, total number of cells within

the image were counted and the intensity/cell was calculated. Intensity is presented as percentage of the *in vitro* only control with no pretreatment.

2.3.8 Cell protection assays

RTG-2 cells were seeded at $1x10^4$ cells/well in 96-well plates and allowed to attach overnight in regular growth media. For each condition there were triplicate wells, and for each assay there was an untreated/uninfected control and an untreated/infected control. Cells were treated with the indicated concentration of dsRNA for 3h or 6h at 20°C in 50µL of media containing L15, 1% P/S, and 2% FBS. When dsRNA concentration was 0.01nM. 6h was selected for treatment to ensure a productive antiviral state prior to infection; 3h was found to be insufficient (data not shown). After dsRNA pretreatment, the virus was added directly to the media to produce the necessary MOI (10 for VHSV, 0.2 or 0.02 for IPNV). Cells were incubated at 17°C for 4-7days until desired accumulation of cytopathic effect (CPE) occurred. Cells were rinsed 2X with PBS and a 5% v/v alamarBlue solution in PBS was added (Invitrogen). Cells were incubated at room temperature for 1h in the dark and fluorescence was measured using a Synergy HT plate reader (BioTek, Winooski, VT, USA). Data are presented as percentage of control, uninfected cells.

2.3.9 RNA extraction, cDNA synthesis, and qRT-PCR

RTG-2 cells were plated at $5x10^5$ cells/well in a 6-well plate and allowed to attach overnight. Media was removed and cells were treated with dsRNA at the noted concentration in full-growth media, or with media only. After the indicated incubation time media was removed and RNA extracted with TRIzol as per manufacturers' instructions (Thermo Fisher Scientific). Possible contaminating DNA was removed using the TURBO DNA-free kit (Fisher Scientific). cDNA was synthesized using iSCRIPT (Bio-Rad) and 1µg of RNA. qRT-PCR has been previously described for the primers used in this study (Poynter and DeWitte-Orr, 2015). A no-

reverse transcriptase (NRT) control was used to identify genomic contamination, a peak earlier than 35 cycles in the NRT control was considered excessive DNA contamination, no samples showed a peak earlier than this threshold. Melting curve analysis was completed (65^{o}C to 95^{o}C with a read every 5s) to determine primer specificity, only single peaks were produced. In addition to the NRT control, primers were designed to span introns for both β-actin and IFN1; as such genomic contamination would produce a much larger product, which would be evident in the melting curve analysis. This technique could not be performed for vig-4, as it is predicted to be intron-less. Additionally, there are two predicted copies of vig-4 in the rainbow trout genome, the primers used in this study would amplify both variants; however, all sequencing performed identified only the published vig-4 sequence (NM_001124333.1).

2.3.10 Statistical analysis

All data presented was derived from at least three independent experiments. Data were graphed and statistically analyzed using GraphPad Prism version 7.00 for Windows, GraphPad Software, La Jolla California USA, www.graphpad.com. Statistical analyses were completed using a one- or two-way ANOVA with Tukey multiple comparison test, alpha = 0.05, P value <0.05 considered significant; qRT-PCR data was log2 transformed prior to analysis.

2.4 Results

2.4.1 dsRNA from different sources bind to the same surface receptor

RTgutGC cells, previously shown to bind poly I:C by SR-As (Poynter et al., 2015), were treated with fluorescently labelled ivt-dsRNA and punctate cell-associated binding was observed, (Fig. 2.1A). Cells were then pretreated with an excess of poly I:C, either high- (HMW) or low-molecular weight (LMW), total CSV v-dsRNA, poly I or poly C (Fig. 2.1A,B). Both sizes of poly I:C and the total v-dsRNA significantly blocked binding of the labeled ivt-dsRNA (Fig. 2.1B). Poly I is a competitive ligand for SRA binding whereas poly C is a molecule of

similar chemical structure that is non-competitive for SRAs. Poly I significantly blocked ivt-dsRNA binding while poly C did not (Fig. 2.1B).

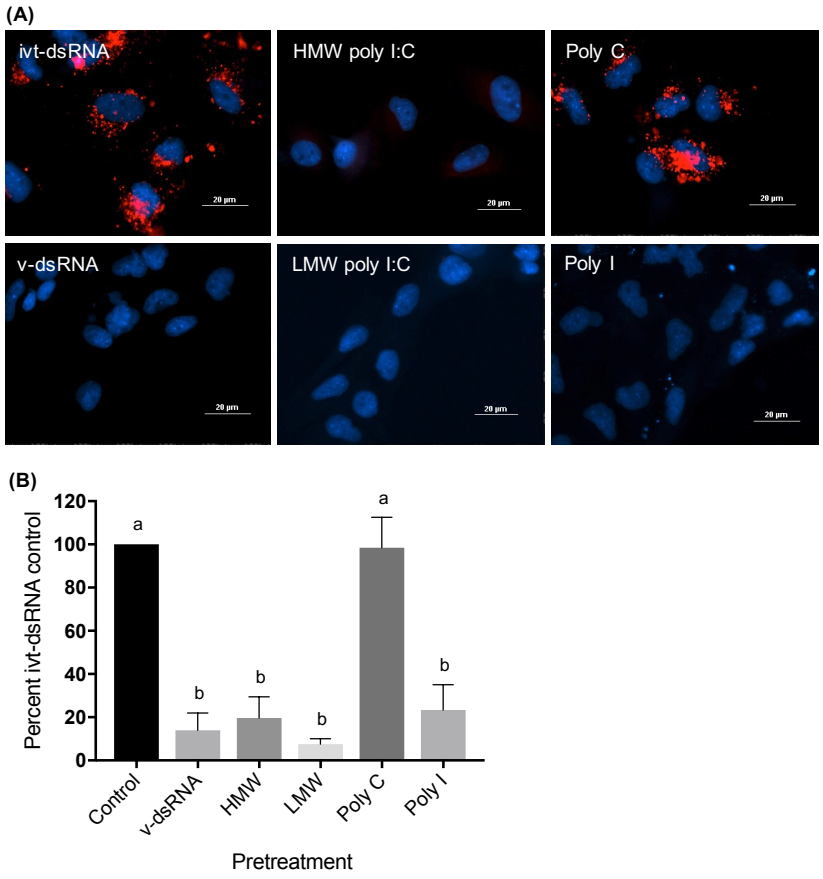

Figure 2.1. *In vitro* transcribed dsRNA, viral dsRNA, and poly I:C bind the same class A scavenger receptor in RTgutGC cells.
RTgutGC cells were pretreated for 3h with high-molecular weight poly I:C (HMW), low-molecular weight poly I:C (LMW), poly I, or poly C at 100µg/mL, or total chum salmon reovirus genome (v-dsRNA) at 40µg/mL, or control media. Cells then received 1.25µg (5µg/mL) of Alexa Fluor 546 labelled CSVseg1 dsRNA (ivt-dsRNA) with 50µg/mL of DEAE-dextran. 6h post treatment cells were formalin fixed and nuclei were counterstained with DAPI; slides were visualized using an inverted fluorescence microscope (Nikon Eclipse TiE with Qi1 camera). (A) Representative images of cells with or without pretreatment, dsRNA = red, nuclei = blue. (B) Fluorescence intensity per cell was quantified using Nikon- NIS-elements software and is presented as percent of the ivt-dsRNA only control, no pretreatment. Data represents three independent replicates and were analyzed statistically by one-way ANOVA, alpha = 0.05; a P value <0.05 considered significant.

2.4.2 v-dsRNA elicits a length-dependent, protective type I IFN response in RTG-2 cells

RTG-2 cells were treated with 10 ng/mL of total CSV v-dsRNA and significant induction of an IFN (IFN1) and an ISG (vig-4) were observed at the transcript level using qRT-PCR at 24h post treatment (Fig. 2.2A). IFN1 transcript production peaked at 3h and was no longer measurable by 24h and vig-4 production peaked at 24h (Fig. 2.2A). Previously concentrations lower than 10ng/mL of ivt-dsRNA have been shown to induce IFN and ISG transcripts in RTG-2 cells (Poynter and DeWitte-Orr, 2015). To test the ability of v-dsRNA to establish a functional antiviral state, RTG-2 cells were pretreated for 3h with 10 ng/mL of total v-dsRNA and then infected with VHSV (MOI: 10) or IPNV (MOI: 0.2; Fig. 2.2B). There was significant protection observed against both viruses when cell viability was measured using alamarBlue.

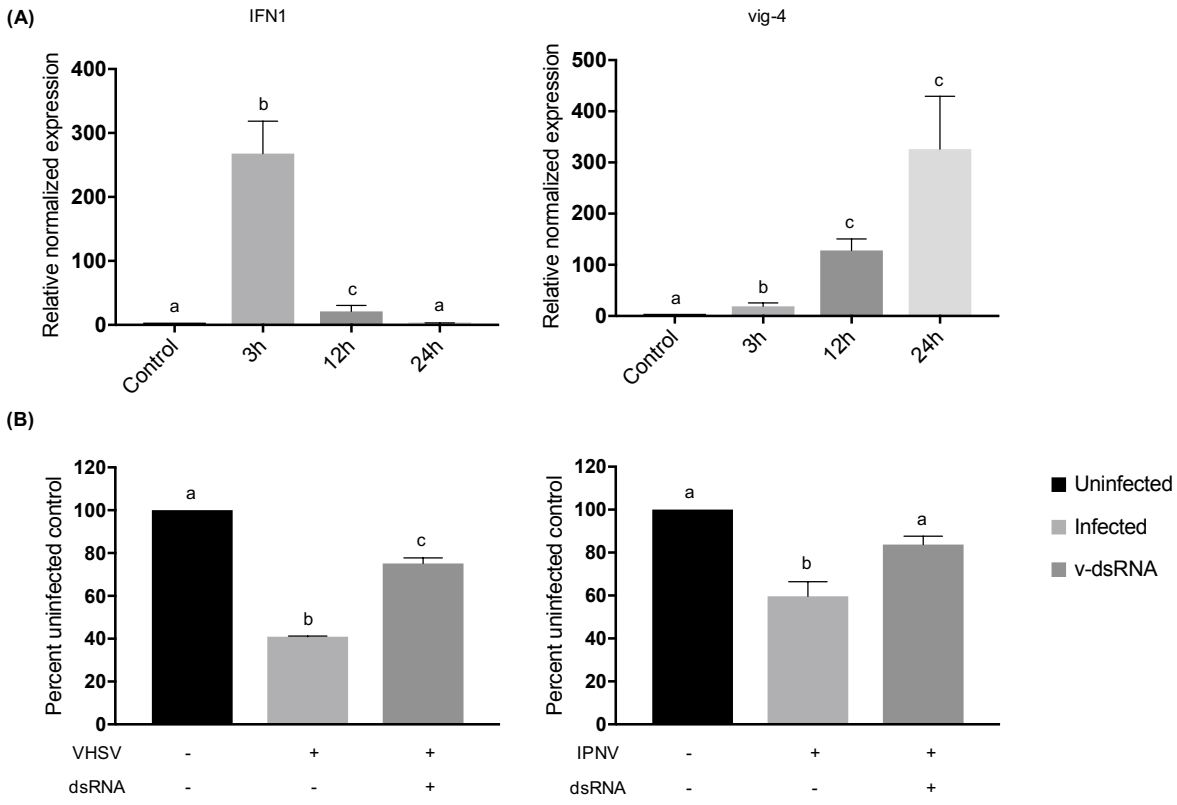

Figure 2.2. Viral dsRNA induces IFN1 and vig-4 transcripts over time and induces a protective antiviral state against viral hemorrhagic septicemia virus (VHSV) and infectious pancreatic necrosis virus (IPNV) in RTG-2 cells.
(A) RTG-2 cells were stimulated with 10ng/mL of total chum salmon reovirus dsRNA (v-dsRNA); IFN1 and vig-4 transcripts were measured by qRT-PCR at 3h, 12h, and 24h, normalized to β-actin, and presented as values relative to an unstimulated control. (B) RTG-2 cells were pretreated with 10ng/mL v-dsRNA for 3h and then infected with VHSV at a multiplicity of infection (MOI) of 10 or IPNV at a MOI of 0.2. After 4-7 days a fluorescent indicator dye, alamarBlue, was used to measure cell viability and data are presented as the percentage of an untreated, uninfected control. Data represents three independent replicates and were analyzed statistically by one-way ANOVA, alpha = 0.05; a P value <0.05 considered significant.

To look at the effects of v-dsRNA length on the immune response, portions of the CSV genome grouped as large, medium, and small segments were isolated and RTG-2 cells were treated with 0.05nM of each molecule for 3h (Fig. 2.3A,B). The concentration used was chosen because in previous studies this concentration demonstrated length effect differences between ivt-dsRNA molecules. Additionally, molar amounts were used to measure the effect of length as

opposed to number of molecules (Poynter and DeWitte-Orr, 2015). It should be noted that these v-dsRNA molecules are different sequences as well as lengths. There was a length-dependent response seen in the RTG-2 production of IFN1 and vig-4 transcripts, with the long segments inducing significantly more IFN1 and vig-4 transcripts than the short segments. For both IFN1 and vig-4 the medium segment fell in the middle range of long and short, and there was a significant difference between long and medium-induced vig-4 production. A corresponding antiviral assay against VHSV and IPNV was completed similarly to the total v-dsRNA assay described above (Fig. 2.3C). While both long and short v-dsRNA protected cells significantly from viral infection, there were no significant differences between the two lengths.

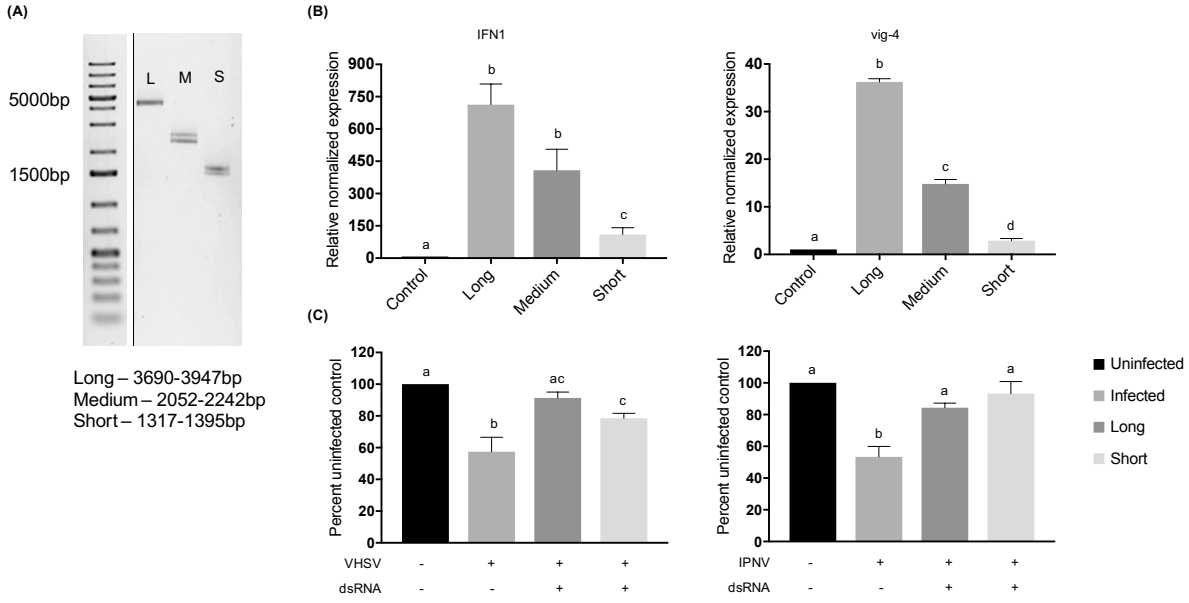

Figure 2.3. Long v-dsRNA segments induces higher levels of IFN1 and vig-4 transcripts but similar antiviral responses against viral hemorrhagic septicemia virus (VHSV) or infectious pancreatic necrosis virus (IPNV) in RTG-2 cells.
Segments of the chum salmon reovirus genome were isolated based on length, segments fell into long (3690-3947bp), medium (2052-2242), or short (1317-1395) segment groups. (A) 20ng of the isolated segments were run on a 1% agarose gel stained with ethidium bromide for visualization. (B) RTG-2 cells were treated with 0.05nM dsRNA for 3h and IFN1 and vig-4 transcripts were measured by qRT-PCR, normalized to β-actin, and presented as values relative to an unstimulated control. (C) RTG-2 cells were pretreated with 0.05nM dsRNA for 3h and then infected with VHSV at a multiplicity of infection (MOI) of 10 or IPNV at a MOI of 0.2. After 4-7 days a fluorescent indicator dye, alamarBlue, was used to measure cell viability and data are presented as the percentage of an untreated, uninfected control. Data represents at least 3 independent replicates and were analyzed statistically by one-way ANOVA, alpha = 0.05; a P value <0.05 considered significant.

2.4.3 Length- and sequence-matched v-dsRNA and ivt-dsRNA induce IFNs and an antiviral state similarly

To compare the IFN response induced by v-dsRNA and ivt-dsRNA directly, v-dsRNA from the CSV genome (segment 6, 2052bp) was isolated and a matching ivt-dsRNA molecule of the same length and sequence was synthesized to match (Fig. 2.4A). Cells were stimulated with 0.01nM of v-dsRNA or ivt-dsRNA respectively. This is a lower molar amount of dsRNA than other assays in this study, due to the difficulty of isolating usable quantities of a single v-dsRNA segment. There was significant induction of both IFN1 and vig-4 transcripts by both

molecules and no significant difference was observed between the ivt-dsRNA and v-dsRNA molecules (Fig. 2.4B). This trend continued with the antiviral assays, where both ivt-dsRNA and v-dsRNA protected cells against IPNV and VHSV-induced cell death, but there were no significant differences in the protection between the two (Fig. 2.4C).

For comparison purposes, a 0.01nM HMW poly I:C (average length 3000bp) control was included for both qRT-PCR and antiviral assays. There was significantly less induction of IFN1 and vig-4 transcript production from the HMW poly I:C at the 3h time point (Figure 2.4B). With VHSV infection all three dsRNA molecules protected similarly; however, with IPNV at an MOI of 0.2 ivt-dsRNA and v-dsRNA provided complete protection (with viability levels similar to uninfected control cells) but poly I:C did not. By an MOI of 0.02 all three dsRNA molecules provided the same amount of protection (Fig. 2.4C).

2.4.4 Molecules of the same length but different sequence had similar effects

To test the effect of sequence on the magnitude of the immune response by RTG-2 cells three length-matched ivt-dsRNAs were made with different sequences, including different source material (2 rainbow trout genes, GAPDH and Mx3, and 1 viral gene, the VHSV G gene), and different nucleotide composition (Fig. 2.5A). IFN1 and vig-4 transcripts were significantly induced following treatment with 0.05nM dsRNA for three hours but no significant differences between the three sequences were detected (Fig. 2.5B). This matched the antiviral assays for both VHSV and IPNV, where protection was seen but no significant differences between molecules (Fig. 2.5C).

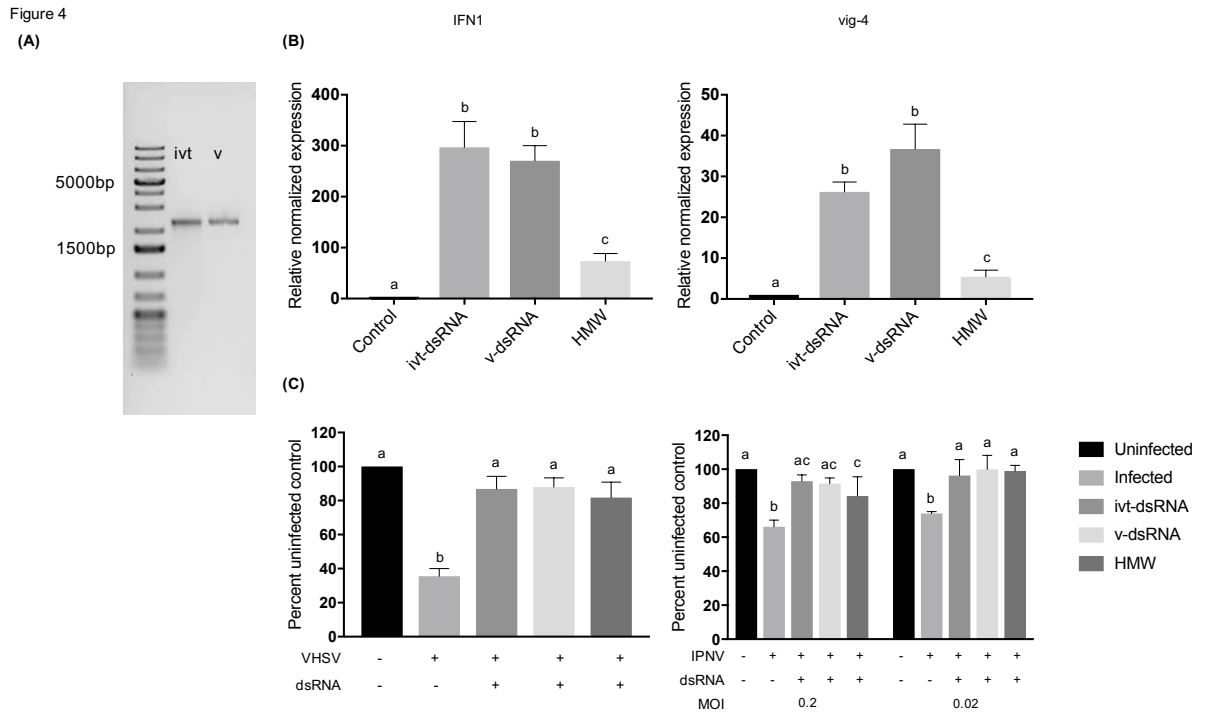

Figure 2.4. Length and sequence matched ivt- and v-dsRNA induced similar levels of IFN1 and vig-4 transcripts and similar antiviral state against VHSV and IPNV infections in RTG-2 cells.

A segment of the chum salmon reovirus genome (segment 6, 2052bp) was isolated (v-dsRNA) and a length and sequence matched dsRNA molecule was transcribed *in vitro* (ivt-dsRNA). High-molecular weight poly I:C (HMW) was included as a treatment control. (A) 20ng of the isolated segments were run on a 1% agarose gel stained with ethidium bromide for visualization. (B) RTG-2 cells were treated with 0.01nM dsRNA for 3h and IFN1 and vig-4 transcripts were measured by qRT-PCR, normalized to β-actin, and presented as values relative to an unstimulated control. (C) RTG-2 cells were pretreated with 0.01nM dsRNA for 6h and then infected with VHSV at a multiplicity of infection (MOI) of 10 or IPNV at a MOI of 0.2 or 0.02. After 4-7 days a fluorescent indicator dye, alamarBlue, was used to measure cell viability and data are presented as the percentage of an untreated, uninfected control. Data represents least 3 independent replicates and were analyzed statistically by one-way ANOVA, panel B, or two-way ANOVA, panel C, alpha = 0.05; a P value <0.05 considered significant.

(A)

Nucleotide distribution				
	%G	%U	%C	%A
Seq1	37	51	65	47
Seq2	55	42	42	61
Seq3	43	46	64	45

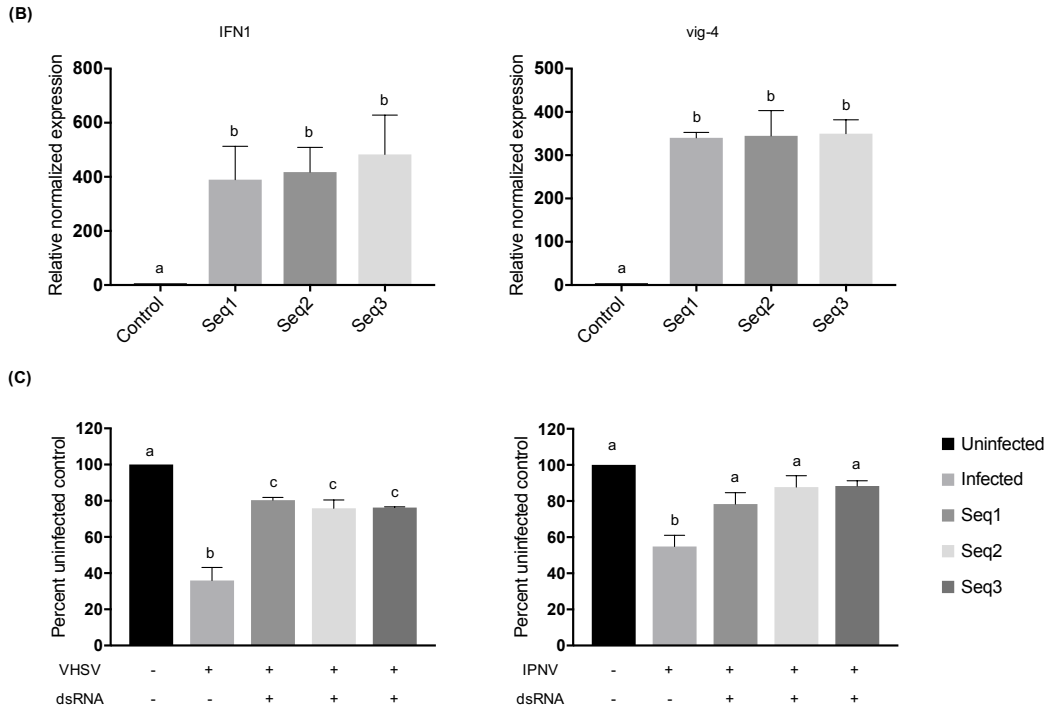

Figure 2.5. ivt-dsRNA of the same length and different sequence induced similar levels of IFN1 and vig-4 transcripts and protective antiviral states against VHSV and IPNV in RTG-2 cells.

Three *in vitro* transcribed dsRNA molecules of the same length but different source sequences were used to test the effects of sequence on innate immune response. (A) Genomatix was used to calculate the nucleotide distribution within the three sequences and the percentage of each nucleotide is shown. (B) RTG-2 cells were treated with 0.05nM dsRNA for 6h and IFN1 and vig-4 transcripts were measured by qRT-PCR, normalized to β-actin, and presented as values relative to an unstimulated control. (C) RTG-2 cells were pretreated with 0.05nM dsRNA for 3h and then infected with VHSV at a multiplicity of infection (MOI) of 10 or IPNV at a MOI of 0.2. After 4-7 days a fluorescent indicator dye, alamarBlue, was used to measure cell viability and data are presented as the percentage of an untreated, uninfected control. Data represents 3 independent replicates and were analyzed statistically by one-way ANOVA, alpha = 0.05; a P value <0.05 considered significant.

2.5 Discussion

While poly I:C is an attractive dsRNA to use in studies of the dsRNA-mediated immune response, it is not biologically relevant and as such is either too potent, such as in mammalian systems, (Carter and De Clercq, 1974) or not potent enough, as has been noted in certain aquatic species, (Strandskog et al., 2011) when modulating the innate immune response. We

hypothesized that ivt-dsRNA would be a better molecule for modulating innate antiviral immune responses, as it has natural sequence variation and defined length. The goal of the present study was to test whether ivt-dsRNA was a comparable surrogate for v-dsRNA and to better understand v-dsRNA and ivt-dsRNA-mediated innate antiviral immune responses using a rainbow trout cell model. This is the first study to investigate v-dsRNA and its effects in an aquatic vertebrate system. The use of the two different cell lines helped provide answers to two separate questions, whether the molecules are bound by a common scavenger receptor and whether the molecules were inducing similar antiviral responses. RTgutGC was used as this cell line has been shown previously to express functional SR-As, surface receptors for dsRNA (Poynter et al., 2015). Additionally, RTG-2 has previously been shown to respond to low concentrations of dsRNA and is permissive to infection by both aquatic viruses used to test the establishment of an antiviral state (Poynter and DeWitte-Orr, 2015; Saint-Jean and Pérez-Prieto., 2006; Kelly et al., 1978).

The dsRNA in this study was delivered extracellularly; they were added directly to the media instead of being transfected into the cell. In a viral infection, dsRNA would be intracellular during its production and released to the extracellular space during a lytic infection where it could be recognized by neighbouring cells. In the case of a dsRNA-based therapy, the dsRNA would be delivered to the cell surface and not to the cytoplasm. If dsRNA-based therapies are viable they need to be able to bind to the cell's surface, thus the mechanism of recognition of ivt-dsRNA compared with v-dsRNA at the cell surface is important to discern. Poly I:C (both LMW and HMW) and v-dsRNA effectively blocked the binding of labelled ivt-dsRNA molecules in RTG-2 cells, suggesting that all three dsRNA molecules do indeed bind SR-As on the cell surface. This is consistent with previous studies in mammals that have shown ivt-dsRNA, poly I:C, and viral dsRNA are bound by SR-As (Limmon et al., 2008; DeWitte-Orr

et al., 2010; Mian et al., 2013; Dansako et al., 2013; Poynter et al., 2017). A study in mouse splenocytes found HMW poly I:C but not LMW was bound by SR-As, and therefore both LMW and HMW poly I:C were tested in the present study for their ability to block binding (Mian et al., 2013). In the present study no differences were observed between LMW and HMW poly I:C's ability to block ivt-dsRNA binding, suggesting SR-A binding capabilities to dsRNA in mice differ from rainbow trout.

Next, the ability of v-dsRNA to induce the IFN pathway and antiviral response was tested. v-dsRNA induced IFN1 and vig-4 transcripts with similar kinetics to what was previously reported with ivt-dsRNA (Poynter et al., 2015) in that IFN1 transcript peaked at 3h and the ISG vig-4 accumulated over time. This antiviral response effectively reduced virus-induced cell death for two important fish pathogens, VHSV-IVb and IPNV. This is the first study in fish to demonstrate v-dsRNA as a stimulant of type I IFN and an inducer of an antiviral state against aquatic viruses.

This is not, however, the first study to use the reovirus genome as a source of v-dsRNA. Previously, the total reovirus genome as well as isolated segments has been used as immune-inducing molecules in mammalian cells (Kato et al., 2008; Alexopoulou et al., 2001; Goubau et al., 2014). One of the first studies of v-dsRNA as an immunostimulant was in 1967 when an isolated reovirus genome was injected into rabbits and induced interferon (Tytell et al., 1967). The cellular response to the reovirus genome has been demonstrated in mouse embryonic fibroblasts (MEFs) and human embryonic kidney cells (HEK293), both cell types producing IFN-β following v-dsRNA treatment (Kato et al., 2008; Goubau et al., 2014). Reoviruses are used for these types of studies due to the relative abundance of dsRNA produced during infection.

Current studies are underway to optimize methods to isolate dsRNA from viruses of other genome types.

Similar to ivt-dsRNA, v-dsRNA induced IFN pathways, and in some cases an antiviral state, in a length dependent manner. The long v-dsRNA molecule induced more IFN1 than short and long v-dsRNA induced more vig-4 transcript than medium and short. At the level of an antiviral state, there were no differences between long and short v-dsRNA induced protection for either VHSV or IPNV infection; however, long v-dsRNA did appear to provide protection similar to control in the VHSV infection model while the short molecule did not (Fig. 2.3C). These differences are indeed subtle, which is unsurprising as the long segment is only 2x the length of the short, whereas previous studies of length have shown an effect with molecules with a 6x and 10x difference in length in RTG-2 cells (Poynter and DeWitte-Orr, 2015). It can then be hypothesized if shorter v-dsRNA molecules were used a greater difference in antiviral assays would be observed. It should be noted that while the molecules are of different lengths they are also of different sequences, and this could be a confounding variable in this study. While future studies may address this issue by digesting native dsRNA genome fragments or ligating fragments together, the present study aimed to focus on native molecules that were as unmodified as possible. Even so, evidence from this study and previous work suggest sequence does not play a role in levels of IFN induction (Peisley and Hur, 2013; Pichlmair et al., 2009).

Next a direct comparison between length and sequence matched v-dsRNA and ivt-dsRNA was performed, and no significant differences were observed between the immune gene transcript induction and antiviral state established by v-dsRNA and the matched ivt-dsRNA. HMW poly I:C, however, even with a much longer average length, was not as effective at inducing IFNs or ISGs and required a lower MOI of IPNV in order to protect cells similarly to

v- or ivt-dsRNA. This data suggests that indeed ivt-dsRNA but not poly I:C could be used as a surrogate for v-dsRNA. Indeed, previous work has shown that poly I:C induced IFN and ISG kinetics differently from ivt-dsRNA in rainbow trout cells (Poynter and DeWitte-Orr, 2015). These differences continue between fish and humans with regard to poly I:C. Human TLR3 responds very strongly to poly I:C, whereas this was not the case for a fish, fugu, (*Takifugu rubripes*) TLR3, which responded most strongly to one length of ivt-dsRNA compared to poly I:C or other lengths of ivt-dsRNA (Matsuo et al., 2008). In vivo, poly I:C has had mixed effects as an antiviral therapy, being an effective protection mechanism against red-spotted grouper necrosis virus (RGNNV) in sevenband grouper (*Epinephelus septemfasciatus*; Nishizawa et al., 2009), but in zebrafish (*Danio reiro)* infected with VHSV poly I:C was able to delay symptoms but only prevented mortality in 5% of fish (Kavaliauskis et al., 2015). Clearly, there is room for increasing the efficacy of dsRNA-based antiviral therapies in fish past the protection that poly I:C can provide.

It should be noted that there are differences between v-dsRNA generated *in situ* with the v-dsRNA isolated for the present study. One difference is the lack of dsRNA-associated proteins in the extracted v-dsRNA. Viruses use many mechanisms to hide dsRNA; one method is the production of proteins that bind dsRNA and effectively hide it from host receptors (Bale et al., 2012). Host cells also have a number of dsRNA-binding proteins that could modify dsRNA availability and potency (DeWitte-Orr and Mossman, 2010). Extracting v-dsRNA through a column or phenol/chloroform extraction would remove these proteins. These dsRNA-associated proteins may have effects on how the cell senses and responds to v-dsRNA. Other modifications that could be influencing the cellular response to dsRNA that would survive extraction include methylation and 5'tri- or di- phosphates (Schaefer et al., 2008; Goubau et al., 2014). Mammalian

reoviruses and poly I:C both have a 5'-diphosphate whereas ivt-dsRNA have 5'-triphosphate termini; both termini are able to activate RIG-I; however, the implication of this difference in rainbow trout is harder to elucidate due to the lack of RIG-I in this fish species (Marq et al., 2011; Martin and Coleman, 1989; Goubau et al., 2014; Chen et al., 2017). Interestingly long ivt-dsRNA (>200bp), which would lack a 5'triphosphate was still able to activate RIG-I in murine embryonic fibroblasts (Kato et a., 2008). The cap status of the dsRNA molecules may also influence the host response; this has been best studied in terms of RIG-I and MDA5. The addition of an M7G cap partially reduces the RIG-I stimulatory properties of dsRNA, whereas 2'O-methylation entirely abrogates RIG-I activation (Schuberth-Wagner et al., 2015). In terms of MDA5, mutant viruses lacking 2'-O-methyltransferase induced higher MDA5-dependent type I IFN expression (Züst et al, 2011). In the present study, v-dsRNA likely has a cap, as reoviruses put a 5' cap on the positive strand of the genomic segments; in comparison, the ivt-dsRNA and poly I:C would not have a m7G cap (Goubau et al., 2014). Kato et al., 2008 found that capped ivt-dsRNA was still able to induce IFN-β production, unfortunately these molecules were not compared to uncapped molecules to determine if this had any positive or negative effects on stimulatory properties. Studies are currently underway to explore the role of different cap modifications on the host innate immune response.

Based on the assumption that ivt-dsRNA can act as a surrogate for v-dsRNA in inducing IFN at the cellular level, and the v-dsRNA vs. ivt-dsRNA comparison performed used molecules with the same sequence, it follows to test whether nucleotide sequence makes a difference. From the results of a group of three ivt-dsRNA containing host or viral sequences it appears as though sequence does not significantly affect ivt-dsRNA's IFN inducing capabilities. This is congruent with the current literature that suggests dsRNA sequence is not a major influence on dsRNA

receptor-binding, as is length and structure (Peisley and Hur, 2013; Pichlmair et al., 2009). Although there is evidence that RIG-I ligands generally have a uridine- or adenosine-rich ribonucleotide sequence and OAS has a four bp specific sequence motif, it is unclear if other receptors have any preference or sequence requirements, or whether there are any sequence preferences for fish dsRNA sensors (Saito and Gale, 2008; Kodym et al., 2009). Sequence may play a role in an antiviral state when RNAi is considered; however, in this system there is an overwhelming IFN-mediated response that likely masks any RNAi effects (Luna et al., 2016).

Overall this study sheds light on the dsRNA-mediated immune response in rainbow trout cells. The findings suggest that v-dsRNA produced by an aquatic reovirus is an interferon-inducing PAMP. There were no significant differences between a v-dsRNA molecule and a length and sequence matched ivt-dsRNA molecules with regards to inducing IFN and ISGs and antiviral state, suggesting that ivt-dsRNA may be useful in studies of interferon and in future antiviral therapies for fish. This study sought to perform functional studies where possible, using antiviral assays to explore the biological relevancy of transcriptional quantification results. These findings contribute to a better understanding of the differences between dsRNA from different sources, which can help facilitate the production of more biologically relevant dsRNA-based therapies.

Acknowledgements

The authors would like to thank Brian Dixon and the members of the DeWitte-Orr and Dixon laboratories for valuable discussions, Julia Pacosz for her assistance with blind measurements, Shreya Jalali for assistance with preliminary sequence studies, and Niels Bols for providing cells, viruses, and grandfatherly support.

Chapter 3: Scavengers for bacteria: Rainbow trout express two functional variants of MARCO that bind to gram-negative and –positive bacteria

Sarah J. Poynter[a] Andrea L. Monjo[b] Gabriella Micheli[c] Stephanie J. DeWitte-Orr[bc]

a Department of Biology, University of Waterloo, 200 University Ave W, Waterloo, ON N2L 3G1, Canada

b Department of Biology, Wilfrid Laurier University, 75 University Ave W, Waterloo, ON N2L 3C5, Canada

c Department of Health Sciences, Wilfrid Laurier University, 75 University Ave W, Waterloo, ON N2L 3C5, Canada

Developmental & Comparative Immunology, 77, pp.95-105. 2017.

3.1 Overview

Class A scavenger receptors (SR-As) are a family of surface-expressed receptors who bind a wide range of polyanionic ligands including bacterial components and nucleic acids and play a role in innate immunity. Macrophage receptor with collagenous structure (MARCO) is a SR-A family member that has been studied in mammals largely for its role in binding bacteria. To date there is little information about SR-As in general and MARCO specifically in fish, particularly what ligands individual SR-A family members bind remains largely unknown. In the present study two novel rainbow trout (rt)MARCO transcript variants have been identified and their sequence and putative protein domains have been analyzed. When overexpressed in CHSE-214, a cell line that appears to lack functional scavenger receptors, GFP-tagged rtMARCO-1 and rtMARCO-2 were able to bind gram-positive, and gram-negative bacteria of both mammalian and aquatic sources. rtMARCO appears to bind bacteria via its scavenger receptor cysteine-rich (SRCR) domain, because SRCR deleted rtMARCO-1 and -2 were unable to bind bacteria. rtMARCO did not show any binding to the yeast cell wall component zymosan or to double-stranded (ds)RNA. This is the first time rainbow trout MARCO sequences have been identified and the first in-depth study exploring their ligand binding profile. This study provides novel insight into the role of rainbow trout MARCO in bacterial innate immunity.

3.2 Introduction

Class A scavenger receptors (SR-As) are surface receptors that perform a broad range of functions in mammals including: cell-cell recognition, macrophage adhesion, endocytosis, phagocytosis, and detection of pathogens as part of the innate immune system (Platt and Gordon, 2001). There are eight classes of scavenger receptors, classes A-H, that were originally described by their ability to bind modified low-density lipoproteins and as such were studied for their role in atherosclerosis (Prabhu Das et al., 2014). SR-As are type II membrane glycoproteins whose family consists of SR-AI/II (Scavenger Receptor class A), MARCO (MAcrophage Receptor with COllagenous domain), SCARA3 (SCAvenger Receptor class A, member 3), SCARA4 (SCAvenger Receptor class A, member 4) and SCARA5 (SCAvenger Receptor class A, member 5). All members share cytoplasmic, transmembrane, α-helical, and collagenous domains, though they differ in the lengths of said domains and in the composition of their C-terminal domains (Whelan et al., 2012). MARCO, the focus of the present study, consists of the typical domains of an SR-A with a scavenger receptor cysteine-rich (SRCR) domain at the proximal end of the extracellular portion of the receptor (Bowdish and Gordon, 2009). In mammals, MARCO is mainly expressed on macrophages of the spleen marginal zone and lymph nodes, as well as on splenic dendritic cells (Elomaa et al., 1995; Granucci et al., 2003). Mammalian MARCO plays in important role in innate immune defenses against bacterial and fungal pathogens (Xu et al., 2017).

The role of SR-As in innate immunity has yet to be clearly elucidated; however, these receptors can bind to a wide range of pathogen-associated molecular patterns (PAMPs). Mammalian SR-As can detect bacteria and their PAMPs including: lipopolysaccharide (LPS), lipoteichoic acid (LTA; Platt and Gordon, 2001), as well as gram-positive and –negative bacteria (Canton et al., 2013). With regards to antiviral innate immunity, SR-As can detect extracellular

nucleic acids, including viral double-stranded RNA, and mediate a type I interferon response in mammals and likely in fish as well (DeWitte-Orr et al., 2009; Poynter et al., 2015). SR-As are also involved in antifungal innate immunity as SCARA4 has been shown to bind yeast as well as the yeast cell well component zymosan (Mori et al., 2014; Jang et al., 2009; Ohtani et al., 2001), while MARCO has been shown to contribute to containing fungal infections in mice (Xu et al., 2017). Considering MARCO in particular, mammalian MARCO binds both gram-positive and -negative bacteria as well as LPS and LTA via its SRCR domain (Arredouani et al., 2005; Elomaa et al., 1998).

Teleost SR-As are an emerging area of study, to date few studies exist looking at these important receptors and there is a serious deficit of functional data. It does appear that teleost fish express MARCO-like receptors and these receptors play a role in innate immunity, at least in response to bacterial infection. A study in common carp (*Cyprinus carpio*) identified two variants of MARCO, similar in structure and regulation during developmental stages and post-infection with *Aeromonas hydrophila* (Feng et al., 2016). In yellow croaker (*Larimichthys crocea*) a MARCO sequence was identified and was upregulated after infection with *Vibrio alginolyticus* (He et al., 2014). A MARCO-like receptor has been identified in red drum (*Sciaenops ocellatus*) and was upregulated by bacterial and viral infection; a recombinant SRCR domain from this protein was purified and bound to bacteria (Qiu et al., 2013). In zebrafish (*Danio rerio)*, MARCO mediated phagocytosis of *Mycobacterium marinum* and the initial pro-inflammatory response to this infection was MARCO-dependent (Benard et al., 2014; Wittamer et al., 2011; Zakrzewska et al., 2010).

The present study sought to identify novel rainbow trout (*Oncorhynchus mykiss*) MARCO sequences, and study the ability of rainbow trout MARCO to function as a surface

receptor in anti-bacterial, -viral or -fungal innate immunity. Two MARCO transcripts, rtMARCO-1 and rtMARCO-2, were identified and analyzed bioinformatically and their binding capabilities were tested. CHSE-214 was chosen to study ligand binding with over-expressed rtMARCO as this cell line demonstrates low bacterial binding capabilities. CHSE-214 is unable to bind extracellular dsRNA (Jensen et al., 2002) and therefore may lack functional class A scavenger receptors (DeWitte-Orr et al., 2010). Both variants, rtMARCO-1 and rtMARCO-2, had domains common to SR-As including an SRCR domain. It was found that rainbow trout rtMARCO-1 and rtMARCO-2 are able to bind Gram-negative and –positive bacteria, but did not bind to zymosan or dsRNA.

3.3 Materials and methods

3.3.1 Cell culture

The rainbow trout monocyte/macrophage cell line RTS-11 and the Chinook salmon (*Oncorhynchus tshawytscha)* embryonic cell line (CHSE-214) used for this study were obtained from N. Bols (University of Waterloo; Ganassin and Bols, 1998; Lannan et al., 1984). Cell lines were grown in 75 cm^2 plastic tissue culture flasks (BD Falcon, Bedford, MA) at 20 °C in Leibovitz's L-15 media (HyClone, Logan, UT) supplemented with 10% (CHSE-214) or 20% (RTS-11) v/v fetal bovine serum (FBS; Fisher Scientific, Fair Lawn, NJ) and 1% v/v penicillin/streptomycin (P/S; 10 mg/mL streptomycin and 10000U/mL penicillin; Fisher Scientific).

3.3.2 Reagents

3.3.2.1. Poly I:C

High molecular weight (HMW) polyinosinic:polycytidylic acid (poly I:C) was purchased from Invivogen and suspended in sterile phosphate buffered saline (PBS) at a concentration of 1 mg/mL, heated for 10 min at 55 °C and cooled at room temperature before being aliquoted and

stored at −20 °C. To solubilize precipitates before use, HMW poly I:C was reheated and cooled to room temperature.

3.3.2.2 Fluorescently labeled E. coli, S. aureus, and zymosan

Fluorescently conjugated *Escherichia coli* (Alexa Fluor 594; K-12 strain), *Staphylococcus aureus* (Alexa Fluor 594: Wood strain without protein A), zymosan (Alexa Fluor 594; *Saccharomyces* cerevisiae) BioParticles were purchased from Molecular Probes (Oregon, USA). Particles were re-suspended in PBS at a concentration of 20 mg/mL and sodium azide (Sigma) was added to a final concentration of 2 mM. Particles were stored at 4 °C.

3.3.2.3 Labeling of Vibrio anguillarum

25 µL of *V. anguillarum* (Obtained from B. Dixon, Waterloo, ON) (1.19×10^{10} CFU/ml; 25 µL was used per well) was pelleted at 10000x*g* for 2min, washed two times in PBS and re-suspended in 25 µL of PBS with Biotium Live-or-dye 350/448 (32002) added at a 1 in 100 dilution. After a 30min room temperature incubation in the dark the bacteria was pelleted, washed 3x with PBS and re-suspended in 25 µL of PBS for immediate use.

3.3.3 Labeling HMW poly I:C

HMW poly I:C was labeled using the ULYSIS labeling kit following manufacturer's instructions (Thermo Fisher). Briefly, 1 µg of HMW poly I:C was precipitated and re-suspended in 20 µL of ULYSIS labeling buffer, heated at 95 °C for 5min and put on ice. Subsequently, 4 µL of labeling buffer as well as 1 µL of ULS labeling solution was added. The solution was heated at 90 °C for 10min, mixed with 75 µL of PBS and run through a BioSpin p30 (Bio-Rad) column to remove unbound fluorophores. dsRNA was added to a 12-well at a concentration of 1 µg/mL.

3.3.4 RNA extraction cDNA synthesis and PCR reactions

RNA was extracted from 1×10^6 RTS-11 cells using TRIzol (Ambion) following manufacturer's instructions. RNA was treated with a DNA-*free* DNA Removal Kit (Ambion).

For cDNA synthesis, 1 µg of RNA was used in a 20 µL iScript reverse transcriptase reaction following manufacturer's instructions exactly (Bio-Rad). Phusion High-Fidelity DNA polymerase (Thermo Scientific) was used with reactions containing 200 µM each dNTP (Fisher scientific), 1X Phusion HF buffer (Thermo Scientific), 0.5 µM each forward and reverse primer, 0.02U/µL Phusion DNA polymerase (Thermo Scientific) and 100 ng of template plasmid (pEGFP-C1-rtMARCO-1 or -2 were used as templates to create SRCR mutant plasmids) or 3 µL of undiluted cDNA (in a 60 µL reaction). A T100 thermocycler (Bio-Rad) was used with the following conditions: 98 °C 30s followed by 30 cycles of 98 °C for 10s, specific TA for 15s (Table 3.1), 72°C for 30 s/kb, followed by a final elongation of 72 °C for 10min and products were held at 4 °C.

Table 3.1. Primer sequences and conditions used in the present study. Target for amplification, primer sequence in the 5′ to 3′ direction, product length, and annealing temperature (TA) are provided. Product length varied depending on the variant of MARCO targeted. Italics denote the extra nucleotides added to facilitate restriction enzyme function, bold sequences are restriction sites. Underlined nucleotides are extra nucleotides added to keep the product in frame.

Target	**Primer (5'-3')**	**Product length (bp)**	**T_A(°C)**
Full-length MARCO	F – ATGGAGACATCAGTAGACAG R – TCACACACACTGCACCCCAG	Marco-1: 1302 Marco-2: 1260	64°C
Cloning MARCO	F –*CGGCCG***CTCGAG**CGGAGACAT CAGTAGACAGAGG R – *GGGCCC***GAATTC**TCACACACA CTGCACCCCGG	Marco-1: 1325 Marco-2: 1283	50°C
Cloning MARCO mutant	R1 –*GCGCCG***GAATTC**TCAACGAGC ACCCCCACCAACAAT	Marco-1: 1060 Marco-2: 1019	50°C
Fragment MARCO	F1 – TCCTCAAAGCTTCACCAGGC F2 – ACAAGGACGAGCTGGAACAC R – ACTGGTCCAGCTGCTCTTTC	F1R – 505 F2R – 357	50°C
Cloning HS-SRAI	F – *GGCGCG***CTCGAG**GCGAGCAGT GGGATCACTTTCACAA R – *GCGCCG***GAATTC**TTATAAAGT GCAAGTGACTCCAGCAT	1382	50°C

3.3.5 Cloning of complete transcript CDS and mutant

The Bowdish lab at McMaster University (Hamilton, ON) generously provided the peGFP-C1 (Clontech) and pCDNA3.1-hSR-AI plasmids used in this study. MARCO rainbow trout primers were designed from the predicted salmon MARCO mRNA sequence (accession number XM_014173984.1) using NCBI primer BLAST. Primer sets used to amplify the full-length sequence of both variants using the protocol described in 3.3.4. Products were sequenced at the Guelph Molecular Services Molecular Biology Unit within Laboratory Services of the University of Guelph (Guelph, ON) and sequences were subsequently analyzed and used for cloning experiments.

3.3.6 Sequence analysis

All sequence analysis was done on deduced rainbow trout amino acid sequences. Protein sequences from all species were found on NCBI. MARCO rainbow trout mRNA sequences were translated into protein sequences using the ExPASy translate tool (http://web.expasy.org/translate/).

3.3.6.1 Bioinformatics analysis – amino acid sequence alignments

Amino acid sequence similarities between rainbow trout MARCO sequences and other species were compared using BLASTp from NCBI. The rainbow trout sequence was always used as the first query sequences for consistency. The pairwise alignment of rtMARCO-1 and rtMARCO-2 was constructed using EMBOSS Needle (EMBL-EBI).

3.3.6.2 Bioinformatics analysis – conserved domains

The cytoplasmic and transmembrane domains were determined using TMHMM software (http://www.cbs.dtu.dk/services/TMHMM) (Whelan et al., 2012). Alpha-helical domains were identified using the PSIPRED protein sequence analysis workbench (http://bioinf.cs.ucl.ac.uk/psipred/) (Whelan et al., 2012). The collagenous and SRCR domains

were determined using NCBI's CDD (http://www-ncbi-nlm-nih-gov.proxy.lib.uwaterloo.ca/Structure/cdd/wrpsb.cgi; E value ≤ 0.01 (Whelan et al., 2012). The protein representations were made using IBS (Illustrator for Biological Sequences; http://ibs.biocuckoo.org/; Liu et al., 2015).

3.3.6.3 Bioinformatics analysis – phylogenetic analysis

A phylogenetic tree was constructed with MEGA7 software (Kumar et al., 2016) using the Neighbor-Joining method based on the amino acid alignment (ClustalW) of full-length MARCO proteins from representative species. The sum of branch length is 7.435. The values next to the branches indicated the confidence probability that the interior branch length is greater than 0 was estimated using the bootstrap test based on 1000 replicates. The evolutionary distances as calculated using the Poisson correction method are provided and presented in units of number of amino acid substitutions/site. Gaps were treated with pairwise deletion and the rate of evolution among sites was considered uniform. SCARA3 and SCARA5 sequences from other fish species were included as non-MARCO SR-A controls.

3.3.7 GFP labeled rtMARCO-1, -2, rtMARCO-1(ΔSRCR), rtMARCO-2(ΔSRCR), hSR-AI vector construction

pEGFP-C1-rtMARCO-1, pEGFP-C1-rtMARCO-2, pEGFP-C1-rtMARCO-1(ΔSRCR) and pEGFP-rtMARCO-2(ΔSRCR) were generated by amplifying the appropriate sequence by PCR using cDNA from RTS-11 and primers described in Table 3.1 pEGFP-C1-hSR-AI was PCR amplified using pCDNA3.1-hSR-AI as a template and primers described in Table 3.1 (100ng/reaction). 60 µL reactions were set up using Phusion High-Fidelity DNA polymerase (Thermo Scientific) as described in section 3.3.2. A T100 thermocycler (Bio-Rad) was used with the following conditions: 98 °C for 30s followed by 30 cycles of 98 °C for 10s, 72 °C for 15s, T_A (Table 3.1) with an annealing time of 30s/kb, followed by a final elongation of 72 °C for

10min and products were held at 4 °C. PCR products were purified using the MinElute PCR purification kit (Qiagen). A double-digest of 1 µg of PCR product and 1 µg of peGFP-C1 plasmid was performed using 10U of *Eco*RI (Roche) and 10U of *Xho*I (Roche) with 1X SureCut buffer H (Roche) in a total volume of 50 µL. PCR products and plasmid were then purified using the MinElute PCR purification kit (Qiagen). Ligation reactions included 50 ng of peGFP-C1 plasmid with a 1:5 ratio of insert and were combined in a 10 µL reaction with 1 µL of T4 Ligase (NEB) and 1X T4 ligation buffer (NEB). Ligations were left overnight at 4 °C and then warmed to room temperature for 15min prior to transformation. Competent JM109 (Promega) cells were transformed with 25 ng of plasmid/insert as per manufacturer's instructions and plated on LB-agar plates with 100 µg/mL kanamycin (Fisher Scientific). Colonies were grown overnight in 6 mL of LB-broth containing 100 µg/mL kanamycin at 37 °C with shaking at 220 rpm in a MaxQ-4000 orbital bench top incubator and shaker. Plasmids were purified using the GenElute Plasmid Miniprep Kit (Sigma) and vectors were to Guelph Molecular Services Molecular Biology Unit within Laboratory Services of the University of Guelph (Guelph, ON) for sequencing to confirm insert sequence and orientation.

3.3.8 rtMARCO and hSR-AI protein overexpression and ligand binding in CHSE-214

3.3.8.1 CHSE-214 transfection

CHSE-214 cells were seeded at 2×10^5 cells/well in a 12-well tissue culture plate (Fisher Scientific). After attaching overnight cells were rinsed one time with PBS and transfected using Fugene6 (Promega). Cells were transfected with 250 ng of plasmid/well at a ratio of 1.5 µL of Fugene6 to 1 µg of plasmid. Initial incubation of plasmid and Fugene6 was done in L-15 (50 µL/µg of plasmid), and the resulting transfection mixture was added to 500 µL L-15 containing 10% (v/v) FBS, but no antibiotics. After 24 h an addition 500 µL of 10% FBS media was added to the cells. The transfection efficiencies (TE) used in the present study were 5–20%

for all GFP-containing vectors transfected into CHSE-214. The transfection conditions were conducted to create low TEs to facilitate isolation of single transfected cells for imaging.

3.3.8.2 Ligand binding assay

At 36 h post-transfection, cells were treated with 500 µL L-15 containing the following ligands for 6 h: *E. coli* (10 µg), *S. aureus* (10 µg), *V. anguillarum* (5.95×10^8 CFU), zymosan (20 µg). For blocking experiments with HMW poly I:C, cells were pretreated with a 100 µg HMW poly I:C in 500 µL L-15 for 30min prior to the addition of 10 µg *E. coli* for 3 h; control cells were treated the same without the addition of HMW poly I:C. After incubation with the ligand-containing media, media was removed and cells were rinsed 3x with PBS, fixed with 10% neutral-buffered formalin for 10min, stained with 10 µg/mL 4′,6-diamidino-2-phenylindole (DAPI) (Fisher Scientific) in PBS, and mounted on slides with SlowFade Gold mounting medium (Fisher Scientific). In the case of *V. anguillarum* the cells were not counterstained with DAPI, as it would interfere with visualization of the bacteria. Cells were left overnight for the mounting media to cure and imaged on a Nikon Eclipse Ti-S fluorescence microscope and analyzed using NIS-Elements software.

3.4 Results

3.4.1 Rainbow trout express 2 variants of MARCO

Two MARCO transcripts were identified in rainbow trout, rtMARCO-1 (accession: KX452014.1) and rtMARCO-2 (accession: KY682703.1; Fig. 3.1), whose expression was confirmed in RTS11 (data not shown) using the MARCO fragment primers (Table 3.1). Both rtMARCO-1 and rtMARCO-2 have consensus sequences shared with other fish MARCO sequences, specifically the RGR VEV and the WGT CDD sequences (bolded in Fig. 3.1), as well as six cysteine residues within the SRCR (highlighted in Fig. 3.1; Yap et al., 2015; He et al., 2014; Feng et al., 2016; Qiu et al., 2013). When compared to other species, including six species

of fish, the only sequences that showed high levels of similarity were to the predicted Atlantic salmon (*Salmo salar)* sequences (Table 3.2). The variant sequences vary in length; however, both sequences have all major domains, including a cytoplasmic, transmembrane, α-helical, collagenous and a SRCR (Fig. 3.2A). The variants have small differences in the lengths of their conserved domains (Fig. 3.2A). Using phylogenetic tree analysis (Fig. 3.2B), fish MARCO sequences clustered with high confidence, and between fish, salmonid MARCO sequences from Atlantic salmon and rainbow trout also clustered together with high confidence. Avian/reptile and mammalian cDNAs each formed their own distinct clusters respectively. Fish SCARA3 and SCARA5 formed individual clusters, separate from MARCO.

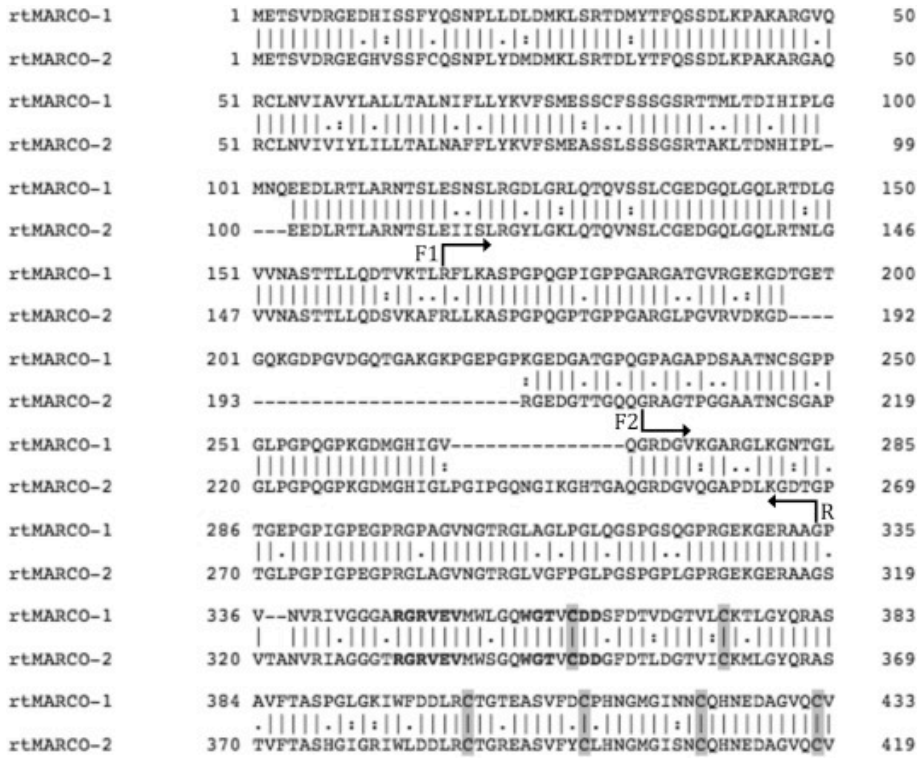

Figure 3.1. Comparison of the amino acid sequence of rainbow trout MARCO variants rtMARCO-1 and -2. Amino acid sequences were deduced using ExPASy and sequences were aligned using EMBOSS Needle pairwise sequence alignment. Approximate location of the fragment primers (Table 3.1) F1, F2, and R are shown with arrows to demonstrate that different sized products would be created by F1/R and F2/R primer sets for different variants; the F1 primer produced a product for variant 1 and F2 produced a product for variant 2. Conserved cysteine residues are highlighted in grey.

Table 3.2. Amino acid sequence similarities between Oncorhynchus mykiss rtMARCO-1 and -2 sequences and other species. Amino acid query cover and identity values were determined using BLASTp. Accession numbers for the protein sequences are listed; *Atlantic salmon sequences are predicted.

	Rainbow trout (*Oncorhynchus mykiss*) **MARCO-1**			Rainbow trout (*Oncorhynchus mykiss*) **MARCO-2**		
	Query cover (%)	**Identity (%)**	**E value**	**Query cover (%)**	**Identity (%)**	**E value**
Atlantic salmon (*Salmo salar*) X1* XP_014020233.1	100	**87**	0	100	**73**	0
Atlantic salmon (*Salmo salar*) X3* XP_014020235.1	100	**85**	0	100	**72**	0
Yellow croaker (*Larimichthys crocea*) AHY18726.1	100	**49**	2e-110	100	**49**	2e-110
Red drum (*Sciaenops ocellatus*) AGH27725.1	100	**48**	6e-110	100	**47**	5e-114
Common carp (*Cyprinus carpio*) LC107820.1	94	**38**	3e-81	94	**37**	3e-76
Zebrafish (*Danio rerio*) AII73713.1	100	**38**	6e-82	100	**37**	1e-80
American alligator (*Alligator mississippiensis*) KYO18128.1	90	**44**	2e-55	89	**44**	2e-54
House mouse (*Mus musculus*) AAA68638.1	92	**32**	1e-58	92	**33**	8e-55
Human (*Homo sapiens*) NP_006761.1	96	**42**	4e-63	93	**32**	2e-55

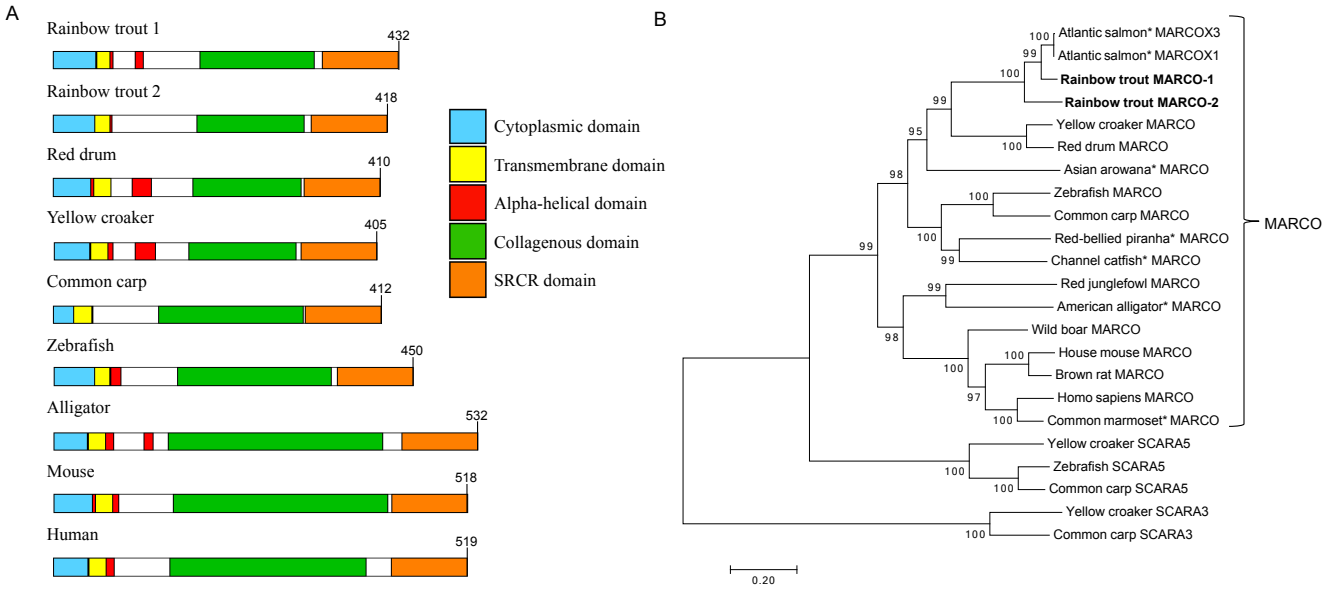

Figure 3.2. The protein domain architecture of rainbow trout (Oncorhynchus mykiss) rtMARCO-1 and -2 and phylogenetic analysis illustrating the relationship between the novel fish MARCO sequences and other fish, reptile, avian and mammalian species.
(A) Structures are scaled based on the length of each domain, total amino acids in each protein sequence is indicated by the number at the end of each protein. The cytoplasmic and transmembrane domains were determined using TMHMM software. α-helical domains were identified using the PSIPRED protein sequence analysis workbench. The collagenous and scavenger receptor cysteine-rich (SRCR) domains were determined using NCBI's Conserved Domain Database (CDD). **(B)** The phylogenetic tree was constructed with the MEGA7 software using the neighbor-joining method based on amino acid alignment (ClustalW) of full-length proteins. Numbers beside the internal branches indicate bootstrap values based on 500 replications. 0.20 scale indicates the genetic distance. *indicates protein is predicted. Accession numbers are as follows: MARCO sequences: Atlantic salmon (*Salmo salar*) X1-XP_014020233.1; Atlantic salmon (*Salmo salar*) X3-XP_014020235.1; Yellow croaker (*Larimichthys crocea*)-AHY18726.1; Red drum (*Sciaenops ocellatus*) AGH27725.1; Common carp (*Cyprinus carpio*) LC107820.1; Zebrafish (*Danio rerio*) AII73713.1; American alligator (*Alligator mississippiensis*) KYO18128.1; House mouse (*Mus musculus*) AAA68638.1; Human (*Homo sapiens*) NP_006761.1; Asian arowana (*Scleropages formosus*) XM_018732274.1; Red-bellied piranha *(Pygocentrus nattereri*) XP_017547716.1; Red jungle fowl (*Gallus gallus*) NP_990067.1; Wild boar (*Sus scrofa*) AEX66158.1; Brown rat (*Rattus norvegicus*) NP_001102481.1; Common marmoset (*Callithrix jacchus*) XP_002749572.1; SCARA5 sequences: Yellow croaker AHY18728.1; Zebrafish NP_001025361.1; Common carp BAU33576.1; SCARA3 sequences: Yellow croaker AHY18727.1; Common carp BAU33572.1.

3.4.2 CHSE-214 overexpressing SR-A express altered morphology

As mentioned in the introduction, CHSE-214 cells were used in this study to monitor MARCO function as this cell line has been shown previously to be unable to bind an SR-A ligand (Jensen et al., 2002) and thus we hypothesized may be negative for functional SR-As. Most cell lines express one to many functional SR-As, and background ligand binding makes it very difficult to determine the role of a single SR-A. In control cultures, without MARCO over expression, CHSE-214 had very low to no background ligand binding, making it an ideal cell line for this study. Human SR-AI (hSR-AI) was used as a positive control for bacterial and dsRNA binding (Limmon et al., 2008; Peiser et al., 2000). CHSE-214 cells expressing either hSR-AI or rtMARCO-1/-2, or rtMARCO-1(ΔSRCR)/-2(ΔSRCR) occasionally showed a distinctly altered morphology that was drastically different than cells expressing the control GFP plasmid alone. This morphology was less evident in cells overexpressing the mutant MARCO sequences compared to wildtype (data not shown). The morphology caused the formation of plasma membrane processes, as well as dendritic projection-like structures (Fig. 3.3). It should be noted not every cell expressing an SR-A showed this extreme appearance, however all did have an altered membrane appearance; often these structures were only visible when the exposure time was increased causing overexposure of the body of the cells.

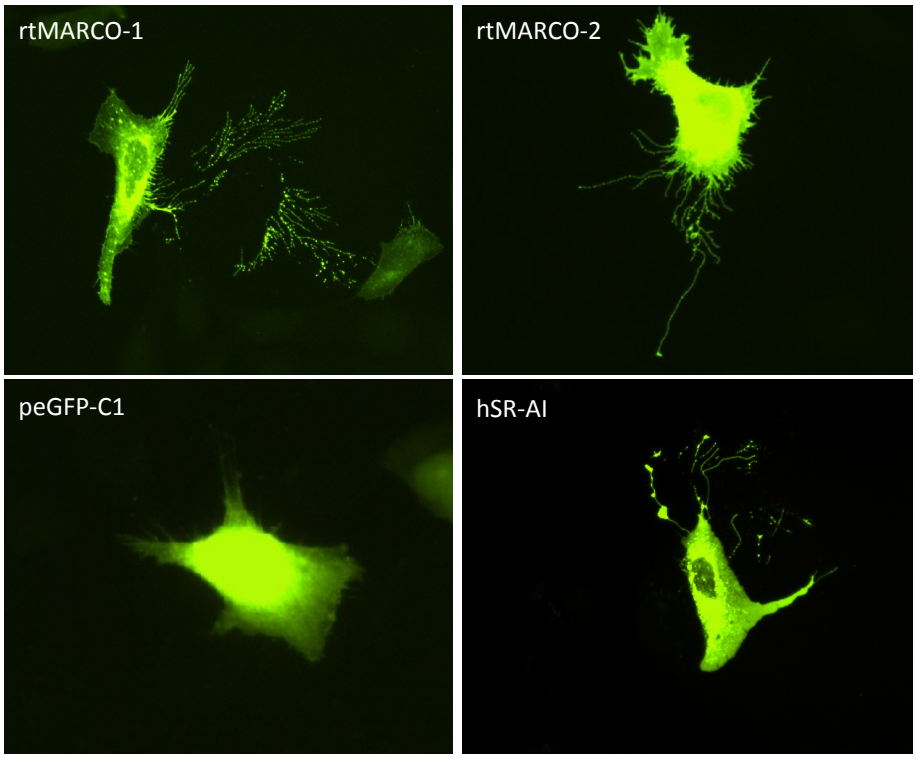

Figure 3.3. Morphological changes induced in CHSE-214 by transfection with GFP-tagged rtMARCO-1, rtMARCO-2 and hSR-AI. CHSE-214 cells were transfected with peGFP-C1 plasmid alone or peGFP-C1 plasmid containing either rtMARCO-1 or -2 sequence or hSR-AI sequence. Three days post-transfection cells were fixed, mounted, and viewed for changes in morphology. Magnification 400x.

3.4.3 Both MARCO variants bind bacteria via their SRCR domains

rtMARCO-1 and -2 showed the same ligand binding profile; both were able to bind to human pathogenic bacteria, including: gram-negative bacteria (*E. coli*) and gram-positive bacteria (*S. aureus*; Fig. 3.4). CHSE-214 cells expressing empty vector (peGFP-C1) did not bind bacteria. CHSE-214 cells overexpressing rtMARCO-1 and -2 also bound the fish bacterial pathogen, *Vibrio anguillarum*. Empty vector expressing control cells did not bind *V. anguillarum*, demonstrating specificity for the receptor (Fig. 3.5). This binding appears to be via the SRCR domain, as both rtMARCO-1(ΔSRCR) and −2(ΔSRCR) lost the ability to bind *E.coli, S. aureus,* and *V. anguillarum* compared to wildtype (Fig. 3.4 and 3.5).

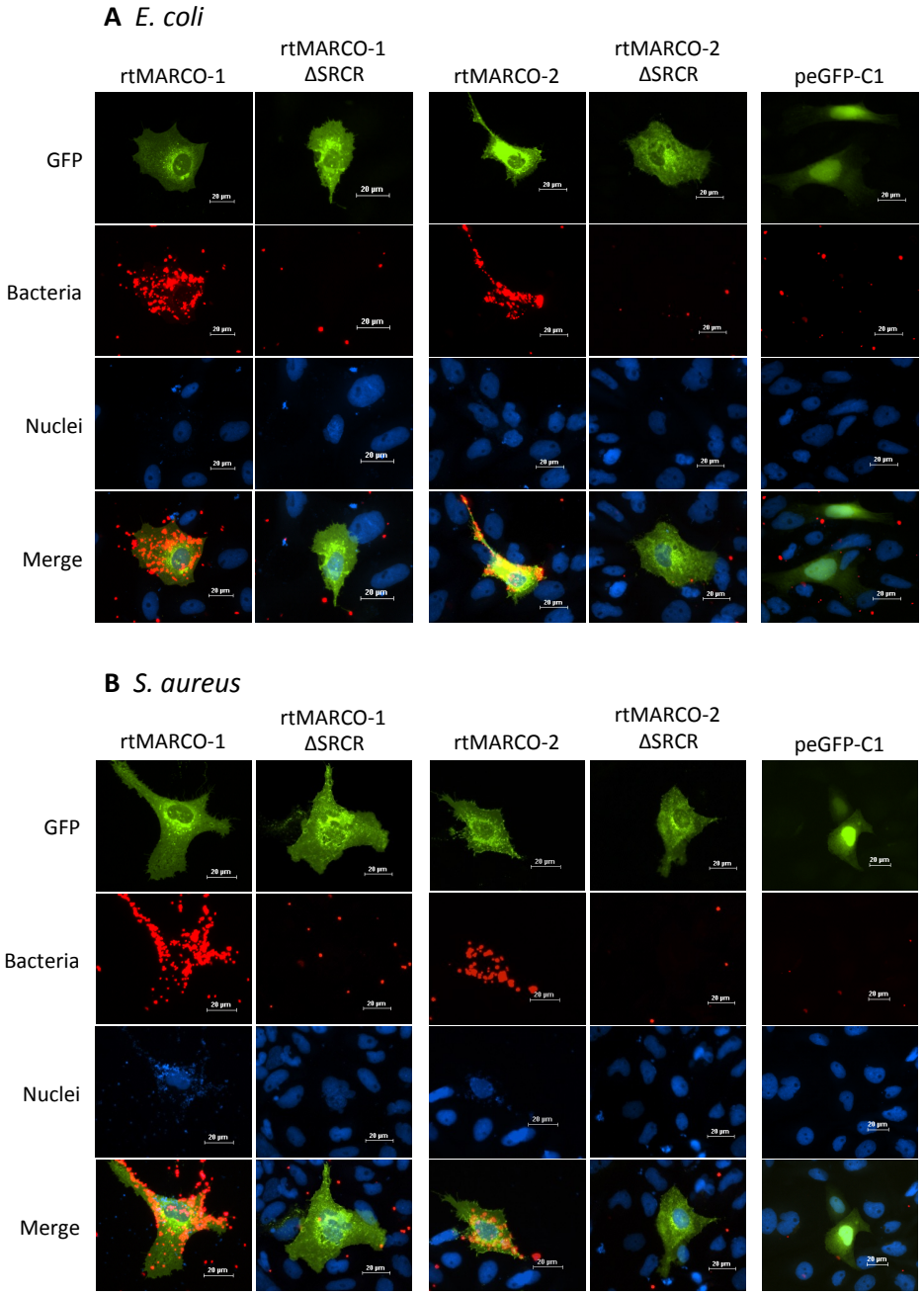

Figure 3.4. Rainbow trout rtMARCO-1 and rtMARCO-2 bind to human gram-negative and gram-positive bacteria through the SRCR domain. CHSE-214 cells were transfected with peGFP-C1 plasmid alone or peGFP-C1 plasmid containing the sequences of full-length rtMARCO-1, rtMARCO-2 or the truncated mutants lacking the scavenger receptor cysteine-rich (SRCR) domain. rtMARCO-1-ΔSRCR, rtMARCO-2ΔSRCR. Three days post-transfection cells were treated with 20 µg/mL of Alexa Fluor 594 labeled heat killed **(A)***Escherichia coli* or **(B)***Staphylococcus aureus* for 6 h. MARCO protein (green), bacteria (red), nuclei were counterstained with DAPI (blue). Magnification 400×.

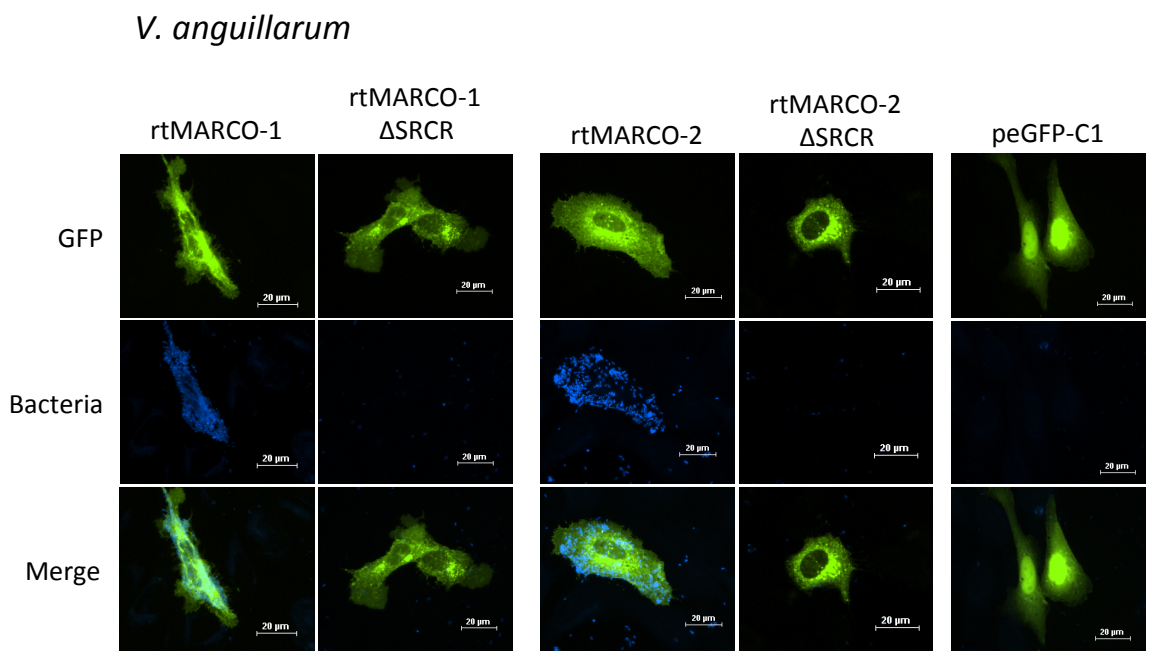

Figure 3.5. Rainbow trout rtMARCO-1 and rtMARCO-2 bind to fish pathogenic gram-negative bacteria through the SRCR domain. CHSE-214 cells were transfected with peGFP-C1 plasmid alone or peGFP-C1 plasmid containing the sequences of full-length rtMARCO-1, rtMARCO-2 or the truncated mutants lacking the scavenger receptor cysteine-rich (SRCR) domain: rtMARCO-1-ΔSRCR, rtMARCO-2ΔSRCR. Three days post-transfection cells were treated with Live-or-Dye labeled *Vibrio anguillarum* (5.95 × 108 CFU) for 6 h. MARCO protein (green), bacteria (blue). Magnification 400×.

3.4.4 rtMARCO do not appear to bind yeast and viral PAMPs

Neither rtMARCO-1 nor −2 were able to bind zymosan or dsRNA at levels detectable by fluorescence microscopy (Figs. 3.6 and 3.7A). Zymosan was able to bind the rainbow trout monocyte/macrophage cell line RTS-11, thus acting as a positive control for visualizing cell-associated zymosan in our system (data not shown). hSRA-I has previously been suggested to bind dsRNA, thus acting as a positive control for binding exogenous dsRNA in our system (Limmon et al., 2008, Fig. 3.7A). DsRNA was unable to block *E.coli* binding to rtMARCO-1 or -2 but did block binding by hSRA-I (Fig. 3.7B).

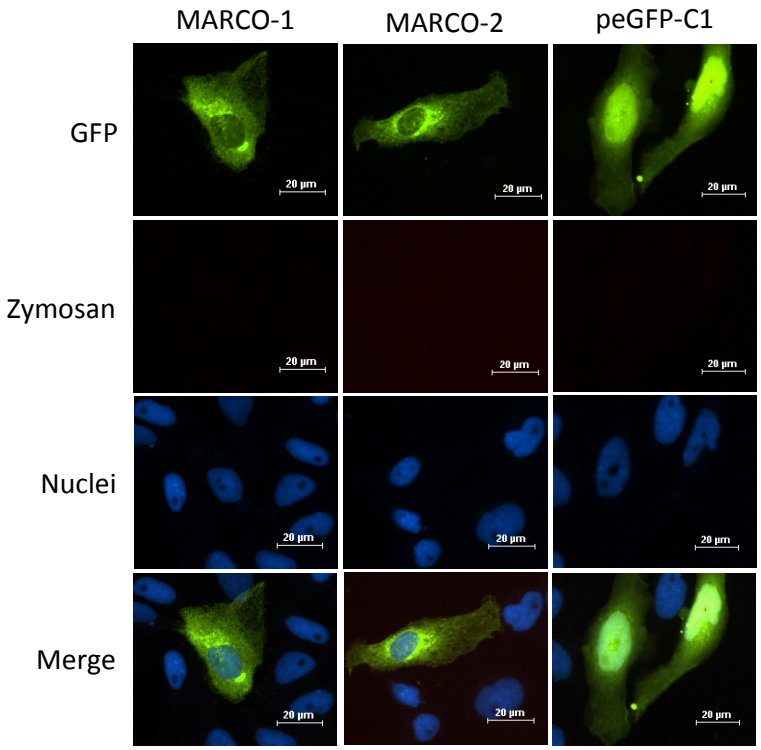

Figure 3.6. Rainbow trout rtMARCO-1 and rtMARCO-2 do not bind to the yeast cell wall component zymosan. CHSE-214 cells were transfected with peGFP-C1 plasmid alone or peGFP-C1 plasmid containing rtMARCO-1 or rtMARCO-2 sequences. Three days post-transfection cells were treated with 40 µg/mL of Alexa Fluor 594 labeled zymosan for 6 h. MARCO protein (green), zymosan (red), nuclei were counterstained with DAPI (blue). A control cell line (RTS-11) that binds zymosan was used as a positive control for visualization of zymosan (not shown). Magnification 400×.

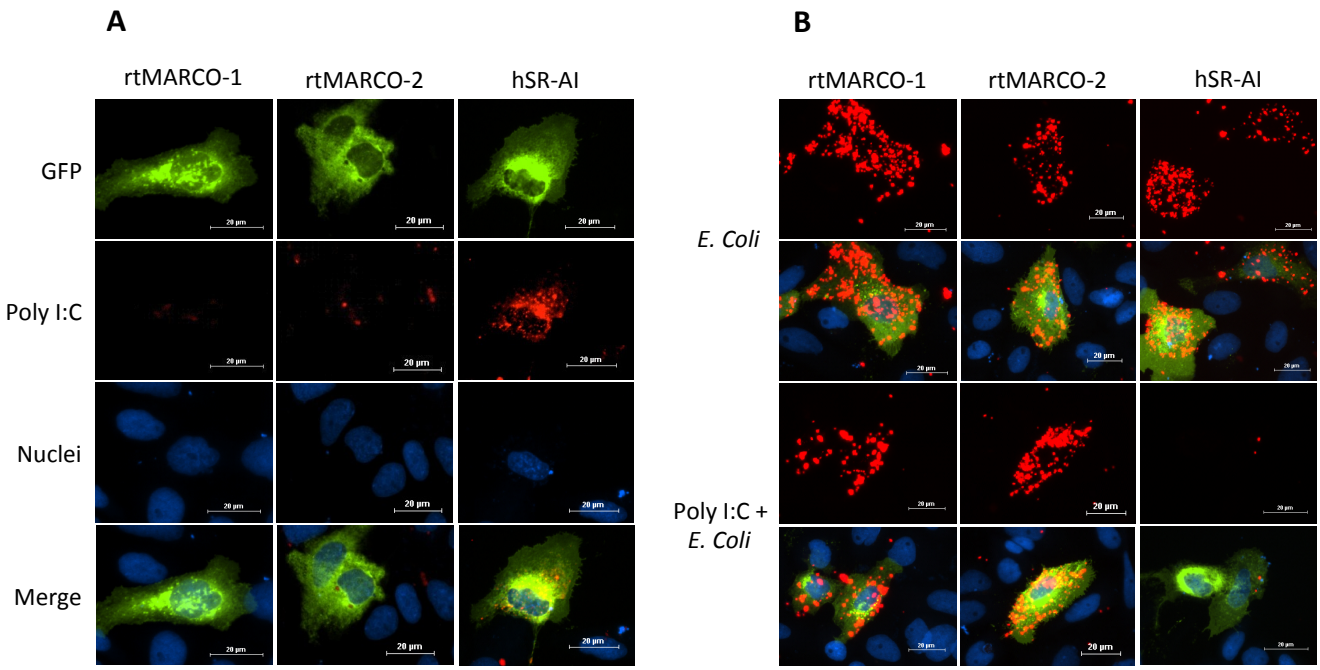

Figure 3.7. Rainbow trout rtMARCO-1 and rtMARCO-2 do not bind the synthetic dsRNA poly I:C but human SRA-I does. CHSE-214 cells were transfected with peGFP-C1 plasmid alone or peGFP-C1 plasmid containing rtMARCO-1 or rtMARCO-2 sequences. Three days post-transfection cells were treated for analysis. (A) Transfected cells were treated with 1 µg/mL of Alexa Fluor 546 labeled high molecular weight poly I:C (HMW) for 6 h. Cells expressing a MARCO protein or the eGFP control (green) did not show any association with dsRNA (red); however cells expressing human SR-AI (hSR-AI) showed robust binding to HMW. (B) Cells were pretreated with 200 µg/mL HMW for 30min, followed by treatment with 20 µg/mL Alexa Fluor 594 labeled heat killed *Escherichia coli* for 3 h. Nuclei were counterstained with DAPI (blue). Magnification 400×.

3.5 Discussion

In this study two rainbow trout MARCO sequences have been identified and analyzed and their ligand binding capabilities were explored. This is not the first report of multiple variants for MARCO in fish. Common carp (*Cyprinus carpio*) also possess two copies of MARCO (also known as SCARA 2; Feng et al., 2016). When comparing MARCO sequences between fish, the sequences had only moderate similarities; however, the conserved domains necessary for function appear to be present in rainbow trout (Fig. 3.2). Of particular importance is the presence of the SRCR in both sequences, as this sequence is believed to be vital for ligand binding in mammalian MARCO receptors (Elomaa et al., 1998; van der Laan et al., 1999). Both sequences

had similar domain architecture and had conserved amino acid residues found across species (Fig. 3.2; Qiu et al., 2013; Yap et al., 2015).

GFP labeled rtMARCO-1 and -2 were overexpressed in CHSE-214 cells, a cell line that is hypothesized to be defective for SR-As as it is unable to respond to extracellular dsRNA (Jensen et al., 2002). Very low background bacterial binding in CHSE-214 cells observed in the present study substantiates this hypothesis. Following overexpression of rtMARCO-1 and -2 it was observed by fluorescence microscopy that some cells demonstrated a perinuclear halo of intense green in addition to a widespread green found throughout the cell, this staining was commented on in a study of SCARA5 (Jiang et al., 2006) and is visible in other MARCO overexpression studies (Hirano et al., 2012) but seldom noted. This staining suggests a localization of the protein to the *trans*-Golgi network (Jiang et al., 2006).

Another notable change was in the morphology of some cells transfected with SR-A containing peGFP-C1 plasmids (Fig. 3.3). While not evident in every transfected cell, many cells transfected with rtMARCO-1, rtMARCO-2, or hSR-AI demonstrated long, filamentous projections. Dendritic-like plasma membrane formations were also observed in studies overexpressing MARCO in a variety of cultured mammalian cells (Pikkarainen et al., 1999; Hirano et al., 2012; Novakowski et al., 2016; Granucci et al., 2003; Grolleau et al., 2003, Ohtani et al., 1999). Why this rearrangement of the membrane occurs is not well understood. MARCO was essential for murine dendritic cell morphological changes mediated by actin during the process of activation (Granucci et al., 2003; Grolleau et al., 2003). Pikkarainen and colleagues found that Rac1 but not cdc42 was involved in MARCO-mediated actin reassembly (Pikkarainen et al., 1999), demonstrating this change in morphology is an active process triggered by signaling cascades within the cell. Thus in the present study, ligand binding as well as intracellular

signaling cascades triggered by rainbow trout MARCO might be conserved when over-expressed in CHSE-214 cells.

Interestingly, similar to what was observed in the present study, previous work with murine and human MARCO demonstrated that the SRCR domain (domain V) of MARCO was important for its induced morphological changes (Pikkarainen et al., 1999; Novakowski et al., 2016). Cells over expressing rtMARCO-1(ΔSRCR) and rtMARCO-2(ΔSRCR) did show reduced production of long filaments; however, short projections were still evident (Figs. 3.4 and 3.5). While this observation may suggest rainbow trout MARCO could play a role in cell membrane morphology, more research into this area is needed.

In fish, MARCO expression is upregulated in response to bacterial infection in common carp, red drum, and yellow croaker; this suggests they may play a role in bacterial recognition (Feng et al., 2016; He et al., 2014). A recombinant SRCR domain from a red drum MARCO-like protein was created and bound gram-negative and gram-positive aquatic bacteria (Qiu et al., 2013). In the present study, both rainbow trout MARCO variants bound robustly to human pathogenic gram-positive and gram-negative bacteria, as well as a fish pathogenic gram-negative bacterium (Figs. 3.4 and 3.5). These results align well with human MARCO, which can also bind *E. coli* and *S. aureus* (Arredouani et al., 2005). It is unsurprising rainbow trout MARCO variants play a role in binding to bacteria as this is a main role of MARCO in other species; it's importance is evident for example in MARCO −/− mice who have an impaired ability to clear S. *pneumoniae* from their lungs (Arredouani et al., 2004). MARCO also plays a role in controlling mycobacterium growth in zebrafish; morpholino knockdown of MARCO showed MARCO was required for phagocytosis of *M. marinum* after infection and this resulted in increased bacterial growth (Benard et al., 2014). Mammalian MARCO receptors bind to the bacterial cell wall

components LPS and LTA; however, gram-negative bacteria such as a *Neisseria meningitides* mutant strain that lacks lipid A are also bound by SR-A and MARCO (Mukhopadhyay et al., 2006). This suggests that there are other bacterial component ligands for scavenger receptors outside of the classic LTA and LPS, this area of study requires further research in both fish and mammals. Indeed, the importance of this receptor in fish bacterial pathogenesis is just beginning to be elucidated.

In mammals the SRCR domain of MARCO is the site of bacterial binding (Elomaa et al., 1998; van der Laan et al., 1999). A naturally occurring variant of MARCO (MARCO II) that is missing the SRCR domain acts as a dominant-negative interfering with MARCO function (Novakowski et al., 2016). The SRCR appears to be mediating ligand binding in rainbow trout as well; rtMARCO-1(ΔSRCR) and rtMARCO-2(ΔSRCR) where the SRCR domain was removed lost their ability to bind both *E.coli*, *S. aureus*, and *V. anguillarum* compared to their wildtype counterparts (Figs. 3.4 and 3.5). Although this data suggests that the SRCR is vital for binding bacteria via rainbow trout MARCO, the possibility cannot be ruled out that the SRCR is also important for protein folding or localization and the loss of receptor binding is the result of receptor misfolding or localization to the cell surface. Clearly further studies are necessary to clearly delineate a role for SRCR specifically in bacterial binding; regardless, it is likely that rtMARCO plays an important role in innate immune sensing of bacteria in rainbow trout.

rtMARCO-1 and -2's ability to bind zyomsan, a fungal cell wall component, was also tested. Zymosan was chosen for testing as a putative ligand for rtMARCO because it was tested as a ligand for human MARCO but appeared not to bind; however, zymosan was a ligand for zebrafish SCARA4 (Fukuda et al., 2011; Jang et al., 2009; Elomaa et al., 1998). In mammals, SCARA4's collagenous domain is necessary for binding bacteria or zymosan (Mori et al., 2014),

a domain also present in MARCO, as such we tested rtMARCO-1 and -2 for any zymosan binding capabilities and none was detected.

SR-As in mammals are key sensors for the innate antiviral immune response, being able to bind double-stranded (ds)RNA, a viral replicative product (DeWitte-Orr et al., 2010; Mian et al., 2013; Limmon et al., 2008). And while the role for MARCO specifically in binding dsRNA is not delineated in any species, red drum MARCO expression was upregulated by viral infection (Qiu et al., 2013). Thus it was possible that rtMARCO was involved in antiviral as well as antibacterial defense. This hypothesis was tested by observing rtMARCO-1 and -2's ability to bind poly I:C, a synthetic dsRNA. hSR-AI was included as a positive control, as hSR-AI was suggested to be the surface receptor for extracellular dsRNA in human epithelial cells (Limmon et al., 2008). Indeed in the present study fluorescently labeled high molecular weight (HMW) poly I:C bound hSR-AI overexpressing CHSE-214 cells (Fig. 3.7A). Pretreating cells with poly I:C prior to treatment with *E.coli* blocked bacterial binding, suggesting both ligands bind the same receptor at the same domain (Fig. 3.7B). These observations were not the same for rtMARCO where neither variant bound fluorescently labeled poly I:C nor could poly I:C block bacterial binding. Taken together these results suggest rainbow trout MARCO may not be involved in binding of dsRNA, or not with high enough affinity to be detected by fluorescence microscopy. It is also possible the GFP-tag that has been added to the protein is somehow interfering with dsRNA binding but not bacterial ligands. Further studies are underway to explore other candidate SR-As in rainbow trout for their role in dsRNA binding.

3.6 Conclusions

Class A scavenger receptors play in important role in innate immunity, with both bacterial, fungal and viral detection. The present study identifies two variants of MARCO, an SR-A family member, and characterizes its ability to bind bacteria but not viral or yeast

pathogen-associated molecular patterns (PAMPs). These findings are important for understanding pathogen-host interactions in fish. As well, MARCO in mammals functions as a co-receptor for other signaling pattern recognition receptors, such as the toll like receptors (Dorrington et al., 2013). Whether rtMARCO functions similarly has yet to be determined, but would broaden its capabilities within the innate immune detection system. Clearly further research is warranted to better understand MARCO in fish and its role as an innate immune sensor.

Acknowledgements

Dr. Niels Bols for kindly providing the cells for these experiments, Dr. Dawn Bowdish for providing the expression vectors, and Dr. Brian Dixon and Shawna Semple for providing the heat killed *Vibrio anguillarum*. Funding for the project was from an NSERC Discovery grant held by SDO and an Ontario Graduate Scholarship held by SJP.

Chapter 4: Identification of three class A scavenger receptors from rainbow trout (*Oncorhynchus mykiss*): SCARA3, SCARA4, and SCARA5

S.J. Poynter[a], A.L. Monjo[b], S.J. DeWitte-Orr[b,c]

[a] Department of Biology, University of Waterloo, Waterloo, Ontario, Canada

[b] Department of Biology, Wilfrid Laurier University, Waterloo, Ontario, Canada

[c] Department of Health Sciences, Wilfrid Laurier University, Waterloo, Ontario, Canada

Fish & Shellfish Immunology, 76, pp.121-125. 2018.

4.1 Overview

Class A scavenger receptors (SR-As) are a family of five surface receptors whose functions in mammals are associated with innate immunity; however, their role in fish immunity requires further elucidation. The present study identifies, performs sequence analysis, and constitutive transcript expression analysis for three SR-A family members, SCARA3, SCARA4 and SCARA5, from rainbow trout. This work will provide a basis for future studies on SR-A function and their role in innate immunity in this economically important fish.

4.2 Short Communication

Class A scavenger receptors (SR-As) are a family of five cell surface receptors, including: scavenger receptor class A I/II (SRAI/II), macrophage receptor with collagenous structure (MARCO), class A scavenger receptor (SCARA) member 3 (SCARA3), member 4 (SCARA4), and member 5 (SCARA5) (Whelan et al., 2012). In mammals, SR-As play important roles in macrophage-mediated clearance of pathogens (van der Laan et al., 1999), atherosclerosis (Moore et al., 2006), uptake of apoptotic cells (Platt et al., 1996), as innate immune sensors (DeWitte-Orr et al., 2009) and as surface receptors mediating virus entry (MacLeod et al., 2015). Mammalian SR-As are able to sense both endogenous ligands, such as modified low-density lipoproteins, and pathogen-associated molecular patterns, such as lipopolysaccharide (LPS) and double-stranded (ds) RNA (Limmon et al., 2008; Peiser et al., 2002). Different SR-As bind to their own set of ligands, with both overlap and exclusivity between them. For example, in mammals all SR-As, with the exception of SCARA3, bind bacteria, whereas only SCARA4 has been shown to bind to the yeast cell wall component zymosan (Jang et al., 2009; Whelan et al., 2012).

To date, SR-As have been identified in several fish species, including: large yellow croaker (*Larimichthys crocea*), zebrafish (*Danio rerio*), pufferfish (*Tetraodon nigroviridis*), common carp (*Cyprinus carpio*), and channel catfish (*Ictalurus punctatus*) (Feng et al., 2016; Fukuda et al., 2011; Guo et al., 2016; He et al., 2014). In rainbow trout (*Oncorhynchus mykiss*) a partial SCARA4 and two full-length MARCO sequences have been identified, but no verified full-length salmonid SR-A sequences are available for SCARA3, SCARA4, or SCARA5 (Poynter et al., 2015; Poynter et al., 2017). In addition to identifying novel SR-As in fish, the cognate ligands of SR- As and downstream functions in fish still require elucidation. In zebrafish, SCARA5 bound LPS, MARCO was required for phagocytosis of a mycobacterium, and

SCARA4 bound to zymosan and *S. aureus* but failed to bind to *E. coli*. SCARA4's binding pattern was different in mammals, where SCARA4 bound zymosan, *S. aureus* and *E. coli* (Benard et al., 2014; Fukuda et al., 2011; Jang et al., 2009; Meng et al., 2012).

In rainbow trout, scavenger receptor ligands were found to bind to two epithelial cell lines that expressed a partial sequence of SCARA4 (Poynter et al., 2015). Two variants of rainbow trout MARCO were identified and found to bind to two gram-negative and one gram-positive bacteria, but did not bind to dsRNA or zymosan (Poynter et al., 2017). To date, identified SR-A functions in fish include: innate immune modulation (Guo et al., 2016; Meng et al., 2012), pathogen clearance (Benard et al., 2014; Meng et al., 2012; Poynter et al., 2017; Qiu et al., 2013), and expression on the surface of nonspecific cytotoxic cells (Kaur et al., 2003). Cumulatively, these studies support the role of SR-As in the immune response, and suggest there are differences between fish and mammalian receptors. In the present study, we have identified the full coding sequence (CDS) of three scavenger receptors in rainbow trout, SCARA3 (accession: MF664681.1), SCARA4 (accession: MF664680.1), and SCARA5 (accession: KX452177.2). We have analyzed the deduced proteins, and looked at their constitutive expression in a panel of tissues isolated from healthy rainbow trout. This work lays the foundation for future functional studies to be performed and therefore contribute to a better understanding of the role of SR-As in teleost fish.

To identify the full-length rainbow trout SCARA3 and SCARA4 sequences, primers were designed based on the predicted sequences previously published on NCBI, XM_021611973.1 and XM_021562976, respectively. SCARA5 degenerate primers were designed based on consensus sequences between an unnamed rainbow trout sequence (CDQ63372.1), zebrafish and yellow croaker SCARA5 sequences (NM_001030190.1 and

NM_001303324.1). RNA was extracted from unstimulated RTgill-W1 (SCARA5) and RTG-2 (SCARA3 and SCARA4) cells, grown as previously described (Poynter and DeWitte-Orr, 2015; Poynter et al., 2015), using TRIzol (Life Technologies, Carlsbad CA, USA) as per manufacturers' instructions and RNA was treated with a DNA-free DNA removal kit (Fisher Scientific, Waltham MA, USA). PCR reactions were performed using Phusion Hot Start II High-Fidelity DNA Polymerase (Thermo Fisher Scientific, Waltham MA, USA) as previously described (Poynter et al., 2017). The PCR reactions were conducted in a T100 Thermal Cycler (Bio-Rad) at the following cycle conditions for SCARA5: 98°C for 30 s, 33 cycles of: 98°C for 7 s, 64°C for 20 s, 72°C for 1 min, 72°C for 10 min and the reaction was held indefinitely at 4°C. The following cycle conditions were used for SCARA3 and SCARA4: 98°C for 30 s, 34 cycles of: 98°C for 5 s, Ta (see Table 4.1) for 10s, 72°C for 1 min, 72°C for 10 min and the reaction was held indefinitely at 4°C. Resultant amplicons were purified using QIAquick Gel Extraction Kit (Qiagen, Hilden, Germany); products with the start or end of the CDS were cloned into pGEM T-easy vectors for sequencing after addition of A overhangs using GoTaq Flexi (Promega). To confirm their identity, PCR products or plasmids were sent to Laboratory Services (University of Guelph, Guelph ON, Canada) for sequence analysis. SCARA5 was sequenced in full; SCARA3 and SCARA4 were sequenced in overlapping fragments that were then assembled in silico to produce the full CDS.

Table 4.1. Primers used for qRT-PCR and sequencing. The forward (F) and reverse (R) primers presented in 5′-3′ direction, amplicon size, and annealing temperature for primers used in this study. SCARA5 was sequenced in full using a single set of primers; SCARA3 and SCARA4 were sequenced from overlapping fragments (using F1/R1 and F2/R2 primer combinations).

Product	Primer sequence (5'-3')	Product length	Annealing Temperature (°C)
Sequencing			
SCARA3F1/R1	F-ATGAAAGAAAGCTATTCTGG R-CCACATCTAGACGGACGCTC	1243	53
SCARA3F2/R2	F-GTTGAGCGGTCTGAAGTCCA R-TCAAGACACCGTGTCTGGGA	1033	65
SCARA4F1/R1	F-ATGCCCACAGACGATTTTGCAG R-CTGACTCGTCCAGGCGTATC	1009	50
SCARA4F2/R2	F-CCGACTACCTGTCCGACTTG R-CTGCATCGAGAAAGGGACCA	656	60
SCARA5F/R	F-ATGGAGAATAGGGCGATGTA R-TTAGGTGTTGCAGGTCACGC	1497	64
qRT-PCR			
SCARA3	F-GAACCTGAACAACACGGTGC R-CCACATCTAGACGGACGCTC	89	55
SCARA4	F-AGGACTCACTGCCCGATCT R-GGCCTCACTCTGCATCGAG	70	55
SCARA5	F-CATGACCCGTATGGAGGACC R-ACAGGCTCTCCAACTTCCAG	104	55

The resultant nucleotide sequence was translated into a deduced amino acid sequence using ExPASy (Artimo et al., 2012). The deduced protein sequences were aligned to other known published sequences using ClustalOmega; common domains were identified using SMART software (Feng et al,. 2016; Schultz et al., 1998) and figures were created using the IBS illustrator program (Liu et al,. 2015). All three scavenger receptor sequences contain a cytoplasmic and transmembrane domain, coiled-coil domain(s), and collagenous domains, as was expected based on sequences from other species, including human (Fig. 4.1A and B; Whelan et al., 2012). Domains were highlighted within the amino acid sequence and a moderate amount of conserved sequence was noted, with a high similarity between fish species (Fig. 1A). The EGRVEVFG and WGTVCDD sequences conserved amongst fish SCARA5 sequences were found in rtSCARA5 (Yap et al., 2015; Fig. 4.1A). Rainbow trout SCARA3 terminated at its collagenous domain,

while SCARA4 ended in a C-type lectin domain and SCARA5 ended in the conserved scavenger receptor cysteine-rich (SRCR) domain. These findings are consistent within respective receptors from other species (Whelan et al., 2012). Nucleotide sequences were aligned with ClustalW (within Mega7) and used to create a phylogenetic tree using Mega7 (Fig. 4.2) (Kumar et al., 2016); mosquito colmedin was included as an outgroup because it contains a transmembrane domain and multiple collagenous domains (Yap et al., 2015). The Neighbor-Joining method (Saitou and Nei, 1987) was used to predict a tree, a bootstrap test of 500 replicates was conducted, the percentage of replicate trees that taxa cluster together has been included next to branches (Felsenstein, 1985). Evolutionary distances were computed using p-distance method (Nei and Kumar, 2000) and units are number of base differences per site. Based on the phylogenetic analysis, each novel rainbow trout SR-A sequence clustered with high confidence with other fish sequences of each respective SR-A. These clusters were independent to those of mammalian SR-As (see Fig. 4.2).

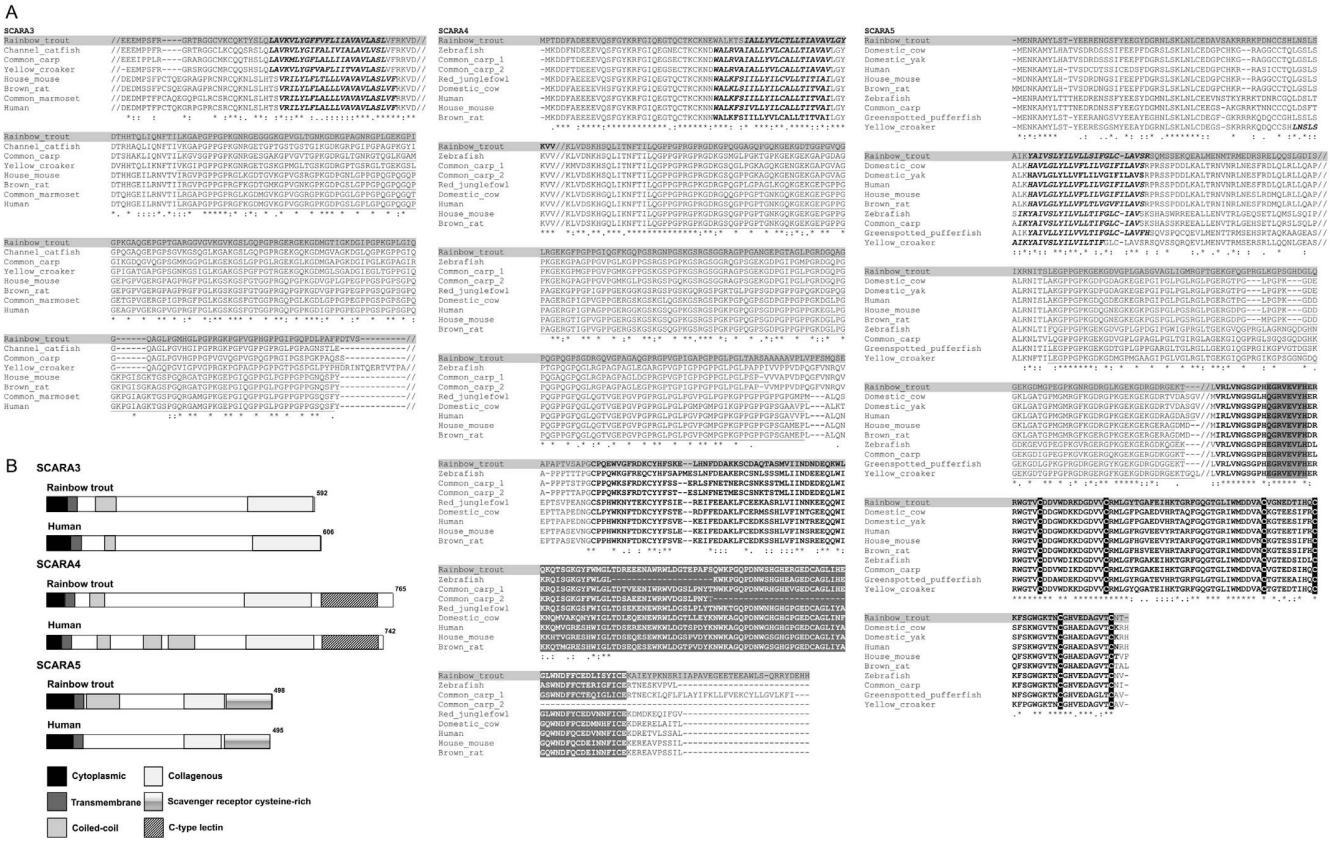

Figure 4.1. Rainbow trout scavenger receptor proteins have similar domains to other species. (A) The deduced rainbow trout SCARA3/4/5 sequences were aligned with known sequences from other fish and mammalian species. Only areas containing conserved domains are shown in this figure. Conserved domains were identified using SMART software and highlighted as followed: C-type lectin domain (grey background with white font), **scavenger receptor cysteine rich domain (SRCR)**, (bolded), conserved cysteines (black background white font), SCARA5 EGRVEVYH and WGTVCDD motifs (grey background black font), collagenous domain (underlined), *transmembrane region* (italics). //indicates a break in the protein sequence. **(B)** A visual representation of the conserved domains within the rainbow trout and human scavenger receptor sequences; domains were identified with SMART software and the illustrations were created using IBS software. Length of protein in amino acids is provided at the end of each protein figure.

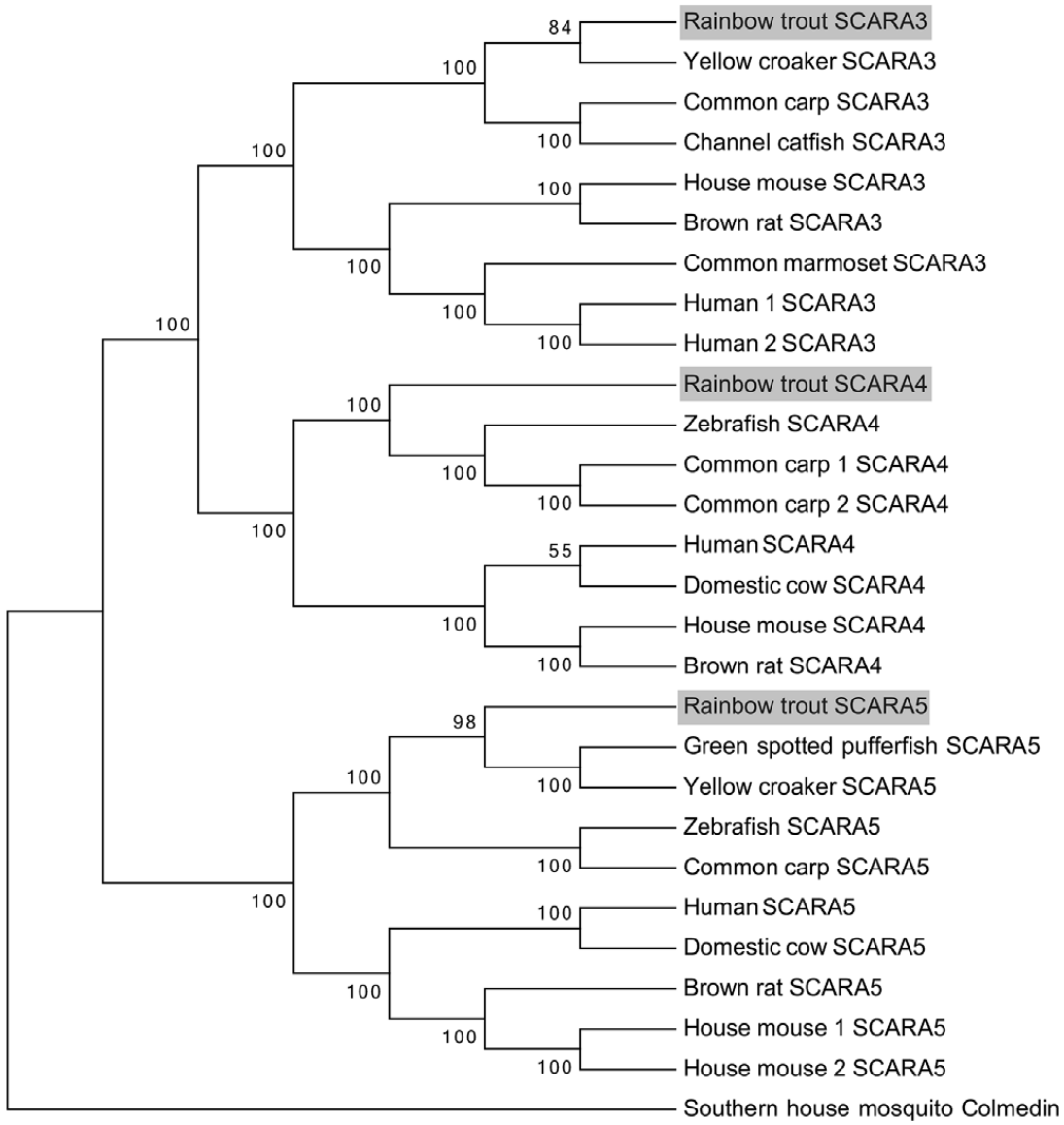

Figure 4.2. Phylogenetic tree analysis of rainbow trout scavenger receptor sequences. Nucleotide sequences were aligned with ClustalW (within Mega7) and used to create a phylogenetic tree using Mega7 with mosquito colmedin included as an outgroup. The Neighbor-Joining method was used to predict a tree, a bootstrap test of 500 replicates was conducted. All sequences were found in the NCBI database and accession numbers can be found in Supplementary Table 4.S.1.

SCARA3, SCARA4, and SCARA5 expression in healthy rainbow trout tissue was measured using qRT-PCR (Fig. 4.3). Tissue samples from four juvenile rainbow trout, between

75g and 210g, were added directly to TRIzol (50mg/mL) and homogenized using a manual homogenizer. RNA was extracted according to manufacturers' instructions and treated with a DNA-free DNA removal kit (Thermo Fisher Scientific). cDNA was synthesized using iScript reverse transcriptase (Bio-Rad) as previously described (Poynter and DeWitte-Orr, 2015). A no-reverse transcriptase (NRT) control reaction was also included for each sample and was then checked via qRT-PCR. Any samples that showed a NRT peak was re-DNase treated as per manufacturers' instructions. SsoFast EvaGreen supermix (Bio-Rad) was used for all qPCR reactions; reactions were assembled and performed as previously described (Poynter and DeWitte-Orr, 2015), primers are listed in Table 4.1. Data were analyzed using a $\Delta\Delta C_t$ method. Specifically, gene expression was normalized to the housekeeping gene (β-actin) and presented as relative to brain (SCARA3 and SCARA5) or spleen (SCARA4). Transcript data from the four different individual fish were pooled and the average expression levels were statistically analyzed using a one-way ANOVA and Tukey's post-hoc test using Kaleidagraph software with a 95% confidence interval (Synergy Software, Reading, PA, v4.1.0).

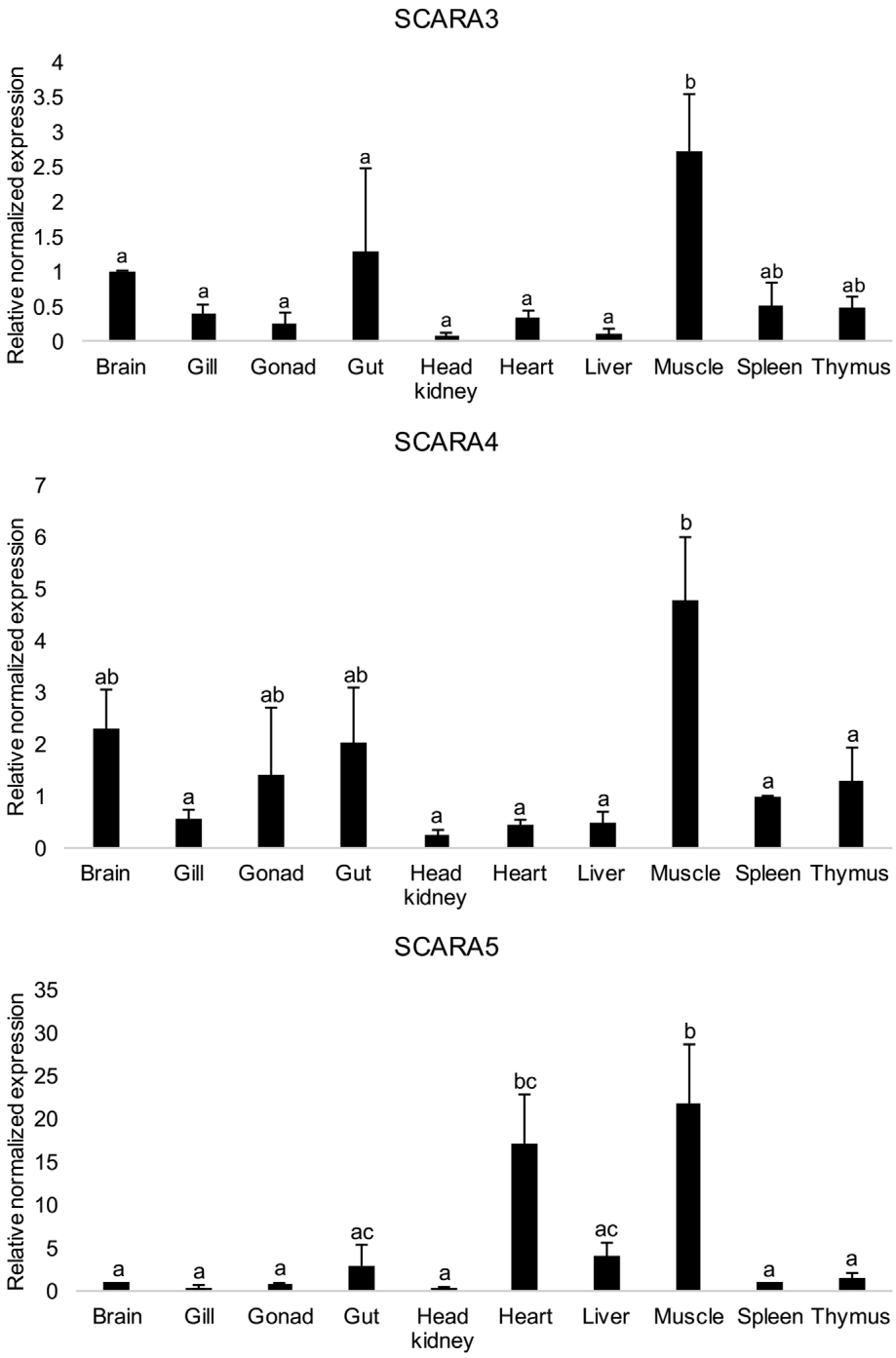

Figure 4.3. Constitutive expression of class A scavenger receptors at the transcript level in healthy rainbow trout tissue. Rainbow trout SCARA3, SCARA4, and SCARA5 expression in healthy, juvenile rainbow trout tissue samples. Data were analyzed using the $\Delta\Delta C_t$ method. Specifically, gene expression was normalized to the housekeeping gene (β-actin) and presented as relative to brain (SCARA3 and SCARA5) or spleen (SCARA4). Samples were taken from four different individual fish, the data were averaged and statistically analyzed using a one-way ANOVA and Tukey's post-hoc test using Kaleidagraph software with a 95% confidence interval (Synergy Software, Reading, PA, v4.1.0).

Tissue expression patterns appeared different between the SR-As; however the only statistically significant difference in expression was seen in the muscle, where SCARA3, SCARA4, and SCARA5 all showed high expression. This observation was similarly made in yellow croaker, where muscle demonstrated high expression of both SCARA3 and SCARA5 (He et al., 2014). Although not statistically significant, there were other constitutive expression patterns observed in rainbow trout that were similar to those observed in yellow croaker for SCARA3 and SCARA5 (He et al., 2014). For example, gut and gill showed low expression for SCARA3 and SCARA5, and SCARA5 expression was higher than SCARA3 in the liver for both species (He et al., 2014). There were also differences observed between the present study in rainbow trout and the yellow croaker study. In yellow croaker SCARA3 expression was the lowest in the gill whereas in rainbow trout this was the case for head kidney (He et al., 2014). There was also greater expression in the spleen and head kidney in yellow croaker compared to other tissues, in rainbow trout spleen and head kidney showed low expression for SCARA3 and SCARA5 (He et al., 2014). It is unclear at present whether the differences observed at the transcript level have physiological implications.

Class A scavenger receptors play an important role in many functions, including maintaining homeostasis and innate immunity. Their identification in rainbow trout will allow for further study of their role in teleost fish.

Acknowledgements

The authors wish to thank Dr. Brian Dixon for his gift of the rainbow trout used in this study and Aaron Frenette for his expertise in dissection. Funding for this project was provided from an NSERC Discovery grant to SDO.

4.3 Appendix

Table 4.S.1 Supplementary data

Sequence	Species name	Accession number
SCARA3		
Yellow croaker	*Larimichthys crocea*	NP_001290286.1
Brown rat	*Rattus norvegicus*	NP_001102340.1
House mouse	*Mus musculus*	NP_766192.1
Common carp	*Cyprinus carpio*	BAU33572.1
Channel catfish	*Ictalurus punctatus*	AHH37855.1
Human 1	*Homo sapiens*	NP_057324.2
Human 2	*Homo sapiens*	NP_878185.1
Common marmoset	*Callithrix jacchus*	JAB42881.1
SCARA4		
Common carp 1	*Cyprinus carpio*	BAU33574.1
Common carp 2	*Cyprinus carpio*	BAU33575.1
House mouse	*Mus musculus*	NP_569716.2
Human	*Homo sapiens*	NP569057.1
Red junglefowl	*Gallus gallus*	NP_001034688.1
Domestic cow	*Bos taurus*	NP_001095313.1
Brown rat	*Rattus norvegicus*	NM_001025721.1
Zebrafish	*Danio rerio*	NM_001122840.1
SCARA5		
Human	*Homo sapiens*	AAH33153.1
Domestic cow	*Bos taurus*	AAI42200.1
House mouse 1	*Mus musculus*	NP_083179.2
House mouse 2	*Mus musculus*	NP_001161790.1
Yellow croaker	*Larimichthys crocea*	NP_001290253.1
Zebrafish	*Danio rerio*	NP_001025361.1
Brown rat	*Rattus norvegicus*	NP_001129327.1
Common carp	*Cyprinus carpio*	BAU33576.1
Greenspotted pufferfish	*Tetraodon nigroviridis*	JQ954963.1
Colmedin		
Southern house mosquito	*Culex quinquefasciatus*	XM_001843280.1

Chapter 5: Two DExD/H-box helicases, DDX3 and DHX9, identified in rainbow trout are able to bind dsRNA

Sarah J Poynter[a], Shanee Herrington-Krause[b], and Stephanie J DeWitte-Orr[bc]

a Department of Biology, University of Waterloo, 200 University Ave W, Waterloo, ON N2L 3G1, Canada

b Department of Biology, Wilfrid Laurier University, 75 University Ave W, Waterloo, ON N2L 3C5, Canada

c Department of Health Sciences, Wilfrid Laurier University, 75 University Ave W, Waterloo, ON N2L 3C5, Canada

5.1 Overview

In mammals, the multi-functional DExH/D-box helicases, DDX3 and DHX9, are nucleic acid sensors with a role in antiviral immunity; their role in innate immunity in fish is not yet understood. In the present study, full-length DDX3 and DHX9 coding sequences were identified in rainbow trout (*Oncorhynchus mykiss)*. Bioinformatic analysis demonstrated both deduced proteins were similar to those of other species, with ~80% identity to other fish species and ~70-75% identity to mammals, and both protein sequences had conserved domains found amongst all species. Phylogenetic analysis revealed clustering of DDX3 and DHX9 with corresponding proteins from other fish. Cellular localization of overexpressed DDX3 and DHX9 was performed using GFP-tagged proteins and endogenous DDX3 localization was measured using immunocytochemistry. In the rainbow trout gonadal cell line, RTG-2, DHX9 localized mostly to the nucleus, while DDX3 was found mainly in the cytoplasm. Tissue distribution from healthy juvenile rainbow trout revealed ubiquitous constitutive expression, highest levels of DDX3 expression were seen in the liver and DHX9 levels were fairly consistent among all tissues tested. Stimulation of RTG-2 cells revealed that DDX3 and DHX9 transcripts were both significantly upregulated by treatment with the dsRNA molecule, poly I:C. A pull-down assay suggested both proteins were able to bind dsRNA. The conserved common domains found between the rainbow trout proteins and other species with defined antiviral roles; combined with the ability for the proteins to bind to dsRNA, suggest these proteins may play an important role in fish innate antiviral immunity.

5.2 Introduction

The DExD/H-box family of helicases includes a diverse array of proteins with multifunctional roles. Each DExD/H-box helicase contains a helicase motif II (DEAD, DEAH, DExD or DExH), as well as at least eight conserved motifs involved in adenosine triphosphate (ATP) binding and hydrolysis, nucleic acid binding, and RNA unwinding (Fullam and Schroder, 2013). The DExD/H domain is well conserved from viruses and bacteria to mammals (Fuller-Pace, 2006). DExD/H-box helicases are involved in nearly all aspects of RNA-related cell processes including pre-mRNA splicing, mRNA export, and translation (Linder and Janowsky, 2011; Tarn and Chang, 2009). In addition to roles in RNA metabolism, some DExD/H-box helicases play a role in the innate antiviral response, acting as sensors for viral nucleic acids and/or affecting downstream signaling events (Zhang et al., 2011; Kim et al., 2010; Miyashita et al., 2011). Sensing viral nucleic acids is a key factor in host recognition of a viral infection; nucleic acids with unique defining features act as pathogen-associated molecular patterns (PAMPs) that are recognized by host-derived pattern recognition receptors (PRRs). Long dsRNA produced during viral infection is one example of a nucleic acid PAMP, length is a distinguishing feature to separate viral dsRNA from host dsRNA. PRRs can be found on the cell surface (ex. class A scavenger receptors), in the endosome (ex. toll-like receptors (TLR) TLR9 or TLR3), or in the cytoplasm, (ex. RIG-I like receptors (RLRs) including RIG-I and MDA5; Takeuchi and Akira, 2010). MDA5 and RIG-I are DExD/H-box helicases that act as dsRNA sensors and play a pivotal role in activating signaling cascades, which culminate in the production of type I interferons (IFN) and the establishment of an antiviral state (Yoneyama et al., 2005). More recently, many other members of the DExD/H-box helicase family are now being recognized for their roles in nucleic acid sensing and mediating immune pathways (Sugimoto et al., 2014).

The present study focused on two DExD/H-box helicases that are not part of the RLR family, DHX9 and DDX3, in rainbow trout (*Oncorhynchus mykiss)*. DDX3 plays an important role in nearly all aspects of RNA metabolism (Schröder et al., 2010). In mammals DDX3 has two forms, DDX3X and DDX3Y, the genes encoding these proteins are found on the X and Y chromosomes respectively (Valiente-Echeverria et al., 2015). DDX3X is widely expressed and has many roles including cell homeostasis, innate immunity, and viral replication; DDX3Y protein is only expressed in the male germline and plays a role in spermatogenesis (Ditton et al., 2004). For the remainder of this study DDX3X will simply be referred to as DDX3. For host innate immunity, DDX3 increases type I IFN production by acting as a viral dsRNA sensor that associates with the adaptor protein IFN-β promoter stimulator 1 (IPS-1) to induce IFNs. DDX3 is also a transcriptional regulator that binds to the IFN-β promoter and enhances transcription (Schröder et al., 2008; Oshiumi et al., 2010A; Soulat et al., 2008). DDX3 reduces influenza A replication via its role in stress granule formation (Raman et al., 2016). In contrast to an antiviral function, DDX3 is also used by viruses to promote viral replication, as has been reported for hepatitis C virus, West Nile virus, and human immunodeficiency virus-1 (HIV-1; Ariumi et al., 2007; Radi et al., 2012; Chahar et al, 2013).

DHX9 (also known as Nuclear DNA helicase II (NDH II) or RNA helicase A (RHA)) has RNA, DNA, and triple-helical DNA structure helicase activity (Zhang and Grosse, 1994; Jain et al. 2010; Lee and Pelletier, 2016). In mammals, DHX9 binds dsRNA and signals through IPS-1 to induce type I IFN (Desmet and Ishii, 2012; Zhang et al., 2011). DHX9 is also a substrate for phosphorylation by the dsRNA-receptor protein kinase R (PKR; Sadler et al., 2009). As with DDX3, in addition to its antiviral activity used by the host, many viruses actively recruit DHX9 to enhance their replication. These viruses include: HIV-1, hepatitis C virus, cytomegalovirus,

adenovirus, hepatitis E, influenza A, classical swine fever virus, and foot and mouth disease virus (Lee and Pelletier, 2016).

Very few studies have explored DHX9 or DDX3 in teleost fish. DHX9 was identified in channel catfish (*Ictalurus punctatus;* Tian et al., 2017) and goldfish (*Carassius auratus;* Silva de Assis et al., 2013), neither study addressed a role for DHX9 in immunity. DDX3 has been identified in goldfish (Silva de Assis et al., 2013), olive (Japanese) flounder (*Paralichthys olivaceus*; Wang et al., 2015), orange-spotted grouper (*Epinephelus coioides*; Liu et al., 2017), and zebrafish (*Danio rerio*; Pradhan et al., 2012). In the olive flounder two DDX3 genes were identified from the transcriptome, DDX3a and DDX3b (Wang et al., 2015). Both genes were expressed in different proportions in a wide variety of tissues, and there were sex-dependent differences in expression, however unlike in mammals these variants are not sex-linked (Wang et al., 2015). Zebrafish DDX3 had differential expression in fish treated with heat-killed *Escherichia coli* (Pradhan et al., 2012). DDX3 from *Epithelioma Papulosum Cyprini* (EPC; a fathead minnow cell line), is a binding partner for the nonvirion (NV) proteins from two novirhabdoviruses, suggesting DDX3 plays an important role in either enhancing innate immunity or promoting virus replication in fish (Biacchesi et al., 2017). Additionally, overexpressed grouper DDX3 protected cells against grouper nervous necrosis virus but did not affect Singapore grouper iridovirus replication and was involved in enhancing IFN-related antiviral pathway components (Liu et al., 2017).

In this study, sequences for DDX3 and DHX9 from rainbow trout were identified and bioinformatically analyzed. Endogenous expression levels of both transcripts were measured in both cell lines and tissues, and the effect of stimulation with the synthetic dsRNA, polyinosinic:

polycytidylic acid (poly I:C) was measured in RTG-2 cells. The ability for DDX3 and DHX9 to bind to dsRNA was explored using *in vitro* transcribed dsRNA.

5.3 Materials and methods

5.3.1 Cell culture

The rainbow trout gonad (RTG-2), rainbow trout gill (RTgill-W1), rainbow trout gut (RTgutGC), and *epithelioma papulosum cyprini* (EPC) cell lines were obtained from N. Bols (University of Waterloo; Fijan et al., 1983; Kawano et al., 2011; Bols et al., 1994; Wolf and Quimby, 1962). Cell lines were grown in 75cm^2 plastic tissue culture flasks (BD Falcon, Bedford, MA, USA) at 20^{o}C (rainbow trout cells) and 25^{o}C (EPC) in Leibovitz's L-15 media (HyClone, Logan, UT, USA) supplemented with 10% v/v fetal bovine serum (FBS; Fisher Scientific, Fair Lawn, NJ, USA), and 1% v/v penicillin/ streptomycin (P/S; 10 mg/mL streptomycin and 10000U/mL penicillin; Fisher Scientific).

5.3.2 CDS Identification

Primers for the full-length coding sequences (CDS) of rainbow trout DDX3 and DHX9 were designed. DDX3 primers were designed from an unnamed rainbow trout protein product (CDQ76520.1) which demonstrated similarity to olive flounder DDX3 variant 1 (AKS43549.1). The DHX9 primers were based on a predicted Atlantic salmon (*Salmo salar*) DHX9 sequence (XM_014190662.1). DDX3 was amplified from start to stop codon using the predicted primers and DHX9 was sequenced in three overlapping fragments, Table 5.1. RNA was extracted from RTG-2 cells using TRIzol reagent (Invitrogen, Carlsbad, CA, USA) and DNase treated using the TURBO DNA-free kit (Fisher Scientific). cDNA was synthesized as per manufacturers' instructions using iScript Reverse Transcriptase Supermix (Bio-Rad, Hercules, CA, USA), 1µg of RNA/20µL reaction. PCR reactions were performed using Phusion High-Fidelity 2x master mix (ThermoFisher Scientific), 0.5µM forward primer, 0.5µM reverse primer, 2µL of cDNA and

nuclease-free water (Fisher Scientific) to a total volume of 20µL. The following protocol was completed in a T100 Bio-Rad thermocycler: 98°C - 30s, 29 cycles of 98°C - 10s, T_a (Table 5.1) - 10s, 72°C - 1min 30s, followed by a final extension at 72°C - 5min. DDX3 was cloned directly into the peGFP-C1 vector for sequencing of the full-length product; DHX9 fragments had A-overhangs added with GoTaq Flexi DNA polymerase (Promega, Madison, WI, USA) as per pGEM T-easy instructions, and were subsequently cloned into pGEM T-easy (Promega) for sequencing prior to full-length cloning into expression vectors.

5.3.3 Full-length DHX9 amplification

To PCR amplify the entire DHX9 sequence a method adapted from Shevchuk et al., 2004 was used. First three overlapping fragments were amplified as described above, Table 5.1. The products were gel purified using the QiaQuick gel extraction kit (Qiagen, Hilden, Germany). A 100µL PCR reaction (reaction A) containing Phusion High-Fidelity 2x master mix and 100ng of each purified product were combined and the following protocol was completed in a T100 Bio-Rad thermocycler: 98°C - 1min followed by 10 cycles of 98°C - 10s, 55°C - 10s, 72°C – 1min 30s. A second 100µl reaction (reaction B) containing Phusion High-Fidelity 2x master mix was created and included 3µl of unpurified reaction A and 0.5µM of DHX9 full-length forward and reverse primers with no tags, Table 5.1. The following protocol was completed: 98°C – 1 min, 34 cycles of 98°C - 10s, 55°C - 10s, 72°C – 2min, followed by 72°C – 5min. The product was then purified using the GeneJET PCR Purification kit (Fisher Scientific) and restriction sites were added using the pEGFP-C1-DHX9 primers from Table 5.1 under the conditions for reaction B. The sequences have been deposited into the NCBI database, DDX3: KY905155 and DHX9 (accession number not yet available).

Table 5.1. Primers, forward (F) and reverse (R), used for sequencing, cloning, and qRT-PCR for DDX3 and DHX9 in rainbow trout. Primer sequences are given in 5'-3' orientation, product size in base pairs (bp) and annealing temperatures (T_a) are reported. Where applicable: extra nucleotides for the GC clamp or to keep a protein in frame are shown in bold, a human influenza hemagglutinin (HA) protein tag sequence is italicized, restriction sites are underlined and reported in the primer name, and the GSG linker sequence is in bold italics.

Primer	Sequence 5'-3'	Size (bp)	T_a (°C)
Sequencing			
DDX3 Full-length	F - ATGAGTCATGTGGCCGTCG R - TTAGTTGCCCCACCAGTCCA	2136	50
DHX9 Frag.	F1-EcoRI - **GCGGCG**GAATTC**A**GCGGACATCAAGAACTTCCTGTAT R1 - AGTACTTGGATCAGGTGGCG	990	50
	F2 - GCTTTTGAGGTGAATGTGGTGGA R2 - TCTGGGGATCTGAGAGTGGA	1257	50
	F3 - ACACCTGGAGATGAACCCAC R3-ApaI - **GCGGGC**GGGCCCCTAATATCCCTGGCCCCCTCCATA	1798	50
DHX9 Full-length	F - ATGGCGGACATCAAGAACTTCCTGTAT R - CTAATATCCCTGGCCCCCTCCATA	3846	55
Cloning			
pCDNA3.1-DDX3-HA	F-EcoRI - **CGGCCG**GAATTCATGAGTCATGTGGCCGTCG R-XhoI - **GCGCCC**CTCGAGTTAGTTGCCCCACCAGTCCA***GG TAG TGGT*** *TACCCATACGATGTTCCAGATTACGCT*	2216	50
pCDNA3.1-DHX9-HA	F-EcoRI - **GCGGCG**GAATTCATGGCGGACATCAAGAACTTCCTGTAT R-XbaI - **GCGCCC**TCTAGACTAATATCCCTGGCCCCCTCCATA***GG TAG TGGT***TACCCATACGATGTTCCAGATTACGCT	3926	50
peGFP-C1-DDX3	F-XhoI - **CGGCCG**CTCGAG***C***GAGTCATGTGGCCGTCG R-EcoRI - **GGGCCC**GAATTCTTAGTTGCCCCACCAGTCCA	2158	50
peGFP-C1-DHX9	F - see DHX9 Frag F1 R - see DHX9 Frag R3	3868	50
qRTPCR			
DDX3 qPCR	F - GAAACCAAGAAGGGAGCGGA R - GGATACTGGTGCAGGCGTAA	70	55
DHX9 qPCR	F - GGGTATTTGAGCCTGTGCCT R - CTTCCTCTGCTCCAGGTTGG	197	55
MDA5 qPCR	F - GGTGTCCTGATGGCTGTGAA R - CCAATGTCTCCTGCTCTGGG	109	55

5.3.4 Bioinformatics

DDX3 and DHX9 nucleotide sequences were translated into deduced amino acid sequences using ExPASy; subsequent analysis was performed on these sequences (Artimo et al., 2012). Conserved motifs found within the DDX and DHX families were identified based on the report by Tian et al., 2017. The amino acid sequences were compared to other published sequences using EMBOSS Needle pairwise sequence alignment and the percent similarity and identity are reported. Amino acid sequences were aligned using ClustalW (within MEGA7) and MEGA7 was used to create a Neighbor-joining tree using the p-distance method (Saitou and Nei, 1987; Kumar et al., 2016; Nei and Kumar, 2000). A bootstrap analysis was done for 1000 replicates, the percentage of replicate trees that create the presented clusters is shown above each branch (Felsenstein, 1985). Conserved domains were identified using the NCBI conserved domain search and figures were created using the IBS illustrator program (Marchler-Bauer et al., 2014; Liu et al., 2015). All accession numbers can be found in Table 5.2.

5.3.5 qRT-PCR

5.3.5.1 RNA extraction

Tissue samples were collected from three juvenile rainbow trout, ranging in weight between 75g and 210g. Tissue was added to TRIzol reagent (50mg tissue/mL TRIozl; Invitrogen) and homogenized with a manual homogenizer. For endogenous expression rainbow trout cells were plated at $1x10^6$ cells in a 6-well plate (BD Falcon), after overnight attachment TRIzol was added to the monolayer. RNA was isolated using TRIzol reagent (Invitrogen) and treated using the TURBO DNA-free kit (Fisher Scientific). For stimulation studies, RTG-2 cells were plated at $8x10^5$ cells in a 6-well plate (BD Falcon) and allowed to attach overnight. Cells were treated with 50µg/mL poly I:C (resuspended in PBS at 10mg/mL; Sigma-Aldrich) in

regular growth media, or media alone, for 4h or 24h. RNA was extracted using the Bio-Rad Aurum RNA extraction kit, including an on-column DNase I digestion (Bio-Rad).

5.3.5.2 cDNA synthesis and qPCR reactions

RNA from tissues and cell lines was reverse transcribed to cDNA using iScript reverse transcriptase as per manufacturers' instructions at 1µg of RNA/20µL reaction. qPCR reactions contained: 2µl of 10^{-1} diluted cDNA, 1X SsoFast EvaGreen Supermix (Bio-Rad, Hercules, CA), 0.2µM forward primer, 0.2µM reverse primer, and nuclease-free water (Fisher Scientific) to a total volume of 10µL, primers listed in Table 5.1. Triplicate technical replicates were performed. qPCR reactions were performed using the CFX Connect Real-Time PCR Detection System (Bio-Rad). The program used for all qPCR reactions was: 98°C - 2 min, 40 cycles of 98°C - 5s, 55°C - 10s, followed by a melting curve completed from 65°C to 95°C with a read every 5s. Product specificity was determined through single PCR melting peaks, and a no-reverse transcriptase (NRT) control reaction was also included for each sample. Data were analyzed using the $\Delta\Delta C_t$ method; gene expression was normalized to the housekeeping gene (β-actin). For tissue and cell culture endogenous expression samples were presented as relative to the gonadal tissue sample or RTG-2 cells. For poly I:C stimulation trials the data are presented as relative to an unstimulated control. Data represent three individual fish or three independent replicates and were statistically analyzed with GraphPad Prism version 7.00 for Mac (GraphPad Software, La Jolla, CA USA, www.graphpad.com). A one-way ANOVA with Tukey's multiple comparison test was used to check for significant differences between data points, a p value<0.05 was considered significant.

5.3.6 Expression vectors and cellular localization

The two plasmids used in this study were peGFP-C1 (Clontech, Mountain View, California, USA) and pCDNA3.1 (+) (Invitrogen). Cloned inserts were amplified using Phusion

High-Fidelity 2x master mix as described in 5.3.2 and 5.3.3 and gel purified using the QiaQuick gel extraction kit (Qiagen). The insert and vector were digested with the two restriction enzymes (FastDigest Thermo Fisher) corresponding to the added restriction sites on the insert, for 1h at 37^{o}C, Table 5.1. A 5:1 ratio of insert to 50ng of vector were ligated with NEB T4 ligase, overnight at 4^{o}C (New England Biolabs, Ipswich MA, USA). Plasmids was transformed into JM109 competent *E. coli* cells (Promega). Positive colonies were cultured overnight in Luria broth containing 100µg/mL of kanamycin or ampicillin (peGFP-C1 or pCDNA3.1 respectively) and plasmids were purified using the GenElute Plasmid Preparation kit (Sigma-Aldrich). For cellular localization, 3x10^{5} RTG-2 cells were plated in 12-well plates (BD Falcon) on glass coverslips. Plasmids were transfected into RTG-2 cells using Fugene6 (Promega) at a ratio of 1µg plasmid to 3µL of Fugene6. At 48h post-transfection cells were fixed using 10% neutral buffered formalin, nuclei were counterstained with 10µg/mL 4',6-diamidino-2-phenylindole (DAPI; Fisher Scientific), and coverslips were mounted on glass slides with SlowFade Gold mounting medium (Fisher Scientific). Images were captured using an inverted fluorescence microscope, Nikon Eclipse TiE with Qi1 camera.

5.3.7 Immunofluorescence

RTG-2 cells were plated at 2x10^{5} cells in a 12-well plate (BD Falcon) on glass coverslips and cells were allowed to attach overnight. Cells were rinsed with PBS before fixation with 10% neutral buffered formalin and permeabilized in 0.1%v/v Triton-X-100 in PBS. After a 1h blocking period in blocking buffer (3% w/v BSA, 3% v/v goat serum, 0.02%v/v Tween-20, in PBS) the primary rabbit anti-DDX3 antibody (CusaBio, CSB-PA002106) was applied at a 1:100 dilution in blocking buffer for 1h. A goat anti-rabbit Fluorescein isothiocyanate (FITC) secondary antibody (Santa Cruz; SC2012) was applied at a 1:200 dilution in blocking buffer for 1h. Nuclei were counterstained with 10µg/mL DAPI (Fisher Scientific) and coverslips were

mounted on glass slides with SlowFade Gold mounting medium (Fisher Scientific). Images were captured using an inverted fluorescence microscope, Nikon Eclipse TiE with Qi1 camera. A secondary only control was used to account for background fluorescence. There have been no reported antibodies that cross-react with teleost DHX9. Cross-reactivity trials with one commercially available DHX9 antibody (A300-854A) were attempted and were unable to detect rainbow trout DHX9; the antigen of most commercial antibodies surveyed did not encompass a conserved area in the rainbow trout protein and therefore were not experimentally tested. DHX9 localization was measured using GFP-tagged protein overexpression and expression was limited to qRT-PCR studies for transcript expression.

5.3.8 Western blotting

Tissue samples from three juvenile rainbow trout, between 75g and 210g, were taken and added directly to lysis buffer. Prior to protein extraction RTG-2, RTgill-W1, and RTgutGC were plated at $1x10^6$ cells in a 6-well tissue culture plate and allowed to attach overnight (BD Falcon). Proteins were extracted from tissue or cells lines using radioimmunoprecipitation assay (RIPA) buffer (50mg tissue/mL or $1x10^6$ cells/250µL; 25mM Tris, 150mM NaCl, 0.1% SDS, 0.5% sodium deoxycholate, 1% Triton-X 100). Before use 2µL/mL of protease inhibitor cocktail (Sigma-Aldrich) was added to RIPA buffer. Proteins were quantified using Bio-Rad Quick Start Bradford Protein Assay (Bio-Rad) and 20µg of protein samples were run on a 10% acrylamide SDS-PAGE gel alongside 5µL of PageRuler Prestained Protein Ladder (Thermo Scientific), after which proteins were transferred onto a polyvinylidene fluoride (PVDF) membrane (Bio-Rad) using the Trans-Blot Turbo system (Bio-Rad) and the mixed molecular weight program (1.3A; up to 25V for 7min). Blots were blocked for 1h in 5% skim milk powder in tris buffered saline with 0.1% Tween 20 (TBS-T). Blots were probed with a 1:2000 dilution of rabbit anti-DDX3 primary antibody (CusaBio, CSB-PA002106) or rabbit anti-β-actin (Sigma-Aldrich, A2066) for

1h at room temperature. Blots were incubated in a 1:4000 dilution of goat anti-rabbit HRP-conjugated secondary antibody (Bio-Rad, 172-1019) for 1h at room temperature. Protein was detected on blots using the chemiluminescent Clarity Western ECL Substrate (Bio-Rad) and images were captured using a VersaDoc Imager (Bio-Rad).

5.3.9 Pull-down assay

EPC cells were seeded at $2x10^6$ cells in a $25cm^2$ flask (BD Falcon). After overnight incubation cells were transfected with 4µg of plasmids for expression of HA-tagged protein and 12µl of Fugene6 transfection reagent in L-15 with 10% FBS and no antibiotics. 72h post-transfection cells were lysed using 500µl of lysis buffer containing 50mM Tris, 150mM NaCl, pH 7.2 and 1%v/v Triton-X-100. Before use 2µl/mL of protease inhibitor cocktail (Sigma-Aldrich) was added to lysis buffer. The cell lysate was mixed with 10µl of anti-HA magnetic beads (Bimake, Houston, TX, USA) that had been equilibrated in tris-buffered saline (TBS). 1µg of *in vitro* transcribed dsRNA, a 200bp molecule of viral sequence (previously described in Poynter and DeWitte-Orr, 2015), was added to the cell mixture and the cell/protein/dsRNA mix was rotated overnight at 4^oC. Beads were washed with TBS until a NanoLite Spectrophotometer (Fisher Scientific) read 0 at absorbance 260nm. The beads were boiled in 20µL of 1x DNA gel loading dye (Fisher Scientific) and an immunoblot was performed using the J2 monoclonal antibody for dsRNA, as previously described (Appendix A). The immunoblot included 1µg of dsRNA ladder (New England BioLabs) and 20ng of the *in vitro* transcribed dsRNA as controls.

5.4 Results

5.4.1 Rainbow trout DDX3 and DHX9 sequence similarity and phylogeny

Full-length coding sequences of DDX3 and DHX9 were identified from rainbow trout cells. The deduced amino acid sequence of DDX3 aligned with 98% similarity to an unnamed rainbow trout protein product in the NCBI database (CDQ76520.1) and 87% similarity to the

olive flounder 2 protein (DDX3b), and out of surveyed sequences had the lowest similarity to brown rat (*Rattus norvegicus*), Table 5.2. DHX9 had an 89.2% similarity to zebrafish and was least similar to the American alligator (*Alligator mississippiensis*), Table 5.2. A Neighbor-joining tree was used to infer evolutionary history; both rainbow trout DDX3 and DHX9 clustered closely with other fish species, unsurprising given the high sequence similarity, Fig. 5.1. The fish species formed a clade separate from the other non-fish species for each protein. The rainbow trout DDX3 clustered more closely to the second variant of olive flounder DDX3 (DDX3b), whereas the other fish species examined clustered with the first olive flounder variant, DDX3a.

Table 5.2. Sequence similarity of rainbow trout DDX3 and DHX9 proteins to other animal species. Emboss Needle pairwise alignment was used to compare the deduced rainbow trout protein sequences to published (A) DDX3 and (B) DHX9 sequences available on NCBI. % identity indicates the percentage of identical matches over reported aligned region, % similarity is the percentage of identical matches as well as similar amino acids (those awarded a positive value from the alignment matrix).

A
DDX3

Species	Accession	% Identity	% Similarity
Rainbow trout *Oncorhynchus mykiss*	CDQ76520.1 unnamed protein product	98.0	98.0
Olive flounder 2 *Paralichthys olivaceus*	AKS43550.1	81.0	87.0
Fathead Minnow *Pimephales promelas*	CZQ42530.1	80.4	85.6
Olive flounder 1 *Paralichthys olivaceus*	AKS43549.1	79.7	83.4
African clawed frog *Xenopus laevis*	NP_001080283.1	73.4	80.9
Western clawed frog *Xenopus tropicalis*	NP_989196.1	73.8	80.7
Domestic cow *Bos taurus*	NM_001192962.1	70.7	78.1
Human *Homo sapiens*	AAC34298.1	70.4	77.9
House mouse *Mus musculus*	NP_034158.1	70.3	77.7
Golden hamster *Mesocricetus auratus*	NM_001281387.1	70.2	77.6
Brown rat *Rattus norvegicus*	NM_001167665.1	68.5	76.0

B
DHX9

Species	Accession	% Identity	% Similarity
Zebrafish *Danio rerio*	NP_001188373.1	80.3	89.2
Japanese pufferfish *Takifugu rubripes*	BAV72136.1	78.3	87.0
African clawed frog *Xenopus laevis*	NP_001087383.1	75.7	85.4
Domestic cow *Bos taurus*	NP_776461.1	74.6	83.5
Human *Homo sapiens*	NM_001357.4	74.8	84.0
Rainbow trout *Oncorhynchus mykiss*	CDQ56455.1 unnamed protein product	73.1	73.3
Brown rat *Rattus norvegicus*	NP_001100654.1	71.4	80.1
House mouse *Mus musculus*	NP_031868.2	70.4	79.1
American alligator *Alligator mississippiensis*	KYO24241.1	56.1	62.8

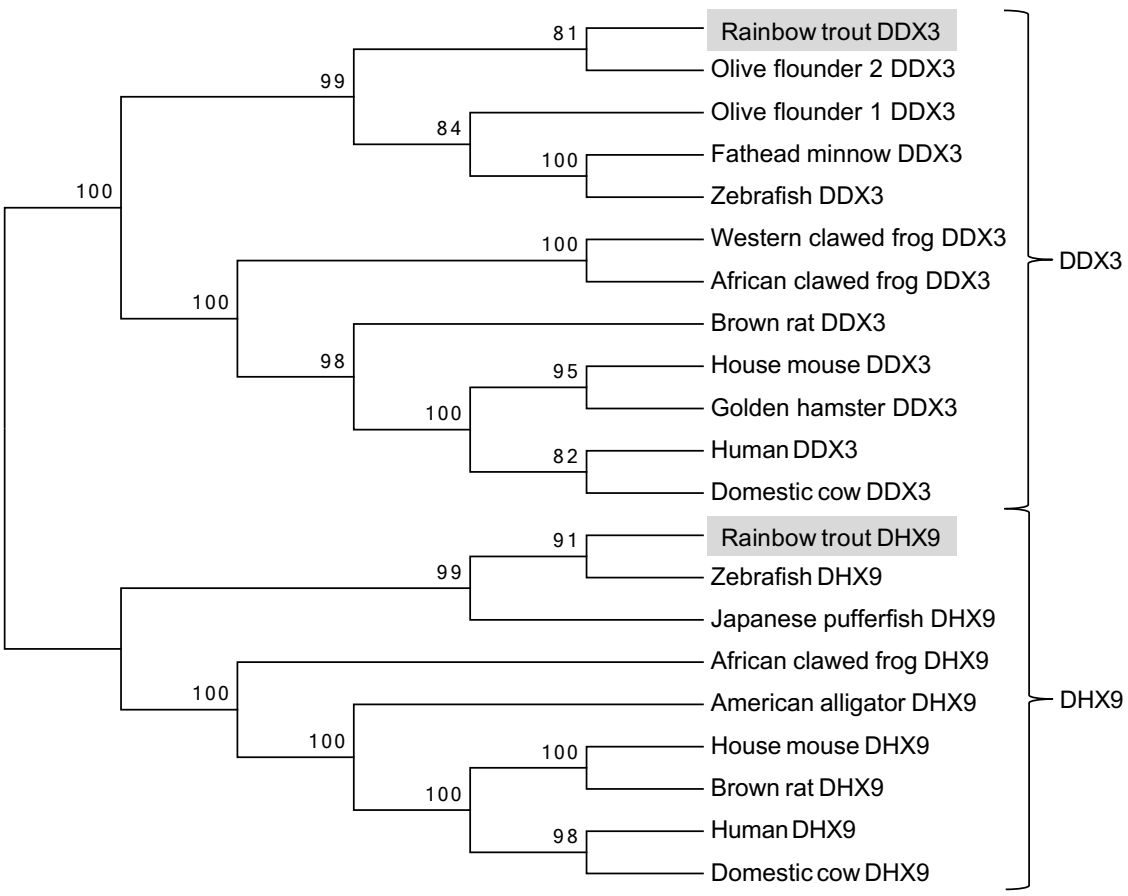

Figure 5.1. Rainbow trout DDX3 and DHX9 cluster closely with respective proteins from other fish species. A Neighbor-joining tree was constructed based on the deduced protein sequence of rainbow trout DDX3 and DHX9 and published protein sequences from NCBI. Analysis was performed using Mega 7 after alignment with ClustalW. 1000 bootstrap replicates were tested and the percentage of replicates trees where the shown taxa clustered together is reported above each branch. Accession numbers are reported in Table 5.2.

5.4.2 Conserved domains and motifs in rainbow trout DDX3 and DHX9

The conserved sequence motifs common to DEAD-box or DExH-box helicases were identified. All DDX3 sequences, including rainbow trout, contained nine conserved motifs (Q, I, Ia, Ib, II (DEAD), III, IV, V and VI), while the DHX9 sequences, including the rainbow trout sequence, contained eight conserved motifs (Q, Ia, Ib, II (DEIH), III, IV, V and VI), Fig. 5.2A (Tian et al., 2017). These motifs were conserved between all animal species included for analysis. NCBI's conserved domain search software was used to identify conserved domains in the rainbow trout DDX3 and DHX9 protein sequences, Fig. 5.2B. The DDX3 proteins contain: a

SRMB domain (COG0513), the superfamily II DNA and RNA helicases; the DEAD_C domain (cd00268) a helicase domain found in members of the DEAD-box family; and the Helicase_C domain, a helicase conserved C-terminal domain, only found in DEAD/H helicases that contains motif III involved in ATP hydrolysis and RNA binding. DHX9 proteins contain: a DEXDc domain (cd00046), found in members of the DEAD-like helicases superfamily and contains an ATP binding site, a putative Mg^{++} binding site; the Helicase_C domain (pfam00271); an HA2 domain (SM00847), a helicase-associated domain found in a diverse set of RNA helicases; two DSRM domains (Smart00358), double-stranded RNA binding motifs, and an OB_NTP_BIND domain (pfam07717), an oligonucleotide/oligosaccharide-binding-fold found in the C-terminus of DEAD-box helicases, generally associated with the HA2 domain.

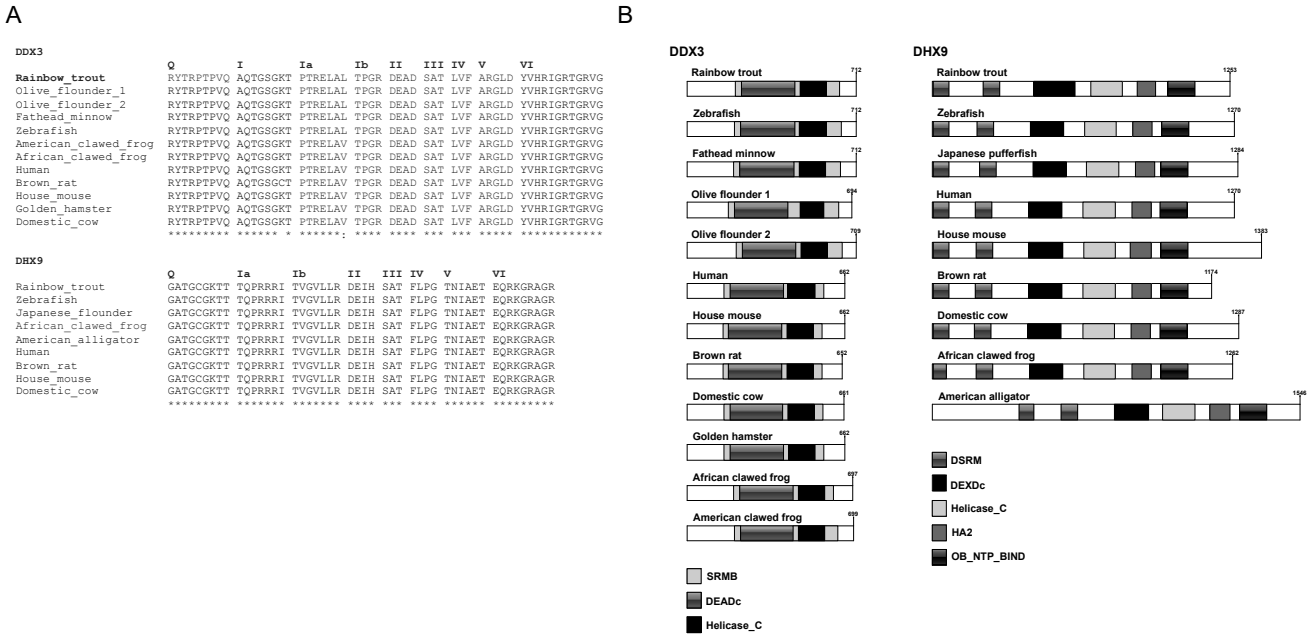

Figure 5.2. Rainbow trout DDX3 and DHX9 proteins have conserved motifs and domains. **(A)** Nine and eight conserved motifs were identified in DDX3 and DHX9 rainbow trout protein sequences respectively, as well as in the amino acid sequences of other species. Amino acids that are identical between all species are marked with an asterisk. **(B)** Conserved domains were identified in the DDX3 and DHX9 proteins using the NCBI conserved domain search and figures were created using the IBS illustrator program. Proteins and domains are drawn to scale with the total length in amino acids is reported at the end of each protein. Accession numbers can be found in Table 5.2. The DDX3 protein domains identified were: the SRMB domain (COG0513), the superfamily II DNA and RNA helicases; the DEAD_C domain (cd00268) a helicase domain found in members of the DEAD-box family; and the Helicase_C domain, a helicase conserved C-terminal domain, only found in DEAD/H helicases. The DHX9 protein domains identified were: a DEXDc domain (cd00046), found in members of the DEAD-like helicases superfamily; the Helicase_C domain (pfam00271); an HA2 domain (SM00847), a helicase-associated domain; two DSRM domains (Smart00358), double-stranded RNA binding motifs, and an OB_NTP_BIND domain (pfam07717), an oligonucleotide/oligosaccharide-binding fold.

5.4.3 Differential cellular localization of DDX3 and DHX9 in rainbow trout cells

Cellular localization of DDX3 and DHX9 was first measured using ectopically expressed proteins. The intracellular location of GFP-tagged DDX3 and DHX9 proteins was monitored in RTG-2 cells using fluorescence microscopy, Fig. 5.3. peGFP-C1-DDX3 localized to the cytoplasm, exhibiting a consistent punctate structure, Fig. 5.3A. Interestingly, when the cellular localization of endogenous DDX3 was measured using immunocytochemistry (ICC; Fig. 5.4) this punctate staining was not reproduced. Using ICC, DDX3 was still cytoplasmic, but with a more diffuse and even staining pattern. peGFP-C1-DHX9 localized mainly to the nucleus, with some cells showing low levels of green fluorescence in the cytoplasm, Fig. 5.3B. Some nuclei exhibited brightly fluorescent punctate structures, while all nuclei exhibited fluorescent exclusion from the nucleoli. Nucleoli were identified by localized DAPI staining exclusion (Sirri et al., 2008), as indicated by arrowheads, Fig. 5.3B.

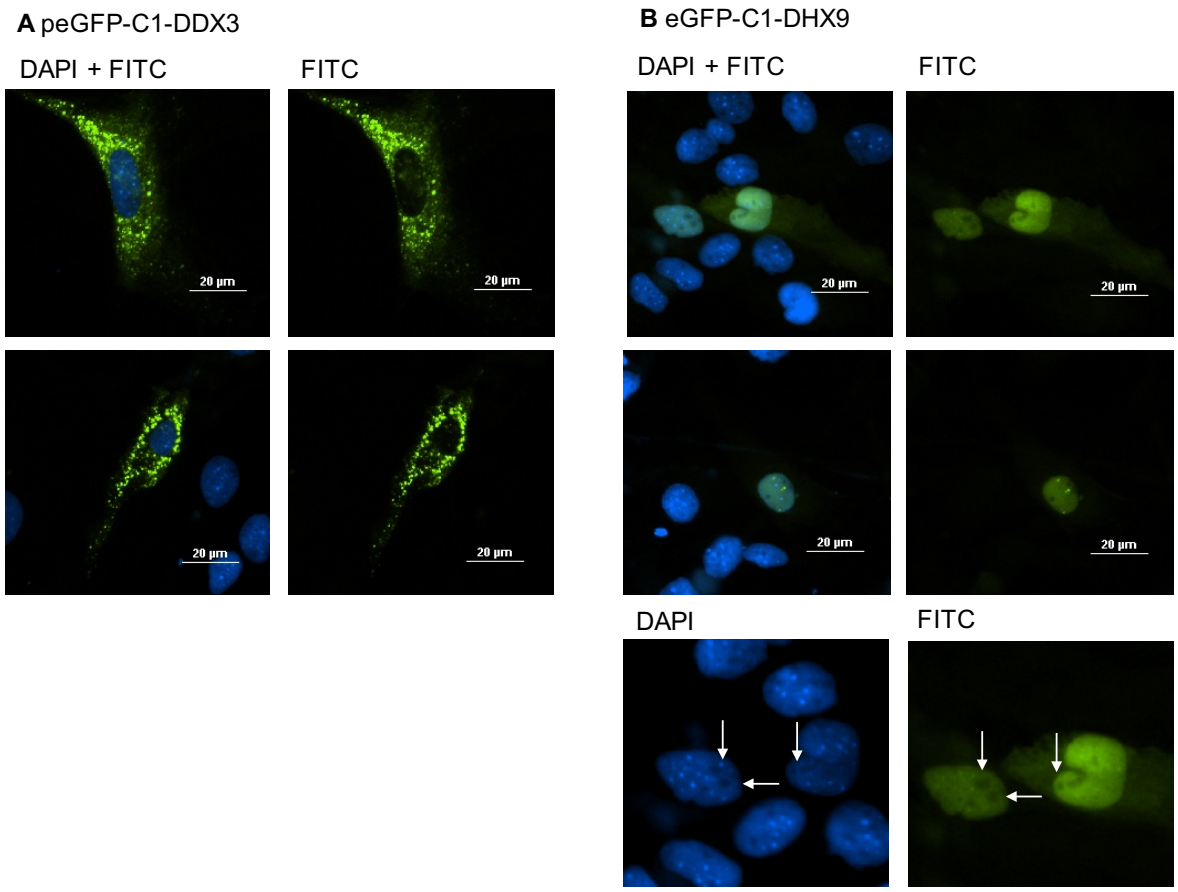

Figure 5.3. In rainbow trout cells, ectopic expression of DDX3 and DHX9 reveals that DDX3 localizes in punctate cytoplasmic structures and DHX9 localizes to the nucleus with nucleolus exclusion. Rainbow trout **(A)** DDX3 and **(B)** DHX9 sequences in the pEGFP-C1 expression vector were overexpressed in RTG-2 cells (GFP; green) and nuclei were counterstained with DAPI (blue). Two different fields of view are shown for each protein. The bottom image of **(B)** is a close-up image of a DHX9-expressing cell with white arrowheads indicating areas of DAPI exclusion in the nucleus, indicating nucleoli, and the corresponding areas of low-FITC expression. Magnification 400 X for both A and B.

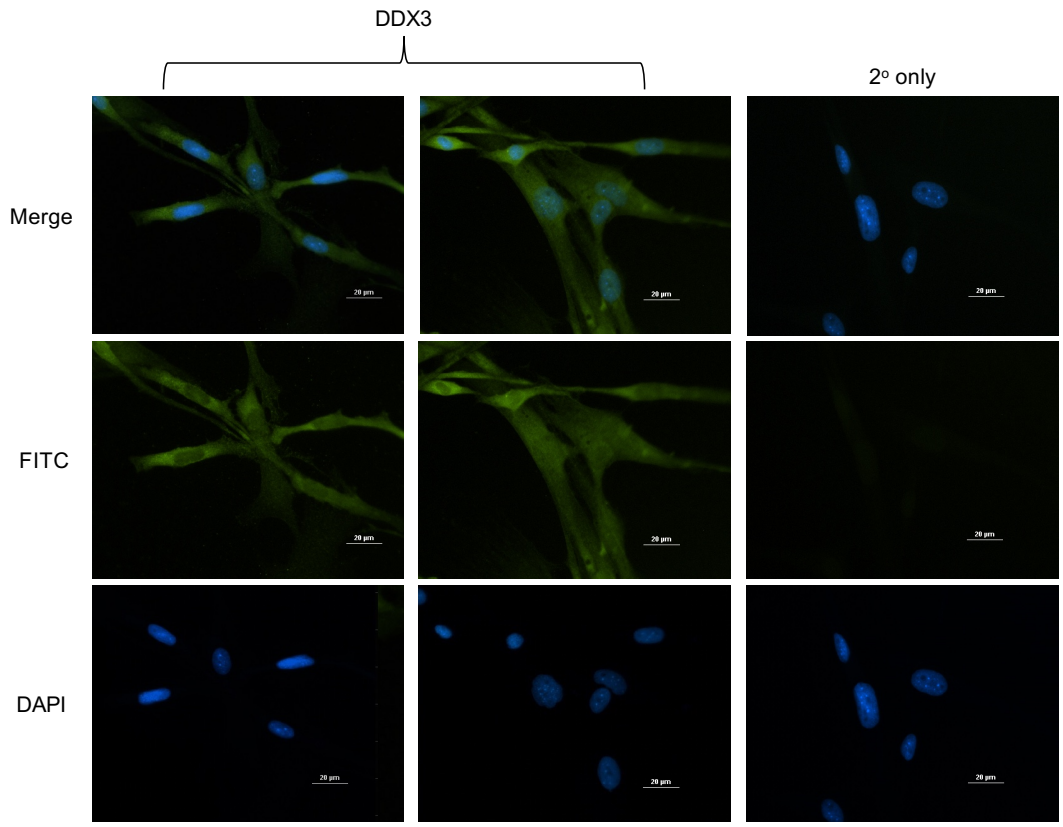

Figure 5.4. Immunocytochemistry for endogenous DDX3 shows localization is cytoplasmic but not punctate. To look at endogenous protein expression an anti-DDX3 antibody was used to detect DDX3 (FITC; green) in unstimulated RTG-2 cells. Nuclei were counterstained with DAPI (blue). A secondary (2^o) only control showed no background FITC signal. Magnification 200X.

5.4.4 Ubiquitous, constitutive expression patterns for DDX3 and DHX9 in rainbow trout tissues and cell lines

DDX3 and DHX9 expression patterns were measured in tissues extracted from juvenile rainbow trout and from three rainbow trout cell lines. Transcripts for DDX3 and DHX9 were found in the ten tissues tested, Fig. 5.5A. Brain and heart showed levels that were elevated higher than gut and liver showed transcript levels higher still, Fig. 5.5A. Head kidney, spleen, thymus, gill, gonad, and muscle showed levels of DDX3 that were not significantly different than gut. While not quantitative, at the protein level gonad, brain and liver showed a trend towards higher amounts of protein being expressed, Fig. 5.5C. The three common rainbow trout cell lines, RTG-

2, RTgutGC, and RTgill-W1 expressed DDX3 transcripts, with no significant difference between the cell lines, Fig. 5,5B. In cell lines at the protein level RTG-2, RTgill-W1, and RTgutGC showed similar levels of DDX3, Fig. 5.5C. DHX9 transcripts were also found in all ten tissues. There were no significant differences between any tissues, however gut showed the highest amounts of transcript, with considerable variability, and gonad had the lowest levels of expression, Fig. 5.5A. In the three cell lines tested there was no significant difference between the cell lines, although there was a slightly increased level of transcript in RTgill-W1 compared to RTG-2 and RTgutGC, Fig. 5.5B.

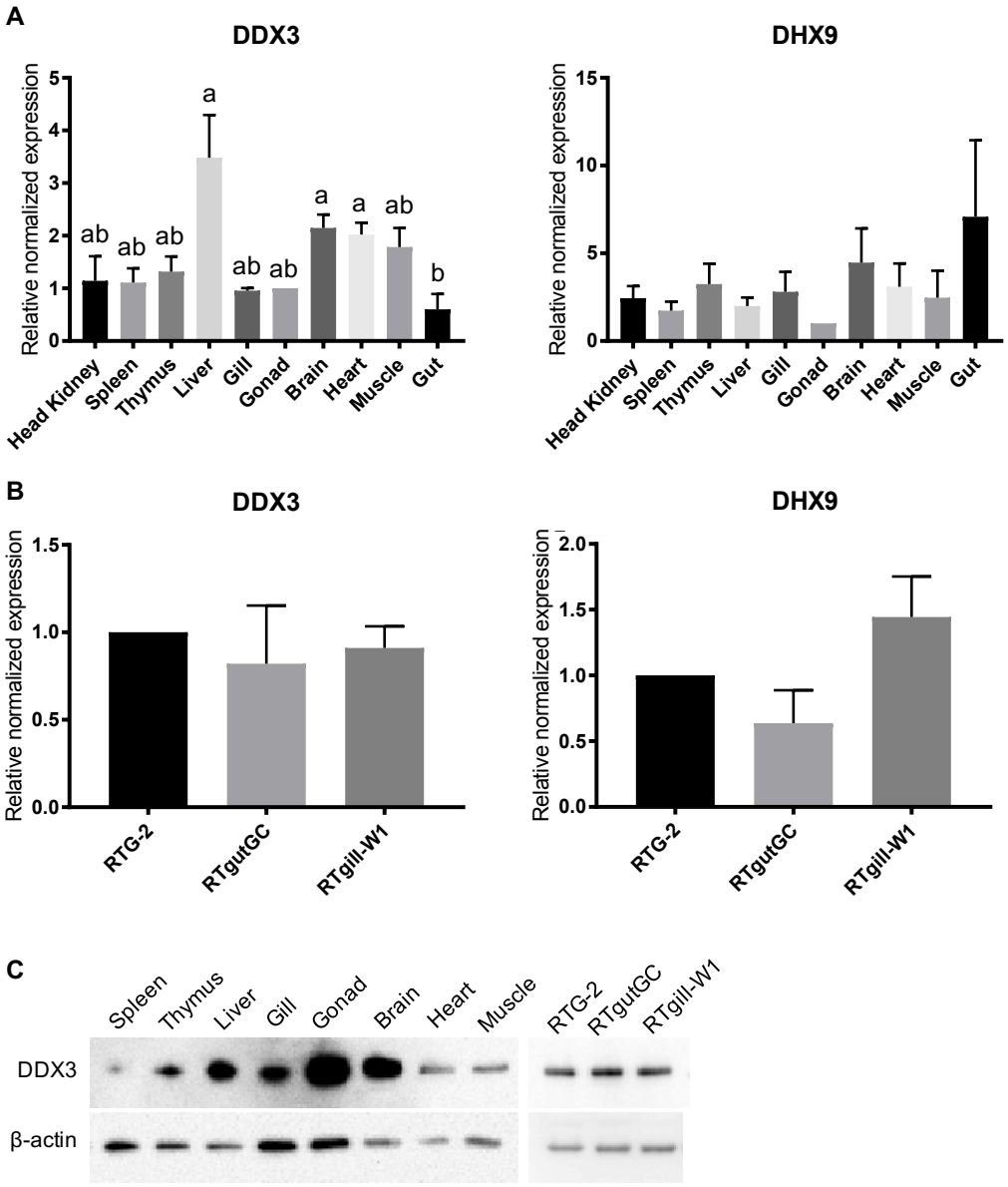

Figure 5.5. DDX3 transcript and protein, and DHX9 transcripts are found across rainbow trout tissues and cell lines. Juvenile rainbow trout tissues were collected and **(A)** qRT-PCR was performed to measure DDX3 and DHX9 transcript levels across tissues. (**B**) DDX3 and DHX9 transcripts in three rainbow trout cell lines, RTG-2, RTgutGC, and RTgill-W, were measured using qRT-PCR. **(A)** and **(B)** Data were analyzed using a $\Delta\Delta C_t$ method, gene expression was normalized to the housekeeping gene (β-actin), and presented as relative expression to the gonadal tissue or RTG-2 cells. N=3, data are presented with the standard error of the mean (SEM). Statistical analysis was performed on log2 transformed data and data were analyzed using a one-way ANOVA and Tukey's multiple comparison test, a p value<0.05 was considered significant. Data points denoted with the same letter were not significantly different from each other, if no letters are present there were no significant differences. **(C)** DDX3 protein expression was measured by Western blot analysis using an anti-DDX3 antibody, anti-β-actin was used as an internal control; data are representative of three individual fish.

5.5.5 Upregulation of DDX3 and DHX9 transcripts by poly I:C stimulation

The effect of dsRNA-stimulation on DDX3 and DHX9 expression levels were measured in RTG-2 cells stimulated with 50µg/mL of poly I:C for 4h and 24h, Fig. 5.6. MDA5, a dsRNA sensor that has previously been shown to increase in expression following poly I:C treatment in RTG-2 cells, was included as a positive control (Chang et al., 2011). While there was a modest and non-significant increase in transcript levels of all three sensors at 4h post-treatment, by 24h transcripts of all three helicases were significantly up-regulated.

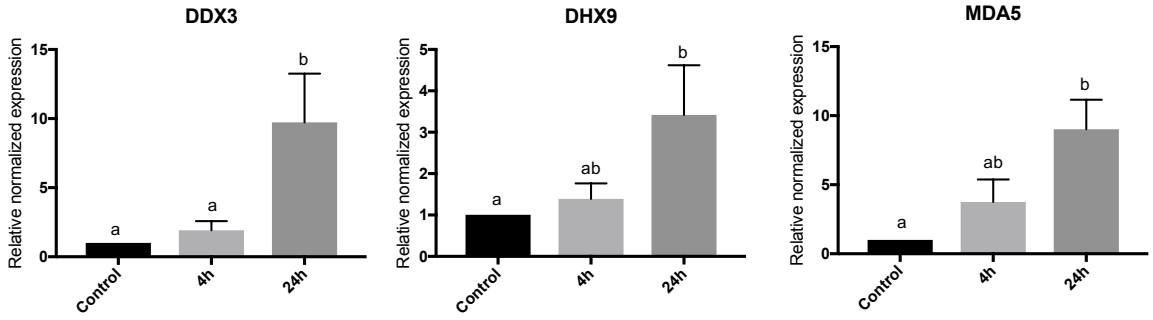

Figure 5.6. dsRNA (poly I:C) stimulation upregulates DDX3, DX9, and MDA5 transcript expression in RTG-2 cells. RTG-2 cells were stimulated extracellularly with 50µg/mL of poly I:C for 4h and 24h. DHX9, DDX3, and MDA5 transcripts were measured using qRT-PCR. Data were analyzed using a $\Delta\Delta C_t$ method; gene expression was normalized to the housekeeping gene (β-actin) and then presented as relative to the unstimulated control. Data represent three individual replicates and are presented with the standard error of the mean (SEM). Data were log2 transformed prior to statistical analysis using a one-way ANOVA with a Tukey's multiple comparison test, and a p value<0.05 was considered significant. Data points labelled with the same letter do not have a statistically different average.

5.5.6 DDX3 and DHX9 are capable of binding dsRNA

The ability of rainbow trout DHX9 and DDX3 to bind dsRNA was measured using pull-down assays. HA-tagged DHX9 and DDX3 proteins were overexpressed in EPC cells and cell lysates were mixed with *in vitro* transcribed dsRNA of 200bp in length. The 200bp molecule was used instead of poly I:C as the defined length produces a very clear band on an immunoblot, unlike the smear produced by poly I:C (Poynter and DeWitte-Orr, 2015). The HA-proteins were

pulled-down using magnetic anti-HA beads and dsRNA was detected in the resulting mixture by immunoblot analysis using the J2 anti-dsRNA antibody. Cell lysate containing DDX3 and DHX9 was able to pull-down dsRNA but the control cell lysate showed no binding to dsRNA, Fig. 5.7. When compared to the dsRNA-only control the dsRNA from the pull-down was a slightly larger size, possibly due to interference from proteins in the cell lysate mixture.

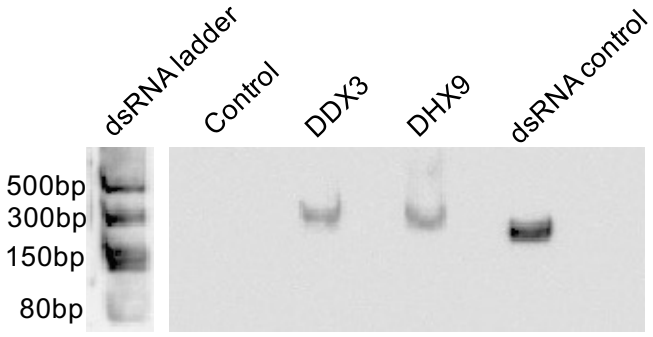

Figure 5.7. Rainbow trout DDX3 and DHX9 bind dsRNA. HA-tagged DDX3 and DHX9 were overexpressed in EPC cells and cell lysate was collected. Cell lysate was mixed with a 200bp *in vitro* transcribed dsRNA molecule. Protein/nucleic acid complexes were pulled down using magnetic anti-HA beads. The resulting pull-down mixture was analyzed for dsRNA using an immunoblot with the J2 antibody, an anti-dsRNA antibody. A control was included, cell lysate isolated from untransfected cells. The dsRNA control lane represents 20ng of *in vitro* transcribed dsRNA loaded onto the gel. This is a representative blot from three independent experiments.

5.5 Discussion

In mammals, DDX3 and DHX9 play important roles in cell homeostasis and innate immunity, however currently there is little knowledge about these helicases in fish. When a phylogenetic analysis was performed on the DDX3 and DHX9 deduced protein sequences, the clustering was as expected based on species relationships; the DDX3 and DHX9 sequences clustered separately from each other, and the fish sequences grouped with other fish over amphibians or mammals. This is congruent with previous studies of DDX3 in grouper and olive flounder, both of which had similar topology in that fish clustered in a separate clade then other

species; olive flounder express a DDX3a and DDX3b and rainbow trout clustered with the DDX3b variant (Liu et al., 2017; Wang et al., 2015). The domains and motifs identified in both rainbow trout DDX3 and DHX9 were conserved across known animal species sequences; indeed, rainbow trout DDX3 and DHX9 contained all the same motifs and domains as the other animal species analyzed. The domains identified with DDX3 and DHX9 are mainly involved with the proteins' role as helicases; DHX9 has two dsRNA binding motifs that are common to all species and have been described in channel catfish as well; these dsRNA binding motifs in mammals are necessary for dsRNA binding (Tian et al., 2017; Zhang et al., 2011). It was therefore unsurprising that DHX9 was able to bind to dsRNA, as demonstrated using a pull-down technique. DDX3 does not have a dsRNA binding motif per se; however, it's capability of binding the dsRNA molecule poly I:C has been reported in mammals and the ability to bind to *in vitro* transcribed dsRNA was seen in this study (Oshiumi et al., 2010B). Instead of using a dsRNA binding motif, DDX3 may be binding dsRNA via its helicase C domain, as was the case for two different DExD/H helicases that sense dsRNA, DHX33 and DHX15 (Liu et al., 2014; Lu et al., 2014). Whether this is the case for DDX3 remains to be elucidated.

DDX3 localized to the cytoplasm of RTG-2 cells, which is consistent with mammalian DDX3 as well as grouper DDX3 (Lee et al., 2008; Liu et al., 2017). This is congruent with DDX3's role as a cytoplasmic sensor for dsRNA, capable of interacting with cytoplasmic signaling proteins such as IPS-1 (Oshiumi et al., 2010A; Oshiumi et al., 2010B). It should be noted that DDX3 does not always localize to the cytoplasm, early studies in HeLa cells found DDX3 located predominantly in the nucleus, and treatment with leptomycin B, an inhibitor of CRM1-mediated nuclear transport, showed accumulation of previously cytoplasmic DDX3 in the nucleus; as such DDX3 is considered a nucleo-cytoplasmic protein (Owsianka and Patel,

1999; Schröder et al., 2010; Ranji and Boris-Lawrie, 2010; Schröder et al., 2008). Similar to mammalian GFP-tagged DDX3, overexpression of rainbow trout peGFP-C1-DDX3 led to punctate cytoplasmic structures; these structures appear to be stress granules in mammals but their identity in fish cells remains unknown (Lai et al., 2008). GFP-tagged DDX3 in grouper also demonstrated cytoplasmic localization, however there were fewer punctate structures and more diffuse staining than what was observed in rainbow trout cell lines, the same vector was used in both studies (peGFP-C1; Liu et al., 2017). peGFP-C1-DHX9 in RTG-2 cells localized almost exclusively to the nucleus in a diffuse pattern with nucleolus exclusion. There were some cells that demonstrated faint expression in the cytoplasm. In mammalian cells DHX9 expression is generally nuclear, one exception is plasmacytoid dendritic cells where DHX9 was found in the cytosol (Kim et al., 2010; Fujita et al., 2005). This is congruent with DHX9's ability to act as a transcriptional regulator (Fuller-Pace, 2006). peGFP-C1-DHX9 expression in RTG-2 was similar to HEK293T cells and HeLa cells where DHX9 localized to the nucleus and was excluded from the nucleolus (Fujita et al., 2005; Capitanio et al., 2017; Fuchosva and Hozak, 2002). This is in opposition to DHX9 expressed in the human bone osteosarcoma cell line U2OS where GFP-DHX9 localized to the nucleolus (Huang and Mitchell, 2008). This difference could possibly be due to the different cell types used for expression studies. While DHX9 is largely a nuclear protein, it has been shown in mammals that DHX9 is able to bind to cytoplasmic IPS-1, along with RIG-I and MDA5 (cytoplasmic proteins) in myeloid dendritic cells, thus at least in some cell types or at low levels DHX9 must be cytoplasmic (Zhang et al., 2011).

Expression of both DDX3 and DHX9 was constitutive across all tissues and cell lines tested, which was also observed in olive flounder and grouper tissue panels (Wang et al., 2015; Liu et al., 2017). This is to be expected as both helicases play roles in maintaining cell

homeostasis (Linder and Janowsky, 2011; Tarn and Chang, 2009). Interestingly, in the olive flounder differences were seen between sexes of the fish, with higher levels of both DDX3 variants being present in the ovary compared to the testis, and differences in both levels of expression and relative variant expression seen in some tissues (Wang et al., 2015). The rainbow trout used in the present study had immature gonads and were not separated by gender, potentially a contributing factor to the variation seen between individuals (Wang et al., 2015). DDX3 transcript expression patterns were similar between rainbow trout and grouper, where liver demonstrated the highest levels of DDX3 transcript expression, brain and heart were moderate and gut demonstrated the lowest levels of expression (Liu et al., 2017). Liver and brain also express high levels of DDX3 in olive flounder (Wang et al., 2015).

DDX3 and DHX9 exhibited increased expression at the transcript level following dsRNA treatment. MDA5, a DExH/D-box helicase and dsRNA sensor, which had been previously shown to be up-regulated following dsRNA treatment was used as a positive control (Chang et al., 2011). This is consistent with grouper DDX3, which was up-regulated 5-fold 24h following poly I:C transfection (Liu et al., 2017). This suggests that DDX3 in fish might be inducible by type I IFN, which is contrary to mammals, where dsRNA (poly I:C) does not appear to up-regulate DDX3 protein (Sparrer and Gack, 2015; Oshiumi et al., 2010A). The mammalian DHX9 promoter sequence contains an interferon-sensitive response element suggesting it is an ISG (Sadler et al., 2009). Mouse and human DDX60, another DExD/H-box helicase family member, were both upregulated in response to recombinant IFN (Goubau et al., 2015). It should be noted that dsRNA treatment is not synonymous with IFN treatment and that dsRNA can induce genes independently of IFNs (Daly and Reich, 1993; Reich et al., 1988). Further studies are necessary to understand DDX3 and DHX9's induction mechanisms.

The present study has demonstrated that rainbow trout express both DDX3 and DHX9. These DExD/H-box helicase family members are structurally similar to their respective proteins in other animal species. In agreement with their roles in cell homeostasis, their expression patterns are ubiquitous and constitutive; however, they are inducible following innate immune stimulation with dsRNA. Finally, this study suggests a role for these proteins as sensors of dsRNA. The present study represents the initial groundwork needed to understand these important yet lesser studied innate immune proteins in fish.

Acknowledgements

The authors wish to thank Dr. Brian Dixon for providing the rainbow trout, Dr. Dawn Bowdish for graciously providing the plasmids used in this study, Jondavid de Jong for his scientific support, Danyel Evseev for the technical information and Dr. Aaron Frenette for his expertise in fish dissections.

Chapter 6: *In vitro* transcribed dsRNA limits viral hemorrhagic septicemia virus (VHSV)-IVb infection in a novel fathead minnow (*Pimephales promelas)* skin cell line

Sarah J Poynter[a], Eric Leis[b], Stephanie J DeWitte-Orr[c]

a Department of Biology, University of Waterloo, Waterloo, ON, CANADA

b La Crosse Fish Health Center, U.S. Fish and Wildlife Service, Onalaska, WI, USA

c Department of Health Sciences, Wilfrid Laurier University, Waterloo, ON, CANADA

6.1 Overview

The farming of baitfish, fish used by anglers to catch predatory fish species, is of economic and ecological importance to North America. Baitfish, including the fathead minnow (*Pimephales promelas),* are susceptible to infection from aquatic viruses, such as viral hemorrhagic septicemia virus (VHSV). VHSV infections can cause mass mortality events amongst farmed fish and can be spread to novel water bodies through the baitfish vector. In this study, a novel skin cell line derived from fathead minnow (FHMskin) is described and its use as a tool to study innate antiviral immune responses and possible therapies is introduced. FHMskin grows optimally in 10% fetal bovine serum and at warmer temperatures, 25-30^{o}C. FHMskin is susceptible and permissive to VHSV-IVb infection, producing high viral titres $7.35x10^{7}$ ($TCID_{50}$/mL) after only 2 days. FHMskin cells do not experience significant dsRNA-induced death after treatment with 50-500ng/mL of *in vitro* transcribed dsRNA for 48h and respond to dsRNA treatment by expressing high levels of three innate immune genes, viperin, ISG15, and Mx1. Pretreatment with dsRNA for 24h significantly protected cells from VHSV-induced cell death, 500ng/mL of dsRNA reduced cell death from 70% to less than 15% at a multiplicity of infection of 0.1. Thus, the novel cell line, FHMskin, represents a new method for producing high tires of VHSV-IVb in culture, and for studying dsRNA-induced innate antiviral responses, with future applications in dsRNA-based antiviral therapeutics.

6.2 Introduction

In recreational angling, baitfish are commonly used by anglers to lure fish. In 2013, the freshwater baitfish industry was valued at $29.37 million USD in the US alone, with fathead minnow (*Pimphales promelas*) accounting for $9.88 million USD (Mor et al., 2017; United States Department of Agriculture, 2014). Not only is baitfish health important due to potential economic loss caused by pathogen-induced fish death, but baitfish could also act as vectors to spread pathogens. For example, in the US the industry ships more than 10 billion fish per year cross country where they are brought to various rivers and lakes with potential for consumption by predatory fish or escape into the environment (Goodwin et al., 2011). In a study of Wisconsin baitfish dealers and importers, 47% of tested cultured and 31% of tested wild fish lots tested positive for at least one virus (McCann, 2012). In the same study fathead minnows were positive for one or more viruses 62% of the time, a higher percentage than the other baitfish tested (McCann, 2012).

Viral hemorrhagic septicemia virus (VHSV) is an aquatic pathogen which has impacted the baitfish industry in Canada and the US. Regulations to prevent the spread of the virus were put in place, including surveillance measures and the restriction of baitfish movement and harvesting locations (Kerr et al., 2012; Bilateral VHSV Surveillance Working Group, 2007). The Great Lakes strain of VHSV, VHSV-IVb, was first identified in the Great Lakes in 2005 (Elsayed et al., 2006; Lumsden et al., 2007). Natural VHSV infections have been documented from several baitfish species, including wild populations of bluntnose minnows (*Pimephales notatus*) (Frattini et al. 2011), emerald shiner (*Notropis atherinoides*) as well as both wild caught and commercial populations of spottail shiners (*Notropis hudsonius*) (Faisal et al. 2012). Experimentally, fathead minnows are permissive to VHSV infection and can shed the virus during infection (Al-Hussinee et al., 2010; Getchell et al., 2013). VHSV can be spread through

the urine, feces, and sexual fluids of infected fish, and there is evidence that predatory fish, such as the Tiger Muskellunge (*Esox masquinongy*), can be infected after eating fathead minnows infected with VHSV-IVb (Getchell et al., 2013). *In vitro*, fathead minnow cell lines are often used to propagate VHSV and to identify the virus in fish tissues (Lumsden et al., 2007; Hope et al., 2010). North American strains of VHSV are efficiently isolated using the cell lines EPC (*Epithelioma Papulosum Cyprini;* fathead minnow), FHM (fathead minnow) or BF-2 (bluegill fry), as recommended by the American Fisheries Society (AFS-Bluebook, 2014) and World Organization for Animal Health (OIE). Fathead minnow cells from connective tissue and muscle (FHM; American Type Culture Collection CCL 42; Gravell and Malsberger, 1965) are permissive to VHSV-IVb, as are EPC (ATCC CRL-2872), originally classified as a carp cell line but has since been reclassified as fathead minnow (Winton et al., 2010; Pham et al., 2013).

There is preliminary evidence suggesting that dsRNA-based antiviral therapies may be effective at controlling VHSV-IVb infections. Studies have used both polyinosinic: polycytdiylic acid (poly I:C), a commercially available toll-like receptor (TLR)3 agonist, and *in vitro* transcribed dsRNA, made *in vitro* using T7 RNA polymerase, to protect rainbow trout cell lines from VHSV-IVb infection (Poynter and DeWitte, 2015). Long dsRNA molecules are pathogen-associated molecular patterns (PAMPs) that are sensed by cytoplasmic sensors such as the RIG-I-like receptors (RLRs) and protein kinase R (PKR), and the endosomal sensor TLR3, to trigger signalling cascades that culminate in the production of the type I interferon (IFN) response (DeWitte-Orr and Mossman, 2010). Type I IFNs are secreted cytokines that induce the expression of a panel of genes known as IFN-stimulated genes (ISGs). These include both receptors and signalling molecules, such as those listed above, and antiviral effectors such as viperin, Mx1, and ISG15 (Poynter and DeWitte-Orr, 2016). In fathead minnow, most aspects of

this pathway have not yet been elucidated, however it is known that fathead minnow cells produce sensors, IFN-related transcription factors, and ISGs at the transcript level in response to the overexpression of an unmethylated CpG DNA motif sensor, TLR9 (Xinxian et al., 2016). In some cell types treatment with long dsRNA induces cell death; for example, in human endothelial cells poly I:C triggers apoptosis (Sun et al., 2011). In teleost fish poly I:C-induced cell death has been observed in several non-salmonid fish cell lines, however to date no formal reports of this phenomena have been published.

In this study, a novel fathead minnow cell line derived from the skin, FHMskin, was established and its optimal growth conditions were characterized. Additionally, FHMskin's ability to support the replication of VHSV-IVb and the potential for *in vitro* transcribed dsRNA to protect the cells from VHSV-IVb infection were also explored.

6.3 Materials and methods

6.3.1 Cell line establishment

Fathead minnows, healthy in appearance, were obtained from the Upper Midwest Environmental Sciences Center (USGS; La Crosse, WI) where they were maintained in clean, continuously flowing well water. Fish were euthanized via cervical dislocation and the dull side of a sterile scalpel was used to scrape skin and scales off the body surface of the fish. Removed tissue was placed in a 50mL conical tube containing MEM-Eagle (M1018; Millipore-Sigma, USA) supplemented with 20% FBS, 1% L-glutamine (200mM), 0.5% $NaHCO_3$ (7.5%), 1% penicillin/streptomycin (10,000units penicillin; 10mg/mL streptomycin), 0.25% Nystatin (10,000units/mL) and 0.1% Gentamicin (50mg/mL). The tube was centrifuged at 400 x g for 10min. The supernatant was then removed and the pellet was resuspended in fresh MEM-Eagle (supplemented as described) in a $25cm^2$ flask (BD Falcon, San Jose, CA, USA). Cells were then incubated at 25°C and observed for confluency. Once a monolayer was formed, the FHMskin

cells were then routinely propagated at a 1:2 or 1:4 ratio. Cells were cultured in T-75 tissue culture flasks (BD Falcon) in L-15 media (Corning, Corning, NY, USA) containing 10% v/v fetal bovine serum (FBS; Fisher Scientific, Fair Lawn, NJ) and 1% v/v penicillin/streptomycin (P/S; 10000U/mL penicillin and10mg/mL streptomycin; Fisher Scientific) prior to experimentation. Cells were detached using TrypLE (Fisher Scientific) and were used between passages 30-40 and for all experiments after seeding cells were allowed to attach overnight at 25^{o}C in 10% FBS media. When not specified, cells were grown at 25^{o}C in 10% FBS media.

6.3.2 Barcoding

The DNA of the FHMskin cell line (passage 37) was extracted using a Qiagen DNEasy Blood and Tissue Kit, following manufacturers' instructions (Qiagen, Hilden, Germany). Two replicates of the FHMskin, an extraction negative control, as well as polymerase chain reaction (PCR) positive and negative controls were sequenced at the cytochrome c oxidase 1 (UCOI, Ivanova et al., 2007) and cytochrome b (UCYTB, Palumbi, 1996) genes. One pGEM®-3Zf(+) Control Template (Life Technologies, Carlsbad, CA, USA) was included on each PCR plate for a sequencing positive control. PCR amplification and cycle sequencing of UCOI and UCYTB were accomplished with the BigDye™ Direct Cycle Sequencing Kit (Life Technologies) following the manufacturers' protocol and using forward primers (from references above) modified with M13 tags to streamline sequencing work. Sequences were purified with a Big Dye XTerminator Purification Kit (Life Technologies) and analyzed on an Applied Biosystems 3500 Genetic Analyzer (Life Technologies). Sequences were then edited using Codon Code Aligner (Version 7.0) and BLASTn searched in Genbank to determine sequence similarity.

6.3.3 Virus propagation

VHSV-IVb isolate U13653 (Pham et al., 2014; Lumsden et al., 2007) was propagated on monolayers of *Epithelioma Papulosum Cyprini* (EPC) cells. Virus infections were performed in

L-15 containing 2% FBS and 1% penicillin at 17°C. Virus-containing media was cleared at 4000 x g and filter sterilized through a 0.45μM filter. The 50% tissue culture infective dose $TCID_{50}$/mL values were quantified according to the Reed and Muench method (1938).

6.3.4 Cell viability measured using alamarBlue

The fluorescent cell metabolism reagent, alamarBlue, was used to measure cell viability. In all cell viability assays, after the indicated treatment or infection, media was removed from the 96-well plate (BD Falcon), cells were rinsed with phosphate buffered saline (PBS; Corning) and 100μL of PBS containing 5% alamarBlue reagent (Invitrogen, Carlsbad, Ca, USA) was added to each well. Cells were incubated for 1h at room temperature in the dark and fluorescence was measured using a BioTek HT Synergy Plate Reader (BioTek, Winooski, VT, USA). All relative fluorescent units (RFUs) were normalized to the uninfected or untreated control RFUs.

6.3.5 In vitro dsRNA transcription

A 750bp dsRNA molecule with a green fluorescent protein (GFP) sequence was made using the MegaScript RNAi kit (Ambion, Carlsbad, CA, USA) following the manufacturers' instructions. A DNA template with T7 promoters on both DNA strands was amplified by PCR using 10ng of peGFP-C1 (Clontech, Mountain View, CA, USA) as a template, 2X Phusion High-Fidelity master mix (Fisher Scientific), 0.5μM forward primer

(5'TAATACGACTCACTATAGGGAGAGTGAGCAAGGGCGAGGAGCTG 3')

and 0.5μM reverse primer

(5'TAATACGACTCACTATAGGGAGATTACTTGTACAGCTCGTCCATGC 3') and up to 50μL with nuclease-free water.

The following protocol was carried out in a Bio-Rad T100 thermocycler (Bio-Rad, Hercules, CA, USA): 98°C - 30s, 34 cycles of 98°C - 10s, 50°C - 10s, 72°C - 30s, followed by 72°C - 5min.

The DNA template was purified using a QIAquick PCR purification kit (Qiagen) and used in the MegaScript RNAi kit as per manufacturers' instructions to produce dsRNA.

6.3.6 β-galactosidase staining

FHMskin cells were seeded at $2x10^5$ cells in a 12-well tissue culture plate (BD Falcon). β-galactosidase activity was detected in cells using the Senescence Cells Histochemical Staining Kit, as per manufacturers' instructions (Sigma-Aldrich, St. Louis, MO, USA). Staining was allowed to continue for 24h at 25°C, at this time the positive control, an early passage (p7) Lake Sturgeon (*Acipenser fulvescens*) cell line (LSskin), showed robust staining. PBS:glycerol (30:70) was used as a mounting media and a glass coverslip was placed on top of cells prior to imaging with a Nikon Eclipse TS100 microscope with a Lumenera Infinity light camera at 100X magnification (Nikon, Tokyo, Japan; Lumenera, Ontario, Canada).

6.3.7 Growth condition optimization

FHMskin cells were seeded at $2x10^5$ cells in a 6-well tissue culture plate (BD Falcon). After overnight attachment at 25°C, cells were moved to different temperatures (all in 10% FBS media) or media was changed to 5% or 0% FBS and cells were incubated at 25°C. Cells were detached in 500µL of trypsin-EDTA (0.25% trypsin, 2.21mM EDTA; Corning) and stained with a final concentration of 0.2% Trypan blue (Invitrogen) to ensure only live cells were counted; cells were then counted using the Countess II FL Automated Cell Counter (Fisher Scientific) at day 0 (after overnight attachment), day 3, and day 5. The cell counts at 25°C and 10% FBS reported in Fig. 6.1B and 6.1C are the same data.

6.3.8 Susceptibility to VHSV-IVb

FHMskin cells were plated at $1x10^4$ cells/well in a 96-well tissue culture plate (BD Falcon). Cells were exposed to a continuous infection of VHSV-IVb at the indicated multiplicity of infection (MOI) in 50µL of growth media containing 2% FBS. Virus was added to the 96h

wells after overnight attachment and then in 24h increments; corresponding controls were treated in the same fashion but media contained no virus. All infections were stopped at the same time and cell viability was measured using alamarBlue reagent as described in section 6.3.4.

6.3.9 Permissiveness to VHSV-IVb

FHMskin cells were plated at $5x10^5$ cells/well in a 6-well tissue culture plate (BD Falcon). VHSV-IVb adsorption was completed in 500µL of 2% FBS media for 2h with gentle rocking at an MOI of 10, and a control was treated the same without virus. Virus or control media was removed and cells were rinsed 3X with PBS before the addition of 2mL of 2% FBS media. Cells were then incubated at 17°C and samples were taken from infected wells at day 0 (immediately after absorption), and 2, 4, and 6 days PI. Control cells were used to ensure cytopathic effects were caused only by viral infection. Cell debris was removed from samples at 8000 x g and VHSV-IVb production was measured by $TCID_{50}$/mL on EPC cells (plated at $2x10^4$ cells/well). Values were calculated using the Reed and Muench method (1938).

6.3.10 Susceptibly to dsRNA-induced death

FHMskin cells were plated at $1x10^4$ cells/well in a 96-well in a tissue culture plate (BD Falcon). Cells were treated with indicated concentration of dsRNA, or no dsRNA for the control wells, in 50µL of growth media (extracellular dsRNA treatment); after 24h and 48h cell viability was measured using alamarBlue reagent as described in section 6.3.4.

6.3.11 RNA extraction, cDNA synthesis, and qRT-PCR

FHMskin cells were plated at $8x10^5$ cells/well in 6-well in a tissue culture plate (BD Falcon). Cells were treated with 1mL of dsRNA-containing growth media (50ng/mL or 500ng/mL) or growth media alone (control). After 24h RNA was extracted using the Bio-Rad Aurum RNA extraction kit (Bio-Rad) with on-column DNase I digestion. Maxima H Minus cDNA Synthesis Master Mix with dsDNase, was used to synthesis cDNA from 1µg of RNA in

a 10µL reaction. qRT-PCR primer sequences for Mx1, ISG15, viperin, and β–actin (Xinxian et al., 2016) were used for the qPCR; reactions contained 1X SsoFast EvaGreen SuperMix (Bio-Rad), 2µL of 10^{-2} diluted cDNA, 0.2µM forward primer, 0.2µM reverse primer, and nuclease-free water to a total volume of 10µL (Fisher Scientific). Triplicate technical replicates were used for each sample/gene, and a no-reverse transcriptase control was included. qPCR reactions were performed using the CFX Connect Real-Time PCR Detection System (Bio-Rad). The program used for all qPCR reactions was: 98°C 2min, 40 cycles of 98°C 5s, 60°C 10s, followed by 95°C for 10s. A melting curve was completed from 65°C to 95°C with a read every 5s. Product specificity was determined through single PCR melting peaks. Data were analyzed using the $\Delta\Delta C_t$ method. Specifically, gene expression was normalized to the housekeeping gene (β-actin) and expressed as fold change over the control group.

6.3.12 Antiviral assays

FHMskin cells were seeded at $1x10^4$ cells/well in a 96-well in a tissue culture plate (BD Falcon). Cells were treated with 50µL of growth media containing 50ng/mL or 500ng/mL of dsRNA or growth media alone (control). After 24h the media was removed and VHSV-IVb was added at the indicated MOI in 50µL of 2% FBS media. After a 2h adsorption, the media was removed and the cells were rinsed 3X with PBS before the addition of 100µL of 2% FBS media. Cells were incubated at 17°C for 3 days prior to quantification of virus propagation by $TCID_{50}$ and analysis of cell viability using alamarBlue reagent, as described in section 6.3.4.

6.3.13 Statistical analyses

All data represent at least three independent trials and are presented with the standard error of the mean (SEM). Data were analyzed and graphed using GraphPad Prism version 7.00 for Mac, GraphPad Software, La Jolla, CA USA, www.graphpad.com. Where indicated in the figure legend data were log2 transformed prior to analysis; a one-way or two-way ANOVA with

a Tukey's or Dunnett's multiple comparison test, as indicated, was used to check for significant differences between all treatments or between the treatments and control group, respectively. A 95% confidence interval was used and a p value <0.05 was considered significant. A letter system has been used to indicate differences between treatments, data points with the same letter did not have significant difference between their means.

6.4 Results

6.4.1 Successful establishment of a fathead minnow skin cell line

A fathead minnow skin cell line was successfully established from healthy juvenile fathead minnows. The identity of the fathead minnow skin cell, FHMskin, was confirmed to be fathead minnow by DNA barcoding (data not shown). FHMskin cells did not show senescence-associated β-galactosidase activity, as can be seen by a lack of blue staining, whereas the positive control lake sturgeon skin cells showed robust blue staining, Fig. 6.1A. The optimal temperature for growth of these cells was determined to be 25°C or 30°C by counting the number of cells at 3 and 5 days when grown at different temperatures. While there was no significant difference between the two temperatures the cells grew slightly better at 25°C so this temperature was used in all subsequent studies, Fig. 6.1B. There was significantly less cell growth at lower temperatures, 4°C and 17°C, compared to the warmer temperatures at both day 3 and day 5, Fig. 6. 1B. FHMskin cells grew best at 10% FBS and there was significantly better growth with the increasing concentrations of FBS, with 5% being preferred to 0% and 10% being superior to 5%, Fig. 6. 1C.

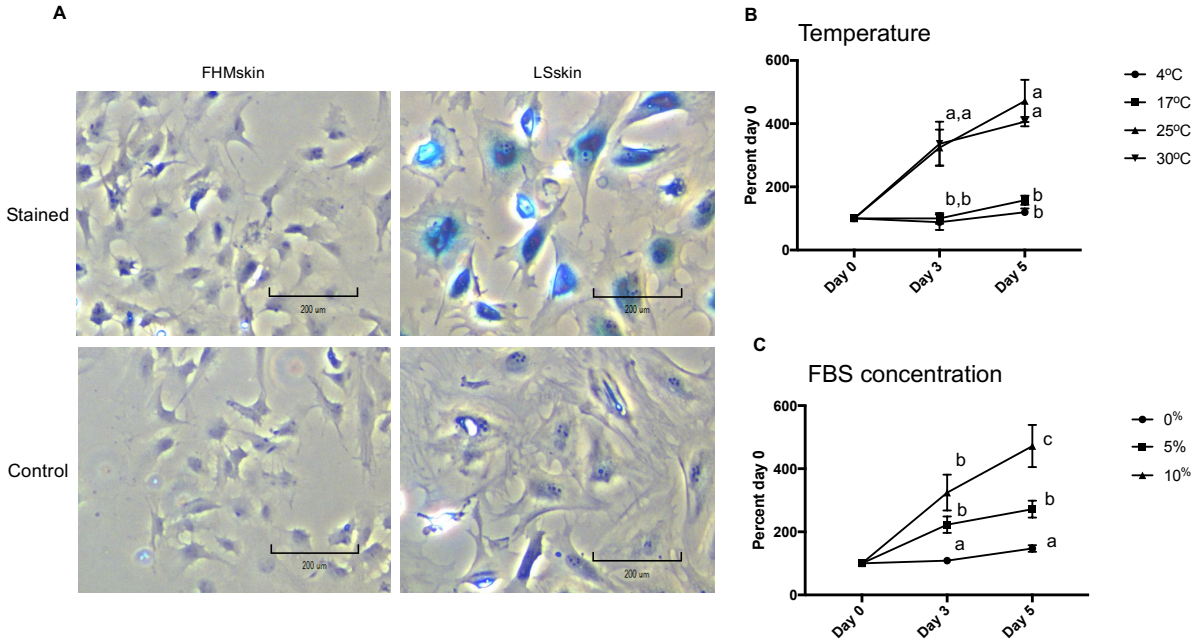

Figure 6.1. FHMskin cells do not show senescence-associated β-galactosidase activity and grow in warm temperatures with 10% FBS. (A) FHMskin cells were fixed and stained using a histochemical stain for β-galactosidase. Blue coloring indicates activity of this enzyme. Lake sturgeon skin (LSskin) cells were included as a positive control, and unstained control cells are shown for both cell lines. A PBS:glycerol (30:70) mounting media and coverslip were applied to cells; images were taken at 100X magnification with a Nikon Eclipse TS100 microscope. Optimal growth conditions for FHMskin cells were measured at **(B)** 4°C, 17°C, 25°C or 30°C (in 10%FBS) or in **(C)** media containing 0%, 5%, or 10% fetal bovine serum (FBS) at 25°C. After 0, 3, and 5 days cells were counted and are presented as a percentage of the day 0 count. N = 3 and data are averages presented with standard error of the mean (SEM). A one-way ANOVA with Tukey's multiple comparison test was performed, a p value <0.05 was considered significant. Data points with the same letter were not statistically different from each other at the given time point.

6.4.2 FHMskin are susceptible and permissive to VHSV-IVb infection

FHMskin cells were continuously infected with VHSV-IVb (MOI = 0.01-10) and cell viability was measured at 24h, 48h, 72h, and 96h post-infection (PI) using the fluorescent cell viability reagent, alamarBlue, Fig. 6.2A. As early as 48h PI significant cell death was measured across all MOIs, and by 96h there was complete decimation of the monolayer and almost no viable cells remained, Fig. 6.2A. To assess the ability for VHSV-IVb to replicate in FHMskin cells, the viral titre produced by the cells was measured as a $TCID_{50}$/mL. FHMskin cells were infected with VHSV by 2h adsorption at an MOI of 10, the cells were then rinsed

and fresh media was added to allow for measurement of new virions and not those from the original virus preparation. To ensure the original virus was adequately removed, a sample was taken after rinsing and considered day 0, the titres from these samples were under $3.2x10^3$ $TCID_{50}$/mL, Fig. 6.2B. Virus titres were measured at 2, 4, and 6 days PI, and by 2 days there was significant a viral titre produced, the average $TCID_{50}$/mL at day 2 was $7.35x10^7$, Fig. 6.2B.

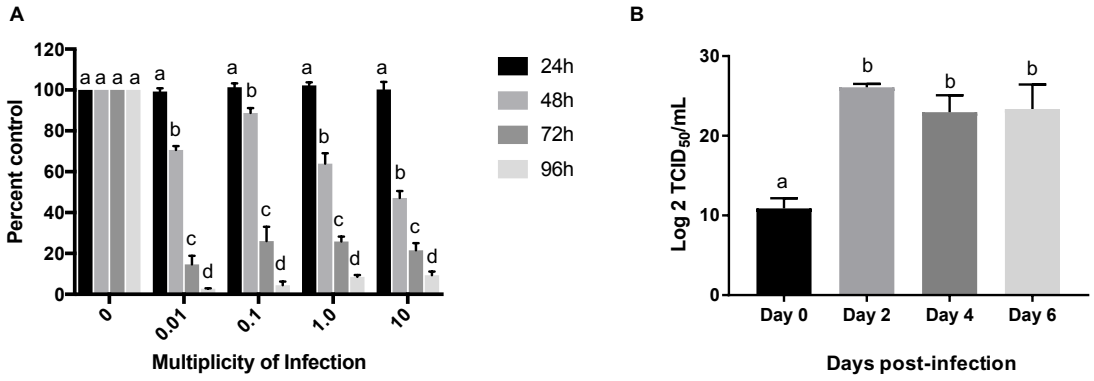

Figure 6.2. FHMskin cells are susceptible and permissive to infection with VHSV-IVb. (A) FHMskin cells were continuously infected with VHSV-IVb at the indicated multiplicity of infection (MOI) for 24-96h. Cell viability was measured using alamarBlue after every 24h post-infection (PI). Data are presented as the percent of the uninfected control cells at the corresponding time point. **(B)** FHMskin cells were infected by 2h adsorption with VHSV-IVb at an MOI of 10. Samples of virus-containing media were collected immediately after adsorption (day 0) and at 2, 4, and 6 days PI. The $TCID_{50}$/mL values were measured for each sample. N = 3 and averages are presented with standard error of the mean (SEM). **(A)** Data were analyzed using a two-way ANOVA with a Tukey's multiple comparison test. **(B)** Data were log2 transformed prior to statistical analysis and analyzed with a one-way ANOVA with Tukey's multiple comparison test. A p value<0.05 was considered significant. Data points with the same letter were not statistically different from each other.

6.4.3 FHMskin are not sensitive to dsRNA-induced cell death at concentrations less than 1μg/mL and respond with the robust production of ISGs

To test whether the cells underwent dsRNA-induced death, FHMskin cells were treated with 0.05μg/mL – 5μg/mL of an *in vitro* transcribed dsRNA molecule for 24h and 48h, after which cell viability was measured using alamarBlue. In this study, the dsRNA molecule contained a GFP sequence, which would not support possible sequence-matched RNAi effects on host or viral proteins (Maillard et al., 2013). GFP has previously been used in shrimp as a

neutral source of dsRNA that is not expected to have any virus-specific effects (Kim et al., 2007). There was moderate, but significant death after 48h at the highest concentrations of dsRNA, 1μg/mL and 5μg/mL, Fig. 6.3A. Due to this decrease in cell viability, all subsequent assays used the concentrations below this limit, 50ng/mL and 500ng/mL, Fig. 6.3A. FHMskin cells treated with 50ng/mL or 500ng/mL of dsRNA for 24h demonstrated significantly higher amounts of viperin, ISG15, and Mx1 at the transcript level compared to untreated controls, as measured by qRT-PCR, Fig. 6.3B. At a concentration of 500ng/mL there was significantly more ISG expression compared to 50ng/mL for all three genes tested, Fig. 6.3B.

6.4.4 dsRNA induced an antiviral state conferring protection against VHSV-IVb

FHMskin cells were pretreated for 24h with 50ng/mL or 500ng/mL of dsRNA. Cells were then infected with VHSV-IVb by 2h adsorption with an MOI of 0.1, Fig. 6.4A, or an MOI of 10, Fig. 6.4B. Cell viability was measured after three days with the cell viability reagent alamarBlue. There was significant protection by both concentrations of dsRNA against both MOIs; the higher concentration, 500ng/mL, of dsRNA protected significantly better than 50ng/mL, Fig. 6.4. The virus titre was measured in dsRNA treated cells and untreated controls. At an MOI of 0.1 there was a significantly higher $TCID_{50}$/mL measured in control infected cells compared to pretreated cells, with a significantly lower $TCID_{50}$/mL in the 500ng/mL dsRNA treatment compared to the 50ng/mL dsRNA treatment, Fig. 6.4A. There was a similar trend seen for an MOI of 10, however there was greater variation and no significant differences between treated and untreated cells was identified, Fig. 6.4B.

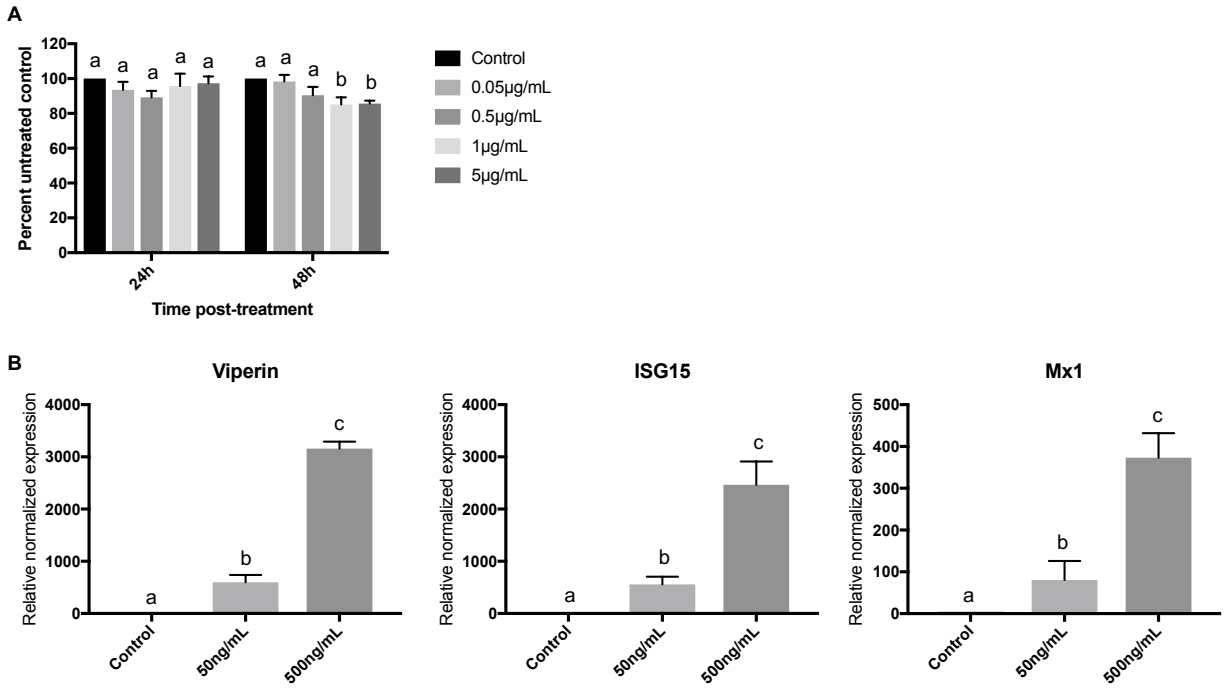

Figure 6.3. FHMskin cells experience moderate dsRNA-induced mortality and dsRNA-treatment induces interferon-stimulated gene production. (A) Cell viability and **(B)** production of interferon-stimulated gene (ISG) transcripts were measured in FHMskin cells treated with *in vitro* transcribed dsRNA. **(A)** Cell viability was measured using alamarBlue 24h and 48h after treatment with increasing concentrations of dsRNA. Data are presented as a percent of the untreated control. **(B)** Cells were stimulated with 50ng/mL or 500ng/mL of dsRNA for 24h and qRT-PCR was used to measure transcript levels of viperin, ISG15, and Mx1. Data were analyzed using a $\Delta\Delta C_t$ method, gene expression was normalized to the housekeeping gene (β-actin), and presented as relative to the untreated control. **(A)** A one-way ANOVA with a Dunnett's post-test was performed for each time point to compare treatments to the control. **(B)** A one-way ANOVA with Tukey's multiple comparison was used to analyze log2 transformed data. A p value <0.05 was considered significant. N=3 and data are presented with the standard error of the mean (SEM). Data points with the same letter were not significantly different.

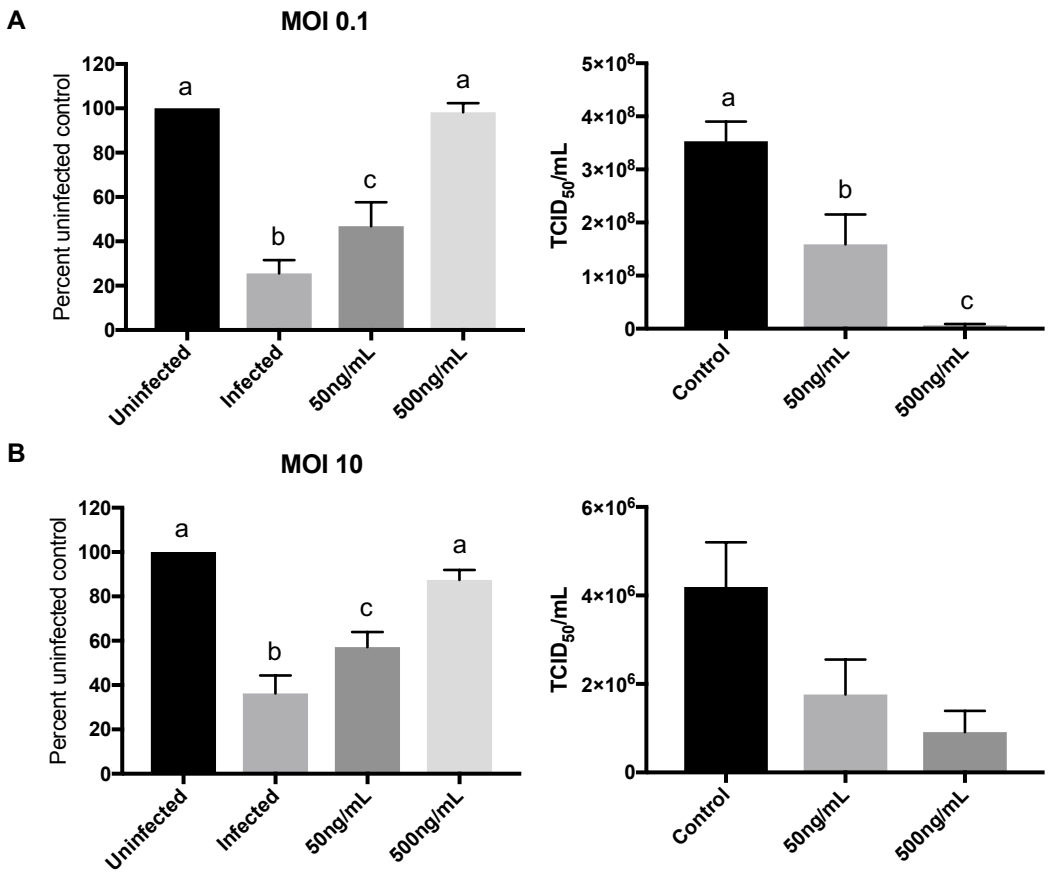

Figure 6.4. dsRNA pretreatment protects FHMskin cells from VHSV-IVb induced cell death and limits viral replication. FHMskin cells were pretreated with 50ng/mL or 500ng/mL dsRNA, after 24h cells were infected by 2h adsorption with VHSV-IVb at a multiplicity of infection (MOI) of **(A)** 0.1 or **(B)** 10**.** 3 days post-infection cell viability was measured using alamarBlue and is presented as percent of the uninfected control. Virus titres were measured by $TCID_{50}$/mL for each treatment. Data are representative of at least three independent replicates and averages are presented with standard error of the mean (SEM). A one-way ANOVA with Tukey's multiple comparison test was used to compare treatments; a p value <0.05 was considered significant. Data points with the same letter were not statistically different from each other, no letters indicates no significant differences between any treatments.

6.5 Discussion

The skin is an important innate immune barrier and of particular importance with respect to VHSV, which can replicate in skin (Harmache et al., 2006; Montero et al., 2011) and can be shed into the water column from infected fish (Kim and Faisal, 2011). Fathead minnow are susceptible to waterborne VHSV as these fish can be infected by immersion (Kibenge and Godoy, 2016; Al-Hussinee et al., 2010). The present study sought to characterize the novel

FHMskin cell line and to investigate the permissiveness and susceptibly of FHMskin to VHSV-IVb infection and whether dsRNA could be used as a therapy to limit VHSV-IVb replication.

This cell line has been passaged >70 times in the last two years since it's development. FHMskin was established at 25^{o}C and then moved to temperatures between 4^{o}C and 30^{o}C. The cell line grew optimally at warmer temperatures, with no significant difference between 25^{o}C and 30^{o}C. Another available fathead minnow cell line from the ATCC is an epithelial cell line, FHM, this cell line grows optimally between 28-34^{o}C (Gravell and Malsberger, 1965). EPC grows between 15-33^{o}C, with optimal growth between 25-30^{o}C (Fijan et al., 1983). This has some correlation with fathead minnow *in vivo*, fish reared at 24^{o}C show optimal body conditions, size, and sexual characteristics; if fish are reared at 28^{o}C the fish are similar in size and reproductive status but have a lower quality (Brian et al., 2011).

The FHMskin cell line was susceptible to VHSV-IVb infection, as demonstrated by virus-induced cytopathic effects (cell death) and was permissive to VHSV-IVb replication, as measured by virus titres. After 48h of infection with an MOI of 10 there was over 50% cell death, and the viral titre was $7.35x10^{7}$ $TCID_{50}$/mL. These values are comparable to VHSV-IVb propagation in EPC cells which produces a $TCID_{50}$/mL of approximately $8x10^{7}$-$2x10^{8}$. Interestingly, it takes EPC cells 5-7 days to produce this high of a titre while FHMskin cells produced this in just 2 days (Vo et al., 2015; Fig 6.2B). FHMskin's ability to support VHSV-IVb replication so quickly has the potential to improve VHSV diagnostic assays, as faster virus replication *in vitro* would allow for identification of virus in a timelier manner, or could improve the sensitivity of current assays over the standard 28-day period. Future work will be necessary to determine if this rapid replication in the FHMskin cell line might also indicate increased assay

sensitivity compared to the cell lines recommended for VHSV diagnosis by the American Fisheries Society and the World Organization for Animal Health.

DsRNA is a potent IFN inducer, and in some cells the activation of these innate immune pathways results in cell death. For example, poly I:C, a commercially available dsRNA molecule is cytotoxic in brown bullhead (*Ictalurus nebulosus)* cells (BB, ATCC - CCL-59) using dosages as little as 5ng/mL (unpublished data). Before exploring dsRNA as an antiviral therapy in fathead minnow cells it was imperative to measure its possible cytotoxic effects. The only cytotoxic effects observed with dsRNA in FHMskin cells were at higher concentrations (1µg/mL and 5µg/mL) for 48h. As there were limited cytotoxic effects, dsRNA's antiviral activity could be pursued at the concentrations where cell death was not observed.

dsRNA was capable of inducing high levels of ISGs at the transcript level in FHMskin cells, suggesting that this cell line is capable of mounting an IFN-mediated innate immune response. The ISG induction patterns were similar to those seen in other fish cell lines. Compared to viperin and ISG15 (known as vig-1 and vig-3 in rainbow trout), the levels of Mx1 transcript were approximately 10-fold lower after induction; this corresponds with previous studies in rainbow trout where Mx1 also showed lower expression levels compared to ISG15 in response to dsRNA stimulation, Fig. 6.3B (Poynter and DeWitte-Orr, 2015). ISG production leads to the establishment of an antiviral state, when a cell is actively inhibiting virus replication. As dsRNA was able to induce ISG production, its ability to induce an effective antiviral state in FHMskin cells was investigated. A dsRNA pretreatment for 24h was able to protect significantly protect FHMskin cells from viral infection, even at lower concentrations, Fig. 6.4. A 24h pretreatment was used as a study in rainbow trout found that prolonged exposure to an antigen increased uptake, this time point is longer than the usual exposure period for fish in a bath treatment setting

(Moore et al., 1998). An *in vivo* study in Chum salmon (*Oncorhynchus keta*) found antiviral protection after a 3h immersion in poly I:C followed by a 4-day waiting period prior to infection (Eaton, 1990). Additionally, studies i*n vivo* found poly I:C treatment protected Japanese flounder (*Paralichthys olivacus*) from VHSV infection, with higher poly I:C doses protecting up to 100% after a 2-day pretreatment (Takami et al., 2010). Previously, *in vitro* transcribed dsRNA pretreatment has been shown to be effective in establishing an anti-VHSV-IVb state in rainbow trout cells (Poynter and DeWitte-Orr, 2015). With *in vitro* transcribed dsRNA's natural sequence variation and tunability with respect to length and sequence, its features outstrip poly I:C's abilities for antiviral therapeutics. Future *in vivo* studies will further clarify the potential for *in vitro* transcribed dsRNA to be used as an antiviral for fathead minnows against virus infection.

The development of the FHMskin cell line contributes to our understanding of dsRNA-mediated immune responses in fathead minnow, an underexplored area of research. The cell line supports rapid and robust replication of VHSV-IVb, making it a useful tool in the study and identification of this virus. The establishment of an antiviral state produced by dsRNA pretreatment in these cells is a first step towards future studies of dsRNA-based therapies in baitfish.

Acknowledgments

The authors wish to thank Dr. Nguyen Vo for his technical advice and scientific support. We would also like to thank Zeb Woiak (Whitney Genetics Laboratory; U.S. Fish and Wildlife Service, Onalaska, WI) for assistance with the molecular identification as well as John Fisher (National Conservation Training Center Library, U.S. Fish and Wildlife Service; Shepherdstown, WV) for help locating reference articles. Usage of trade names does not imply endorsement by the United States Government.

Chapter 7: General discussion and future directions

7.1 Understanding fish immunology

Fish play an important role in the ecosystem, the global and Canadian economies, and in human health as a food source. A better understanding of fish immune systems will allow for the design of better vaccines, adjuvants, and antiviral therapies to support the aquaculture industry, an industry that in 2016 in Canada alone produced 120,000 tonnes of finfish worth $1.25 billion CAD (Fisheries and Oceans Canada, 2016). It should be noted that innate immune responses are similar but not identical between mammals and fish. One example of this is that of TLR4, in mammals this is a well-defined receptor for bacterial lipopolysaccharide (LPS), whereas in fish TLR4 is not involved in LPS signaling (Sepulcre et al., 2009). While "fish" immunology is frequently compared to "mammalian" immunology, it is important to recognize these titles represent a vast diversity of species (Tort et al., 2003). Just as there are differences in the immune response between mammals, such as those between a mouse and human, differences exist between fish species as well (Mestas et al., 2004). An example of these differences is exemplified in the Atlantic cod (*Gadus morhua*); the majority of fish have the genes for the major histocompatibility complex II, but these genes have been lost in Atlantic cod (Star et al., 2011). Another example would be that of the dsRNA-receptor RIG-I; while this receptor is found in most salmonids, it has not been located in rainbow trout (*Oncorhynchus mykiss*) and is an example of a potential erroneous assumption that could be made if all fish, even fish within the same family, were treated as the same without experimental confirmation (Biacchesi et al., 2009; Chen et al., 2017).

One objective of this thesis was to compare the immune responses induced in rainbow trout cells by dsRNA that is made by a virus (v-dsRNA), made in the lab by *in vitro* transcription (ivt-dsRNA), and commercially available (polyinosinic polycytidylic acid (poly I:C)). From this

study it was proposed that ivt-dsRNA with sequence variation is a better tool to study natural dsRNA responses than the synthetic poly I:C. Differences in responses to dsRNA between fish species was tested when dsRNA responses were tested in a novel cell line derived from fathead minnow (*Pimephales promelas*). Similar to rainbow trout, the fathead minnow cells expressed antiviral gene transcripts and a robust antiviral response to treatment with ivt-dsRNA. These findings were expected as the dsRNA pathways are well-conserved and there are few fish cell lines that do not respond to dsRNA. Additionally, it has been previously demonstrated that VHSV-IVb replication is limited by the type I IFN response induced by ivt-dsRNA (Poynter and DeWitte-Orr, 2015). Future studies will continue to explore the difference between sources of dsRNA, and *in vitro* and *in vivo* trials in different fish species will help to elucidate antiviral pathways induced by dsRNA, and how conserved these pathways are between fish species.

7.2 dsRNA as an adjuvant or antiviral therapy in fish

To the author's knowledge only dsRNA in the form of poly I:C has been tested for its efficacy as an antiviral therapy and vaccine adjuvant in some fish species. There is a great deal of variation in the effectiveness of poly I:C as an antiviral therapy, depending on the fish species being test and in some cases temperature. Pre-treatment with poly I:C has shown almost complete protection against viral infection in several fish species, including nervous necrosis virus (NNV) infection in sevenband grouper (*Epinephelus septemfasciatus*), viral hemorrhagic septicemia virus (VHSV) infection in Olive flounder (*Paralichthys olivaceus*), and infectious hematopoietic necrosis virus (IHNV) infection in rainbow trout (Nishizawa et al., 2009; Avunje et al., 2017; Kim et al., 2009). Interestingly, poly I:C was used successfully as a curative antiviral drug in sevenband grouper. Oh and colleagues demonstrated that fish treated with poly I:C 20 days post-infection (PI) from a natural occurrence of NNV had 6.3% mortality whereas fish that did not receive the poly I:C had a cumulative mortality reaching 90% (Oh et al., 2012). An

earlier study where fish were experimentally infected as opposed to becoming naturally infected from the environment did not see this curative effect; further studies will be needed to explore the potential of poly I:C to prevent virus-induced death (Nishizawa et al., 2009). In rock bream (*Oplegnathus fasciatus*) infected with rock bream iridovirus (RBIV) for two days prior to treatment with poly I:C there was a final mortality of 100%, but a substantial delay in this mortality (Jung et al., 2017).

There are cases where poly I:C was not particularly effective at protecting fish from viral infection; rock bream pre-treated with poly I:C showed protection from RBIV at 20^{o}C but not at 23^{o}C or 26^{o}C. At the higher temperatures there was 100% mortality, although there were some delays in mortality in the poly I:C treated group. At 20^{o}C there was 33.4% survivorship in the poly I:C treated group compared to 0% in the untreated group (Jung et al., 2017). In zebrafish (*Danio* rerio) only 5% of fish were protected from VHSV infection after pre-treatment with poly I:C, there was a notable delay in the mortality of the fish treated with poly I:C but the end result was still substantial mortality (Kavaliauskis et al., 2015).

At least two studies have tested poly I:C as an adjuvant for fish vaccines, in one case it was a combination of CpG DNA and poly I:C, and in the other study it was poly I:C stabilized with chitosan. The addition of CpG/poly I:C enhanced the protective effect of an inactivated vaccine against salmonid alphavirus in Atlantic Salmon (*Salmo salar*), but did not result in increased levels of neutralizing antibodies (Thim et al., 2012). In zebrafish, the chitosan stabilized poly I:C injected with an inactivated VHSV vaccine produced significant protection against VHSV, however the plasma from surviving fish also did not have neutralizing antibodies (Kavaliauskis et al., 2015). While there are examples of poly I:C performing as a prophylactic antiviral treatment, and at least one example of poly I:C rescuing infected fish, there are also

cases where poly I:C is less effective and in several studies, poly I:C only delayed fish mortality. It is also unclear if this molecule can function as a strong adjuvant. Future directions for this project focus on comparing the immuno-stimulatory antiviral and adjuvant properties of ivt-dsRNA to poly I:C.

7.3 Pattern-recognition receptors and functional studies

A better understanding of rainbow trout pattern-recognition receptors (PRRs) will help elucidate the immune pathways induced by viral pathogen-associated molecular patterns (PAMPs). While mammalian models can be used as a guide to form a hypothesis for the function and ligand-binding profile of aquatic animal PRRs, experimental evidence is needed to clarify their function, for a better understanding of their similarities and differences to mammals. The first step to understanding the functionality of these receptors is to clone the coding sequences, as has been done in this thesis for SCARA3, SCARA4, SCARA5, MARCO-1, MARCO-2, DDX3, and DHX9. Analysis of the conserved domains and motifs within these proteins suggests similarity of function to counterparts from other species. So far, with the PRRs identified in this manuscript, all domains have been similar to known sequences; however, with any new PRRs that are identified, missing domains would be of great interest and could give an indication of a difference in function. Following their identification, the next steps are to perform functional assays to identify the cognate ligands for these receptors. Unfortunately, these functional assays have many hindrances and hurdles that need to be overcome. GFP-tagged MARCO-1 and MARCO-2 were successfully transiently overexpressed in fish cells and saw functional binding to bacterial ligands. Overexpression studies with SCARA3/4/5 in fish cells were attempted, however, these studies were unsuccessful. To date it is unknown if this is because a) the proteins were not functional when overexpressed or b) if the proteins simply did not bind to any of the tested ligands, as the ligands were predicted based on studies in mammals.

Ligand binding has been studied in this thesis using transient transfection protocols to engineer cells to express the PRR of interest. There are several problems with this strategy. Fish cells have low transfection efficiencies compared to the levels reached in mammalian cells. This combined with their lower metabolism makes over expression studies challenging. For example, while mammalian cell lines can be transfected with almost 100% efficiency, fish cell transfection is often below 10% (Bonetta, 2005; Schiøtz et al., 2011). EPC cells are by far the most efficient for transfections and after extensive optimization the transfection efficiencies were 15-45% depending on the method of counting positive cells (Lopez et al., 2001; Schiøtz et al., 2011; Collet et al., 2018). In addition to the low transfection efficiency, studying type I IFN-mediated responses with transient transfected DNA has a unique difficulty, transfected DNA itself causes type I IFN production, with plasmid DNA acting as a PAMP (Li et al., 2005; Sobhkhez et al., 2017). A study found that injecting Atlantic salmon *in vivo* with control plasmid induced several immune genes without the presence of an insert (Sobhkhez et al., 2017). The creation of cell lines stably expressing these receptors are currently underway using traditional stable transfection methods, in hopes of having a less transient system in order to test ligand binding.

The CRISPR/Cas-9 system is a useful tool that among many applications can be used to create knock-in or knock-out cell lines. Currently the application of CRISPER/Cas-9 has been successful in fish cells and is a tool that will be utilized in future studies (Chakrapani et al., 2016). One issue with any knock-down system in fish is the whole-genome duplication event in teleost fish, and a second genome duplication event in salmonids, creating an incredible range of genetic variation (Glasauer and Neuhauss, 2014; Collet et al., 2018). In order to efficiently knockdown a gene, all the different variants should be identified and considered to achieve complete knockdown.

An additional future direction that would help to elucidate the function of PRRs is to create bioactive recombinant proteins. Traditionally recombinant proteins are produced by bacteria. However, there are limitations of using a prokaryotic system to produce a eukaryotic protein in a functional form as the post-translational modifications may not be appropriate or present and the chaperones within the bacteria may not facilitate proper folding of the protein (Brondyk, 2009). One way this can be overcome is to employ a eukaryotic protein expression system, such as baculoviruses and insect cells lines. This technology is not new for fish proteins, the insect cell line SF-9 and a recombinant baculovirus was used to produce recombinant active growth fish hormone in 1994, and in the future the recombinant dsRNA sensors may be produced using this method (Tsai et al., 1994). The expression of the surface class A scavenger receptors will be particularly cumbersome as the proteins are trimeric and membrane bound, but the extracellular domains can be produced as soluble proteins, as has been done for mammalian MARCO and a fish MARCO scavenger-receptor cysteine rich (SRCR) domain; full-length, active recombinant mammalian SR-A proteins have also been purified successfully (Qiu et al., 2013; Sankala et al., 2002; Baid et al., 2018). Once purified these proteins can be used for various ligand-protein interaction assays, such as surface plasmon resonance, bacteria-binding assays performed using fluorescent ligands and protein coated coverslips, or ELISA analysis (Qiu et al., 2013; Sankala et al., 2002).

7.4 Synthetic PAMPs

The study of PAMPs relies on the use of synthetic molecules to mimic those produced by pathogens. Some naturally occurring PAMPs, like lipopolysaccharide (LPS) from bacteria, can be purchased already purified, this is not the case for virally produced dsRNA; even with naturally occurring LPS the purity of these preparations is often questioned as contaminants such as other PAMPs may be present (Rutledge et al., 2011). There are many reasons research to date

has relied on poly I:C, synthetic molecules tend to be more cost effective. For example, when using the RNAi Megascript kit to produce dsRNA, this kit is approximately $26 for one reaction that can yield up to 50-100µg of dsRNA, although in this lab yields are generally lower, approximately 50µg. Poly I:C cost depends on the brand, but for example EMD Millipore™ Calbiochem poly I:C is approximately $100 for 10mg, approximately $1 for 100µg. Poly I:C is also easier to use, a simple reconstitution step produces a stock concentration, to create *in vitro* transcribed dsRNA a DNA template must be prepared followed by the transcription reaction, a digestion, and a purification. The yield can also vary depending on the reaction and the template, and some optimization is needed. However, compared with the complexities of extracting virus-produced dsRNA, the *in vitro* molecule preparation is much simpler, cheaper and requires less time and optimization.

Poly I:C is not a naturally occurring molecule and host cells have not evolved to sense and respond to this molecule (Löseke et al., 2008). While *in vitro* transcribed dsRNA may have some downfalls compared to poly I:C, it has many advantages in terms of biological relevancy and is more efficient to produce than extracting viral dsRNA. *In vitro* transcribed dsRNA provides a researcher with the option to control length and sequence, modified nucleotides can be added to the transcription reaction, or post-transcriptional modifications such as capping or tailing can be added using enzymatic reactions. In this thesis *in vitro* dsRNA was used where possible as an alternative to poly I:C. Rainbow trout and fathead minnow cells both respond robustly to *in vitro* transcribed dsRNA by producing type I IFNs and an antiviral state. It was demonstrated the rainbow trout proteins DDX3 and DHX9 were able to bind to *in vitro* transcribed dsRNA using a pull-down assay.

7.5 Final Conclusions

The contents of this thesis provide evidence that dsRNA with natural sequence variation and defined length, is an important viral PAMP for the innate immune response in fish cells. The use of the synthetic IFN-inducer poly I:C has been questioned and *in vitro* transcribed dsRNA has been suggested as a more biologically accurate substitute. Future studies using different fish species and different aquatic viruses will help elucidate the conservation of these findings for broader applications. Identification of novel receptors in rainbow trout cells lays the groundwork for future studies to better understand the role of these receptors and their similarities and differences to mammalian homologs. The functional study of the dsRNA surface receptor MARCO showed an unexpected finding that the receptor variants did not bind to dsRNA, this emphasizes the need to further characterize receptors identified in fish for their functional purpose. Future studies will translate the *in vitro* studies performed here to *in vivo* studies in whole fish. *In vivo* studies will clarify the potential for *in vitro* transcribed dsRNA to be used as an antiviral therapy or vaccine adjuvant to prevent the massive losses in aquaculture caused by viral disease.

References

Ablasser, A., Bauernfeind, F., Hartmann, G., Latz, E., Fitzgerald, K.A. and Hornung, V., 2009. RIG-I-dependent sensing of poly (dA: dT) through the induction of an RNA polymerase III–transcribed RNA intermediate. *Nature Immunology*, *10*(10), p.1065.

AFS-FHS (American Fisheries Society-Fish Health Section). 2014. FHS blue book: suggested procedures for the detection and identification of certain finfish and shellfish pathogens, 2014 edition. Accessible at: http://afs-fhs.org/bluebook/bluebook-index.php.

Aggad, D., Mazel, M., Boudinot, P., Mogensen, K.E., Hamming, O.J., Hartmann, R., Kotenko, S., Herbomel, P., Lutfalla, G. and Levraud, J.P., 2009. The two groups of zebrafish virus-induced interferons signal via distinct receptors with specific and shared chains. *The Journal of Immunology*, *183*(6), pp.3924-3931.

Akira, S. and Hemmi, H., 2003. Recognition of pathogen-associated molecular patterns by TLR family. *Immunology Letters*, *85*(2), pp.85-95.

Al-Hussinee, L., Huber, P., Russell, S., LePage, V., Reid, A., Young, K.M., Nagy, E., Stevenson, R.M.W. and Lumsden, J.S., 2010. Viral haemorrhagic septicaemia virus IVb experimental infection of rainbow trout, *Oncorhynchus mykiss* (Walbaum), and fathead minnow, *Pimphales promelas* (Rafinesque). *Journal of Fish Diseases, 33*(4), pp.347- 360.

Alexopoulou, L., Holt, A.C., Medzhitov, R. and Flavell, R.A., 2001. Recognition of double-stranded RNA and activation of NF-κB by Toll-like receptor 3. *Nature*, *413*(6857), p.732.

Alvarez-Torres, D., Garcia-Rosado, E., Fernandez-Trujillo, M.A., Bejar, J., Alvarez, M.C., Borrego, J.J. and Alonso, M.C., 2013. Antiviral specificity of the *Solea senegalensis* Mx protein constitutively expressed in CHSE-214 cells. *Marine Biotechnology*, *15*(2), pp.125-132.

Angus, A.G., Dalrymple, D., Boulant, S., McGivern, D.R., Clayton, R.F., Scott, M.J., Adair, R., Graham, S., Owsianka, A.M., Targett-Adams, P. and Li, K., 2010. Requirement of cellular DDX3 for hepatitis C virus replication is unrelated to its interaction with the viral core protein. *Journal of General Virology*, *91*(1), pp.122-132.

Ariumi, Y., 2014. Multiple functions of DDX3 RNA helicase in gene regulation, tumorigenesis, and viral infection. *Frontiers in Genetics*, *5*, article 423.

Ariumi, Y., Kuroki, M., Abe, K.I., Dansako, H., Ikeda, M., Wakita, T. and Kato, N., 2007. DDX3 DEAD-box RNA helicase is required for hepatitis C virus RNA replication. *Journal of Virology*, *81*(24), pp.13922-13926.

Arredouani, M., Yang, Z., Ning, Y., Qin, G., Soininen, R., Tryggvason, K. and Kobzik, L., 2004. The scavenger receptor MARCO is required for lung defense against pneumococcal pneumonia and inhaled particles. *Journal of Experimental Medicine*, *200*(2), pp.267-272.

Arredouani, M.S., Palecanda, A., Koziel, H., Huang, Y.C., Imrich, A., Sulahian, T.H., Ning, Y.Y., Yang, Z., Pikkarainen, T., Sankala, M., and Vargas, S.O., 2005. MARCO is the major binding receptor for unopsonized particles and bacteria on human alveolar macrophages. *Journal of Immunology, 175* (9), pp. 6058-6064.

Artimo, P., Jonnalagedda, M., Arnold, K., Baratin, D., Csardi, G., De Castro, E., Duvaud, S., Flegel, V., Fortier, A., Gasteiger, E. and Grosdidier, A., 2012. ExPASy: SIB bioinformatics resource portal. *Nucleic Acids Research*, *40*(W1), pp.W597-W603.

Assefa, A. and Abunna, F., 2018. Maintenance of Fish Health in Aquaculture: Review of Epidemiological Approaches for Prevention and Control of Infectious Disease of Fish. *Veterinary Medicine International*, *2018*.

Au-Yeung, N., Mandhana, R. and Horvath, C.M., 2013. Transcriptional regulation by STAT1 and STAT2 in the interferon JAK-STAT pathway. *Jak-Stat*, *2*(3), p.e23931.

Avunje, S. and Jung, S.J., 2017. Poly (I: C) and imiquimod induced immune responses and their effects on the survival of olive flounder (*Paralichthys olivaceus*) from viral haemorrhagic septicaemia. *Fish & Shellfish Immunology*, *71*, pp.338-345.

Baid, K., Nellimarla, S., Huynh, A., Boulton, S., Guarné, A., Melacini, G., Collins, S.E. and Mossman, K.L., 2018. Direct binding and internalization of diverse extracellular nucleic acid species through the collagenous domain of class A scavenger receptors. *Immunology and Cell Biology,* epub ahead of print.

Bale, S., Julien, J.P., Bornholdt, Z.A., Kimberlin, C.R., Halfmann, P., Zandonatti, M.A., Kunert, J., Kroon, G.J., Kawaoka, Y., MacRae, I.J. and Wilson, I.A., 2012. Marburg virus VP35 can both fully coat the backbone and cap the ends of dsRNA for interferon antagonism. *PLoS Pathogens,. 8*(9), e1002916.

Belgnaoui, S.M., Paz, S. and Hiscott, J., 2011. Orchestrating the interferon antiviral response through the mitochondrial antiviral signaling (MAVS) adapter. *Current Opinion in Immunology*, *23*(5), pp.564-572.

Benard, E.L., Roobol, S.J., Spaink, H.P., and Meijer, A.H., 2014. Phagocytosis of mycobacteria by zebrafish macrophages is dependent on the scavenger receptor Marco, a key control factor of pro-inflammatory signalling. *Developmental & Comparative Immunology, 47* (2), pp. 223-233.

Benmansour, A., Basurco, B., Monnier, A.F., Vende, P., Winton, J.R. and de Kinkelin, P., 1997. Sequence variation of the glycoprotein gene identifies three distinct lineages within field

isolates of viral haemorrhagic septicaemia virus, a fish rhabdovirus. *Journal of General Virology, 78*(11), pp.2837-2846.

Bevilacqua, P.C. and Cech, T.R., 1996. Minor-groove recognition of double-stranded RNA by the double-stranded RNA-binding domain from the RNA-activated protein kinase PKR. *Biochemistry*, *35*(31), pp.9983-9994.

Biacchesi, S., LeBerre, M., Lamoureux, A., Louise, Y., Lauret, E., Boudinot, P. and Brémont, M., 2009. Mitochondrial antiviral signaling protein plays a major role in induction of the fish innate immune response against RNA and DNA viruses. *Journal of Virology*, *83*(16), pp.7815-7827.

Biacchesi, S., Mérour, E., Chevret, D., Lamoureux, A., Bernard, J. and Brémont, M., 2017. NV proteins of fish novirhabdovirus recruit cellular PPM1Bb protein phosphatase and antagonize RIG-I-mediated IFN induction. *Scientific Reports*, *7*, p.44025.

Bilateral VHSV Surveillance Working Group, 2007. Surveillance Proposal for Viral Hemorrhagic Septicemia Virus In Freshwater Fish in Canada and the United States. Canadian Food Inspection Agency, Aquatic Animal Health Division Great Lakes Fish Health Committee U. S. Department of Agriculture Animal and Plant Health Inspection Service U.S. Fish and Wildlife Service

Boeras, I., Song, Z., Moran, A., Franklin, J., Brown, W.C., Johnson, M., Boris-Lawrie, K. and Heng, X., 2016. DHX9/RHA binding to the PBS-segment of the genomic RNA during HIV-1 assembly bolsters virion infectivity. *Journal of Molecular Biology*, *428*(11), pp.2418-2429.

Bols, N.C., Barlian, A., Chirino-Trejo, M., Caldwell, S.J., Goegan, P. and Lee, L.E.J., 1994. Development of a cell line from primary cultures of rainbow trout, *Oncorhynchus mykiss* (Walbaum), gills. *Journal of Fish Diseases*, *17*(6), pp.601-611.

Bonetta, L. 2005. The inside scoop—evaluating gene delivery methods. *Nature Methods, 2,* pp. 875-883.

Boudinot, P., Massin, P., Blanco, M., Riffault, S. and Benmansour, A., 1999. vig-1, a new fish gene induced by the rhabdovirus glycoprotein, has a virus-induced homologue in humans and shares conserved motifs with the MoaA family. *Journal of Virology*, *73*(3), pp.1846-1852.

Bowdish, D.M., and Gordon, S., 2009. Conserved domains of the class A scavenger receptors: evolution and function. *Immunological Reviews, 227* (1), pp. 19-31.

Bowdish, D.M., Sakamoto, K., Kim, M.J., Kroos, M., Mukhopadhyay, S., Leifer, C.A., Tryggvason, K., Gordon, S. and Russell, D.G., 2009. MARCO, TLR2, and CD14 are required for macrophage cytokine responses to mycobacterial trehalose dimycolate and Mycobacterium tuberculosis. *PLoS Pathogens*, *5*(6), p.e1000474.

Brian, J.V., Beresford, N., Margiotta-Casaluci, L. and Sumpter, J.P., 2011. Preliminary data on the influence of rearing temperature on the growth and reproductive status of fathead minnows *Pimephales promelas*. *Journal of Fish Biology*, *79*(1), pp.80-88.

Brondyk, W.H., 2009. Selecting an appropriate method for expressing a recombinant protein. *Methods in Enzymology*, *463*, pp. 131-147.

Brubaker, S.W., Bonham, K.S., Zanoni, I. and Kagan, J.C., 2015. Innate immune pattern recognition: a cell biological perspective. *Annual Review of Immunology*, *33*, pp.257-290.

Canton, J., Neculai, D., Grinstein, S., 2013. Scavenger receptors in homeostasis and immunity. *Nature Reveiws Immunology,. 13* (9), pp. 621-634.

Capitanio, J.S., Montpetit, B. and Wozniak, R.W., 2017. Human Nup98 regulates the localization and activity of DExH/D-box helicase DHX9. *eLife*, *6*, pp. e18825.

Carter, W.A. and De Clercq, E., 1974. Viral infection and host defense. *Science, 186*(4170), pp. 1172-1178.

Chahar, H.S., Chen, S. and Manjunath, N., 2013. P-body components LSM1, GW182, DDX3, DDX6 and XRN1 are recruited to WNV replication sites and positively regulate viral replication. *Virology*, *436*(1), pp.1-7.

Chakrapani, V., Patra, S.K., Panda, R.P., Rasal, K.D., Jayasankar, P. and Barman, H.K., 2016. Establishing targeted carp TLR22 gene disruption via homologous recombination using CRISPR/Cas9. *Developmental & Comparative Immunology*, *61*, pp.242-247.

Chang, M., Collet, B., Nie, P., Lester, K., Campbell, S., Secombes, C.J. and Zou, J., 2011. Expression and functional characterization of the RIG-I-like receptors MDA5 and LGP2 in Rainbow trout (*Oncorhynchus mykiss*). *Journal of Virology*, *85*(16), pp.8403-8412.

Chang, M., Nie, P., Collet, B., Secombes, C.J. and Zou, J., 2009. Identification of an additional two-cysteine containing type I interferon in rainbow trout *Oncorhynchus mykiss* provides evidence of a major gene duplication event within this gene family in teleosts. *Immunogenetics. 61*(4), pp. 315-325.

Chaves-Pozo, E., Zou, J., Secombes, C.J., Cuesta, A. and Tafalla, C., 2010. The rainbow trout (*Oncorhynchus mykiss*) interferon response in the ovary. *Molecular Immunology*, *47*(9), pp.1757-1764.

Chen, S.N., Zou, P.F. and Nie, P., 2017. Retinoic acid-inducible gene I (RIG-I)-like receptors (RLRs) in fish: current knowledge and future perspectives. *Immunology, 151,* pp.16-25.

Chen, Y.M., Su, Y.L., Shie, P.S., Huang, S.L., Yang, H.L. and Chen, T.Y., 2008. Grouper Mx confers resistance to nodavirus and interacts with coat protein. *Developmental & Comparative Immunology*, *32*(7), pp.825-836.

Chin, K.C. and Cresswell, P., 2001. Viperin (cig5), an IFN-inducible antiviral protein directly induced by human cytomegalovirus. *Proceedings of the National Academy of Sciences*, *98*(26), pp.15125-15130.

Chiu, Y.H., MacMillan, J.B. and Chen, Z.J., 2009. RNA polymerase III detects cytosolic DNA and induces type I interferons through the RIG-I pathway. *Cell*, *138*(3), pp.576-591.

Collet, B., Collins, C. and Lester, K., 2018. Engineered cell lines for fish health research. *Developmental & Comparative Immunology*, *80*, pp.34-40.

Compton, T., Kurt-Jones, E.A., Boehme, K.W., Belko, J., Latz, E., Golenbock, D.T. and Finberg, R.W., 2003. Human cytomegalovirus activates inflammatory cytokine responses via CD14 and Toll-like receptor 2. *Journal of Virology*, *77*(8), pp.4588-4596.

Crosse, K.M., Monson, E.A., Beard, M.R. and Helbig, K.J., 2018. Interferon-Stimulated Genes as Enhancers of Antiviral Innate Immune Signaling. *Journal of Innate Immunity, 10* (2)*,* pp. 85–93.

Cui, H., Yan, Y., Wei, J., Huang, X., Huang, Y., Ouyang, Z. and Qin, Q., 2011. Identification and functional characterization of an interferon regulatory factor 7-like (IRF7-like) gene from orange-spotted grouper, *Epinephelus coioides. Developmental & Comparative Immunology*, *35*(6), pp.672-684.

Daly, C., and Reich, N.C., 1993. Double-stranded RNA activates novel factors that bind to the interferon-stimulated response element. *Molecular and Cellular Biology*, *13*(6), pp.3756-3764.

Dansako, H., Yamane, D., Welsch, C., McGivern, D.R., Hu, F., Kato, N. and Lemon, S.M., 2013. Class A scavenger receptor 1 (MSR1) restricts hepatitis C virus replication by mediating toll-like receptor 3 recognition of viral RNAs produced in neighboring cells. *PLoS Pathogens*, *9*(5), p.e1003345.

Desmet, C.J. and Ishii, K.J., 2012. Nucleic acid sensing at the interface between innate and adaptive immunity in vaccination. *Nature Reviews Immunology*, *12*(7), p.nri3247.

DeWitte-Orr, S.J., Mehta, D.R., Collins, S.E., Suthar, M.S., Gale, M. and Mossman, K.L., 2009. Long double-stranded RNA induces an antiviral response independent of IFN regulatory factor 3, IFN-β promoter stimulator 1, and IFN. *The Journal of Immunology*, *183*(10), pp.6545-6553.

DeWitte-Orr, S.J. and Mossman, K.L., 2010. dsRNA and the innate antiviral immune response. *Future Virology, 5*(3), pp.325-341.

DeWitte-Orr, S.J., Collins, S.E., Bauer, C.M., Bowdish, D.M. and Mossman, K.L., 2010. An accessory to the 'Trinity': SR-As are essential pathogen sensors of extracellular dsRNA,

mediating entry and leading to subsequent type I IFN responses. *PLoS Pathogens*, *6*(3), p.e1000829.

DeWitte-Orr, S.J., Mehta, D.R., Collins, S.E., Suthar, M.S., Gale, M. and Mossman, K.L., 2009. Long double-stranded RNA induces an antiviral response independent of IFN regulatory factor 3, IFN-β promoter stimulator 1, and IFN. *The Journal of Immunology*, *183*(10), pp.6545-6553.

Diamond, M.S., 2014. IFIT1: a dual sensor and effector molecule that detects non-2′-O methylated viral RNA and inhibits its translation. *Cytokine & Growth Factor Reviews*, *25*(5), pp.543-550.

Ditton, H.J., Zimmer, J., Kamp, C., Rajpert-De Meyts, E. and Vogt, P.H., 2004. The AZFa gene DBY (DDX3Y) is widely transcribed but the protein is limited to the male germ cells by translation control. *Human Molecular Genetics*, *13*(19), pp.2333-2341.

Doherty, L., Poynter, S.J., Aloufi, A. and DeWitte-Orr, S.J., 2016. Fish viruses make dsRNA in fish cells: characterization of dsRNA production in rainbow trout (*Oncorhynchus mykiss*) cells infected with viral haemorrhagic septicaemia virus, chum salmon reovirus and frog virus 3. *Journal of Fish Diseases*, *39*(9), pp.1133-1137.

Dopazo, C.P., Bandin, I., Rivas, C., Cepeda, C. and Barja, J.L., 1996. Antigenic differences among aquareoviruses correlate with previously established genogroups. *Diseases of Aquatic Organisms*, *26*(2), pp.159-162.

Dorrington, M.G., Roche, A.M., Chauvin, S.E., Tu, Z., Mossman, K.L., Weiser, J.N. Bowdish, D.M., 2013. MARCO is required for TLR2-and Nod2-mediated responses to Streptococcus pneumoniae and clearance of pneumococcal colonization in the murine nasopharynx. *Journal of Immunology, 190* (1), pp. 250-258.

Dunne, D.W., Resnick, D., Greenberg, J., Krieger, M. and Joiner, K.A., 1994. The type I macrophage scavenger receptor binds to gram-positive bacteria and recognizes lipoteichoic acid. *Proceedings of the National Academy of Sciences*, *91*(5), pp.1863-1867.

Durfee, L.A., Lyon, N., Seo, K. and Huibregtse, J.M., 2010. The ISG15 conjugation system broadly targets newly synthesized proteins: implications for the antiviral function of ISG15. *Molecular Cell*, *38*(5), pp.722-732.

Eaton, W.D., 1990. Anti-viral activity in four species of salmonids following exposure to poly inosinic: cytidylic acid. *Disease of Aquatic Organisms*, *9*(3), pp.193-8.

Elomaa, O., Kangas, M., Sahlberg, C., Tuukkanen, J., Sormunen, R., Liakka, A., Thesleff, I., Kraal, G., Tryggvason, K., 1995. Cloning of a novel bacteria-binding receptor structurally related to scavenger receptors and expressed in a subset of macrophages. *Cell 80* (4), pp. 603-609.

Elomaa, O., Sankala, M., Pikkarainen, T., Bergmann, U., Tuuttila, A., Raatikainen-Ahokas, A., Sariola, H. and Tryggvason, K., 1998. Structure of the human macrophage MARCO receptor and characterization of its bacteria-binding region. *Journal of Biological Chemistry*, *273*(8), pp.4530-4538.

Faisal, M., Shavalier, M., Kim, R.K., Millard, E.V., Gunn, M.R., Winters, A.D., Schulz, C.A., Eissa, A., Thomas, M.V., Wolgamood, M. and Whelan, G.E., 2012. Spread of the emerging viral hemorrhagic septicemia virus strain, genotype IVb, in Michigan, USA. *Viruses*, 4(5), pp.734-760.

Felsenstein J., 1985. Confidence limits on phylogenies: An approach using the boostrap. *Evolution, 39*, pp.783-791.

Feng, S., Jiang, Y., Zhang, S., Dong, C., Jiang, L., Peng, W., Mu, X., Sun, X. and Xu, P., 2016. Genome wide identification of scavenger receptors class A in common carp (*Cyprinus carpio*) and their expression following Aeromonas hydrophila infection. *Fish & Shellfish Immunology*, *54*, pp.60-67.

Fijan, N., Sulimanović, D., Bearzotti, M., Muzinić, D., Zwillenberg, L.O., Chilmonczyk, S., Vautherot, J.F. and De Kinkelin, P., 1983. Some properties of the epithelioma papulosum cyprini (EPC) cell line from carp *Cyprinus carpio*. *Annales de l'Institut pasteur/Virologie*, *134*(2), pp. 207-220.

Fijan, N., Sulimanović, D., Bearzotti, M., Muzinić, D., Zwillenberg, L.O., Chilmonczyk, S., Vautherot, J.F. and De Kinkelin, P., 1983, April. Some properties of the epithelioma papulosum cyprini (EPC) cell line from carp Cyprinus carpio. In *Annales de l'Institut pasteur/Virologie,* 134(2), pp. 207-220. Elsevier Masson.

Fisheries and Oceans Canad, 2016. 2016 Canadian Aquaculture Production Statistics. Statistics Canada. Table 003-0001 - Aquaculture, production and value, annual, CANSIM (database). http://www.dfo-mpo.gc.ca/stats/aqua/aqua16-eng.htm.

Food and Agriculture Organization of the United Nations. 2016. *The State of World Fisheries and Aquaculture 2016. Contributing to food security and nutrition for all.* Rome. 200 pp.

Frattini, S.A., Groocock, G.H., Getchell, R.G., Wooster, G.A., Casey, R.N., Casey, J.W. and Bowser, P.R., 2011. A 2006 survey of viral hemorrhagic septicemia (VHSV) virus type IVb in New York State waters. *Journal of Great Lakes Research*, 37(1), pp.194-198.

Fuchsova, B. and Hozak, P., 2002. The localization of nuclear DNA helicase II in different nuclear compartments is linked to transcription. *Experimental cell research, 279*(2), pp.260-270.

Fujita H, Ohshima T, Oishi T, Aratani S, Fujii R, Fukamizu A and Nakajima T., 2005. Relevance of nuclear localization and functions of RNA helicase A. *International Journal of Molecular Medicine, 15*, pp. 555- 560.

Fukuda, M., Ohtani, K., Jang, S.J., Yoshizaki, T., Mori, K.I., Motomura, W., Yoshida, I., Suzuki, Y., Kohgo, Y. and Wakamiya, N., 2011. Molecular cloning and functional analysis of scavenger receptor zebrafish CL-P1. *Biochimica et Biophysica Acta (BBA)-General Subjects*, *1810*(12), pp.1150-1159.

Fullam, A. and Schröder, M., 2013. DExD/H-box RNA helicases as mediators of anti-viral innate immunity and essential host factors for viral replication. *Biochimica Et Biophysica Acta (BBA)-Gene Regulatory Mechanisms, 1829*(8), pp.854-865.

Fuller-Pace, F.V., 2006. DExD/H box RNA helicases: multifunctional proteins with important roles in transcriptional regulation. *Nucleic Acids Research, 34*(15), pp.4206-4215.

Ganassin, R.C., Bols, N.C., 1998. Development of a monocyte/macrophage-like cell line, RTS11, from rainbow trout spleen. *Fish & Shellfish Immunology, 8,* pp. 457-476.

Garbelli, A., Beermann, S., Di Cicco, G., Dietrich, U. and Maga, G., 2011. A motif unique to the human DEAD-box protein DDX3 is important for nucleic acid binding, ATP hydrolysis, RNA/DNA unwinding and HIV-1 replication. *PLoS One*, *6*(5), p.e19810.

Garcia, M.A., Meurs, E.F. and Esteban, M., 2007. The dsRNA protein kinase PKR: virus and cell control. *Biochimie*, *89*(6-7), pp.799-811.

Getchell, R.G., Cornwell, E.R., Groocock, G.H., Wong, P.T., Coffee, L.L., Wooster, G.A. and Bowser, P.R., 2013. Experimental transmission of VHSV genotype IVb by predation. *Journal of Aquatic Animal Health, 25*(4), pp.221-229.

Glasauer, S.M. and Neuhauss, S.C., 2014. Whole-genome duplication in teleost fishes and its evolutionary consequences. *Molecular Genetics and Genomics*, *289*(6), pp.1045-1060.

Goodwin, A.E., Peterson, J.E., Meyers, T.R. and Money, D.J., 2004. Transmission of exotic fish viruses: the relative risks of wild and cultured bait. *Fisheries, 29*(5), pp.19-23.

Goubau, D., der Veen, A.G., Chakravarty, P., Lin, R., Rogers, N., Rehwinkel, J., Deddouche, S., Rosewell, I., Hiscott, J. and Reis e Sousa, C., 2015. Mouse superkiller-2-like helicase DDX60 is dispensable for type I IFN induction and immunity to multiple viruses. *European Journal of Immunology*, *45*(12), pp.3386-3403.

Goubau, D., Schlee, M., Deddouche, S., Pruijssers, A.J., Zillinger, T., Goldeck, M., Schuberth, C., Van der Veen, A.G., Fujimura, T., Rehwinkel, J. and Iskarpatyoti, J.A., 2014. Antiviral immunity via RIG-I-mediated recognition of RNA bearing 5′-diphosphates. *Nature*, *514*(7522), p.372.

Gough, P.J. and Gordon, S., 2000. The role of scavenger receptors in the innate immune system. *Microbes and Infection*, *2*(3), pp.305-311.

Granucci, F., Petralia, F., Urbano, M., Citterio, S., Di Tota, F., Santambrogio, L. and Ricciardi-Castagnoli, P., 2003. The scavenger receptor MARCO mediates cytoskeleton rearrangements in dendritic cells and microglia. *Blood*, *102*(8), pp.2940-2947.

Gravell, M. and Malsberger, R.G., 1965. A permanent cell line from the fathead minnow (*Pimephales promelas*). *Annals of the New York Academy of Sciences*, *126*(1), pp.555-565.

Grolleau, A., Misek, D.E., Kuick, R., Hanash, S. and Mulé, J.J., 2003. Inducible expression of macrophage receptor Marco by dendritic cells following phagocytic uptake of dead cells uncovered by oligonucleotide arrays. *The Journal of Immunology*, *171*(6), pp.2879-2888.

Groocock, G.H., Getchell, R.G., Wooster, G.A., Britt, K.L., Batts, W.N., Winton, J.R., Casey, R.N., Casey, J.W. and Bowser, P.R., 2007. Detection of viral hemorrhagic septicemia in round gobies in New York State (USA) waters of Lake Ontario and the St. Lawrence River. *Diseases of Aquatic Organisms, 76*(3), pp.187-192.

Guo, D.Y., Cao, C., Zhang, X.Y., Xiang, L.X. and Shao, J.Z., 2016. Scavenger receptor SCARA5 acts as an HMGB1 recognition molecule negatively involved in HMGB1-mediated inflammation in fish models. *The Journal of Immunology*, *197*(8), pp.3198-3213.

Harmache, A., LeBerre, M., Droineau, S., Giovannini, M. and Brémont, M., 2006. Bioluminescence imaging of live infected salmonids reveals that the fin bases are the major portal of entry for Novirhabdovirus. *Journal of Virology, 80*(7), pp.3655-3659.

He, J., Liu, H. and Wu, C., 2014. Identification of SCARA3, SCARA5 and MARCO of class A scavenger receptor-like family in *Pseudosciaena crocea*. *Fish & Shellfish Immunology*, *41*(2), pp.238-249.

Heinicke, .A., Wong, C.J., Lary, J., Nallagatia, S.R., Diegelman-Parente, A., Zheng, X., Cole, J.L., Bevilacqua, P.C. (2009). RNA Dimerization Promotes PKR Dimerization and Activation. *Journal of Molecular Biology, 390*(2): 319-338.

Helbig, K.J., Eyre, N.S., Yip, E., Narayana, S., Li, K., Fiches, G., McCartney, E.M., Jangra, R.K., Lemon, S.M. and Beard, M.R., 2011. The antiviral protein viperin inhibits hepatitis C virus replication via interaction with nonstructural protein 5A. *Hepatology*, *54*(5), pp.1506-1517.

Hirano, S., Fujitani, Y., Furuyama, A. and Kanno, S., 2012. Macrophage receptor with collagenous structure (MARCO) is a dynamic adhesive molecule that enhances uptake of carbon nanotubes by CHO-K1 cells. *Toxicology and applied pharmacology*, *259*(1), pp.96-103.

Holland, J.W., Bird, S., Williamson, B., Woudstra, C., Mustafa, A., Wang, T., Zou, J., Blaney, S.C., Collet, B. and Secombes, C.J., 2008. Molecular characterization of IRF3 and IRF7

in rainbow trout, Oncorhynchus mykiss: functional analysis and transcriptional modulation. *Molecular Immunology*, *46*(2), pp.269-285.

Hope, K.M., Casey, R.N., Groocock, G.H., Getchell, R.G., Bowser, P.R. and Casey, J.W., 2010. Comparison of Quantitative RT-PCR with Cell Culture to Detect Viral Hemorrhagic Septicemia Virus (VHSV) IVb Infections in the Great Lakes. *Journal of Aquatic Animal Health*, *22*(1), pp.50-61.

Hovanessian, A.G. and Justesen, J., 2007. The human 2′-5′ oligoadenylate synthetase family: unique interferon-inducible enzymes catalyzing 2′-5′ instead of 3′-5′ phosphodiester bond formation. *Biochimie*, *89*(6-7), pp.779-788.

Hu, Y., Huang, Y., Liu, J., Zhang, J., Qin, Q. and Huang, X., 2018A. TBK1 from orange-spotted grouper exerts antiviral activity against fish viruses and regulates interferon response. *Fish & Shellfish Immunology*, *73*, pp.92-99.

Hu, Y.W., Zhang, J., Wu, X.M., Cao, L., Nie, P. and Chang, M.X., 2018B. TBK1 isoforms negatively regulate type I interferon induction by inhibiting TBK1-IRF3 interaction and IRF3 phosphorylation. *Frontiers in Immunology*, *9*, p.84.

Huang, M., and Mitchell, B.S., 2008. Guanine nucleotide depletion mediates translocation of nucleolar proteins, including RNA helicase A (DHX-9). *Nucleosides, Nucleotides, and Nucleic Acids*, *27*(6-7), pp.704-711.

Huang, X., Huang, Y., Cai, J., Wei, S., Ouyang, Z. and Qin, Q., 2013. Molecular cloning, expression and functional analysis of ISG15 in orange-spotted grouper, *Epinephelus coioides*. *Fish & Shellfish Immunology*, *34*(5), pp.1094-1102.

Huang, Y., Zhang, J., Ouyang, Z., Liu, J., Zhang, Y., Hu, Y., Huang, X. and Qin, Q., 2018. Grouper MAVS functions as a crucial antiviral molecule against nervous necrosis virus infection. *Fish & Shellfish Immunology*, *72*, pp.14-22.

Ivanova, N.V., Zemlak, T.S., Hanner, R.H. and Hebert, P.D., 2007. Universal primer cocktails for fish DNA barcoding. *Molecular Ecology Resources,* 7(4), pp.544-548.

Ivashkiv, L.B. and Donlin, L.T., 2014. Regulation of type I interferon responses. *Nature Reviews Immunology*, *14*(1), p.36.

Jacobs, B.L. and Langland, J.O., 1996. When two strands are better than one: the mediators and modulators of the cellular responses to double-stranded RNA. *Virology*, *219*(2), pp.339-349.

Jacquemont, B. and Roizman, B., 1975. RNA synthesis in cells infected with herpes simplex virus. X. Properties of viral symmetric transcripts and of double-stranded RNA prepared from them. *Journal of Virology*, *15*(4), pp.707-713.

Jain, A., Bacolla, A., Chakraborty, P., Grosse, F., and Vasquez, K.M., 2010, Human DHX9 helicase unwinds triple-helical DNA structures. *Biochemistry, 49*, pp. 6992-6999.

Jang, S., Ohtani, K., Fukuoh, A., Yoshizaki, T., Fukuda, M., Motomura, W., Mori, K., Fukuzawa, J., Kitamoto, N., Yoshida, I. and Suzuki, Y., 2009. Scavenger receptor collectin placenta 1 (CL-P1) predominantly mediates zymosan phagocytosis by human vascular endothelial cells. *Journal of Biological Chemistry*, *284*(6), pp.3956-3965.

Jensen, I. and Robertsen, B., 2002. Effect of double-stranded RNA and interferon on the antiviral activity of Atlantic salmon cells against infectious salmon anemia virus and infectious pancreatic necrosis virus. *Fish & Shellfish Immunology*, *13*(3), pp.221-241.

Jensen, I., Larsen, R. and Robertsen, B., 2002. An antiviral state induced in Chinook salmon embryo cells (CHSE-214) by transfection with the double-stranded RNA poly I: C. *Fish & Shellfish Immunology*, *13*(5), pp.367-378.

Ji, J., Rao, Y., Wan, Q., Liao, Z. and Su, J., 2018. Teleost-Specific TLR19 Localizes to Endosome, Recognizes dsRNA, Recruits TRIF, Triggers both IFN and NF-κB Pathways, and Protects Cells from Grass Carp Reovirus Infection. *The Journal of Immunology*, *200*(2), pp.573-585.

Jiang, M., Österlund, P., Sarin, L.P., Poranen, M.M., Bamford, D.H., Guo, D. and Julkunen, I., 2011. Innate immune responses in human monocyte-derived dendritic cells are highly dependent on the size and the 5′ phosphorylation of RNA molecules. *The Journal of Immunology*, *187*(4), pp.1713-1721.

Jiang, Y., Oliver, P., Davies, K.E. and Platt, N., 2006. Identification and characterization of murine SCARA5, a novel class A scavenger receptor that is expressed by populations of epithelial cells. *Journal of Biological Chemistry*, *281*(17), pp.11834-11845.

Jung, M.H. and Jung, S.J., 2017. Protective immunity against rock bream iridovirus (RBIV) infection and TLR3-mediated type I interferon signaling pathway in rock bream (*Oplegnathus fasciatus*) following poly (I: C) administration. *Fish & Shellfish Immunology*, *67*, pp.293-301.

Kariko, K. and Weissman, D., 2007. Naturally occurring nucleoside modifications suppress the immunostimulatory activity of RNA: implication for therapeutic RNA development. *Current Opinion in Drug Discovery and Development*, *10*(5), p.523.

Kato, H., Takeuchi, O., Mikamo-Satoh, E., Hirai, R., Kawai, T., Matsushita, K., Hiiragi, A., Dermody, T.S., Fujita, T. and Akira, S., 2008. Length-dependent recognition of double-stranded ribonucleic acids by retinoic acid–inducible gene-I and melanoma differentiation–associated gene 5. *Journal of Experimental Medicine*, *205*(7), pp.1601-1610.

Kato, H., Takeuchi, O., Sato, S., Yoneyama, M., Yamamoto, M., Matsui, K., Uematsu, S., Jung, A., Kawai, T., Ishii, K.J. and Yamaguchi, O., 2006. Differential roles of MDA5 and RIG-I helicases in the recognition of RNA viruses. *Nature*, *441*(7089), p.101.

Kaur, H., Jaso-Friedmann, L. and Evans, D.L., 2003. Identification of a scavenger receptor homologue on nonspecific cytotoxic cells and evidence for binding to oligodeoxyguanosine. *Fish & Shellfish Immunology*, *15*(3), pp.169-181.

Kavaliauskis, A., Arnemo, M., Kim, S.H., Ulanova, L., Speth, M., Novoa, B., Dios, S., Evensen, Ø., Griffiths, G.W. and Gjøen, T., 2015. Use of Poly (I: C) stabilized with chitosan as a vaccine-adjuvant against viral hemorrhagic septicemia virus infection in zebrafish. *Zebrafish*, *12*(6), pp.421-431.

Kawai, T. and Akira, S., 2008. Toll-like Receptor and RIG-1-like Receptor Signaling. *Annals of the New York Academy of Sciences*, *1143*(1), pp.1-20.

Kawai, T. and Akira, S., 2010. The role of pattern-recognition receptors in innate immunity: update on Toll-like receptors. *Nature Immunology*, *11*(5), p.373.

Kawano, A., Haiduk, C., Schirmer, K., Hanner, R., Lee, L.E.J., Dixon, B. and Bols, N.C., 2011. Development of a rainbow trout intestinal epithelial cell line and its response to lipopolysaccharide. *Aquaculture Nutrition*, *17*(2), pp. e241-e252.

Kelly, R.K., Souter, B.W. and Miller, H.R., 1978. Fish cell lines: comparisons of CHSE-214, FHM, and RTG-2 in assaying IHN and IPN viruses. *Journal of the Fisheries Board of Canada*, *35*(7), pp.1009-1011.

Kerr, S. J. 2012. The management of bait in Ontario: a review. Fisheries Policy Section, Biodiversity Branch. Ontario Ministry of Natural Resources. Peterborough, Ontario. 49 p. + appendices.

Kibenge, S.B., and Godoy, M.G. 2016. *Aquaculture Virology*, Elsevier

Kim, C.S., Kosuke, Z., Nam, Y.K., Kim, S.K. and Kim, K.H., 2007. Protection of shrimp (*Penaeus chinensis*) against white spot syndrome virus (WSSV) challenge by double-stranded RNA. *Fish & Shellfish Immunology*, *23*(1), pp.242-246.

Kim, H.J., Oseko, N., Nishizawa, T. and Yoshimizu, M., 2009. Protection of rainbow trout from infectious hematopoietic necrosis (IHN) by injection of infectious pancreatic necrosis virus (IPNV) or Poly (I: C). *Diseases of Aquatic Organisms*, *83*(2), pp.105-113.

Kim, R. and Faisal, M., 2011. Emergence and resurgence of the viral hemorrhagic septicemia virus (Novirhabdovirus, Rhabdoviridae, Mononegavirales). *Journal of Advanced Research*, *2*(1), pp.9-23.

Kim, T., Pazhoor, S., Bao, M., Zhang, Z., Hanabuchi, S., Facchinetti, V., Bover, L., Plumas, J., Chaperot, L., Qin, J. and Liu, Y.J., 2010. Aspartate-glutamate-alanine-histidine box motif

(DEAH)/RNA helicase A helicases sense microbial DNA in human plasmacytoid dendritic cells. *Proceedings of the National Academy of Sciences*, *107*(34), pp.15181-15186.

Kim, W.S., Kim, S.R., Kim, D., Kim, J.O., Park, M.A., Kitamura, S.I., Kim, H.Y., Kim, D.H., Han, H.J., Jung, S.J. and Oh, M.J., 2009. An outbreak of VHSV (viral hemorrhagic septicemia virus) infection in farmed olive flounder *Paralichthys olivaceus* in Korea. *Aquaculture*, *296*(1-2), pp.165-168.

Kodym, R., Kodym, E. and Story, M.D., 2009. 2′-5′-Oligoadenylate synthetase is activated by a specific RNA sequence motif. *Biochemical and Biophysical Research Communications*, *388*(2), pp.317-322.

Kumar, S., Stecher, G., and Tamura K., 2016. MEGA7: Molecular Evolutionary Genetics Analysis version 7.0 for bigger datasets. *Molecular Biology and Evolution, 33*(7), pp.1870-1874.

Kumar, M. and Carmichael, G.G., 1998. Antisense RNA: function and fate of duplex RNA in cells of higher eukaryotes. *Microbiology and Molecular Biology Reviews*, *62*(4), pp.1415-1434.

Laghari, Z.A., Chen, S.N., Li, L., Huang, B., Gan, Z., Zhou, Y., Huo, H.J., Hou, J. and Nie, P., 2018. Functional, signalling and transcriptional differences of three distinct type I IFNs in a perciform fish, the mandarin fish *Siniperca chuatsi. Developmental & Comparative Immunology*, *84*, pp.94-108.

Lai, M.C., Lee, Y.H.W. and Tarn, W.Y., 2008. The DEAD-Box RNA helicase DDX3 associates with export messenger ribonucleoproteins as well as Tip-associated protein and participates in translational control. *Molecular Biology of the Cell*, *19*(9), pp.3847-3858.

Langevin, C., Van Der Aa, L.M., Houel, A., Torhy, C., Briolat, V., Lunazzi, A., Harmache, A., Bremont, M., Levraud, J.P. and Boudinot, P., 2013. Zebrafish ISG15 exerts a strong antiviral activity against RNA and DNA viruses and regulates the interferon response. *Journal of Virology*, *87*(18), pp.10025-10036.

Lannan, C., Fryer, J. and Kimura, T., 1981. Isolation of a new reovirus from chum salmon in Japan. *Fish Pathology*, *15*(3-4), pp.155-162.

Lannan, C.N., Winton, J.R. and Fryer, J.L., 1984. Fish cell lines: establishment and characterization of nine cell lines from salmonids. *In vitro*, *20*(9), pp.671-676.

Lee, C.G., da Costa Soares, V., Newberger, C., Manova, K., Lacy, E. and Hurwitz, J., 1998. RNA helicase A is essential for normal gastrulation. *Proceedings of the National Academy of Sciences*, *95*(23), pp.13709-13713.

Lee, C.S., Dias, A.P., Jedrychowski, M., Patel, A.H., Hsu, J.L. and Reed, R., 2008. Human DDX3 functions in translation and interacts with the translation initiation factor eIF3. *Nucleic Acids Research*, *36*(14), pp.4708-4718.

Lee, J.Y., Marshall, J.A. and Bowden, D.S., 1994. Characterization of rubella virus replication complexes using antibodies to double-stranded RNA. *Virology*, *200*(1), pp.307-312.

Lee, T. and Pelletier, J., 2016. The biology of DHX9 and its potential as a therapeutic target. *Oncotarget*, *7*(27), pp.42716-42739.

Lee, T., Di Paola, D., Malina, A., Mills, J.R., Kreps, A., Grosse, F., Tang, H., Zannis-Hadjopoulos, M., Larsson, O. and Pelletier, J., 2014. Suppression of the DHX9 helicase induces premature senescence in human diploid fibroblasts in a p53-dependent manner. *Journal of Biological Chemistry*, *289*(33), pp.22798-22814.

Leung, T.L. and Bates, A.E., 2013. More rapid and severe disease outbreaks for aquaculture at the tropics: implications for food security. *Journal of Applied Ecology*, *50*(1), pp.215-222.

Levraud, J.P., Boudinot, P., Colin, I., Benmansour, A., Peyrieras, N., Herbomel, P. and Lutfalla, G., 2007. Identification of the zebrafish IFN receptor: implications for the origin of the vertebrate IFN system. *The Journal of Immunology*, *178*(7), pp.4385-4394.

Levy, D.E., Marié, I.J. and Durbin, J.E., 2011. Induction and function of type I and III interferon in response to viral infection. *Current Opinion in Virology*, *1*(6), pp.476-486.

Li, C., Ge, L.L., Li, P.P., Wang, Y., Dai, J.J., Sun, M.X., Huang, L., Shen, Z.Q., Hu, X.C., Ishag, H. and Mao, X., 2014. Cellular DDX3 regulates Japanese encephalitis virus replication by interacting with viral un-translated regions. *Virology*, *449*, pp.70-81.

Li, J., Zhou, M., Peng, L., Sun, W., Yang, P., Yan, J. and Feng, H., 2015. Identification and characterization of IKKε gene from grass carp *Ctenopharyngodon idella*. *Fish & Shellfish Immunology*, *47*(1), pp.255-263.

Li, S., Wilkinson, M., Xia, X., David, M., Xu, L., Purkel-Sutton, A. and Bhardwaj, A., 2005. Induction of IFN-regulated factors and antitumoral surveillance by transfected placebo plasmid DNA. *Molecular Therapy*, *11*(1), pp.112-119.

Limmon, G.V., Arredouani, M., McCann, K.L., Minor, R.A.C., Kobzik, L. and Imani, F., 2008. Scavenger receptor class-A is a novel cell surface receptor for double-stranded RNA. *The FASEB Journal*, *22*(1), pp.159-167.

Lin, L., Li, Y., Pyo, H.M., Lu, X., Raman, S.N.T., Liu, Q., Brown, E.G. and Zhou, Y., 2012. Identification of RNA helicase A as a cellular factor that interacts with influenza A virus NS1 protein and its role in the virus life cycle. *Journal of Virology*, *86*(4), pp.1942-1954.

Linder, P. and Jankowsky, E., 2011. From unwinding to clamping—the DEAD box RNA helicase family. *Nature Reviews Molecular Cell Biology*, *12*(8), pp.505-516.

Liu, J., Huang, X., Yu, Y., Zhang, J., Ni, S., Hu, Y., Huang, Y. and Qin, Q., 2017. Fish DDX3X exerts antiviral function against grouper nervous necrosis virus infection. *Fish & Shellfish Immunology*, *71*, pp.95-104.

Liu, T.K., Zhang, Y.B., Liu, Y., Sun, F. and Gui, J.F., 2011. Cooperative roles of fish PKZ and PKR in IFN-mediated antiviral response. *Journal of Virology*, pp.JVI-05849.

Liu, W., Xie, Y., Ma, J., Luo, X., Nie, P., Zuo, Z., Lahrmann, U., Zhao, Q., Zheng, Y., Zhao, Y., Xue, Y., 2015. IBS: an illustrator for the presentation and visualization of biological sequences. *Bioinformatics, 31*(20), pp.3359-3361.

Liu, Y., Lu, N., Yuan, B., Weng, L., Wang, F., Liu, Y.J. and Zhang, Z., 2014. The interaction between the helicase DHX33 and IPS-1 as a novel pathway to sense double-stranded RNA and RNA viruses in myeloid dendritic cells. *Cellular & Molecular Immunology*, *11*(1), p.49.

Lloyd, R.M. and Shatkin, A.J., 1992. Translational stimulation by reovirus polypeptide sigma 3: substitution for VAI RNA and inhibition of phosphorylation of the alpha subunit of eukaryotic initiation factor 2. *Journal of Virology*, *66*(12), pp.6878-6884.

Long, H. and Sun, L., 2014. CsIFIT1, an interferon-induced protein with tetratricopeptide repeat, inhibits viral infection in tongue sole (*Cynoglossus semilaevis*). *Fish & Shellfish Immunology*, *41*(2), pp.231-237.

Loo, Y.M., Fornek, J., Crochet, N., Bajwa, G., Perwitasari, O., Martinez-Sobrido, L., Akira, S., Gill, M.A., García-Sastre, A., Katze, M.G. and Gale, M., 2008. Distinct RIG-I and MDA5 signaling by RNA viruses in innate immunity. *Journal of Virology*, *82*(1), pp.335-345.

Lopez, A., Fernandez-Alonso, M., Rocha, A., Estepa, A. and Coll, J.M., 2001. Transfection of epithelioma papulosum cyprini (EPC) carp cells. *Biotechnology Letters*, *23*(6), pp.481-487.

Lorenzen, E., Carstensen, B. and Olesen, N.J., 1999. Inter-laboratory comparison of cell lines for susceptibility to three viruses: VHSV, IHNV and IPNV. *Diseases of Aquatic Organisms, 37*(2), pp.81-88.

Löseke, S., Grage-Griebenow, E., Heine, H., Wagner, A., Akira, S., Bauer, S. and Bufe, A., 2006. In vitro-Generated Viral Double-Stranded RNA in Contrast to Polyinosinic: Polycytidylic Acid Induces Interferon-α in Human Plasmacytoid Dendritic Cells. *Scandinavian Journal of Immunology*, *63*(4), pp.264-274.

Lu, G., Reinert, J.T., Pitha-Rowe, I., Okumura, A., Kellum, M., Knobeloch, K.P., Hassel, B. and Pitha, P.M., 2006. ISG15 enhances the innate antiviral response by inhibition of IRF-3 degradation. *Cellular and Molecular Biology*, *52*(1), pp.29-41.

Lu, H., Lu, N., Weng, L., Yuan, B., Liu, Y.J. and Zhang, Z., 2014. DHX15 senses double-stranded RNA in myeloid dendritic cells. *The Journal of Immunology*, *193*(3), pp.1364-1372.

Lumsden, J.S., Morrison, B., Yason, C., Russell, S., Young, K., Yazdanpanah, A., Huber, P., Al-Hussinee, L., Stone, D. and Way, K., 2007. Mortality event in freshwater drum *Aplodinotus grunniens* from Lake Ontario, Canada, associated with viral haemorrhagic septicemia virus, Type IV. *Diseases of Aquatic Organisms, 76*(2), pp.99-111.

Luna, J.M., Wu, X. and Rice, C.M., 2016. Present and not reporting for duty: dsRNAi in mammalian cells. *The EMBO journal*, *35*(23), pp.2499-2501.

MacLeod, D.T., Nakatsuji, T., Wang, Z., Di Nardo, A. and Gallo, R.L., 2015. Vaccinia virus binds to the scavenger receptor MARCO on the surface of keratinocytes. *Journal of Investigative Dermatology*, *135*(1), pp.142-150.

MacLeod, D.T., Nakatsuji, T., Yamasaki, K., Kobzik, L. and Gallo, R.L., 2013. HSV-1 exploits the innate immune scavenger receptor MARCO to enhance epithelial adsorption and infection. *Nature Communications*, *4*, p.1963.

Maillard, P.V., Ciaudo, C., Marchais, A., Li, Y., Jay, F., Ding, S.W. and Voinnet, O., 2013. Antiviral RNA interference in mammalian cells. *Science*, *342*(6155), pp.235-238.

Majde, J.A., Brown, R.K., Jones, M.W., Dieffenbach, C.W., Maitra, N., Krueger, J.M., Cady, A.B., Smitka, C.W. and Maassab, H.F., 1991. Detection of toxic viral-associated double-stranded RNA (dsRNA) in influenza-infected lung. *Microbial pathogenesis*, *10*(2), pp.105-115.

Marchler-Bauer, A., Derbyshire, M.K., Gonzales, N.R., Lu, S., Chitsaz, F., Geer, L.Y., Geer, R.C., He, J., Gwadz, M., Hurwitz, D.I. and Lanczycki, C.J., 2014. CDD: NCBI's conserved domain database. *Nucleic Acids Research*, *43*(D1), pp. D222-D226.

Marq, J.B., Hausmann, S., Veillard, N., Kolakofsky, D. and Garcin, D., 2011. Short double-stranded RNAs with an overhanging 5′ ppp-nucleotide, as found in arenavirus genomes, act as RIG-I decoys. *Journal of Biological Chemistry*, *286*(8), pp.6108-6116.

Martin, C.T. and Coleman, J.E., 1989. T7 RNA polymerase does not interact with the 5'-phosphate of the initiating nucleotide. *Biochemistry*, *28*(7), pp.2760-2762.

Matsuo, A., Oshiumi, H., Tsujita, T., Mitani, H., Kasai, H., Yoshimizu, M., Matsumoto, M. and Seya, T., 2008. Teleost TLR22 recognizes RNA duplex to induce IFN and protect cells from birnaviruses. *The Journal of Immunology*, *181*(5), pp.3474-3485.

McCann, R., 2012. Viral survey of fathead minnows, golden shiners, and white suckers from baitfish dealers in Wisconsin. *Master's Degree Thesis, University of Wisconsin*.

Meng, Z., Zhang, X.Y., Guo, J., Xiang, L.X. and Shao, J.Z., 2012. Scavenger receptor in fish is a lipopolysaccharide recognition molecule involved in negative regulation of NF-κB activation by competing with TNF receptor-associated factor 2 recruitment into the TNF-α signaling pathway. *The Journal of Immunology*, *189*(8), pp.4024-4039.

Mestas, J. and Hughes, C.C., 2004. Of mice and not men: differences between mouse and human immunology. *The Journal of Immunology*, *172*(5), pp.2731-2738.

Mian, M.F., Ahmed, A.N., Rad, M., Babaian, A., Bowdish, D. and Ashkar, A.A., 2013. Length of dsRNA (poly I: C) drives distinct innate immune responses, depending on the cell type. *Journal of leukocyte biology*, *94*(5), pp.1025-1036.

Milne, D.J., Campoverde, C., Andree, K.B., Chen, X., Zou, J. and Secombes, C.J., 2018. The discovery and comparative expression analysis of three distinct type I interferons in the perciform fish, meagre (*Argyrosomus regius*). *Developmental & Comparative Immunology*, *84*, pp.123-132.

Miyashita, M., Oshiumi, H., Matsumoto, M. and Seya, T., 2011. DDX60, a DEXD/H box helicase, is a novel antiviral factor promoting RIG-I-like receptor-mediated signaling. *Molecular and Cellular Biology*, *31*(18), pp.3802-3819.

Montero, J., Garcia, J., Ordas, M.C., Casanova, I., Gonzalez, A., Villena, A., Coll, J. and Tafalla, C., 2011. Specific regulation of the chemokine response to viral hemorrhagic septicemia virus at the entry site. *Journal of Virology, 85*(9), pp.4046-4056.

Moore, K.J. and Freeman, M.W., 2006. Scavenger receptors in atherosclerosis: beyond lipid uptake. *Arteriosclerosis, Thrombosis, and Vascular Biology*, *26*(8), pp.1702-1711.

Mor, S.K., Phelps, N.B., Ng, T.F.F., Subramaniam, K., Primus, A., Armien, A.G., McCann, R., Puzach, C., Waltzek, T.B. and Goyal, S.M., 2017. Genomic characterization of a novel calicivirus, FHMCV-2012, from baitfish in the USA. *Archives of Virology, 162*(12), pp.3619-3627.

Mori, K., Ohtani, K., Jang, S., Kim, Y., Hwang, I., Roy, N., Matsuda, Y., Suzuki, Y. and Wakamiya, N., 2014. Scavenger receptor CL-P1 mainly utilizes a collagen-like domain to uptake microbes and modified LDL. *Biochimica et Biophysica Acta (BBA)-General Subjects*, *1840*(12), pp.3345-3356.

Mortensen, H.F., Heuer, O.E., Lorenzen, N., Otte, L. and Olesen, N.J., 1999. Isolation of viral haemorrhagic septicaemia virus (VHSV) from wild marine fish species in the Baltic Sea, Kattegat, Skagerrak and the North Sea. *Virus Research*, *63*(1-2), pp.95-106.

Mukhopadhyay, S., Chen, Y., Sankala, M., Peiser, L., Pikkarainen, T., Kraal, G., Tryggvason, K. and Gordon, S., 2006. MARCO, an innate activation marker of macrophages, is a class A scavenger receptor for Neisseria meningitidis. *European Journal of Immunology*, *36*(4), pp.940-949.

Myong, S., Cui, S., Cornish, P.V., Kirchhofer, A., Gack, M.U., Jung, J.U., Hopfner, K.P. and Ha, T., 2009. Cytosolic Viral Sensor RIG-I Is a 5'-Triphosphate–Dependent Translocase on Double-Stranded RNA. *Science*, *323*(5917), pp.1070-1074.

Nei M., and Kumar, S., 2000. *Molecular Evolution and Phylogenetics*. Oxford University Press, New York.

Nellimarla, S., Baid, K., Loo, Y.M., Gale, M., Bowdish, D.M. and Mossman, K.L., 2015. Class A Scavenger Receptor–Mediated Double-Stranded RNA Internalization Is Independent of Innate Antiviral Signaling and Does Not Require Phosphatidylinositol 3-Kinase Activity. *The Journal of Immunology*, *195*(8), pp.3858-3865.

Nicholson, A.W., 1996. Structure, reactivity, and biology of double-stranded RNA. *Progress in Nucleic Acid Research and Molecular Biology*, 52, pp. 1-65.

Nims, L., Fryer, J.L. and Pilcher, K.S., 1970. Studies of replication of four selected viruses in two cell lines derived from salmonid fish. *Proceedings of the Society for Experimental Biology and Medicine*, *135*(1), pp.6-12.

Nishizawa, T., Takami, I., Kokawa, Y. and Yoshimizu, M., 2009. Fish immunization using a synthetic double-stranded RNA Poly (I: C), an interferon inducer, offers protection against RGNNV, a fish nodavirus. *Diseases of Aquatic Organisms*, *83*(2), pp.115-122.

Novakowski, K.E., Huynh, A., Han, S., Dorrington, M.G., Yin, C., Tu, Z., Pelka, P., Whyte, P., Guarné, A., Sakamoto, K. and Bowdish, D.M., 2016. A naturally occurring transcript variant of MARCO reveals the SRCR domain is critical for function. *Immunology & Cell Biology*, *94*(7), pp.646-655.

O'Farrell, C., Vaghefi, N., Cantonnet, M., Buteau, B., Boudinot, P. and Benmansour, A., 2002. Survey of transcript expression in rainbow trout leukocytes reveals a major contribution of interferon-responsive genes in the early response to a rhabdovirus infection. *Journal of Virology*, *76*(16), pp.8040-8049.

Oates, A.C., Wollberg, P., Pratt, S.J., Paw, B.H., Johnson, S.L., Ho, R.K., Postlethwait, J.H., Zon, L.I. and Wilks, A.F., 1999. Zebrafish stat3 is expressed in restricted tissues during embryogenesis and stat1 rescues cytokine signaling in a STAT1-deficient human cell line. *Developmental Dynamics*, *215*(4), pp.352-370.

Oh, M.J., Takami, I., Nishizawa, T., Kim, W.S., Kim, C.S., Kim, S.R. and Park, M.A., 2012. Field tests of Poly (I: C) immunization with nervous necrosis virus (NNV) in sevenband grouper, *Epinephelus septemfasciatus* (Thunberg). *Journal of Fish Diseases*, *35*(3), pp.187-191.

Ohtani, K., Suzuki, Y., Eda, S., Kawai, T., Kase, T., Keshi, H., Sakai, Y., Fukuoh, A., Sakamoto, T., Itabe, H. and Suzutani, T., 2001. The membrane-type collectin CL-P1 is a scavenger receptor on vascular endothelial cells. *Journal of Biological Chemistry*, *276*(47), pp.44222-44228.

Okahira, S., Nishikawa, F., Nishikawa, S., Akazawa, T., Seya, T. and Matsumoto, M., 2005. Interferon-β induction through Toll-like receptor 3 depends on double-stranded RNA structure. *DNA and Cell Biology*, *24*(10), pp.614-623.

Olive, C., 2012. Pattern recognition receptors: sentinels in innate immunity and targets of new vaccine adjuvants. *Expert Review of Vaccines*, *11*(2), pp.237-256.

Ørpetveit, I., Küntziger, T., Sindre, H., Rimstad, E. and Dannevig, B.H., 2012. Infectious pancreatic necrosis virus (IPNV) from salmonid fish enters, but does not replicate in, mammalian cells. *Virology Journal*, *9*(1), p.228.

Oshiumi, H., Ikeda, M., Matsumoto, M., Watanabe, A., Takeuchi, O., Akira, S., Kato, N., Shimotohno, K. and Seya, T., 2010B. Hepatitis C virus core protein abrogates the DDX3 function that enhances IPS-1-mediated IFN–beta induction. *PLoS One*, *5*(12), p.e14258.

Oshiumi, H., Sakai, K., Matsumoto, M. and Seya, T., 2010A. DEAD/H BOX 3 (DDX3) helicase binds the RIG-I adaptor IPS-1 to up-regulate IFN-β-inducing potential. *European Journal of Immunology*, *40*(4), pp.940-948.

Owsianka, A.M. and Patel, A.H., 1999. Hepatitis C virus core protein interacts with a human DEAD box protein DDX3. *Virology, 257*(2), pp.330-340.

Palumbi, SR. 1996. Nucleic acids II: the polymerase chain reaction. In: Hillis, DM, Moritz, C & Mable, BK eds. Molecular systematics. Sinauer Publishing: Sunderland, MA, pp. 205-248.

Peiser, L., Mukhopadhyay, S. and Gordon, S., 2002. Scavenger receptors in innate immunity. *Current opinion in immunology*, *14*(1), pp.123-128.

Peiser, L., Gough, P.J., Kodama, T. and Gordon, S., 2000. Macrophage class A scavenger receptor-mediated phagocytosis of Escherichia coli: role of cell heterogeneity, microbial strain, and culture conditions in vitro. *Infection and Immunity*, *68*(4), pp.1953-1963.

Peisley, A. and Hur, S., 2013. Multi-level regulation of cellular recognition of viral dsRNA. *Cellular and Molecular Life Sciences*, *70*(11), pp.1949-1963.

Peisley, A., Jo, M.H., Lin, C., Wu, B., Orme-Johnson, M., Walz, T., Hohng, S. and Hur, S., 2012. Kinetic mechanism for viral dsRNA length discrimination by MDA5 filaments. *Proceedings of the National Academy of Sciences*, *109*(49), pp.E3340-E3349.

Pestka, S., Krause, C.D. and Walter, M.R., 2004. Interferons, interferon-like cytokines, and their receptors. *Immunological Reviews, 202*(1), pp.8-32.

Pham, P.H., Huang, Y.J., Chen, C. and Bols, N.C., 2014. Corexit 9500 inactivates two enveloped viruses of aquatic animals but enhances the infectivity of a nonenveloped fish virus. *Applied and Environmental Microbiology*, *80*(3), pp.1035-1041.

Pham, P.H., Lumsden, J.S., Tafalla, C., Dixon, B. and Bols, N.C., 2013. Differential effects of viral hemorrhagic septicaemia virus (VHSV) genotypes IVa and IVb on gill epithelial and spleen macrophage cell lines from rainbow trout (*Oncorhynchus mykiss*). *Fish & Shellfish Immunology, 34*(2), pp.632-640.

Pichlmair, A., Schulz, O., Tan, C.P., Rehwinkel, J., Kato, H., Takeuchi, O., Akira, S., Way, M., Schiavo, G. and e Sousa, C.R., 2009. Activation of MDA5 requires higher-order RNA structures generated during virus infection. *Journal of Virology*, *83*(20), pp.10761-10769.

Pikkarainen, T., Brännström, A. and Tryggvason, K., 1999. Expression of macrophage MARCO receptor induces formation of dendritic plasma membrane processes. *Journal of Biological Chemistry*, *274*(16), pp.10975-10982.

Platt, N., Suzuki, H., Kurihara, Y., Kodama, T. and Gordon, S., 1996. Role for the class A macrophage scavenger receptor in the phagocytosis of apoptotic thymocytes in vitro. *Proceedings of the National Academy of Sciences*, *93*(22), pp.12456-12460.

Platt, N. and Gordon, S., 2001. Is the class A macrophage scavenger receptor (SR-A) multifunctional?—The mouse's tale. *The Journal of clinical investigation*, *108*(5), pp.649-654.

Plüddemann, A., Neyen, C. and Gordon, S., 2007. Macrophage scavenger receptors and host-derived ligands. *Methods*, *43*(3), pp.207-217.

Poynter, S.J., Monjo, A.L., Micheli, G. and DeWitte-Orr, S.J., 2017. Scavengers for bacteria: Rainbow trout have two functional variants of MARCO that bind to gram-negative and–positive bacteria. *Developmental & Comparative Immunology*, *77*, pp.95-105.

Poynter, S.J., Weleff, J., Soares, A.B. and DeWitte-Orr, S.J., 2015. Class-A scavenger receptor function and expression in the rainbow trout (*Oncorhynchus mykiss*) epithelial cell lines RTgutGC and RTgill-W1. *Fish & shellfish immunology*, *44*(1), pp.138-146.

Poynter, S., Lisser, G., Monjo, A. and DeWitte-Orr, S., 2015A. Sensors of infection: viral nucleic acid PRRs in fish. *Biology*, *4*(3), pp.460-493.

Poynter, S.J. and DeWitte-Orr, S.J., 2016. Fish interferon-stimulated genes: The antiviral effectors. *Developmental & Comparative Immunology*, *65*, pp.218-225..

Poynter, S.J. and DeWitte-Orr, S.J., 2015. Length-dependent innate antiviral effects of double-stranded RNA in the rainbow trout (*Oncorhynchus mykiss*) cell line, RTG-2. *Fish & Shellfish Immunology*, *46*(2), pp.557-565.

Poynter, S.J. and DeWitte-Orr, S.J., 2016. Fish interferon-stimulated genes: The antiviral effectors. *Developmental & Comparative Immunology*, *65*, pp.218-225.

Poynter, S.J. and DeWitte-Orr, S.J., 2017. Visualizing Virus-Derived dsRNA Using Antibody-Independent and-Dependent Methods. In *Innate Antiviral Immunity*, pp. 103-118. Humana Press, New York, NY.

Poynter, S.J. and DeWitte-Orr, S.J., 2015. Length-dependent innate antiviral effects of double-stranded RNA in the rainbow trout (Oncorhynchus mykiss) cell line, RTG-2. *Fish & Shellfish Immunology*, *46*(2), pp.557-565.

Poynter, S.J., Monjo, A.L., Micheli, G. and DeWitte-Orr, S.J., 2017. Scavengers for bacteria: Rainbow trout have two functional variants of MARCO that bind to gram-negative and–positive bacteria. *Developmental & Comparative Immunology*, *77*, pp.95-105.

Poynter, S.J., Weleff, J., Soares, A.B. and DeWitte-Orr, S.J., 2015B. Class-A scavenger receptor function and expression in the rainbow trout (*Oncorhynchus mykiss*) epithelial cell lines RTgutGC and RTgill-W1. *Fish & Shellfish Immunology*, *44*(1), pp.138-146.

Prabhu Das, M., Bowdish, D., Drickamer, K., Febbraio, M., Herz, J., Kobzik, L., Krieger, M., Loike, J., Means, T.K., Moestrup, S.K. and Post, S., 2014. Standardizing scavenger receptor nomenclature. *The Journal of Immunology*, *192*(5), pp.1997-2006.

Pradhan, A., Khalaf, H., Ochsner, S.A., Sreenivasan, R., Koskinen, J., Karlsson, M., Karlsson, J., McKenna, N.J., Orbán, L. and Olsson, P.E., 2012. Activation of NF-κB protein prevents the transition from juvenile ovary to testis and promotes ovarian development in zebrafish. *Journal of Biological Chemistry*, *287*(45), pp.37926-37938.

Purcell, M.K., Laing, K.J. and Winton, J.R., 2012. Immunity to fish rhabdoviruses. *Viruses*, *4*(1), pp.140-166.

Qiu, R., Sun, B.G., Li, J., Liu, X. and Sun, L., 2013. Identification and characterization of a cell surface scavenger receptor cysteine-rich protein of *Sciaenops ocellatus*: bacterial interaction and its dependence on the conserved structural features of the SRCR domain. *Fish & Shellfish Immunology*, *34*(3), pp.810-818.

Radi, M., Falchi, F., Garbelli, A., Samuele, A., Bernardo, V., Paolucci, S., Baldanti, F., Schenone, S., Manetti, F., Maga, G. and Botta, M., 2012. Discovery of the first small molecule inhibitor of human DDX3 specifically designed to target the RNA binding site: towards the next generation HIV-1 inhibitors. *Bioorganic & Medicinal Chemistry Letters*, *22*(5), pp.2094-2098.

Rahman, M.M., Liu, J., Chan, W.M., Rothenburg, S. and McFadden, G., 2013. Myxoma virus protein M029 is a dual function immunomodulator that inhibits PKR and also conscripts RHA/DHX9 to promote expanded host tropism and viral replication. *PLoS Pathogens*, *9*(7), p.e1003465.

Raman, S.N.T., Liu, G., Pyo, H.M., Cui, Y.C., Xu, F., Ayalew, L.E., Tikoo, S.K. and Zhou, Y., 2016. DDX3 interacts with influenza A virus NS1 and NP proteins and exerts antiviral function through regulation of stress granule formation. *Journal of Virology*, *90*(7), pp.3661-3675.

Ranjan, P., Bowzard, J.B., Schwerzmann, J.W., Jeisy-Scott, V., Fujita, T. and Sambhara, S., 2009. Cytoplasmic nucleic acid sensors in antiviral immunity. *Trends in Molecular Medicine*, *15*(8), pp.359-368.

Ranji, A. and Boris-Lawrie, K., 2010. RNA helicases: emerging roles in viral replication and the host innate response. *RNA Biology*, *7*(6), pp.775-787.

Rebl, A., Goldammer, T. and Seyfert, H.M., 2010. Toll-like receptor signaling in bony fish. *Veterinary Immunology and Immunopathology*, *134*(3-4), pp.139-150.

Reed, L.J. and Muench, H., 1938. A simple method of estimating fifty per cent endpoints. *American Journal of Epidemiology*, *27*(3), pp.493-497.

Reich, N., Pine, R., Levy, D.A. and Darnell, J.E., 1988. Transcription of interferon-stimulated genes is induced by adenovirus particles but is suppressed by E1A gene products. *Journal of Virology, 62*(1), pp.114-119.

Reikine, S., Nguyen, J.B. and Modis, Y., 2014. Pattern recognition and signaling mechanisms of RIG-I and MDA5. *Frontiers in Immunology*, *5*, p.342.

Richmond, J.Y. and Hamilton, L.D., 1969. Foot-and-mouth disease virus inhibition induced in mice by synthetic double-stranded RNA (polyriboinosinic and polyribocytidylic acids). *Proceedings of the National Academy of Sciences*, *64*(1), pp.81-86.

Robertsen, B., 2008. Expression of interferon and interferon-induced genes in salmonids in response to virus infection, interferon-inducing compounds and vaccination. *Fish & Shellfish Immunology*, *25*(4), pp.351-357.

Robertsen, B., 2006. The interferon system of teleost fish. *Fish & Shellfish Immunology*, *20*(2), pp.172-191.

Røkenes, T.P., Larsen, R. and Robertsen, B., 2007. Atlantic salmon ISG15: expression and conjugation to cellular proteins in response to interferon, double-stranded RNA and virus infections. *Molecular Immunology*, *44*(5), pp.950-959.

Rutledge, H.R., Jiang, W., Yang, J., Warg, L.A., Schwartz, D.A., Pisetsky, D.S. and Yang, I.V., 2012. Gene expression profiles of RAW264. 7 macrophages stimulated with preparations of LPS differing in isolation and purity. *Innate Immunity*, *18*(1), pp.80-88.

Sadler, A.J., Latchoumanin, O., Hawkes, D., Mak, J. and Williams, B.R., 2009. An antiviral response directed by PKR phosphorylation of the RNA helicase A. *PLoS Pathogens*, *5*(2), p.e1000311.

Saint-Jean, S.R. and Pérez-Prieto, S.I., 2006. Interferon mediated antiviral activity against salmonid fish viruses in BF-2 and other cell lines. *Veterinary Immunology and Immunopathology*, *110*(1-2), pp.1-10.

Saito, T. and Gale, M., 2008. Differential recognition of double-stranded RNA by RIG-I–like receptors in antiviral immunity. *Journal of Experimental Medicine*, *205*(7), pp.1523-1527.

Saito, T., Hirai, R., Loo, Y.M., Owen, D., Johnson, C.L., Sinha, S.C., Akira, S., Fujita, T. and Gale, M., 2007. Regulation of innate antiviral defenses through a shared repressor domain in RIG-I and LGP2. *Proceedings of the National Academy of Sciences*, *104*(2), pp.582-587.

Saitou, N., and Nei, M., 1987. The neighbor-joining method: A new method for reconstructing phylogenetic trees. *Molecular Biology and Evolution, 4*, pp.406-425.

Sankala, M., Brännström, A., Schulthess, T., Bergmann, U., Morgunova, E., Engel, J., Tryggvason, K. and Pikkarainen, T., 2002. Characterization of recombinant soluble macrophage scavenger receptor MARCO. *Journal of Biological Chemistry*, *277*(36), pp.33378-33385.

Santiago-García, J., Kodama, T. and Pitas, R.E., 2003. The class A scavenger receptor binds to proteoglycans and mediates adhesion of macrophages to the extracellular matrix. *Journal of Biological Chemistry*, *278*(9), pp.6942-6946.

Scagnolari, C., Midulla, F., Selvaggi, C., Monteleone, K., Bonci, E., Papoff, P., Cangiano, G., Di Marco, P., Moretti, C., Pierangeli, A. and Antonelli, G., 2012. Evaluation of viral load in infants hospitalized with bronchiolitis caused by respiratory syncytial virus. *Medical Microbiology and Immunology*, *201*(3), pp.311-317.

Schaefer, M., Pollex, T., Hanna, K. and Lyko, F., 2008. RNA cytosine methylation analysis by bisulfite sequencing. *Nucleic Acids Research*, *37*(2), pp.e12-e12.

Schafer, T.W. and JUN, R.L., 1970. Interferon required for viral resistance induced by poly I. poly C. *Nature*, *226*(5244), p.449.

Schiøtz, B.L., Rosado, E.G., Baekkevold, E.S., Lukacs, M., Mjaaland, S., Sindre, H., Grimholt, U. and Gjøen, T., 2011. Enhanced transfection of cell lines from Atlantic salmon through nucoleofection and antibiotic selection. *BMC Research Notes*, *4*(1), p.136.

Schneider, W.M., Chevillotte, M.D. and Rice, C.M., 2014. Interferon-stimulated genes: a complex web of host defenses. *Annual review of Immunology*, *32*, pp.513-545.

Schönborn, J., Oberstraβ, J., Breyel, E., Tittgen, J., Schumacher, J. and Lukacs, N., 1991. Monoclonal antibodies to double-stranded RNA as probes of RNA structure in crude nucleic acid extracts. *Nucleic Acids Research*, *19*(11), pp.2993-3000.

Schröder, M., 2010. Human DEAD-box protein 3 has multiple functions in gene regulation and cell cycle control and is a prime target for viral manipulation. *Biochemical Pharmacology*, *79*(3), pp.297-306.

Schröder, M., Baran, M. and Bowie, A.G., 2008. Viral targeting of DEAD box protein 3 reveals its role in TBK1/IKKε-mediated IRF activation. *The EMBO Journal*, *27*(15), pp.2147-2157.

Schuberth-Wagner, C., Ludwig, J., Bruder, A.K., Herzner, A.M., Zillinger, T., Goldeck, M., Schmidt, T., Schmid-Burgk, J.L., Kerber, R., Wolter, S. and Stümpel, J.P., 2015. A conserved histidine in the RNA sensor RIG-I controls immune tolerance to N1-2′ O-methylated self RNA. *Immunity*, *43*(1), pp.41-51.

Schultz, J., Milpetz, F., Bork, P. and Ponting, C.P., 1998. SMART, a simple modular architecture research tool: identification of signaling domains. *Proceedings of the National Academy of Sciences*, *95*(11), pp.5857-5864.

Secombes, C.J. and Zou, J., 2017. evolution of interferons and interferon Receptors. *Frontiers in Immunology*, *8*, p.209.

Sepulcre, M.P., Alcaraz-Pérez, F., López-Muñoz, A., Roca, F.J., Meseguer, J., Cayuela, M.L. and Mulero, V., 2009. Evolution of lipopolysaccharide (LPS) recognition and signaling: fish TLR4 does not recognize LPS and negatively regulates NF-κB activation. The *Journal of Immunology,* 182(4), pp.1836-1845.

Shevchuk, N.A., Bryksin, A.V., Nusinovich, Y.A., Cabello, F.C., Sutherland, M. and Ladisch, S., 2004. Construction of long DNA molecules using long PCR-based fusion of several fragments simultaneously. *Nucleic Acids Research*, *32*(2), pp.e19-e19.

Shi, J., Zhang, Y.B., Liu, T.K., Sun, F. and Gui, J.F., 2012. Subcellular localization and functional characterization of a fish IRF9 from crucian carp *Carassius auratus*. *Fish & Shellfish Immunology*, *33*(2), pp.258-266.

Shih, J.W. and Lee, Y.H.W., 2014. Human DExD/H RNA helicases: emerging roles in stress survival regulation. *Clinica Chimica Acta*, *436*, pp.45-58.

Silva de Assis, H.C., Simmons, D.B., Zamora, J.M., Lado, W.E., Al-Ansari, A.M., Sherry, J.P., Blais, J.M., Metcalfe, C.D. and Trudeau, V.L., 2013. Estrogen-like effects in male goldfish co-exposed to fluoxetine and 17 alpha-ethinylestradiol. *Environmental Science & Technology*, *47*(10), pp.5372-5382.

Sirri, V., Urcuqui-Inchima, S., Roussel, P. and Hernandez-Verdun, D., 2008. Nucleolus: the fascinating nuclear body. *Histochemistry and Cell Biology*, *129*(1), pp.13-31.

Skjesol, A., Hansen, T., Shi, C.Y., Thim, H.L. and Jørgensen, J.B., 2010. Structural and functional studies of STAT1 from Atlantic salmon (*Salmo salar*). *BMC Immunology*, *11*(1), p.17.

Sobhkhez, M., Krasnov, A., Chang, C.J. and Robertsen, B., 2017. Transcriptome analysis of plasmid-induced genes sheds light on the role of type I IFN as adjuvant in DNA vaccine against infectious salmon anemia virus. *PloS One*, *12*(11), p.e0188456.

Soto-Rifo, R. and Ohlmann, T., 2013. The role of the DEAD-box RNA helicase DDX3 in mRNA metabolism. *Wiley Interdisciplinary Reviews: RNA*, *4*(4), pp.369-385.

Soulat, D., Bürckstümmer, T., Westermayer, S., Goncalves, A., Bauch, A., Stefanovic, A., Hantschel, O., Bennett, K.L., Decker, T. and Superti-Furga, G., 2008. The DEAD-box helicase DDX3X is a critical component of the TANK-binding kinase 1-dependent innate immune response. *The EMBO Journal*, *27*(15), pp.2135-2146.

Sparrer, K.M. and Gack, M.U., 2015. Intracellular detection of viral nucleic acids. *Current Opinion in Microbiology*, *26*, pp.1-9.

Star, B., Nederbragt, A.J., Jentoft, S., Grimholt, U., Malmstrøm, M., Gregers, T.F., Rounge, T.B., Paulsen, J., Solbakken, M.H., Sharma, A. and Wetten, O.F., 2011. The genome sequence of Atlantic cod reveals a unique immune system. *Nature*, *477*(7363), p.207.

Strandskog, G., Villoing, S., Iliev, D.B., Thim, H.L., Christie, K.E. and Jørgensen, J.B., 2011. Formulations combining CpG containing oliogonucleotides and poly I: C enhance the magnitude of immune responses and protection against pancreas disease in Atlantic salmon. *Developmental & Comparative Immunology*, *35*(11), pp.1116-1127.

Sugimoto, N., Mitoma, H., Kim, T., Hanabuchi, S. and Liu, Y.J., 2014. Helicase proteins DHX29 and RIG-I cosense cytosolic nucleic acids in the human airway system. *Proceedings of the National Academy of Sciences*, *111*(21), pp.7747-7752.

Sun, F., Zhang, Y.B., Liu, T.K., Gan, L., Yu, F.F., Liu, Y. and Gui, J.F., 2010. Characterization of fish IRF3 as an IFN-inducible protein reveals evolving regulation of IFN response in vertebrates. *The Journal of Immunology*, *185*(12), pp.7573-7582.

Sun, R., Zhang, Y., Lv, Q., Liu, B., Jin, M., Zhang, W., He, Q., Deng, M., Liu, X., Li, G. and Li, Y., 2011. Toll-like receptor 3 (TLR3) induces apoptosis via death receptors and

mitochondria by up-regulating the transactivating p63 isoform α (TAP63α). *Journal of Biological Chemistry*, *286*(18), pp.15918-15928.

Svingerud, T., Solstad, T., Sun, B., Nyrud, M.L.J., Kileng, Ø., Greiner-Tollersrud, L. and Robertsen, B., 2012. Atlantic Salmon Type I IFN subtypes show differences in antiviral activity and cell-dependent expression: evidence for high IFNb/IFNc–producing cells in fish lymphoid tissues. *The Journal of Immunology*, *189*(12), pp.5912-5923.

Taghavi, M., Khosravi, A., Mortaz, E., Nikaein, D. and Athari, S.S., 2017. Role of pathogen-associated molecular patterns (PAMPS) in immune responses to fungal infections. *European Journal of Pharmacology*, *808*, pp.8-13.

Takami, I., Kwon, S.R., Nishizawa, T. and Yoshimizu, M., 2010. Protection of Japanese flounder *Paralichthys olivaceus* from viral hemorrhagic septicemia (VHS) by Poly (I: C) immunization. *Diseases of Aquatic Organisms*, *89*(2), pp.109-115.

Takeuchi, O. and Akira, S., 2010. Pattern recognition receptors and inflammation. *Cell*, *140*(6), pp.805-820.

Tang, R.S. and Draper, D.E., 1994. On the use of phasing experiments to measure helical repeat and bulge loop-associated twist in RNA. *Nucleic Acids Research*, *22*(5), pp.835-841.

Tarn, W.Y. and Chang, T.H., 2009. The current understanding of Ded1p/DDX3 homologs from yeast to human. *RNA Biology*, *6*(1), pp.17-20.

Thim, H.L., Iliev, D.B., Christie, K.E., Villoing, S., McLoughlin, M.F., Strandskog, G. and Jørgensen, J.B., 2012. Immunoprotective activity of a Salmonid Alphavirus Vaccine: comparison of the immune responses induced by inactivated whole virus antigen formulations based on CpG class B oligonucleotides and poly I: C alone or combined with an oil adjuvant. *Vaccine*, *30*(32), pp.4828-4834.

Thompson, M.R., Kaminski, J.J., Kurt-Jones, E.A. and Fitzgerald, K.A., 2011. Pattern recognition receptors and the innate immune response to viral infection. *Viruses*, *3*(6), pp.920-940.

Tian, C., Tan, S., Bao, L., Zeng, Q., Liu, S., Yang, Y., Zhong, X. and Liu, Z., 2017. DExD/H-box RNA helicase genes are differentially expressed between males and females during the critical period of male sex differentiation in channel catfish. *Comparative Biochemistry and Physiology Part D: Genomics and Proteomics, 22*, pp.109-119.

Tort, L., Balasch, J.C. and Mackenzie, S., 2003. Fish immune system. A crossroads between innate and adaptive responses. *Inmunología*, *22*(3), pp.277-286.

Tsai, H.J., Chen, H.M. and Lo, C.F., 1994. Secretory synthesis of active recombinant fish growth hormone by insect cells using a baculovirus vector. *Canadian Journal of Fisheries and Aquatic Sciences*, *51*(1), pp.1-7.

Tytell, A.A., Lampson, G.P., Field, A.K. and Hilleman, M.R., 1967. Inducers of interferon and host resistance. 3. Double-stranded RNA from reovirus type 3 virions (reo 3-RNA). *Proceedings of the National Academy of Sciences*, *58*(4), pp.1719-1722.

United States Department of Agriculture. 2014. 2013 Census of Aquaculture, volume 3. Table 4, pp 8.

United States Department of the Interior. 2007. Detection of viral hemorrhagic septicemia virus. USGS FS 2007-3055. US Department of the Interior, US Geological Survey. Fact Sheets.

Valiente-Echeverría, F., Hermoso, M.A. and Soto-Rifo, R., 2015. RNA helicase DDX3: at the crossroad of viral replication and antiviral immunity. *Reviews in Medical Virology*, *25*(5), pp.286-299.

van de Veerdonk, F.L., Kullberg, B.J., van der Meer, J.W., Gow, N.A. and Netea, M.G., 2008. Host–microbe interactions: innate pattern recognition of fungal pathogens. *Current Opinion in Microbiology*, *11*(4), pp.305-312.

van der Laan, L.J., Döpp, E.A., Haworth, R., Pikkarainen, T., Kangas, M., Elomaa, O., Dijkstra, C.D., Gordon, S., Tryggvason, K. and Kraal, G., 1999. Regulation and functional involvement of macrophage scavenger receptor MARCO in clearance of bacteria in vivo. *The Journal of Immunology*, *162*(2), pp.939-947.

Virtue, E.R., Marsh, G.A., Baker, M.L. and Wang, L.F., 2011. Interferon production and signaling pathways are antagonized during henipavirus infection of fruit bat cell lines. *PLoS One*, *6*(7), p.e22488.

Vo, N.T., Bender, A.W., Ammendolia, D.A., Lumsden, J.S., Dixon, B. and Bols, N.C., 2015. Development of a walleye spleen stromal cell line sensitive to viral hemorrhagic septicemia virus (VHSV IVb) and to protection by synthetic dsRNA. *Fish & Shellfish Immunology, 45*(1), pp.83-93.

Wang, B., Zhang, Y.B., Liu, T.K., Shi, J., Sun, F. and Gui, J.F., 2014. Fish viperin exerts a conserved antiviral function through RLR-triggered IFN signaling pathway. *Developmental & Comparative Immunology*, *47*(1), pp.140-149.

Wang, H. and Ryu, W.S., 2010. Hepatitis B virus polymerase blocks pattern recognition receptor signaling via interaction with DDX3: implications for immune evasion. *PLoS Pathogens*, *6*(7), p.e1000986.

Wang, W., Zhang, M., Xiao, Z.Z. and Sun, L., 2012. *Cynoglossus semilaevis* ISG15: a secreted cytokine-like protein that stimulates antiviral immune response in a LRGG motif-dependent manner. *PLoS One*, *7*(9), p.e44884.

Wang, X., Hinson, E.R. and Cresswell, P., 2007. The interferon-inducible protein viperin inhibits influenza virus release by perturbing lipid rafts. *Cell Host & Microbe*, *2*(2), pp.96-105.

Wang, Z., Liu, W., Song, H., Wang, H., Liu, J., Zhao, H., Du, X. and Zhang, Q., 2015. Comparative Evolution of Duplicated Ddx3 Genes in Teleosts: Insights from Japanese Flounder*, Paralichthys olivaceus*. *G3: Genes| Genomes| Genetics*, *5*(8), pp.1765-1773.

Weber, F., Wagner, V., Rasmussen, S.B., Hartmann, R. and Paludan, S.R., 2006. Double-stranded RNA is produced by positive-strand RNA viruses and DNA viruses but not in detectable amounts by negative-strand RNA viruses. *Journal of Virology*, *80*(10), pp.5059-5064.

Whelan, F.J., Meehan, C.J., Golding, G.B., McConkey, B.J. and Bowdish, D.M., 2012. The evolution of the class A scavenger receptors. *BMC Evolutionary Biology*, *12*(1), p.227.

Winton, J., Batts, W., DeKinkelin, P., LeBerre, M., Bremont, M. and Fijan, N., 2010. Current lineages of the epithelioma papulosum cyprini (EPC) cell line are contaminated with fathead minnow, *Pimephales promelas,* cells. *Journal of Fish Diseases, 33*(8), pp.701-704.

Wittamer, V., Bertrand, J.Y., Gutschow, P.W. and Traver, D., 2011. Characterization of the mononuclear phagocyte system in zebrafish. *Blood, 117* (26), pp. 7126-7135.

Wolf, K. and Quimby, M.C., 1962. Established eurythermic line of fish cells in vitro. *Science*, *135*(3508), pp.1065-1066.

Wu, Y.C., Lu, Y.F. and Chi, S.C., 2010. Anti-viral mechanism of barramundi Mx against betanodavirus involves the inhibition of viral RNA synthesis through the interference of RdRp. *Fish & Shellfish Immunology*, *28*(3), pp.467-475.

Xiao, J., Yan, C., Zhou, W., Li, J., Wu, H., Chen, T. and Feng, H., 2017. CARD and TM of MAVS of black carp play the key role in its self-association and antiviral ability. *Fish & Shellfish Immunology*, *63*, pp.261-269.

Xinxian, W., Peng, J., Guixiang, T., Jinjin, W., Xiaocong, Z., Junqiang, H., Xianle, Y. and Hong, L., 2016. Effect of common carp (*Cyprinus carpio*) TLR9 overexpression on the expression of downstream interferon-associated immune factor mRNAs in epithelioma papulosum cyprini cells. *Veterinary Immunology and Immunopathology, 170*, pp.47-53.

Xu, J., Flaczyk, A., Neal, L.M., Fa, Z., Eastman, A.J., Malachowski, A.N., Cheng, D., Moore, B.B., Curtis, J.L., Osterholzer, J.J. and Olszewski, M.A., 2017. Scavenger receptor MARCO orchestrates early defenses and contributes to fungal containment during cryptococcal infection. *The Journal of Immunology*, *198*(9), pp.3548-3557.

Yap, N.V., Whelan, F.J., Bowdish, D.M. and Golding, G.B., 2015. The evolution of the scavenger receptor cysteine-rich domain of the class A scavenger receptors. *Frontiers in Immunology*, *6*, p.342.

Yoneyama, M., Kikuchi, M., Matsumoto, K., Imaizumi, T., Miyagishi, M., Taira, K., Foy, E., Loo, Y.M., Gale, M., Akira, S. and Yonehara, S., 2005. Shared and unique functions of the DExD/H-box helicases RIG-I, MDA5, and LGP2 in antiviral innate immunity. *The Journal of Immunology*, *175*(5), pp.2851-2858.

Yoneyama, M., Onomoto, K., Jogi, M., Akaboshi, T. and Fujita, T., 2015. Viral RNA detection by RIG-I-like receptors. *Current Opinion in Immunology*, *32*, pp.48-53.

Zakrzewska, A., Cui, C., Stockhammer, O.W., Benard, E.L., Spaink, H.P. and Meijer, A.H., 2010. Macrophage-specific gene functions in Spi1-directed innate immunity. *Blood*, *116* (3), pp. 1-11.

Zani, I.A., Stephen, S.L., Mughal, N.A., Russell, D., Homer-Vanniasinkam, S., Wheatcroft, S.B. and Ponnambalam, S., 2015. Scavenger receptor structure and function in health and disease. *Cells*, *4*(2), pp.178-201.

Zhang, B.C., Zhang, J., Xiao, Z.Z. and Sun, L., 2014A. Rock bream (*Oplegnathus fasciatus*) viperin is a virus-responsive protein that modulates innate immunity and promotes resistance against megalocytivirus infection. *Developmental & Comparative Immunology*, *45*(1), pp.35-42.

Zhang, J., Zhang, Y.B., Wu, M., Wang, B., Chen, C. and Gui, J.F., 2014B. Fish MAVS is involved in RLR pathway-mediated IFN response. *Fish & Shellfish Immunology*, *41*(2), pp.222- 230.

Zhang, L., Nie, L., Cai, S.Y., Chen, J. and Chen, J., 2018. Role of a macrophage receptor with collagenous structure (MARCO) in regulating monocyte/macrophage functions in ayu, *Plecoglossus altivelis. Fish & Shellfish Immunology, 74*, pp.141-151.

Zhang, S., and Grosse, F., 1994. Nuclear DNA helicase II unwinds both DNA and RNA. *Biochemistry, 33,* pp. 3906-3912.

Zhang, S., Herrmann, C. and Grosse, F., 1999. Pre-mRNA and mRNA binding of human nuclear DNA helicase II (RNA helicase A). *Journal of Cell Science*, *112*(7), pp.1055-1064.

Zhang, Z., Yuan, B., Lu, N., Facchinetti, V. and Liu, Y.J., 2011. DHX9 pairs with IPS-1 to sense double-stranded RNA in myeloid dendritic cells. *The Journal of Immunology*, *187*(9), pp.4501-4508.

Zhou, X., Michal, J.J., Zhang, L., Ding, B., Lunney, J.K., Liu, B. and Jiang, Z., 2013. Interferon induced IFIT family genes in host antiviral defense. *International Journal of Biological Sciences*, *9*(2), p.200.

Zou, J., Bird, S. and Secombes, C., 2010. Antiviral sensing in teleost fish. *Current Pharmaceutical Design*, *16*(38), pp.4185-4193.

Zou, J., Gorgoglione, B., Taylor, N.G., Summathed, T., Lee, P.T., Panigrahi, A., Genet, C., Chen, Y.M., Chen, T.Y., Hassan, M.U. and Mughal, S.M., 2014A. Salmonids have an extraordinary complex type I IFN system: characterization of the IFN locus in rainbow trout *Oncorhynchus mykiss* reveals two novel IFN subgroups. *The Journal of Immunology*, *193*(5), pp.2273-2286.

Zou, J., Tafalla, C., Truckle, J. and Secombes, C.J., 2007. Identification of a second group of type I IFNs in fish sheds light on IFN evolution in vertebrates. *The Journal of Immunology*, *179*(6), pp.3859-3871.

Zou, P.F., Chang, M.X., Li, Y., Zhang, S.H., Fu, J.P., Chen, S.N. and Nie, P., 2015. Higher antiviral response of RIG-I through enhancing RIG-I/MAVS-mediated signaling by its long insertion variant in zebrafish. *Fish & Shellfish Immunology*, *43*(1), pp.13-24.

Zou, P.F., Chang, M.X., Xue, N.N., Liu, X.Q., Li, J.H., Fu, J.P., Chen, S.N. and Nie, P., 2014B. Melanoma differentiation-associated gene 5 in zebrafish provoking higher interferon-promoter activity through signalling enhancing of its shorter splicing variant. *Immunology*, *141*(2), pp.192-202.

Züst, R., Cervantes-Barragan, L., Habjan, M., Maier, R., Neuman, B.W., Ziebuhr, J., Szretter, K.J., Baker, S.C., Barchet, W., Diamond, M.S. and Siddell, S.G., 2011. Ribose 2′-O-methylation provides a molecular signature for the distinction of self and non-self mRNA dependent on the RNA sensor Mda5. *Nature Immunology*, *12*(2), p.137.

Appendix A: Visualizing virus-derived dsRNA using antibody-independent and –dependent methods

Sarah J. Poynter[1] and Stephanie J. DeWitte-Orr[2]

1. University of Waterloo, Department of Biology, Waterloo, Canada
2. Wilfrid Laurier University, Department of Health Sciences, Waterloo, Canada

The final publication is available at SpringerLink via https://doi.org/10.1007/978-1-4939-7237-1_5

Innate Antiviral Immunity (pp. 103-118). Humana Press, New York, NY. 2017.

A.1 Overview

Long double-stranded RNA molecules are produced as a byproduct of viral replication. Studying virus-derived dsRNA is important for understanding virus replication, understanding host responses to virus infections, and as a diagnostic tool for virus presence and replication. Here we describe four different techniques for visualizing dsRNA; two antibody-dependent methods, immunoblotting and immunocytochemistry, as well as two antibody-independent methods, differential digestion and acridine orange staining. The benefits and disadvantages of each technique are also discussed.

A.2 Introduction

Virus replication leads to the production of dsRNA, either as a genomic fragment, replication intermediate, replicative by-product, or potentially transcribed from viral DNA by host machinery (1,2). These long dsRNA molecules act as an indicator of a viral infection, as healthy host cells do not contain dsRNA molecules >40bp (3). Virus-derived (v)dsRNA molecules are recognized by host expressed pattern-recognition receptors (PRRs) and can induce a strong innate antiviral immune response (1). Many viruses have evolved mechanisms to evade dsRNA-induced innate antiviral mechanisms (4). Thus studying (v)dsRNA is important for: i. understanding virus replication, ii. understanding host responses to virus infection, and iii. as a diagnostic tool for virus presence (for dsRNA genome viruses) and replication.

Viral dsRNA is clearly an important molecule, worthy of study; however, the methods used to detect these virus-produced molecules can be difficult to execute. There are a number of ways to visualize and distinguish dsRNA from other nucleic acids; a few examples are provided here. Differential nuclease digestion can be used as dsRNA is sensitive to RNase III but resistant to RNase A and T1 under high salt conditions (3, 5, 6, 7). There are three commercially available dsRNA antibodies, J2, K1, and K2 that can be used for immunoblotting or immunocytochemistry (ICC) (6, 8, 9, 10). Acridine orange (AO) stained agarose gels can be used to look for dsRNA in total RNA extractions from virus-infected cells, as AO stains single-stranded nucleic acids red and double-stranded nucleic acids green (11); however AO staining will not differentiate dsDNA and dsRNA so this method alone is not enough to confirm dsRNA presence if there is a possibility of contaminating DNA. Ideally more than one technique should be employed when looking to confirm the presence of dsRNA.

The methods for each aforementioned technique are described here, with advantages and disadvantages compared in Table A.1. These techniques allow for identification and

visualization of dsRNA within virus-infected cells. An aquareovirus, chum salmon reovirus (CSV), is used as a model in this paper as it has a dsRNA genome and is an effective positive control for (v)dsRNA (9). The dsRNA detection methods described here include both antibody-dependent and -independent assays. The antibody-dependent assays include ICC, Fig. A.1, and a dsRNA immunoblot, Fig. A.2. The strength of these assays include: providing information of the size of the dsRNA produced (dsRNA immunoblot) and indicating cellular localization (ICC), all while relying on the specificity of a monoclonal antibody. In addition, ICC is the only technique described here that does not require extraction of nucleic acids, as such there is no risk of dsRNA being formed during the extraction process. Uninfected cells serve as an effective negative control, as the J2 antibody cannot detect dsRNA <40bp (8). These assays however are time consuming and require specialized equipment. The antibody-independent assays use an RNA extraction method (from virus-infected cells; the same RNA used in the immunoblot), combined with either differential nuclease digestion and detection with ethidium bromide (EtBr), Fig. A.3, or AO staining, Fig. A.4, and require less specialized equipment. AO stain is combined with agarose gel electrophoresis to differentially stain ssRNA red and dsRNA green. It has been suggested that RNA extraction methods using phenol/chloroform (ex. TRIzol) can cause dsRNA formation (12). We have not observed this in our controls, in fact, we have found commercial RNA extraction kits often are ineffective at extracting large (v)dsRNA molecules. The two antibody-independent detection methods for (v)dsRNA have different strengths (described in Table A.1). It should be noted that these two methods could also be combined; a differential digestion can be followed by AO staining in addition to or in place of EtBr. When comparing fluorescence stains, EtBr is a more sensitive stain than AO, but the need to differentiate ssRNA

and dsRNA could outweigh sensitivity in some cases. As always, the detection method must be chosen based on the requirements of the researcher.

Table A.1. A summary of select techniques used to visualize dsRNA.

Method	Benefits	Disadvantages
Antibody (J2)-dependent		
Immunoblot	• dsRNA length and amounts can be determined • Does not require digestion to remove ssRNA prior to detection • Specific	• Nucleic acids must be extracted • Specialized equipment needed
Immunocytochemistry	• dsRNA location within cell can be determined • No nucleic acid extraction needed • Specific	• No information on size • Specialized equipment needed
Antibody-independent		
Differential digestion	• No antibody required • No specialized equipment needed	• Possible loss of dsRNA during RNase A inactivation step • Nucleic acids must be extracted
Acridine orange	• Allows for differentiation of RNA strandedness • No specialized equipment needed	• Lower sensitivity than ethidium bromide • Does not differentiate dsDNA from dsRNA • Nucleic acids must be extracted

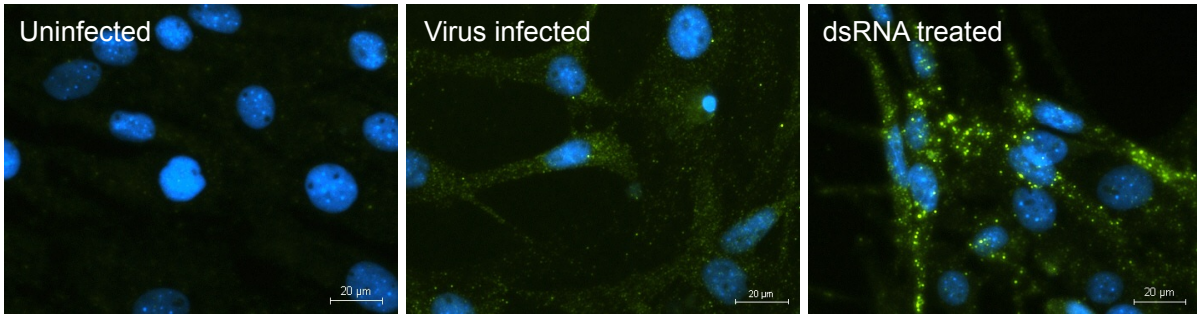

Figure A.1. Immunocytochemistry to detect chum salmon reovirus (CSV) dsRNA in rainbow trout gonadal cells (RTG-2) using the J2 antibody. Cells were infected with CSV (TCID50/mL: $1.5x10^4$) for 5 days, treated with media containing 10µg/mL in vitro transcribed dsRNA for 12h, or treated with control media. A 2^o only control showed no green signal (data not shown). Cells were counterstained with DAPI (green = dsRNA, blue = nuclei). Magnification 200X.

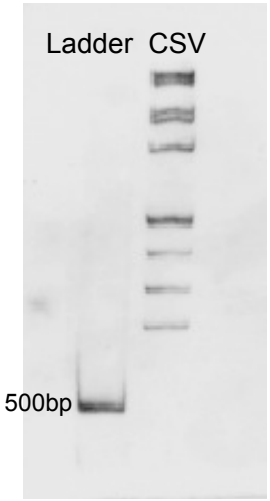

Figure A.2. dsRNA immunoblot detecting dsRNA from chum salmon reovirus (CSV) infected Chinook salmon embryonic (CHSE-214) cells. Cells were infected with $TCID_{50}$/mL $1.5x10^5$ virus for 7 days prior to RNA extraction. 5µg of total RNA from CSV-infected cells was used in this experiment, and dsRNA was detected using the J2 antibody. 1µg of dsRNA ladder was also included. Total RNA from uninfected CHSE-214 cells has no bands (data not shown).

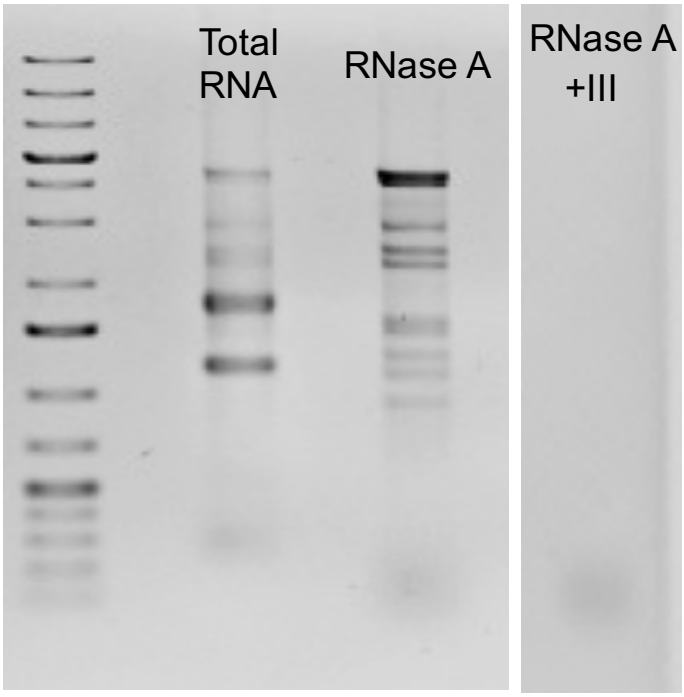

Figure A.3. Differential digestion confirming the presence of dsRNA from total RNA extracted from virus-infected cells. Cells were infected with $1.5x10^5$ virus for 7 days prior to RNA extraction. 0.5µg of total RNA, 10µg of total RNA treated with RNase A or RNase A and RNase III were run on an agarose gel alongside 0.5µg O'Generuler 1kb plus. The gel was stained with ethidium bromide and visualized under UV transillumination.

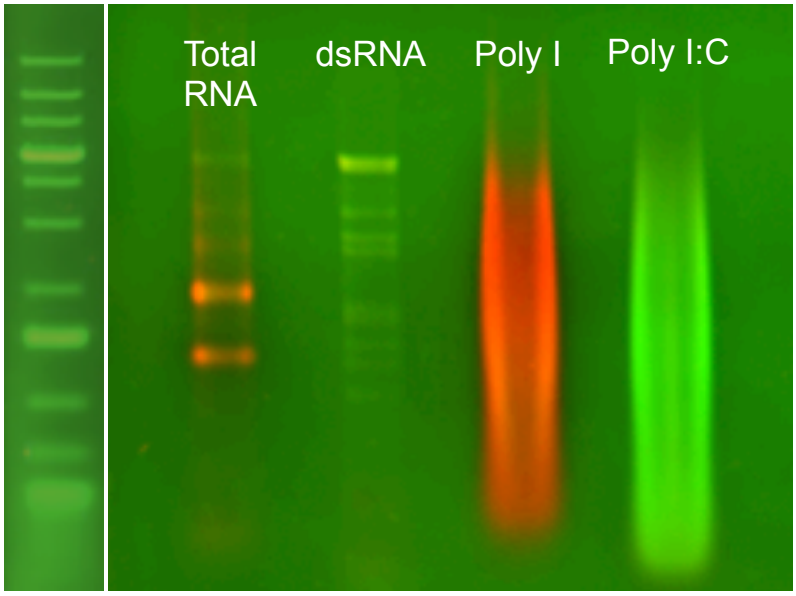

Figure A.4. Acridine orange stain used to visualize nucleic acids with colorimetric indication of strandedness. RTG-2 cells were infected with $1.5x10^5$ chum salmon reovirus (CSV) for 7 days prior to RNA extraction. 0.5µg of total RNA, dsRNA isolated from 10µg of total RNA digested with RNase A (dsRNA) were run on an agarose gel alongside 0.5µg O'Generuler 1kb plus. 4µg of poly I (ssRNA) and poly I:C (dsRNA) were run as controls. The gel was stained with acridine orange. Double stranded nucleic acids stain green and single stranded nucleic acids stain red with this stain.

A.3 Materials

A.3.1 RNA extraction

1. TRIzol reagent (15596-018, Ambion).
2. 75% (v/v) Ethanol: Combine 7.5mL of 100% ethanol with 2.5mL molecular biology grade water. Store at room temperature.
3. 100% Isopropanol.
4. Chloroform.
5. Nuclease-free molecular biology grade water.
6. Microcentrifuge tubes.
7. Tabletop centrifuge (speed of at least 12000xg).

A.3.2 Immunocytochemistry

1. ICC blocking solution (3% w/v BSA; 3% v/v goat serum, 0.02% v/v): In a 50mL Falcon tube dissolve, 1.5g bovine serum albumin, 1.5mL goat serum, in 48.49mL phosphate buffered saline (PBS), add 10µL Tween-20. Mix thoroughly by inverting tube. Filter through 0.22µM filter and store at 4^{o}C (*see* **Note 1**).
2. Permeablization solution (0.5% v/v Triton-X): Mix 50µL Triton-X in 10mL of PBS. Prepare fresh.
3. Permeablization solution (0.1% Triton-X): Mix 10µL, 0.5% (v/v), Triton-X in 10mL of PBS. Prepare fresh.
4. 4′,6-Diamidine-2′-phenylindole dihydrochloride (DAPI, 5mg/mL): To prevent product loss reconstitute entire container of DAPI at once. To 10mg of DAPI add 2mL of molecular biology grade water. Mix thoroughly by vortexing. Divide into 10µL aliquots and store at -20^{o}C protected from light.
5. Circular cover glass 18mm diameter.
6. Microscope slides 3” x 1” x 1mm.
7. SlowFade Gold Antifade mountant (S36936, Fisher Scientific).
8. 1X PBS with magnesium and calcium.
9. 1X PBS without magnesium and calcium.
10. Goat-anti mouse Dylight 488 antibody (Cedarlane, CLAS09-632).
11. J2 monoclonal antibody (1mg/mL) (Scicons English and Scientific Consulting Kft, Hungary): To 200µg add 200µL molecular biology grade water. Mix thoroughly by pipetting and let sit at room temperature for 15min. Centrifuge the tube at max speed in a tabletop centrifuge for 5min to remove aggregates. Divide into 5µL aliquots and store at -20^{o}C.

A.3.3 dsRNA Immunoblot

A.3.3.1 Polyacrylamide gel electrophoresis (PAGE)

1. 40% (v/v) Acrylamide/BIS solution (Bio-Rad).
2. 10% (w/v) Ammonium persulfate (APS): Add 1g of APS solution to 10mL of MilliQ water; mix by vortexing. Divide into 100µL aliquots and store at -20^{o}C.
3. Tetramethylethylenediamine (TEMED).
4. dsRNA ladder (N0363S, NEB).
5. Orange DNA Loading Dye (6X) (R0631, Thermo Scientific).Tris-borate ethylenediaminetetraacetic acid (EDTA) (TBE; 5X): 445mM Tris base, 445mM borate, 10mM EDTA. Combine 54g of Tris base, 27.5g of boric acid and 20mL of 0.5M (pH 8.0) EDTA. Bring up to 1L with MilliQ water. Mix with a magnetic stir bar until clear. Store at room temperature.
6. Mini-protein electrophoresis system (Bio-Rad).

A.3.3.2 Membrane Transfer

1. Trans-Blot Turbo Transfer System (Bio-Rad).
2. MagnaLift Nylon Membrane 0.45µM.
3. Extra thick western blotting filter paper (88620; Thermo Scientific)

A.3.3.3 Immunoblotting

1. Tris-buffered saline (TBS; 10X): 200mM Tris, 1.5M NaCl (pH 7.6). Dissolve 24g Tris base and 88g of NaCl in 1L of MilliQ water. Adjust pH to 7.6 with concentrated HCl. Store at room temperature.
2. TBS-T: TBS containing 0.1% (v/v) Tween-20. Add 1mL of Tween-20 to 1L of TBS. Mix thoroughly by inversion. Store at room temperature.

3. Blocking solution: 5% (w/v) skim milk in TBS-T. Combine 1g of skim milk powder with 20mL of TBS-T. Make fresh.
4. 1^{o} Antibody dilution solution: 2% (w/v) bovine serum albumin (BSA) in TBS-T. Dissolve 0.2g of BSA to 10mL of TBS-T. Make fresh.
5. 2^{o} Antibody dilution solution: 5% (w/v) skim milk in TBS-T. Combine 1g of skim milk powder with 20mL of TBS-T. Make fresh.
6. J2 monoclonal antibody (Scicons), *see* 2.2.
7. Goat-anti mouse horseradish peroxidase (HRP) antibody.

A.3.3.4 ECL Detection

1. Clarity Western ECL substrate (Bio-Rad)
2. VersaDoc Imaging System or similar system capable of imaging chemiluminescence (Bio-Rad)

A.3.4 Nuclease Digestion

1. RNase A (R6148, Sigma-Aldrich); dilute 1 to 10 in molecular biology grade water. Mix thoroughly with vortex. Prepare fresh.
2. RNase III and RNase III digestion buffer (Fisher Scientific).
3. Molecular biology grade 5M NaCl (Fisher Scientific).
4. Poly inosinic: poly cytidylic acid (poly I:C, 10mg/mL) (1530, Sigma-Aldrich). To prevent product loss, reconstitute entire container of poly I:C at once. To a 25mg container add 2.5mL of PBS. Invert bottle to mix solution. Heat in a 55^{o}C water bath for 15min and then let cool at room temperature for 30min. Divide into 20µL aliquots and store at -20^{o}C.
5. Poly inosinic acid (poly I; 10mg/mL) (P4154, Sigma-Aldrich). To prevent product loss reconstitute entire container of poly I at once. To a 25mg container add 2.5mL of

molecular biology grade water. Invert bottle to mix solution. Heat in a 55°C water bath for 15min. Divide into 20µL aliquots and store at -20°C.

6. O'GeneRuler 1Kb Plus DNA ladder (SM1343, Thermo Scientific).

A.3.5 Agarose Gel

1. Mini-Sub Cell GT Cell (Bio-Rad).
2. Orange DNA Loading Dye (6X) (R0631, Thermo Scientific).
3. O'Generuler 1kb plus ladder.
4. Tris-acetate EDTA (TAE, 50X): 2M Tris, 1M acetic acid, 50mM EDTA. Dissolve 242g Tris base, 18.61g EDTA, and 57,1mL of acetic acid in 1liter of MilliQ water. Store at room temperature.
5. Ethidium bromide (EtBr) stain (0.5µg/mL). Dilute 10µLof 10mg/mL stock EtBr in 200mL of MilliQ water. Store at room temperature away from UV light for up to 1 month.
6. Agarose (1% w/v in TAE). For a mini-gel combine 40mL of 1XTAE with 0.4g of agarose in a Bench Pint (OD260 Inc). Microwave for approximately 1.5min until clear. Swirl under cold water until you are able to touch the Bench Pint, and then pour into mold.
7. Orange DNA Loading Dye (6X) (R0631, Thermo Scientific).

A.3.6 Acridine Orange

1. Acridine orange (AO) stain (15µg/mL). Measure 30mg of AO in a container big enough to fit the gel you are staining, add 200mL of MilliQ water. Mix on a rocking platform at a low speed until there are no visible precipitates Prepare fresh.

A.4 Methods

Carry out all steps at room temperature and with room temperature reagents, unless specified. If not specified otherwise PBS is without magnesium and calcium.

A.4.1 Immunocytochemistry

All wash steps will be 500µL/well for 1min; to easily remove media or wash solution invert plate over a collection dish.

1. Plate cells in 12-well plate containing glass coverslips at a medium-confluency, for RTG-2 cells (13) 200,000cells/well in a total volume of 1mL.
2. Incubate overnight at normal growth temperature to allow for re-attachment of cells.
3. Infect cells with a sub-lethal titre of your virus of interest (in this case $TCID_{50}$/mL $1.5x10^4$, in 500µL of media with 5% fetal bovine serum (FBS). Treat uninfected control wells with 500µL of infection media – without virus. A positive control can be included (in this case, 10µg/mL *in vitro* transcribed dsRNA for 12h (*see* **Note 2).**
4. Incubate for the required amount of time at a permissive temperature (5 days at 17°C for our example), after this time there may be some beginning signs of cytopathic effects, but the monolayer should be largely intact.
5. Remove media from all wells and wash 1x with PBS (+Mg+Ca).
6. To fix the cells add 500µL/well 10% neutral buffered formalin and incubate for 10min.
7. Wash cells 3x with PBS.
8. To permeabilize the cells add 500µL/well of freshly prepared 0.5% Triton-X in PBS and incubate for 15min (*see* **Note 3).**
9. Wash cells 3x with PBS.
10. To block nonspecific binding, add 500µL ICC blocking solution to all wells and incubate for 1h.
11. Wash cells 1x with PBS.
12. Using a pipette tip, ensure that no coverslips are touching the walls of the well, as this

can draw the antibody solution off the coverslip.

13. Dilute J2 (1^o) antibody 1:200 in ICC blocking solution and add 40µL/coverslip; add ICC blocking solution alone to 2^o antibody-only control and full control wells (no virus, 1^o or 2^o antibodies).
14. Incubate for 1h in a humidified chamber; a Styrofoam cooler with wet paper towel at the bottom will suffice.
15. Wash cells 3x with PBS.
16. Using a pipette tip ensure that no coverslips are touching the walls of the well.
17. Dilute goat anti-mouse Dylight 488 (2^o) antibody 1:200 in IF blocking solution and add 40µL/coverslip; add IF blocking solution alone to full control well. Incubate for 1h in a humidified chamber in the dark.
18. Rinse 3x with PBS
19. To counterstain nuclei, dilute DAPI 1:1000 to 5µg/mL in PBS and add 300µL/well. Incubate for 5min in the dark
20. Wash 3x with PBS and 1x with MilliQ water to remove residual salt.
21. To mount coverslips, add 3µL of SlowFade Gold Antifade mountant to glass slides and using tweezers place coverslips cell-side down into mounting media.
22. Incubate overnight at room temperature in the dark to cure mounting media.
23. Visualize with a fluorescence microscope at 200x magnification (we use a Nikon Eclipse TiE with Qi1 camera and Nikon NIS-Elements software; *see* **Note 4)**.

A.4.2 Extraction of viral dsRNA from cells (RNA generated used for A.4.3, A.4.4 and A.4.5)

1. Infect a T-75 flask of cells with your virus of choice at a sufficient titre, which will need to be determined (for this example, CHSE-214 cells (14) were infected with CSV ($1.5x10^5$).

2. Incubate at permissive temperature (17^{o}C in this case) until cells are showing advanced cytopathic effects but prior to complete annihilation of monolayer (5-7 days with CSV).
3. Aspirate media from the flask.
4. Add 1.2mL of TRIzol reagent. Coat cell growing surface with TRIzol by gently tilting the flask. Scrape cells and collect cell/TRIzol mixture in a 1.5mL microcentrifuge tube. The mix is split into two separate tubes of 600µL to facilitate processing.
5. Complete RNA extraction as per manufacturers instructions. Steps are as follows.
6. To each 600µL of TRIzol add 0.12mL of chloroform and shake vigorously for approximately 30seconds.
7. Incubate for 3min at room temperature.
8. Centrifuge at max speed in a tabletop microcentrifuge (13200xg) for 15min at 4^{o}C.
9. Transfer the clear upper aqueous phase (this phase contains RNA) to a new microcentrifuge tube, taking care to not to remove any of the white or pink phases.
10. To precipitate the RNA, Add 0.3mL of 100% isopropanol to the aqueous phase. Shake vigorously and incubate at room temperature for 10min.
11. Centrifuge at max speed in a tabletop microcentrifuge for 10min at 4^{o}C. Ensure the hinge of the tube is facing up so the pellet may be located. The pellet of RNA may be very small, draw off the supernatant by placing a pipette on the opposite side of the tube.
12. To wash the RNA add 0.6mL of 75% ethanol. Centrifuge at max speed in a tabletop microcentrifuge for 5min at 4^{o}C.
13. Remove the 75% ethanol carefully, to avoid displacing the pellet of RNA.
14. Let the tube dry upside down on a KimWipe for 15min.
15. Resuspend the pellet in 30µL of molecular biology grade water.

16. Heat at 55^{o}C for 15min. Let cool at room temperature for 15min.

17. Quantify RNA using a NanoDrop Lite Spectrophotometer (*see* **Note 5).**

A.4.3 dsRNA Immunoblot

All steps are performed at room temperature unless otherwise specified; all rinses are for 5min with gentle rocking.

A.4.3.1 Polyacrylamide gel electrophoresis (PAGE)

1. Prepare a 30% acrylamide gel by combining 3.9mL MilliQ water, 1.5mL of 40% acrylamide/Bis solution, 600µL 10x TBE buffer, 100µL 10% APS in MilliQ water, and 5µL of TEMED in a 15mL Falcon tube, ensuring APS and TEMED are added last.
2. Mix thoroughly but quickly to ensure gel is poured before polymerization occurs in the Falcon tube. Using a P1000 pipette to transfer solution into the Mini-PROTEAN Tetra handcast system (Bio-Rad), add comb for wells, allow to polymerize approximately 20-30min. There is no stacking layer for this gel. Check the leftover gel solution in the Falcon tube; once this solution is solidified the gel should be as well.
3. Assemble the gel apparatus and fill with 1X TBE. Do not use the running buffer meant for a western blot.
4. Load 2µL (1µg) of dsRNA ladder mixed with 8µL of molecular biology grade water and 2µL of 6X Orange DNA Loading Dye into the dsRNA ladder lane. All sample lanes should contain 5µg of RNA mixed with 6X loading dye. (*see* **Note 6,7,8**)
5. Run gel at 140V for 2.5-3h. (*see* **Note 9**)

A.4.3.2 Transfer

1. Cut 2 sheets of extra thick paper and a nylon membrane to the size of the gel.
2. Soak paper and membranes in 0.5X TBE for 1-2min, until saturated.

3. Set up membrane/filter/gel stack with 1 layer of extra thick paper, nylon membrane, acrylamide gel, 1 layer extra thick paper (Fig. A.5).
4. Roll out any air bubbles using a roller or clean test tube.
5. Using Bio-Rad Turbo Semi-Dry Transfer apparatus, set transfer to 400mA (max 25V) for 90minutes, the actual transfer will vary between 100-200mA for the majority of the transfer.

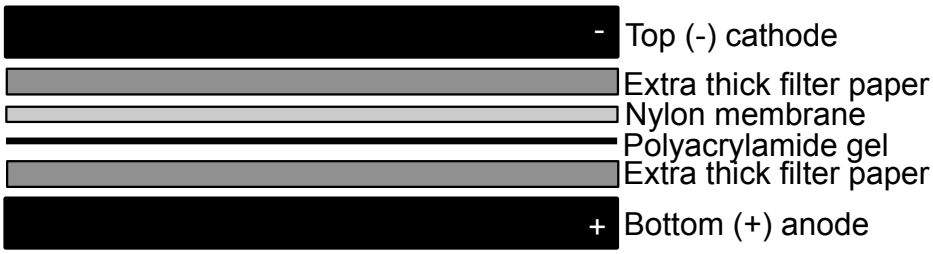

Figure A.5. The order of assembly for a dsRNA immunoblot transfer. From the bottom anode up, the stack should include a layer of extra thick filter paper, a nylon membrane, the polyacrylamide gel, and another layer of extra thick filter paper. The membrane and filter paper should be presoaked in transfer buffer (0.5X TBE).

A.4.3.3 Immunoblot

1. Remove membrane from stack carefully using tweezers; transfer to a container of a size to fit the membrane flat, and block in 5% skim milk TBS-T solution for 1h on a rocking platform set to a low speed.
2. Pour off block solution: rinse 3x with TBS-T.
3. Add J2 antibody diluted 1:2000 in TBS-T with 2% BSA (*see* **Note 10**).
4. Incubate overnight at 4^{o}C with gentle rocking on a rocking platform set to a low speed.
5. Remove primary antibody solution; collect for re-use.
6. Rinse 3x with TBS-T.
7. Add secondary antibody, goat-anti mouse HRP, 1:2000 in 5% skim milk TBS-T for 1h on a rocking platform set to a low speed, now at room temperature.

A.4.3.4 Detection

1. Remove secondary antibody solution, rinse 2x with TBS-T and 1x with TBS
2. Mix equal parts Bio-Rad clarity luminol/enhancer solution and Bio-Rad clarity peroxide solution; a total of 0.5mL is sufficient for one membrane using this technique. This solution must be made immediately before use.
3. Place blot onto transparent sheet protector, cover with clarity substrate taking care to remove bubbles; incubate for 5min, keeping the membrane in the dark.
4. Blot along the edges of the membrane using a KimWipe to remove any excess reagent, leaving membrane in sheet protector. Do not touch membrane directly.
5. Image using VersaDoc imager or other imager set to Ultra Chemiluminescence for 30s-1min (*see* **Note 11, 12).**

A.4.4 Differential Digestion + EtBr stained agarose gel electrophoresis

1. Combine 20µg of total RNA with 4µL of 10^{-1} diluted RNase A + 4µL of 5M NaCl and bring volume to 40µL with molecular biology grade water.
2. Incubate for 15min at room temperature.
3. Add 400µL of TRIzol (RNase A inactivation step).
4. Perform TRIzol extraction as per manufacturers instructions, resuspending pellet in 20µL of molecular biology grade water, *see* 3.2.
5. Keep RNA on ice until ready for downstream use. For long-term storage store at -80^{o}C
6. Take 10µL of the dsRNA solution and add 5µL of RNase III + 2µL of RNase III buffer + 3µL molecular biology grade water.
7. Incubate at 37^{o}C for 1h

8. Mix 10µL of the single digest with 2µL of 6X loading dye and 20µL of the double digest with 4µL of loading dye. Both samples will contain the same amount of starting RNA, 10µg.
9. Run both the single digestion and double digestion on a 1% agarose (w/v) gel in 1X TAE buffer prepared in a horizontal slab gel mold, Wide Mini-Sub Cell GT Cell (Bio-Rad). The gel will use 40mL of 1% agarose. 4µL (0.5µg) of O'Generuler 1kb plus ladder is also included on the gel (*see* **Note 13).**
10. Run the gel at 80V for approximately 90min in 1X TAE buffer.
11. Transfer gel to a container with 200mL of 0.5µg/mL EtBr in MilliQ water and incubate for 15min at room temperature
12. Transfer to a container with 300mL of MilliQ water to destain for 15-20min.
13. Visualize using VersaDoc transilluminator, UV setting for EtBr, exposure time 5s.

A.4.5 Acridine orange stained agarose gel

1. Prepare a 1% agarose gel (w/v) in 1X TAE buffer, in a horizontal slab gel mold, Wide Mini-Sub Cell GT Cell (Bio-Rad). The gel will use 40mL of 1% agaraose.
2. Mix samples with 6X loading dye (to a final 1X loading dye) and add to wells. In Fig. A.4 the samples include:
    a. 0.5µg O'GeneRuler 1kb plus
    b. 0.5 µg total RNA extracted from virus-infected cells
    c. 10 µg of RNaseA treated total RNA (starting concentration) extracted from virus-infected cells (this treatment should demonstrate dsRNA)
    d. 4 µg of poly inosinic acid (poly I) (ssRNA control) (*see* **Note 14**)
    e. 4 µg of poly I:C (dsRNA control) (*see* **Note 15**)
3. Run the gel at 80V for approximately 90min in 1X TAE buffer.

4. Stain gel in 200mL of 15µg/mL acridine orange in MilliQ water for 10min at room temperature.
5. Destain for 30-60min in 300mL of MilliQ water; checking the gel at 15min intervals. (*see* **Note 16, 17**)
6. Visualize using VersaDoc transilluminator, for AO set two custom channels: AO-red: 695bp, blue LED, 0.5x gain, 1x1bin; AO-green: 530band pass (bp), blue LED, 0.5xgain, 1x1bin.
7. Overlap AO images using multi-channel viewer (*see* **Note 18**).

A.5 Notes

1. Triton-X and Tween-20 are viscous reagents, however it is very important they are pipetted accurately; to accomplish these we make a 50% solution prior to pipetting (for immunocytochemistry blocking buffer and Triton-X solution the dilution is made in PBS, for immunoblotting the dilution is made in MilliQ water).
2. *In vitro* dsRNA, in this case a 200bp molecule made using the MEGAscript RNAi kit (Thermo Fisher Scientific), works as a stronger positive control compared to poly I:C. This is because J2 in some cases can have a 10x lower affinity for poly I:C compared to other forms of dsRNA (8). If you are interested in looking at poly I:C the K1 antibody form Scicons would be a better choice.
3. We have found this combination of fixative/permeablization effective to see viral dsRNA in both the cytoplasm and nucleus of fish cells. We have found that 0.1% Triton-X in PBS is best for visualizing *in vitro* dsRNA. It is entirely possible this would not be sufficient in some cases; we have not used other methods in our lab but other options for fixation/permeablization could include using cold methanol, acetone, or perhaps not permeablizing to look at surface dsRNA.

4. Fish cells have high autofluorescence in the green spectrum, make sure to use an exposure that does not result in high background in the full control treatment.
5. There could be residual DNA contamination in this RNA, for the immunoblot DNA contamination is not an issue as the antibody is specific, a digestion that is stopped with a second TRIzol extraction will also remove any DNA contamination in our experience. If you are using a downstream application straight from here you should strongly consider DNase treating the RNA.
6. 5µg of total RNA was sufficient as the dsRNA in this sample is abundant. If there is a lower amount of dsRNA within the total RNA sample or the abundance is unknown we recommended running a greater amount of RNA, for example in the past we have found 20µg necessary.
7. If you want a membrane transfer control, you can also load a pre-stained protein ladder into an additional well. The dye in the RNA samples will not remain on the membrane but the protein ladder will, this can be useful to ensure you did not make any mistakes such as building your stack upside down.
8. If you think your sample is very large and you are interested in knowing the exact size this ladder will not be helpful as it only has bands up to 500bp; you can use *in* vitro transcribed dsRNA of a longer length or a viral genome (preferably segmented) if available.
9. This time will require optimization depending on your sample, usually viral dsRNA length is reflected in the length of the genome and as such the molecules are quite large. This time/speed puts a 500bp dsRNA ladder band at the bottom of the gel.

10. Diluting the antibody in TBS-T with BSA allows the antibody to be frozen, thawed and reused. This strategy has been very successful for us and we have freeze/thawed the same antibody solution 3-4 times without any apparent decrease in sensitivity.
11. If the dsRNA in your sample is at a very low concentration you may need to do a very long exposure time. If this is the case it may be beneficial to cut off the ladder, as the ladder signal will be strong and might interfere with visualizing a fainter band. The ladder is generally so strong that a visible brown band can be seen with the naked eye.
12. It is recommended to image the gel after the five-minute incubation, however the membrane can be still be imaged several hours after the addition of the substrate.
13. dsRNA migrates slightly slower than dsDNA on an agarose gel; this means the dsDNA ladder such as O'GeneRuler 1kb plus will not be an entirely accurate means of sizing your dsRNA molecules. For our purposes however it has been sufficient. If you are interested in getting the most accurate size you can run the dsRNA marker used in the immunoblot, but the same issues will remain that the ladder does not have a band higher than 500bp, so once again you will have to create an in vitro molecule to accurately assess larger sized dsRNA molecules.
14. ssRNA from total RNA is not always a reliable control because it can have secondary structures that might interfere with the red/green staining. Poly I is an commercially available ssRNA that works well as a ssRNA control.
15. Poly I:C is a commercially available dsRNA molecule that works well as a positive control for dsRNA. The DNA ladder will also function positive control for double-strandedness. However it is less relevant, as a DNA molecule for our purposes. An in

vitro dsRNA would also be a good control, but these molecules are more expensive to produce and may not be as readily available.

16. Gels can be stained in AO and EtBr, however the AO stain must be completed first as the EtBr seems to interfere with the AO coloring.
17. The destain period can be increased if the background is too high, an overnight destain can drastically reduce the background; however as the nucleic acids will start to diffuse out of gel you lose sensitivity, especially in the smaller and fainter bands; larger, strong bands look clear and well-stained in our experience.
18. If the gel is understained all nucleic acids will visualize green, this is why having a strong single-stranded control is important to include.

A.6 Works cited

1. Jacobs BL, Langland JO (1996) When two strands are better than one: the mediators and modulators of the cellular responses to double-stranded RNA. *Virol 219*(2): 339-349

2. Ablasser A, Bauernfeind F, Hartmann G, Latz E, Fitzgerald KA, Hornung V (2009) RIG-I-dependent sensing of poly (dA: dT) through the induction of an RNA polymerase III–transcribed RNA intermediate. *Nature Immunol 10*(10): 1065-1072.

3. DeWitte-Orr SJ, Mossman KL (2010) dsRNA and the innate antiviral immune response. *Future Virol* 5(3): 325-341

4. Alcami A, Koszinowski UH (2000) Viral mechanisms of immune evasion. *Immunol Today* 21(9): 447-455

5. Edy VG, Szekely M, Loviny T, Dreyer C (1976) Action of Nucleases on Double-Stranded RNA. *European J Biochem* 61(2): 563-572

6. Weber F, Wagner V, Rasmussen SB, Hartmann R, Paludan SR (2006) Double-Stranded RNA Is Produced by Positive-Strand RNA Viruses and DNA Viruses but Not in Detectable Amounts by Negative-Strand RNA Viruses. *J. Virol* 80(10): 5059-5064

7. Aloni Y (1972) Extensive symmetrical transcription of simian virus 40 DNA in virus-yielding cells. *PNAS* 69(9): 2404-2409

8. Schonborn J, Oberstraβ J, Breyel E, Tittgen J, Schumacher J, Lukacs N (1991) Monoclonal antibodies to double-stranded RNA as probes of RNA structure in crude nucleic acid extracts. *Nucleic Acids Res 19*(11): 2993-3000

9. Doherty L, Poynter SJ, Aloufi A, DeWitte-Or SJ (2016) Fish viruses make dsRNA in fish cells: characterization of dsRNA production in rainbow trout (*Oncorhynchus mykiss)* cells infected with viral haemorrhagic septicaemia virus, chum salmon reovirus and frog virus 2. *J Fish Dis* 39: 1133-1137.

10. Lukács N (1994). Detection of virus infection in plants and differentiation between coexisting viruses by monoclonal antibodies to double-stranded RNA. *J Virol Methods* 47(3): 255-272

11. Pichlmair A, Schulz O, Tan CP, Rehwinkel J, Kato H, Takeuchi O, Akira S, Way M, Schiavo G, Reis e Sousa C (2009) Activation of MDA5 requires higher-order RNA structures generated during virus infection. *J Virol. 83*(20): 10761-10769

12. Borst P, Weissmann C (1965) Replication of viral RNA, 8. Studies on the enzymatic mechanism of replication of ms2 RNA. *Proc Natl Acad Sci USA* 54(3): 982–987

13. Wolf K, Quimby MC (1962) Established Eurythermic Line of Fish Cells in vitro. *Science* 23(3508): 1065-1066

14. Lannan CN, Winton JR, Fryer JL (1984) Fish cell lines: establishment and characterization of nine cell lines from salmonids. *In vitro 20*(9): 671-676

Appendix B: Fish interferon-stimulated genes: The antiviral effectors

Sarah J. Poynter[a], Stephanie J. DeWitte-Orr[b]

a Department of Biology, 200 University Ave W, Waterloo, ON N2L 3G1, Canada

b Department of Health Sciences and Biology, 75 University Ave W, Waterloo, ON N2L 3G1, Canada

The final publication is available at Elsevier via https://doi.org/10.1016/j.dci.2016.07.011

Developmental & Comparative Immunology 65: 218-225. 2016.

B.1 Overview

Type I interferons (IFN) are the cornerstone cytokine of innate antiviral immunity. In response to a viral infection, IFN signaling results in the expression of a diverse group of genes known as interferon-stimulated genes (ISGs). These ISGs are responsible for interfering with viral replication and infectivity, helping to limit viral infection within a cell. In mammals, many antiviral effector ISGs have been identified and the antiviral mechanisms are at least partially elucidated. In fish fewer ISGs have been identified and while there is evidence they limit viral infection, almost nothing is known of their respective antiviral mechanisms. This review discusses seven ISGs common to mammals and fish and three ISGs that are unique to fish. The lack of understanding regarding fish ISG's antiviral effector functions is highlighted and draws attention to the need for research in this aspect of aquatic innate immunity.

B.2. Introduction

When a cell senses a viral infection an alarm is raised and the cell begins to defend itself via the innate immune response; mediated by type I interferons (IFNs). IFNs are cytokines that signal in an autocrine and paracrine fashion to ultimately establish an antiviral state, which can make cells refractive to virus replication (Fig. B.1; Zhang and Gui, 2012). Fish type I IFNs fall into two groups, group 1 and 2, based on the number of cysteines they contain (2 and 4 respectively; Zhang and Gui, 2012). IFN is secreted from the cell and binds to its cognate receptor (IFNAR), whose binding triggers the Janus kinase - signal transduction and activator of transcription (JAK-STAT) signaling pathway. Fish IFNs and their subsequent signaling pathways have been previously reviewed in detail (Zhang and Gui, 2012). In fish, like in mammals, JAK-STAT signaling leads to the formation of interferon-stimulated gene (ISG)-factor 3 (ISGF3) that binds to the IFN-stimulated regulatory element (ISRE) of various ISGs (Schneider et al., 2014) inducing the expression of hundreds of antiviral genes (Schneider et al., 2014; Zhang and Gui, 2012). ISGs are the workhorses of the innate antiviral response; they are the effector molecules that work together to limit every step of a virus's replication. The healthy cell maintains these proteins at low levels to limit inappropriate activation while keeping the cell poised to respond to legitimate viral infections (Schneider et al., 2014). As a second safety mechanism, many ISGs are produced in inactive forms and remain inactive until the cell is infected with a virus (Haller and Kochs, 2002; Schneider et al., 2014). There is also a subset of ISGs that function as pattern recognition receptors (PRRs), ISGs, and antiviral effectors combined, such as PKR (dsRNA-dependent protein kinase) and the OAS (oligoadenylate synthetase)/RNaseL pathway (Schneider et al., 2014).

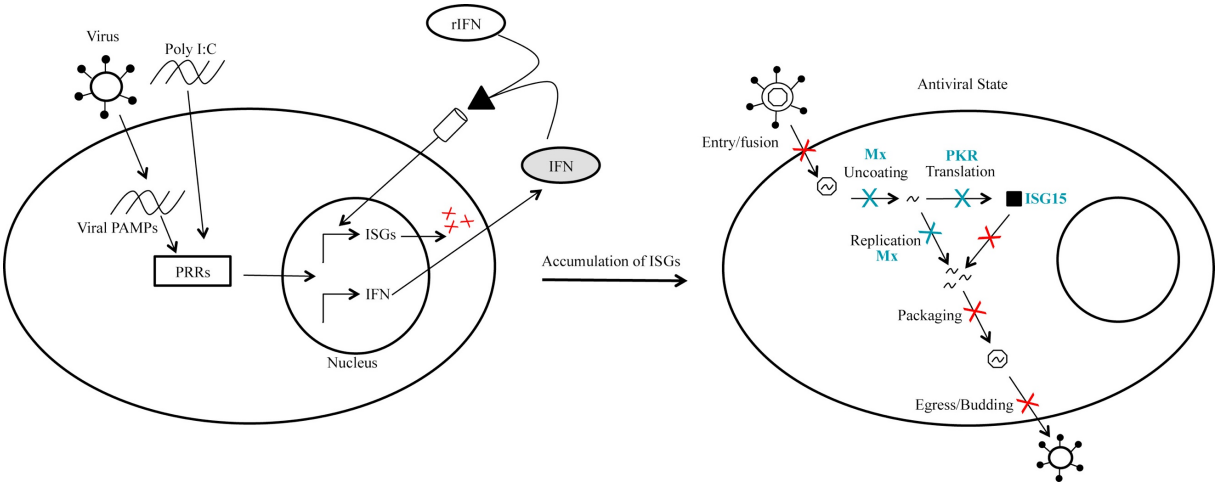

Figure B.1. IFN-stimulated gene induction and function. ISGs (with the exception of PKR which is also a PRR) are generally not expressed or expressed at low levels in unstimulated cells, but are highly expressed upon stimulation. Three common experimental stimulants of ISGs are recombinant/endogenous IFN, synthetic dsRNA (poly I:C), and virus infection. With the exception of VigB319, ISG56, TRIM8 and TRIM39, which have not been shown to be induced by IFN, all other ISGs discussed in this review have been shown to be induced by virus infection, poly I:C, and IFN. Once ISGs accumulate within a cell, known as the antiviral state, the cell can defend itself from a virus infection. ISGs are capable of protecting the cell against virus infection at every different stage of virus replication. Red X's indicate steps of virus replication shown to be blocked by ISGs in mammals, while blue X's indicate steps of virus replication blocked by both the fish and mammalian homologue of the ISG. ISG15 is listed in blue, as it can bind to viral and cellular proteins in fish, but it is unclear what stage of the viral life cycle they hinder. PRR = pattern recognition receptor, PAMP = pathogen-associated molecular pattern, IFN = interferon, ISG = IFN-stimulated genes, poly I:C = poly inosinic: poly cytidylic acid, rIFN = recombinant IFN.

While hundreds of ISGs have been identified only a small subset have been shown definitely to have antiviral effectiveness. In 2011 over 380 human ISGs were cloned into expression vectors and overexpressed in human cells to identify antiviral activity against a range of viruses (Schoggins et al., 2011). A study of this magnitude in fish has not yet been conducted. As ISGs are so numerous, this review has focused on ISGs who are proven antiviral effectors or believed to directly limit viral replication, including: viperin (virus inhibitory protein, endoplasmic reticulum-associated), ISG15, ISG56, viral hemorrhagic septicemia virus (VHSV)-induced gene (Vig)-B319, Mx, TRIM39, TRIM8 and grass carp hemorrhagic virus (GCHV)-

induced gene (Gig)-1 and -2. Fish viperin, ISG15, ISG56, Mx, PKR, TRIM8, and TRIM39 have mammalian homologues while the expression of Vig-B319, Gig-1 and -2 appears to be fish specific. The fish species in which these ISGs have been identified are summarized in Table B.1 and a comparison of antiviral activity, antiviral mechanism, and cellular location of mammalian and fish ISGs can be found in Table B.2. Modulation of the innate immune response is an excellent candidate approach to developing broad antiviral strategies. As fish in general and aquaculture in particular are economically important on a global scale; the purpose of this review is to highlight areas lacking understanding in the field of fish ISGs in order to encourage much needed research in the hopes of developing novel antiviral therapies.

Table B.1. A summary of fish species from which each listed ISGs has been identified. Only complete transcript sequences published on NCBI haven been included in this table. Predicted or putative sequences have not been included. * = similar or –like sequence; + = ISG56.

ISG	Species with NCBI-published whole mRNA transcripts		
Viperin	*Carassius auratus**	*Epinephelus coidoides*	*Oplegnathus fasciatus*
	Cyprinus carpio	*Esox lucius*	*Salmo salar*
	Danio rerio	*Onchorhynchus mykiss*	*Sciaenops ocellatus*
ISG15	*Channa argus*	*O. fasciatus*	*S. salar**
	Cynoglossus semilaevis	*Paralichthys olivaceus*	*S. ocellatus*
	D. rerio	*Hippoglossus hippoglossus*	*Scophthalmus maximus*
	Gadus morhua	*O. mykiss*	*Sebastes schlegelii*
ISG56	*O. mykiss+*		
Vig-B319	*O. mykiss*	*E. coioides*	
Mx	*Anguilla Anguilla*	*E. fuscoguttatus*	*Rachycentron canadum*
	A. japonica	*Gobiocypris rarus*	*S. salar*
	C. auratus	*H. hippoglossus*	*S. maximus*
	Cirrhinus mrigala	*Ictalurus punctatus*	*Seriola lalandi*
	Ctenopharyngodon idella	*Labeo rohita Lates calcarifer*	*Siniperca chuatsi*
	D. rerio	*O. mykiss*	*Solea senegalensis*
	Dicentrarchus labrax	*O. fasciatus*	*Sparus aurata*
	E. akaara	*P. olivaceus*	*Squaliobarbus curriculus*
	E. coioides	*Pseudosciaena crocea*	
Gig1	*C. auratus*	*C. idella*	
Gig2	*C. auratus*	*E. coioides*	
	D. rerio		
PKR	*C. auratus*	*O. fasciatus*	
	C. idella	*P. olivaceus*	
	D. rerio	*S.salar*	
	O. mykiss		
Trim39			
Trim 8	*D. rerio*		

Table B.2. Comparison of mechanisms of action and location of expression within the cell, between mammalian and fish ISGs, and virus families able to induce ISGs in specific fish species. The antiviral mechanism, cellular location (when active), and effectiveness against viral family have been compared. The host species and the viral family that the ISG has been effective against have been listed for fish, bolded viral families indicate virus families that have been shown to be limited by the mammalian ISG homologue as well.

MAMMALS				FISH				
	Mechanism	Location	Ref.	Mechanism	Location	Host species	Family	Ref.
Viperin	Binds viral proteins; limits viral budding, replication and enzyme activity	Cytoplasm	1	ND	Cytoplasm	*Oplegnathus fasciatus* *Carassius carassius*	Iridoviridae Reovirus	8
ISG15	ISGylation of host and viral proteins modulates function	Cytoplasm	2	ISGylation of viral and host proteins	Nucleus/cytoplasm	*Danio rerio* *D. rerio/Cynoglossus semilaevis* *Epinephelus coioides* *D. rerio*	Birnaviridae Iridoviridae Nodaviridae Rhabdoviridae	9
ISG56	Binds eIF3 inhibiting transcription; sequesters viral 5′PPP-RNA	Cytoplasm/ mitochondria	3	ND	ND	*C. semilaevis*	Iridoviridae	10
Vig-B319	NA	NA		ND	ND	*E. coioides*	Nodaviridae	11
Mx	Binds viral proteins, thus blocking function (example binding nucleoprotein)	Nucleus/cytoplasm	4	Interaction with coat protein and RNA-dependent RNA polymerase	Nucleus/cytoplasm	*Sparus aurata/Salmo salar/ Solea senegalensis* *S. aurata* *E. coioides/Lates calcarifer* *S. salmo* *Gobiocypris rarus/ Ctenopharyngodon idella* *S. aurata/Paralichthys olivaceus/S. senegalensis*	**Birnaviridae** Iridoviridae Nodaviridae **Orthomyxoviridae** **Reoviridae** **Rhabdoviridae**	12
Gig1	NA	NA	NA	ND	Cytoplasm	*C. idella/C. carassius*	Reoviridae	13
Gig2	NA	NA	NA	ND	Cytoplasm	*D. rerio* *C. idella* *D. rerio*	Iridoviridae Reoviridae Rhabdoviridae	14
PKR	Inhibits protein translation through phosphorylation of eIF2a; signal transducer in immune pathways	Nucleus/cytoplasm	5	Inhibits protein translation through phosphorylation of eIF2a	Cytoplasm	*P. olivaceus* *C. carassius*	**Rhabdoviridae** Reoviridae	15
Trim39	Direct antiviral mechanism unknown: Induces genes involved in type I IFN and antiviral responses	Nucleus	6	ND	Cytoplasm	*E. coioides* *E. coioides*	Iridoviridae Nodaviridae	16
Trim8	Direct antiviral mechanism unknown: Modulates expression of inflammatory pathway proteins	Nucleus/Cytoplasm	7	ND	Cytoplasm	*E. coioides* *E. coidoides*	Iridoviridae Nodaviridae	17

1: Wang et al., 2007, Helbig et al., 2011, Chin and Cresswell, 2001; **2:**Cunha et al., 1996; Okumura et al., 2006; Skaug and Chen, 2010; **3**: Zhou et al., 2013; Li et al., 2009; **4**: Haller et al., 2007; Kochs and Haller, 1999; Engelhardt et al., 2004; **5:**Jeffrey et al., 1995; Balachandran et al., 2000; Der and Lau, 1995; Kumar et al., 1994, **6**: Suzuki et al., 2016; Kurata et al., 2013; **7:**Okumura et al., 2010; Tomar et al., 2012; **8:**Zhang et al., 2014; Wang et al., 2014A, 2014B**9:**Langevin et al., 2013; Huang et al., 2013; Furnes et al., 2009; Wang et al., 2012; **10:**Long and Sun, 2014; **11:**Yeh et al., 2014; **12:**Lin et al., 2006; Trobridge et al., 1997; Fernández-Trujillo et al., 2015; Leong et al., 1998; Kibenge et al., 2005; Caipang et al., 2003; Peng et al., 2012; Chen et al., 2008, Su et al., 2009, Fernandez-Trujillo et al., 2011, Alvarez-Torres et al., 2013; Wu et al., 2010; **13:**Sun et al., 2014; Sun et al., 2013, 2013; **14:**Li et al., 2012, **15:**Zhu et al., 2008, 2009, Liu et al., 2011, **16:**Wang et al., 2016; **17:**Huang et al., 2016.

B.3. Viperin

Viperin (also known as vig-1) is a well-characterized ISG with multiple antiviral activities in mammals; these include interfering with viral budding through inhibition of specific enzymes, and inhibiting viral genome replication through binding to viral proteins required for replication and assembly (Chin and Cresswell, 2001; Helbig et al., 2011; Wang et al., 2007). Viperin associates with the cytosolic face of the endoplasmic reticulum (ER) until viral infection and then relocates to the cytoplasm, in lipid droplets or foci in the cytoplasm to inhibit virus replication (Chin and Cresswell, 2001; Helbig et al., 2011; Wang et al., 2007). One mammalian virus, human cytomegalovirus (HCMV), hijacks viperin and induces its expression then redirects it to the mitochondria where it increases viral entry (Seo et al., 2011).

Fish express an ISG with a high sequence similarity to human and murine viperin; however, its mechanism of action in fish is not well understood (Boudinot et al., 1999). Fish viperin is a demonstrated IFN-inducible protein that has been identified in many fish species (Table B.1). The antiviral effects of viperin in both fish cells and whole animals have been shown; for example overexpression of viperin resulted in an antiviral state in crucian carp (*Carassius carassius*) cells against GCHV and in rock bream (*Oplegnathus fasciatus)* fish against megalocytivirus (Wang et al., 2014A; Zhang et al., 2014). As is seen in infected mammalian cells, rock bream viperin localized to the ER in uninfected cells and dissociated from the ER to the cytoplasm after viral infection (Table B.2; Chin and Cresswell, 2001; Nasr et al., 2012; Zhang et al., 2014).

B.4. ISG15

ISG15 (also known as vig-3) is a small protein with many roles in mammalian immunity; it is a ubiquitin-like protein that covalently binds to its target protein in a process known as ISGylation (O'Farrell et al., 2002; Schneider et al., 2014). Current evidence suggests that ISG15's

antiviral activity may be non-specific, as it conjugates to both host and viral proteins, thus its mechanism for preferentially targeting viral proteins might be its ability to conjugate newly synthesized proteins of which there would be many in a virus infected cell (Durfee et al., 2010). Interestingly, ISGylation has been found to have both stabilizing and destabilizing effects on its target proteins, but it is not clear how this is accomplished (Durfee et al., 2010; Lu et al., 2006; Schneider et al., 2014). ISG15 conjugates to a lysine residue in the NS1 protein of influenza A and one outcome of this was the inhibition its ability to interact with importing A, leading to decreased viral replication (Zhao et al., 2010).

ISG15 has been identified in many fish species and is induced by IFN (Table B.1; Røkenes et al., 2007). As in humans, the LRGG motif of fish ISG15 is crucial for antiviral activity (Langevin et al., 2013; Wang et al., 2012). Fish ISG15 conjugates to viral proteins within infected cells, however the effect of this ISGylation is not understood (Langevin et al., 2013; Røkenes et al., 2007). Zebrafish (*Danio rerio)* ISG15 was found to conjugate to the P and N proteins of infectious hematopoietic necrosis virus (IHNV) and Atlantic salmon (*Salmo salar*) ISG15 was found conjugated to infectious salmon anemia virus (ISAV) proteins (Langevin et al., 2013). ISG15 in fish shows broad antiviral activity against many fish viruses, as seen with overexpression of orange-spotted grouper ISG15 in grouper spleen cells inhibiting grouper nervous necrosis virus (GNNV) and overexpression of zebrafish ISG15 in *Epithelioma Papulosum Cyprini* (EPC) cells inhibited VHSV and IHNV; and after knockdown of ISG15 by RNAi led to an increase in megalocytivirus viral load in tongue sole head kidney lymphocytes (HKL) (Huang et al., 2013; Langevin et al., 2013; Wang et al., 2012). ISG15 was shown to localize to the cytoplasm after viral infection or poly I:C stimulation (Huang et al., 2013). ISG15, however, does not confer protection against all fish viruses, for example in orange-spotted

grouper (*Epinephelus coioides*) ISG15 provided protection against GNNV but was not effective in reducing Singapore grouper iridovirus (SGIV) viral transcripts (Huang et al., 2013). Where ISG15 is ineffective ISGylation is not seen, thus ISG15 is either not effective against these viruses or the viruses have fast acting countermeasures against ISG15 (Huang et al., 2013).

Mammalian ISG15, in addition to conjugating to intracellular proteins, is secreted and has cytokine activity (Bogunovic et al., 2013). This may also be the case for fish as ISG15 was found in the supernatants of poly I:C stimulated Atlantic salmon leucocytes (Røkenes et al., 2007); this secreted property of ISG15 was also found in tongue sole (*Cynoglossus semilaevis*), where megalocytovirus infection of HKL led to secretion of ISG15 (Wang et al., 2012). Recombinant tongue sole ISG15 was able to activate head kidney macrophages and enhance immune gene expression in HKL (Wang et al., 2012). Treating tongue sole HKLs with extracellular recombinant ISG15 decreased viral load, and enhanced antibody-mediated inhibition of virus infection (Wang et al., 2012). In contrast to mammalian ISG15, and perhaps other fish, tongue sole ISG15 appeared to exert most of its antiviral activity through its extracellular role as opposed to its intracellular protein conjugation mechanisms (Wang et al., 2012).

B.5. ISG56

Mammalian ISG56 (also known as IFIT1) is a member of the IFIT family of proteins (Zhou et al., 2013). ISG56 in mammals has demonstrated antiviral properties; however, its mechanism is not thoroughly elucidated and appears complex. One antiviral mechanism of ISG56 is interference with viral transcription through binding to eukaryotic initiation factor (eIF)3 or binding/sequestering viral 5′PPP-RNA or non-2′-O methylated viral RNA (Zhou et al., 2013; Diamond, 2014). Fish also express members of the IFIT family, including ISG56 (O'Farrell et al., 2002).

As in mammals, fish ISG56 proteins contain tetratricopeptide repeat domains and transcription is upregulated in response to viral infection (Long and Sun, 2014; O'Farrell et al., 2002; Zhou et al., 2013). While fish ISG56 has been shown to have antiviral effects, its mechanism of action is poorly understood. Overexpression of ISG56 in tongue sole limited megalocytivirus replication and knockdown of ISG56 enhanced replication (Long and Sun, 2014). Rainbow trout (*Oncorhynchus mykiss*) express Vig-4, which shares sequence similarity with ISG56 and another IFIT family member, ISG58 (O'Farrell et al., 2002). While there is no direct evidence for ISG56 being IFN-inducible in fish, transfection of fish cells with IRF3 or stimulation with poly I:C, an IFN-stimulating molecule, increased ISG56 or Vig-4 expression respectively, suggesting IFN-inducibility (Huang et al., 2015; Poynter and DeWitte-Orr, 2015).

B.6. Mx

Mx proteins are dynamin-like GTPases with antiviral activity. For example in mammals, Mx1 induces a broad antiviral state by forming oligomers around viral nucleocapsids, ultimately targeting them for degradation (Schneider et al., 2014). While some aspects of its antiviral mechanism understood, many details of Mx's antiviral mechanism are not fully elucidated (Schneider et al., 2014). Mx isoforms vary between animals: humans and mice express 2 and rat express 3 forms of Mx, fish express many forms of Mx ranging from 1 in many fish species to 7 in zebrafish (Lin et al., 2006; Leong et al., 1998). Fish Mx is also interferon inducible and exhibits broad antiviral activity (Alvarez-Torres et al., 2013; Holland et al., 2008).

As with mammalian Mxs, fish Mxs have antiviral properties against a wide range of viruses while some viruses are unaffected by Mx activity (Alvarez-Torres et al., 2013; Meier et al., 1990). Different Mx isoforms in fish show different antiviral ranges, as is seen in mammals, but interestingly fish Mx isoforms show interactions that have not been noted in mammals. Gilthead seabream (*Sparus aurata*) expressing Mx1, Mx2, and Mx3 individually

showed antiviral activity; however, these Mxs also interacted with each other, synergistically or antagonistic, depending on the virus that was infecting the cells (Fernández-Trujillo et al., 2015). It is hypothesized that interactions between different Mx isoform combinations create different oligomer conformations; if different isoforms are present in the oligomer ring it could affect the virus-targeting domain and alter its antiviral activity (Fernández-Trujillo et al., 2015). As with mammals, fish Mx proteins have different mechanisms of action. In grouper Mx was shown to limit GNNV replication through direct interactions, specifically it was seen that the coat protein of the virus binds to the effector domain of Mx (Chen et al., 2008). In barramundi (*Lates calcarifer*) it was found that increased Mx expression led to a decrease in nervous necrosis virus (NNV) RNA-dependent RNA polymerase (RdRp) activity; Mx co-localized and co-precipitated with viral RdRp indicating a direct interaction (Wu et al., 2010). It appears Mx directs RdRp to the perinuclear area for degradation; mammalian MxA has been found in to also inhibit viral polymerase activity. In some cases, purified recombinant MxA inhibited the viral polymerase of vesicular stomatitis virus (VSV) and nuclear-modified human MxA inhibits viral polymerase of *Thogoto* virus and influenza virus (Wu et al., 2010; Schwemmle et al., 1995; Turan et al., 2004; Weber et al., 2000). There has been an emphasis on the study of fish Mx, and more is known about this ISG than any other; however it is necessary to continue studying Mx, to identify different isoforms from fish species and identify their varying mechanisms of action for limiting viral infections.

B.7. Vig-B319

Vig-B319 was first identified in VHSV-infected rainbow trout head kidney cells (O'Farrell et al., 2002). It is not yet confirmed that vig-B319 is IFN-induced; however, as with ISG56, poly I:C does stimulate vig-B319 suggesting it could be mediated by IFN (unpublished data). This seemingly fish-specific ISG was first identified in orange-spotted grouper and called

EcVig. EcVig was found to have four isoforms, EcVigA-D, with EcVig-A being the major isoform (Yeh et al., 2014). All four EcVig isoforms were induced by viral infection and overexpression of EcVigA resulted in protection against a NVV infection (Yeh et al., 2014). Vig-B319 is an understudied ISG in fish that warrants further investigation.

B.8. Gig1 and Gig2

As with vig-B319, the Gig family members are ISGs specific to fish that do not appear to have human homologues (Sun et al., 2014). Gig1 and Gig2 expression is upregulated in response to virus infection, and both promoters contain ISREs (Sun et al., 2013, 2014; Li et al., 2012). The IFN-inducibility and IFN-dependence of Gig1 and Gig2 are unclear; recombinant IFN did not induce Gig1 or Gig2 in Grass carp (*Ctenopharyngodon idella*); however, recombinant IFN induced Gig2 in zebrafish and Gig1 in crucian carp (Jiang et al., 2009; Li et al., 2012; Sun et al., 2013; Zhang and Gui, 2004). In crucian carp blastulae cells no observable Gig1 was present prior to stimulation; however, after poly I:C or viral infection, Gig 1 was found in cytoplasm upon viral infection and limited GCHV replication (Sun et al., 2014). The antiviral mechanisms of these ISGs are still unknown. Overexpression of fish Gig proteins limits viral replication and induces a protective antiviral state; Gig1 and Gig2 have protective activity against GCHV, Gig2 has demonstrated effectiveness against spring viremia of carp virus (SVCV) and *Rana grylio* virus (RGV) (Li et al., 2012; Sun et al., 2013, 2014). Again, further research is necessary to understand the induction and expression patterns for Gig1 and Gig2 as well as its mechanism of action.

B.9. TRIM39 and TRIM8

The tripartite motif (TRIM) family of proteins is an emerging group of antiviral ISGs. While some TRIMs are constitutively expressed and believed to interfere with early viral infection, other TRIMs are induced by IFNs and may function to limit later stages of virus

replication (Nisole et al., 2005; Carthagena et al., 2009). In a panel of 72 human TRIM genes, 9 were shown to be upregulated by IFN (Carthagena et al., 2009). TRIM proteins contain a RING (Really Interesting New Gene) finger domain, one or two B-box domains and a coiled-coil region; they have many cellular functions including differentiation, development and cell proliferation (Carthagena et al., 2009; Nisole et al., 2005). Several mammalian TRIMs have antiviral properties based mainly on their function as E3-ubiquitin ligases, and there are a number of current reviews of mammalian TRIMs discussing their actions in detail (Rajsbaum et al., 2014; McNab et al., 2011). Briefly, a TRIM8/10/11/56 complex in mouse was able to inhibit HIV entry and TRIM8/25/31/56 was able to interfere with N-MLV entry (Uchil et al., 2008). TRIM8 was also found to have a role in innate immunity signaling, as it was able to mediate activation of NF-kB (Li et al., 2011). TRIM39 is common to mammals and fish; gain-of-function of mammalian TRIM39R induces genes involved with the type I IFN response and antiviral defenses (Kurata et al., 2013). TRIM39 has many additional roles in cell homeostasis control, including mediating apoptosis, cell cycle, and cytostasis (Zhang et al., 2012).

Fish have a larger number of TRIMs compared to mammals, in fact a new virus-induced TRIM subfamily, called finTRIMs, were first identified in rainbow trout (Van Der Aa et al., 2009). finTRIMs from various species cluster into a separate group from TRIM39 (fish and human), TRIM25 (fish, human, chicken, Xenopus), TRIM39 (Xenopus, fish, human; Van Der Aa et al., 2009). While the antiviral roles of fish TRIMs are only now beginning to be studied, two of these proteins TRIM39 and TRIM8, have been preliminarily explored (Wang et al., 2016; Huang et al., 2016). It should be noted that neither TRIM has been shown to be induced by IFN directly, but both were upregulated after poly I:C treatment (Wang et al., 2016; Huang et al., 2016). While there is a lack of confirmed full length TRIM8 or TRIM39 mRNA sequences

published on NCBI (as noted in Table B.1), there are many predicted sequences available. A gene involved in erythrocyte differentiation in zebrafish, which is closely related to TRIM39 has been identified, called blood-thirsty (bty or btr) (Yergeau et al., 2005). The zebrafish subfamily of btr genes is homologous to human TRIM39 (Zhang et al., 2015). Grouper TRIM39 was upregulated in response to virus challenge with an iridovirus. As with many ISGs, grouper TRIM39 localized to the cytoplasm in aggregates when transfected into cells (Wang et al., 2016). While there is a role for TRIM39 in cell cycle progression in fish, as is seen in mammals, antiviral activity was also observed, as overexpression significantly inhibited both SGIV and red-spotted grouper necrosis virus (RGNNV; Wang et al., 2016). TRIM8 was upregulated by SGIV and was most significantly increased at early stages of infection. Over-expression of TRIM8 *in vitro* in the grouper spleen (GS) cell line resulted in inhibition of both SGIV and RGNNV replication, possibly via enhanced IRF-3 or IRF-7-induced ISRE promoter activity (Huang et al., 2016). Further research into the complex roles of finTRIMs and other TRIMs from fish is necessary to fully understand whether or not these molecules are solely involved in regulating antiviral signaling pathways or if they limit virus replication directly.

B.10. PKR

The double-stranded RNA-dependent protein kinase (PKR) is unique in this review as it functions as both a pattern recognition receptor (PRR) and an antiviral effector. As it is a PRR, PKR is expressed constitutively prior to stimulation with IFN (Balachandran et al., 2000). Following dsRNA binding and dimerization PKR becomes an active kinase that phosphorylates the eukaryotic-translation initiation factor 2α (eIF2α) (Balachandran et al., 2000). This phosphorylation inhibits protein translation within the cell, inhibiting viral replication. PKR also plays a role in signal transduction; it is able to activate NF-κB by phosphorylating IκB-α and also plays a role in IFN signaling; it has been recently reported that PKR plays a crucial role in

the signal transduction of the dsRNA sensor MDA5 (Pham et al., 2016; Kumar et al., 1994; Der and Lau, 1995). Additionally, PKR can induce apoptosis within virus-infected cells (Gill and Esteban, 2000). As PKR has a broad range of antiviral effector mechanisms, many viruses have developed methods evading PKR-mediated antiviral activities (discussed in section B.11).

PKR homologs have also been identified in a variety of fish species (Table B.1). As with mammals, fish PKR is also induced by IFN (Liu et al., 2011), contains at least two tandem dsRNA-binding motifs (dsRBMs), is constitutively expressed at low levels, and is able to inhibit protein translation (Zenke et al., 2010; del Castillo et al., 2012; Hu et al., 2016). At least two dsRBMs were required for binding dsRNA and triggering protein translation inhibition (Hu et al., 2016). Grass carp PKR has three dsRBMs, two of which are similar to mammalian dsRBMs while the third, dsRBM1, is unique to fish (Hu et al., 2016). PKR in Japanese flounder *(Paralichthys olivaceus)* and crucian carp inhibited the replication of Scophthalmus maximus rhabdovirus (SMRV) and GCHV respectively via its eIF2α phosphorylation activity (Zhu et al., 2008; Liu et al., 2011). While study into the antiviral role for PKR in fish has begun, very little is known regarding PKR's alternative roles, such as inducing apoptosis or signaling, in fish.

We would be remiss if we failed to examine PKZ while discussing PKR in fish. PKZ is a fish-specific PKR-like molecule that has Z-DNA binding domains instead of dsRBMs (Rothenburg et al., 2005). PKZ is also able to phosphorylate eIF2 α and inhibit protein translation (Yang et al., 2011). Although there is less direct evidence for antiviral effectiveness of PKZ, in crucian carp it was shown that PKZ was able to inhibit replication of GCRV. PKZ and PKR appear to have non-redundant roles as overexpression or knockdown of both resulted in a stronger antiviral response compared to either protein alone; notably PKR showed stronger antiviral properties than PKZ (Liu et al., 2011).

B.11. Fish virus countermeasures

The virus-host cell battle is hardly one-sided, aquatic viruses have developed methods for modulating host-produced ISGs. This battle is not restricted to mammalian viruses, fish viruses can interfere with host antiviral responses; for example, many ranaviruses are able to modulate PKR activity (Grayfer et al., 2012). Some fish viruses have the ability to prevent the induction of Mx. In two salmon head kidney cell lines infectious pancreatic necrosis virus (IPNV) blocked Mx protein expression (Jensen and Robertsen, 2002). This was further supported by studies in rainbow trout fibroblast cells where IPNV induced IFN transcription but hindered the activation of the Mx promoter (Collet et al., 2007). At least two IPNV viral proteins are suspected to be antagonists for the Mx promoter, viral nonstructural protein VP5 and protease VP4 (Skjesol et al., 2009). ISAV produces a 7i protein which is an interferon-signaling antagonist, as was seen by its ability to limit Mx-promoter activation and transcript levels, however it did not affect levels of IFN transcripts (McBeath et al., 2006). In a separate study ISAV proteins from segment 7 and 8 were found to independently down-regulate type I IFN promoter activity; interestingly the protein from segment 8 binds dsRNA and poly-A ssRNA (García-Rosado et al., 2008). There are only a handful of studies investigating virus immune evasion strategies in fish; this is another area of research that requires further elucidation.

B.12. Conclusions

In conclusion, it appears as though fish and mammals express similar arsenals of ISG combatants to battle a viral infection. There are a small number of identified ISGs that are present in fish but not mammals and there are many ISGs that have been found in mammals but not yet in fish; however, this is not necessarily because they do not exist in fish, but that they have not yet been identified. While some fish ISGs have been cloned and induction patterns are somewhat known, very little is known about their mechanism of antiviral activity (Table B.2). Further

research is necessary to identify novel fish ISGs and characterize their mechanisms for limiting virus replication. Research into similarities and differences between mammalian and fish ISGs would guide our understanding of the evolution of innate antiviral immunity. ISGs are the front line of defense against viral infection and a lack of understanding of the mechanism of these molecules in fish greatly hinders our understanding of the host antiviral response and the development of novel antiviral therapeutics.

Acknowledgements

The authors with to thank Alex Siopiolosz for his editing assistance and NSERC (419367-2012 RGPIN) for funding.

B.13. Works cited

Alvarez-Torres, D., Garcia-Rosado, E., Fernandez-Trujillo, M.A., Bejar, J., Alvarez, M.C., Borrego, J.J., Alonso, M.C., 2013. Antiviral specificity of the *Solea senegalensis* Mx protein constitutively expressed in CHSE-214 cells. Mar. Biotechnol. 15, 125-132. http://dx.doi.org/10.1007/s10126-012-9478-8.

Balachandran, S., Roberts, P.C., Brown, L.E., Truong, H., Pattnaik, A.K., Archer, D.R., Barber, G.N., 2000. Essential role for the dsRNA-dependent protein kinase PKR in innate immunity to viral infection. Immunity 13, 129-141.

Bogunovic, D., Boisson-Dupuis, S., Casanova, J., 2013. ISG15: leading a double life as a secreted molecule. Exp. Mol. Med. 45, e18. http://dx.doi.org/10.1038/ emm.2013.36.

Boudinot, P., Massin, P., Blanco, M., Riffault, S., Benmansour, A., 1999. Vig-1, a new fish gene induced by the rhabdovirus glycoprotein, has a virus-induced homologue in humans and shares conserved motifs with the MoaA family. J. Virol. 73, 1846-1852.

Caipang, C.M.A., Hirono, I., Aoki, T., 2003. In vitro inhibition of fish rhabdoviruses by Japanese flounder, *Paralichthys olivaceus* Mx. Virol 317, 373-382. http:// dx.doi.org/10.1016/j.virol.2003.08.040.

Carthagena, L., Bergamaschi, A., Luna, J.M., David, A., Uchil, P.D., Mothes, W., Hazan, U., Transy, C., Pancino, G., 2009. Human TRIM gene expression in response to interferons. PLoS One 4, e4894. http://dx.doi.org/10.1371/ journal.pone.0004894.

Chen, Y., Su, Y., Shie, P., Huang, S., 2008. Grouper Mx confers resistance to nodavirus and interacts with coat protein. Dev. Comp. Immunol. 32, 825-836. http:// dx.doi.org/10.1016/j.dci.2007.12.003.

Chin, K., Cresswell, P., 2001. Viperin (cig5), an IFN-inducible antiviral protein directly induced by human cytomegalovirus. PNAS 99, 15125-15130.

Collet, B., Munro, E.S., Gahlawat, S., Acosta, F., Garcia, J., Roemelt, C., Zou, J., Secombes, C.J., Ellis, A.E., 2007. Infectious pancreatic necrosis virus suppresses type I interferon signalling in rainbow trout gonad cell line but not in Atlantic salmon macrophages. Fish. Shellfish Immunol. 22, 44-56. http://dx.doi.org/ 10.1016/j.fsi.20 06.03.011.

Cunha, J.D., Knight, E., Haast, A.L., Truitt, R.L., Borden, E.C., 1996. Immunoregulatory properties of ISG15, an interferon-induced cytokine. PNAS 93, 211-215.

del Castillo, C.S., Hikima, J., Ohtani, M., Jung, T., Aoki, T., 2012. Characterization and functional analysis of two PKR genes in fugu (*Takifugu rubripes*). Fish. Shellfish Immunol. 32, 79-88. http://dx.doi.org/10.1016/j.fsi.2011.10.022.

Der, S.D., Lau, A.S., 1995. Involvement of the double-stranded-RNA-dependent kinase PKR in interferon expression and interferon-mediated antiviral activity. Proc. Natl. Acad. Sci. U. S. A. 92, 8841-8845.

Diamond, M.S., 2014. IFIT1: a dual sensor and effector molecule that detects non-2^{0}- O methylated viral RNA and inhibits its translation. Cytokine Growth Factor Rev. 25 (5), 543-550.

Durfee, L.A., Lyon, N., Seo, K., Huibregtse, J.M., 2010. The ISG15 conjugation system broadly targets newly synthesized Proteins: implications for the antiviral function of ISG15. Mol. Cell 38, 722-732. http://dx.doi.org/10.1016/ j.molcel.2010.05.002.

Engelhardt, O.G., Pandolfi, P., Haller, O., 2004. Mx1 GTPase accumulates in distinct nuclear domains and inhibits influenza A virus in cells that lack promyelocytic leukaemia protein nuclear bodies. J. Gen. Virol. 85, 2315-2326. http:// dx.doi.org/10.1099/vir.0.79795-0.

Fernandez-Trujillo, M.A., García-Rosado, E., Alonso, M.C., Alvarez, M.C., Bejar, J., 2015. Synergistic effects in the antiviral activity of the three Mx proteins from gilthead seabream (*Sparus aurata*). Vet. Immunol. Immunopathol. http:// dx.doi.org/10.1016/j.vetimm.2015.08.007.

Ferna ndez-Trujillo, M.A., García-Rosado, E., Alonso, M.C., Borrego, J.J., Alvarez, M.C., Bejar, J., 2011. Differential antiviral activity of Mx1, Mx2 and Mx3 proteins from gilthead seabream (*Sparus aurata*) against infectious pancreatic necrosis virus (IPNV). Mol. Immunol. 49 (12), 107-114.

Furnes, C., Kileng, Ø., Hanssen, C., Seppola, M., Jensen, I., Robertsen, B., 2009. Atlantic cod (*Gadus morhua L.*) possesses three homologues of ISG15 with different expression kinetics and conjugation properties. Dev. Comp. Immunol. 33, 123-1246. http://dx.doi.org/10.1016/j.dci.2009.07.005.

García-Rosado, E., Markussen, T., Kileng, Ø., Baekkevold, E.S., Robertsen, B., Mjaaland, S., Rimstad, E., 2008. Molecular and functional characterization of two infectious salmon anaemia virus (ISAV) proteins with type I interferon antagonizing activity. Virus Res. 133 (2), 228-238.

Gill, J., Esteban, M., 2000. Induction of apoptosis by the dsRNA-dependent protein kinase (PKR): mechanism of action. Apoptosis 5 (2), 107-114.

Grayfer, L., Robert, J., Andino, F.D.J., Chen, G., Chinchar, G., 2012. Immune evasion strategies of ranaviruses and innate immune responses to these emerging pathogens. Viruses 4, 1075-1092. http://dx.doi.org/10.3390/v4071075.

Haller, O., Kochs, G., 2002. Interferon-induced Mx Proteins: dynamin-like GTPases with antiviral activity. Traffic 3, 710-717.

Haller, O., Stertz, S., Kochs, G., 2007. The Mx GTPase family of interferon-induced antiviral proteins. Microbes Inf. 9, 1636-1643. http://dx.doi.org/10.1016/ j.micinf.2007.09.010.

Helbig, K.J., Eyre, N.S., Yip, E., Narayana, S., Li, K., Fiches, G., Mccartney, E.M., Jangra, R.K., Lemon, S.M., Beard, M.R., 2011. The antiviral protein viperin inhibits hepatitis C virus replication via interaction with nonstructural protein 5A. Hepatol 1506-1517. http://dx.doi.org/10.1002/hep.24542.

Holland, J.W., Bird, S., Williamson, B., Woudstra, C., Mustafa, A., Wang, T., Zou, J., Blaney, S.C., Collet, B., Secombes, C.J., 2008. Molecular characterization of IRF3 and IRF7 in rainbow trout, *Oncorhynchus mykiss*: functional analysis and tran- scriptional modulation. Mol. Immunol. 46, 269-285. http://dx.doi.org/10.1016/ j.molimm.2008.08.265.

Huang, X., Huang, Y., Cai, J., Wei, S., Ouyang, Z., Qin, Q., 2013. Molecular cloning, expression and functional analysis of ISG15 in orange-spotted grouper, *Epinephelus coioides*. Fish. Shellfish Immunol. 34, 1094-1102. http://dx.doi.org/ 10.1016/j.fsi.2013.01.010.

Huang, Y., Huang, X., Cai, J., OuYang, Z., Wei, S., Wei, J., Qin, Q., 2015. Identification of orange-spotted grouper (*Epinephelus coioides*) interferon regulatory factor 3 involved in antiviral immune response against fish RNA virus. Fish. Shellfish Immunol. 42, 345-352. http://dx.doi.org/10.1016/j.fsi.2014.11.025.

Huang, Y., Yu, Y., Yang, Y., Yang, M., Zhou, L., 2016. Fish TRIM8 exerts antiviral roles through regulation of the proinflammatory factors and interferon signaling. Fish. Shellfish Immunol. 54, 435-444. http://dx.doi.org/10.1016/ j.fsi.2016.04.138.

Hu, Y., Fan, L., Wu, C., Wang, B., Sun, Z., Hu, C., 2016. Identification and function analysis of the three dsRBMs in the N terminal dsRBD of grass carp (*Ctenopharyngodon idella*) PKR. Fish. Shellfish Immunol. 50, 91-100. http:// dx.doi.org/10.1016/j.fsi.2016.01.011.

Jeffrey, I.W., Kaderit, S., Meurs, E.F., Metzger, T., Bachmann, M., Schwemmle, M., Hovanessian, A.G., Clemens, M.J., 1995. Nuclear localization of the interferon- inducible protein kinase PKR in human cells and transfected mouse cells. Exp. Cell Res. 218, 17-27.

Jensen, I., Robertsen, B., 2002. Effect of double-stranded RNA and interferon on the antiviral activity of Atlantic salmon cells against infectious salmon anemia virus and infectious pancreatic necrosis virus. Fish. Shellfish Immunol. 13, 221-241. http://dx.doi.org/10.1006/fsim.2001.0397.

Jiang, J., Zhang, Y., Li, S., Yu, F., Sun, F., Gui, J., 2009. Expression regulation and functional characterization of a novel interferon inducible gene Gig2 and its promoter. Mol. Immunol. 46, 3131-3140. http://dx.doi.org/10.1016/ j.molimm.2009.05.183.

Kibenge, M.J., Munir, K., Kibenge, F.S., 2005. Constitutive expression of Atlantic salmon Mx1 protein in CHSE-214 cells confers resistance to infectious salmon anaemia virus. Virol. J. 2 (1), 75.

Kochs, G., Haller, O., 1999. Interferon-induced human MxA GTPase blocks nuclear import of Thogoto virus nucleocapsids. PNAS 96, 2082-2086.

Kumar, A., Haque, J., Lacosteo, J., Hiscotrr, J., Williams, B.R.G., 1994. Double-stranded RNA-dependent protein kinase activates transcription factor NF-KB by phosphorylating 1KcB. PNAS 91, 6288-6292.

Kurata, R., Tajima, A., Yonezawa, T., Inoko, H., 2013. TRIM39R, but not TRIM39B, regulates type I interferon response. Biochem. Biophys. Res. Commun. 436, 90-95.

http://dx.doi.org/10.1016/j.bbrc.2013.05.064.

Langevin, C., van der Aa, L.M., Houel, A., Torhy, C., Briolat, V., Lunazzi, A., Harmache, A., Bremont, M., Levraud, J.P., Boudinot, P., 2013. Zebrafish ISG15 exerts a strong antiviral activity against RNA and DNA viruses and regulates the interferon response. J. Virol. 87, 10025-10036. http://dx.doi.org/10.1128/ JVI.01294-12.

Leong, J.C., Trobridge, G.D., Kim, C.H.Y., 1998. Interferon-inducible Mx proteins in fish. Immunol. Rev. 166, 349-364.

Li, Y., Li, C., Xue, P., Zhong, B., Mao, A., Ran, Y., Chen, H., Wang, Y., Yang, F., 2009. ISG56 is a negative-feedback regulator of virus-triggered signaling and cellular, 106, 7945-7950.

Li, Q., Yan, J., Mao, A.P., Li, C., Ran, Y., Shu, H.B., Wang, Y.Y., 2011. Tripartite motif 8 (TRIM8) modulates TNFa-and IL-1betriggered NF-kB activation by targeting TAK1 for K63-linked polyubiquitination. PNAS 108 (48), 19341-19346.

Li, S., Sun, F., Zhang, Y.B., Gui, J.F., Zhang, Q.Y., 2012. Identification of DreI as an antiviral factor regulated by RLR signaling pathway. PLoS One 7, e32427. http:// dx.doi.org/10.1371/journal.pone.003242.

Lin, C., Abraham, J., John, C., Lin, C., Chang, C., 2006. Inhibition of nervous necrosis virus propagation by fish Mx proteins. Biochem. Biophys. Res. Commun. 351, 534-539. http://dx.doi.org/10.1016/j.bbrc.2006.10.063.

Liu, T., Zhang, Y., Liu, Y., Sun, F., Gui, J., 2011. Cooperative roles of fish PKZ and PKR in IFN-mediated antiviral response. J. Virol. 85 (23) http://dx.doi.org/10.1128/ JVI.05849-11.

Long, H., Sun, L., 2014. CsIFIT1, an interferon-induced protein with tetratricopeptide repeat, inhibits viral infection in tongue sole (*Cynoglossus semilaevis*). Fish. Shellfish Immunol. 41, 231-237. http://dx.doi.org/10.1016/j.fsi.2014.09.006.

Lu, G., Reinert, J.T., Pitha-Rowe, I., Okumura, A., Kellum, M., Knobeloch, K.P., Hassel, B., Pitha, P.M., 2006. ISG15 enhances the innate antiviral response by inhibition of IRF-3 degradation. Cell. Mol. Biol. 52, 29-41.

McBeath, A.J., Collet, B., Paley, R., Duraffour, S., Aspehaug, V., Biering, E., Secombes, C.J., Snow, M., 2006. Identification of an interferon antagonist protein encoded by segment 7 of infectious salmon anaemia virus. Virus Res. 115 (2), 176-184.

McNab, F.W., Rajsbaum, R., Stoye, J.P., O'Garra, A., 2011. Tripartite-motif proteins and innate immune regulation. Curr. Opin. Immunol. 23 (1), 46-56.

Meier, E., Kunz, G., Haller, O., Arnheiter, H., 1990. Activity of rat Mx proteins against a rhabdovirus. J. Virol. 64, 6263-6269.

Nasr, N., Maddocks, S., Turville, S.G., Harman, A.N., Woolger, N., Helbig, K.J., Wilkinson, J., Bye, C.R., Wright, T.K., Rambukwelle, D., Donaghy, H., Beard, M.R., Cunningham, A.L., 2012.

HIV-1 infection of human macrophages directly in- duces viperin which inhibits viral production. Blood 120, 778-789. http:// dx.doi.org/10.1182/blood-2012-01-407395.

Nisole, S., Stoye, J.P., Saïb, A., Hill, M., 2005. TRIM family proteins: retrovial re- striction and antiviral defence. Nat. Rev. Microbiol. 3, 799-808. http:// dx.doi.org/10.1038/nrmicro1248.

O'Farrell, C., Vaghefi, N., Cantonnet, M., Buteau, B., Boudinot, P., Benmansour, A., 2002. Survey of transcript expression in rainbow trout leukocytes reveals a major contribution of interferon-responsive genes in the early response to a rhabdovirus infection. J. Virol. 76, 8040-8049.

Okumura, A., Lu, G., Pitha-rowe, I., Pitha, P.M., 2006. Innate antiviral response targets HIV-1 release by the induction of ubiquitin-like protein ISG15. PNAS 103, 1-6.

Okumura, F., Matsunaga, Y., Katayama, Y., Nakayama, K.I., Hatakeyama, S., 2010. TRIM8 modulates STAT3 activity through negative regulation of PIAS3. J. Cell Sci. 123, 2238-2245. http://dx.doi.org/10.1242/jcs.068981.

Peng, L., Yang, C., Su, J., 2012. Protective roles of grass carp *Ctenopharyngodon idella* Mx isoforms against grass carp reovirus. PLoS One 7, 1-16. http://dx.doi.org/ 10.1371/journal.pone.0052142.

Pham, A.M., Santa Maria, F.G., Lahiri, T., Friedman, E., Marie , I.J., Levy, D.E., 2016. PKR transduces MDA5-dependent signals for type I IFN induction. PLoS Pathog. 12 (3), e1005489.

Poynter, S.J., DeWitte-Orr, S.J., 2015. Length-dependent innate antiviral effects of double-stranded RNA in the rainbow trout (*Oncorhynchus mykiss*) cell line, RTG- 2. Fish. Shellfish Immunol. 46, 557-565.

Rajsbaum, R., Garcia-Sastre, A., Versteeg, G.A., 2014. TRIMmunity: the roles of the TRIM E3-ubiquitin ligase family in innate antiviral immunity. J. Mol. Biol. 426 (6), 1265-1284.

Røkenes, T.P., Larsen, R., Robertsen, B., 2007. Atlantic salmon ISG15: expression and conjugation to cellular proteins in response to interferon, double-stranded RNA and virus infections. Mol. Immunol. 44, 950-959. http://dx.doi.org/10.1016/ j.molimm.2006.03.016.

Rothenburg, S., Deigendesch, N., Dittmar, K., Koch-nolte, F., Haag, F., Lowenhaupt, K., Rich, A., 2005. A PKR-like eukaryotic initiation factor 2a kinase from zebrafish contains Z-DNA binding domains instead of dsRNA binding domains. PNAS 102, 1602-1607.

Schneider, W.M., Chevillotte, M.D., Rice, C.M., 2014. Interferon-stimulated genes: a complex web of host defenses. Annu. Rev. Immunol. 32, 513-545. http:// dx.doi.org/10.1146/annurev-immunol-032713-120231.

Schoggins, J.W., Wilson, S.J., Panis, M., Murphy, M.Y., Jones, C.T., Bieniasz, P., Rice, C.M., 2011. type I interferon antiviral response. Nature 472, 481-485. http://dx.doi.org/10.1038/nature09907.

Schwemmle, M., Weining, K.C., Richter, M.F., Schumacher, B., Staeheli, P., 1995. Vesicular stomatitis virus transcription inhibited by purified MxA protein. Virol 206 (1), 545-554.

Seo, J.Y., Yaneva, R., Hinson, E.R., Cresswell, P., 2011. Human cytomegalovirus directly induces the antiviral protein viperin to enhance infectivity. Science 332, 1093-1097.

Skaug, B., Chen, Z.J., 2010. Minireview emerging role of ISG15 in antiviral immunity. Cell 143, 187-190. http://dx.doi.org/10.1016/j.cell.2010.09.033.

Skjesol, A., Aamo, T., Hegseth, M.N., Robertsen, B., Jørgensen, J.B., 2009. The interplay between infectious pancreatic necrosis virus (IPNV) and the IFN system: IFN signaling is inhibited by IPNV infection. Virus Res. 143, 53-60. http:// dx.doi.org/10.1016/j.virusres.2009.03.004.

Su, J., Yang, C., Zhu, Z., Wang, Y., Jang, S., Liao, L., 2009. Enhanced grass carp reovirus resistance of Mx-transgenic rare minnow (*Gobiocypris rarus*). Fish. Shellfish Immunol. 26 (6), 828-835.

Sun, C., Liu, Y., Hu, Y., Fan, Q., Li, W., Yu, X., Mao, H., Hu, C., 2013. Gig1 and Gig2 homologs (CiGig1 and CiGig2) from grass carp (*Ctenopharyngodon idella*) display good antiviral activities in an IFN-independent pathway. Dev. Comp. Immunol. 41, 477-483. http://dx.doi.org/10.1016/j.dci.2013.07.007.

Sun, F., Zhang, Y., Jiang, J., Wang, B., Chen, C., Zhang, J., Gui, J., 2014. Gig1, a novel antiviral effector involved in fish interferon response. Virology 448, 322-332. http://dx.doi.org/10.1016/j.virol.2013.10.029.

Suzuki, M., Watanabe, M., Nakamaru, Y., Yakagi, D., Takahashi, H., Fukuda, S., Hatakeyama, S., 2016. TRIM39 negatively regulates the NFkB-mediated signaling pathway through stabilization of Cactin. Cell Mol. Life Sci. 73 (5), 1085-1101.

Tomar, D., Sripada, L., Prajapati, P., Singh, R., Singh, A.K., Singh, R., 2012. Nucleo-cytoplasmic trafficking of TRIM8, a novel oncogene, is involved in positive regulation of TNF induced NF- k B Pathway. PLoS One 7. http://dx.doi.org/ 10.1371/journal.pone.0048662.

Trobridge, G.D., Chiou, P.P., Leong, J.C., 1997. Cloning of the rainbow trout (*Oncorhynchus mykiss*) Mx2 and Mx3 cDNAs and characterization of trout Mx protein expression in salmon cells. J. Virol. 71, 5304-5311.

Turan, K., Mibayashi, M., Sugiyama, K., Saito, S., Numajiri, A., Nagata, K., 2004. Nuclear MxA proteins form a complex with influenza virus NP and inhibit the transcription of the engineered influenza virus genome. Nuc. Acids Res. 32 (2), 643-652.

Uchil, P.D., Quinlan, B.D., Chan, W., Luna, J.M., Mothes, W., 2008. TRIM E3 ligases interfere with early and late stages of the retroviral life cycle. PLOS Pathog. 4 (2) http://dx.doi.org/10.1371/journal.ppat.0040016.

Van Der Aa, L.M., Levraud, J., Yahmi, M., Lauret, E., Briolat, V., Herbomel, P., Benmansour,

A., Boudinot, P., 2009. A large new subset of TRIM genes highly diversified by duplication and positive selection in teleost fish. BMC 23, 1-23. http://dx.doi.org/10.1186/1741-7007-7-7.

Wang, B., Zhang, Y.B., Liu, T.K., Shi, J., Sune, F., Gui, J.F., 2014a. Fish viperin exerts a conserved antiviral function through RLR-triggered IFN signaling pathway. Dev. Comp. Immunol. 47, 140-149. http://dx.doi.org/10.1016/j.dci.2014.07.006.

Wang, B., Zhang, Y., Liu, T., Gui, J., 2014b. Sequence analysis and subcellular localization of crucian carp *Carassius auratus* viperin. Fish. Shellfish Immunol. 39, 168-177. http://dx.doi.org/10.1016/j.fsi.2014.04.025.

Wang, W., Zhang, M., Xiao, Z.Z., Sun, L., 2012. *Cynoglossus semilaevis* ISG15: a secreted cytokine-like protein that stimulates antiviral immune response in a LRGG motif-dependent manner. PLoS One 7, 1-11. http://dx.doi.org/10.1371/ journal.pone.0044884.

Wang, X., Hinson, E.R., Cresswell, P., 2007. Article the interferon-inducible protein viperin inhibits influenza virus release by perturbing lipid rafts. Cell Host Microbe 2, 96-105. http://dx.doi.org/10.1016/j.chom.2007.06.009.

Wang, W., Huang, Y., Yu, Y., Yang, Y., Xu, M., Chen, X., 2016. Fish TRIM39 regulates cell cycle progression and exerts its antiviral function against iridovirus and nodavirus. Fish. Shellfish Immunol. 50, 1-10. http://dx.doi.org/10.1016/ j.fsi.2016.01.016.

Weber, F., Haller, O., Kochs, G., 2000. MxA GTPase blocks reporter gene expression of reconstituted Thogoto virus ribonucleoprotein complexes. J. Virol. 74 (1), 560-563.

Wu, Y., Lu, Y., Chi, S., 2010. Anti-viral mechanism of barramundi Mx against betanodavirus involves the inhibition of viral RNA synthesis through the interference of RdRp. Fish. Shellfish Immunol. 28, 467-475. http://dx.doi.org/10.1016/ j.fsi.2009.12.008.

Yang, P., Wu, C., Li, W., Fan, L., Lin, G., Hu, C., 2011. Cloning and functional analysis of PKZ (PKR-like) from grass carp (*Ctenopharyngodon idellus*). Fish. Shellfish Immunol. 31, 1173e1178. http://dx.doi.org/10.1016/j.fsi.2011.10.012.

Yeh, Y.C., Hsu, Y.J., Chen, Y.M., Lin, H.Y., Yang, H.L., Chen, T.Y., Wang, H.C., 2014. EcVig, a novel grouper immune-gene associated with antiviral activity against NNV infection. Dev. Comp. Immunol. 43, 68-75. http://dx.doi.org/10.1016/ j.dci.2013.10.014.

Yergeau, D.A., Cornell, C.N., Parker, S.K., Zhou, Y., Detrich, H.W., 2005. Bloodthirsty, an RBCC/TRIM gene required for erythropoiesis in zebrafish. Dev. Biol. 283, 97-112. http://dx.doi.org/10.1016/j.ydbio.2005.04.006.

Zenke, K., Kwon, Y., Hong, K., 2010. Molecular cloning and expression analysis of double-stranded RNA-dependent protein kinase (PKR) in rock bream (*Oplegnathus fasciatu*s). Vet. Immunol. Immunopathol. 133, 290e295. http:// dx.doi.org/10.1016/j.vetimm.2009.08.009.

Zhang, B.C., Zhang, J., Xiao, Z.Z., Sun, L., 2014. Rock bream (*Oplegnathus fasciatus*) viperin is a virus-responsive protein that modulates innate immunity and promotes resistance against

megalocytivirus infection. Dev. Comp. Immunol. 45, 35-42. http://dx.doi.org/10.1016/j.dci.2014.02.001.

Zhang, Y., Gui, J., 2004. Identification of two novel interferon-stimulated genes from cultured CAB cells induced by UV-inactivated grass carp hemorrhage virus. Dis. Aquat. Organ 60, 1-9. http://dx.doi.org/10.3354/dao060001.

Zhang, L., Mei, Y., Fu, N., Guan, L., Xie, W., Liu, H., Yu, C., Yin, Z., Yu, V.C., You, H., 2012. TRIM39 regulates cell cycle progression and DNA damage responses via stabilizing p21, 109, 20937-20942. http://dx.doi.org/10.1073/pnas.1300201110.

Zhang, Y.B., Gui, J.F., 2012. Molecular regulation of interferon antiviral response in fish. Dev. Comp. Immunol. 38, 193-202. http://dx.doi.org/10.1016/ j.dci.2012.06.003.

Zhang, X., Zhao, H., Chen, Y., Luo, H., Yang, P., Yao, B., 2015. A zebrafish (*Danio rerio*) bloodthirsty member 20 with E3 ubiquitin ligase activity involved in immune response against bacterial infection. Biochem. Biophys. Res. Commun. 457, 83-89. http://dx.doi.org/10.1016/j.bbrc.2014.12.081.

Zhao, C., Hsiang, T.Y., Kuo, R.L., Krug, R.M., 2010. ISG15 conjugation system targets the viral NS1 protein in influenza A virus infected cells. Proc. Natl. Acad. Sci. 107 (5), 2253-2258.

Zhou, X., Michal, J.J., Zhang, L., Ding, B., Lunney, J.K., Liu, B., Jiang, Z., 2013. Interferon induced IFIT family genes in host antiviral defense. Int. J. Biol. Sci. 9, 200-208. http://dx.doi.org/10.7150/ijbs.5613.

Zhu, R., Zhang, Y., Zhang, Q., Gui, J., 2009. Subcellular localization and inductive expression of the dsRNA-dependent protein kinase PKR from Japanese flounder, *Paralichthys olivaceus*. Prog. Nat. Sci. 19 (10), 1227-1234.

Zhu, R., Zhang, Y.B., Zhang, Q.Y., Gui, J.F., 2008. Functional domains and the antiviral effect of the double-stranded RNA-dependent protein kinase PKR from *Paralichthys olivaceus*. J. Virol. 82 (14), 6889-6901.